Development and Application of a Consumable-Free Modulator for Comprehensive Two-Dimensional Gas Chromatography

by

Matthew Edwards

A thesis

presented to the University of Waterloo

in fulfillment of the

thesis requirement for the degree of

Doctor of Philosophy

in

Chemistry

Waterloo, Ontario, Canada, 2024

Examining Committee Membership

The following served on the Examining Committee for this thesis. The decision of the Examining Committee is by majority vote.

External Examiner	Phillip Marriott Professor School of Chemistry Monash University
Supervisor	Tadeusz Gorecki Professor Department of Chemistry University of Waterloo
Internal Member	Janusz Pawliszyn Professor Department of Chemistry University of Waterloo
Internal Member	W. Scott Hopkins Associate Professor Department of Chemistry University of Waterloo
Internal-external Member	Roland Hall Professor Department of Biology University of Waterloo

Author's Declaration

This thesis consists of material all of which I authored or co-authored: see Statement of Contributions included in the thesis. This is a true copy of the thesis, including any required final revisions, as accepted by my examiners.

I understand that my thesis may be made electronically available to the public.

Statement of Contributions

Chapter 1 is based on two papers written and co-authored by the writer of this thesis. Chapter 2 and 3 are original work completed by the writer of this thesis. Chapter 4 is based on a combination of original work and papers co-authored by the writer of this thesis. Chapter 5 is based on a paper written by the author. Specific contributions to co-authored works are detailed at the beginning of the chapter in which they are contained.

The following publications have been used in this work:

Chapter 1:

M. Edwards, A. Mostafa, T. Gorecki, "Modulation in comprehensive two-dimensional gas chromatography: 20 years of innovation," *Analytical and Bioanalytical Chemistry,* vol. 401, pp. 2335-2349, 2011.

A. Mostafa, M. Edwards, T. Górecki, "Optimization aspects of comprehensive two-dimensional gas chromatography," *Journal of Chromatography A,* vol. 1255, pp. 38-55, 2012.

Chapter 4:

G. Ntlhokwe, A.G.J. Tredoux, T. Górecki, M. Edwards, J. Vestner, M. Muller, L. Erasmus, E. Joubert, J. Christel Cronje, A. de Villiers, "Analysis of honeybush tea (Cyclopia spp.) volatiles by comprehensive two-dimensional gas chromatography using a single-stage thermal modulator," *Analytical and Bioanalytical Chemistry,* vol. 409, pp. 4127-4138, 2017.

A.M. Muscalu, M. Edwards, T. Gorecki, E.J. Reiner, "Evaluation of a single-stage consumable-free modulator for comprehensive two-dimensional gas chromatography: Analysis of polychlorinated biphenyls, organochlorine pesticides and chlorobenzenes," *Journal of Chromatography. A,* vol. 1391, pp. 93-101, 2015.

M.R. Jacobs, M. Edwards, T. Górecki, P.N. Nesterenko, R.A. Shellie, "Evaluation of a miniaturised single-stage thermal modulator for comprehensive two-dimensional gas chromatography of petroleum contaminated soils," *Journal of Chromatography A,* vol. 1463, pp. 162-168, 2016.

Chapter 5:

M. Edwards, T. Górecki, "Inlet backflushing device for the improvement of comprehensive two-dimensional gas chromatographic separations," *Journal of Chromatography A,* vol. 1402, pp. 110-123, 2015.

Abstract

Comprehensive two-dimensional gas chromatography (GC×GC), is a separation method recognized as offering far greater peak capacity than conventional one-dimensional separations. Today, the most frequently used GC×GC systems require consumables such as liquid N_2 for the trapping function of the modulator. Although these systems are recognized as being very effective, their initial and running costs are a hindrance to more widespread use. A consumable-free, single-stage thermal modulator for GC×GC has been developed to overcome these problems. The device traps analytes through the use of a specially prepared coated stainless steel capillary compressed between two ceramic cooling pads. Analytes are thermally released from the trap into the secondary column via resistive heating. Thermal treatment of the trapping capillary plays an important role in the function of the device and advanced imaging and material characterization techniques were used to reveal changes in the stationary phase coating of the trap. These experiments revealed the polydimethylsiloxane stationary phase coating was being converted to carbon doped, oxygen rich silica nanoparticles. These spherical particles coated the internal surface of the capillary evenly and provided an effective and highly sorptive phase for use in GC×GC modulation. This modulator's performance was evaluated by applying it to real world analytical challenges. Samples such as honeybush tea volatiles, polychlorinated biphenyls, perfumes and petroleum products were successfully analyzed with performance comparable to commercially available instruments. This work demonstrates the single-stage, consumable-free GC×GC modulation system described herein is an excellent instrumental option for analysts across a wide breadth of application areas in the world of complex volatile and semi-volatile analysis.

Acknowledgements

I would like to thank my supervisor, Professor Tadeusz Górecki, for the opportunity to join his research group. Under his supervision I was able to develop the necessary skillset and experience to acquire meaningful employment in the field of analytical chemistry, with a particular focus on multidimensional gas chromatography. Thank you for your leadership and professionalism.

Thank you to my committee members, Professor Scott Hopkins and Professor Janusz Pawliszyn, for reading my thesis and providing their support and guidance. I would also like to thank my external examiner, Professor Phillip Marriott, and my internal examiner, Professor Roland Hall, for participating in the evaluation committee of my work and examining my thesis.

Thank you to Hiruy Haile of the Waterloo Machine Shop for his guidance and support during the many hours we spent together. Thank you to the University of Waterloo WAT Lab for their help in acquiring the SEM, XPS and EDX data.

Thank you to my children, Matthew and Mitchell, for giving me the time and space necessary to complete this work and always putting a smile on my face. You are both incredible young men.

Lastly, my deepest appreciation and love to my wife, Marianne, for your love, patience and support of my pursuits. You are the catalyst to my success and I am eternally grateful for you.

Dedication

I dedicate this thesis to my grandparents, John and June Dekoning.

Table of Contents

List of Figures

List of Tables

List of Abbreviations

1D	One-dimensional
^{1}D	First dimension
$^{1}d_{c}$	^{1}D column diameter
$^{1}d_{f}$	^{1}D column film thickness
$^{1}\Delta p$	Pressure drop in the ^{1}D
$^{1}\Delta p/\Delta p_{T}$	Pressure drop in the ^{1}D compared to the total pressure drop
^{1}l	^{1}D column length
$^{1}R_{s}$	^{1}D resolution
$^{1}t_{R}$	First dimension retention time
^{1}u	^{1}D column linear velocity
$^{1}u_{opt}$	^{1}D column optimal linear velocity
$^{1}w_{h}$	^{1}D peak width
2D	Two-dimensional
^{2}D	Second dimension
$^{2}d_{c}$	^{2}D column diameter
$^{2}d_{f}$	^{2}D column film thickness
$^{2}\Delta p$	Pressure drop in the ^{2}D
^{2}l	^{2}D column length
$^{2}R_{s}$	^{2}D resolution
$^{2}t_{R}$	Second dimension retention time
^{2}u	^{2}D column linear velocity
$^{2}W_{1/2}$	Peak width at half height in the second dimension
$^{2}w_{h}$	^{2}D peak width
2D-PAGE	Two-dimensional polyacrylamide gel electrophoresis
2D-TAG	Thermal desorption aerosol comprehensive two-dimensional gas-chromatography mass spectrometry system
2D-TLC	Two-dimensional thin-layer chromatography
ALS	Automatic liquid sampler
CAR/PDMS	Carboxen/polydimethylsiloxane
CBs	Chlorobenzenes
CFT	Capillary flow technology
CMD	Comprehensive multidimensional
CPU	Central processing unit
DC	Direct current
d_{f}	Film thickness

DFM	Differential flow modulator
DVM	Diaphragm flow modulator
EI	Electron ionization
FAME	Fatty acid methyl ester
FF	Fuel farm
fg	Femtogram
FID	Flame ionization detection
GC	Gas chromatography
GC×GC	Comprehensive two-dimensional gas chromatography
HCA	Hierarchical clustering analysis
HS-SPME	Headspace-solid phase microextraction
id	Internal diameter
IDL	Instrument detection limit
LMCS	Longitudinally modulated cryogenic system
LN_2	Liquid nitrogen
LOD	Limit of detection
m	Metres
MC	Modulator capillary
MD	Multidimensional
mL	Millilitres
mm	Millimetres
MPH	Main power house
MS	Mass spectrometer
µg	Microgram
µm	Micrometer
m_s	Solute mass
ms	Millisecond
mV	Millivolt
N	Peak capacity
n_1	Peak capacity column 1
n_2	Peak capacity column 2
nm	Nanometre
OCs	Organochlorine pesticides
PA	Polyacrylate
PAHs	Polycyclic aromatic hydrocarbons
PCA	Principal component analysis
PCBs	Polychlorinated biphenyls
PCDD/Fs	Dibenzo-p-dioxins/polychlorinated dibenzofurans
PCM	Pneumatic Control Module
PDMS	Polydimethylsiloxane
PDMS/CAR	Polydimethylsiloxane/carboxen

PDMS/CAR/DVB	Polydimethylsiloxane/carboxen/divinylbenzene
PDMS/DVB	Polydimethylsiloxane/divinylbenzene
PEG	Polyethylene glycol
PHC	Petroleum hydrocarbon contamination
PLOT	Porous layer open tubular
P_M	Modulation Period
POPs	Persistent organic pollutants
ppm	Parts per million
PSU	Power Supply Unit
qMS	Quadrupole mass spectrometer
qTOF	Quadrupole time-of-flight
RPM	Revolutions per minute
RSH	Rotating slotted heater
RTM	Rotating thermal modulator
S/SL	Split/Splitless
SAB	Special Antarctic blend
SCD	Sulfur chemiluminescence detector
SPME	Solid-phase microextraction
T_e	Elution temperature
TDM	Thermal desorption modulator
TEC	Thermoelectric Cooler
TF-SPME	Thin-film solid-phase microextraction
TIM	Thermal independent modulator
TOF	Time-of-flight
TOF MS	Time-of-flight mass spectrometer
VOCs	Volatile organic compounds
Vp	Peak area
WCOT	Wall coated open tubular

Chapter 1. Introduction to multidimensional separations[1]

1.1 Introduction

It has been nearly 120 years since the Russian-Italian botanist Mikhail Tswett revealed in the Journal of the German Botanical Society his seminal papers describing the chromatographic separation of plant pigments on a packed column of calcium carbonate [1, 2]. Since this time several brilliant chemists have significantly improved our ability to separate chemical mixtures into their individual components, and efforts to increase this ability continue to this day. Readers interested in learning more about the fascinating history of chromatography are directed to references [3-5]. Single column separations have continuously been and remain standard practice today. However, effective separation of complex mixtures remains a significant challenge. Several authors including Giddings, Davis and Guiochon have published important works describing the theoretical limitations of one-dimensional (1D) separation techniques in great detail [6-8]. The ability of a single column separation technique to resolve a mixture of compounds is often described in terms of its peak capacity, *n*, which is calculated for some retention time window. For one to be able to always resolve 98 % of the components in a sample, the peak capacity must exceed the number of components by a factor of 100 [9]. An often cited

[1] This chapter is based on the following publications:

M. Edwards, A. Mostafa, T. Gorecki, "Modulation in comprehensive two-dimensional gas chromatography: 20 years of innovation," *Analytical and Bioanalytical Chemistry,* vol. 401, pp. 2335-2349, 2011.

Author contributions include original concept, primary manuscript contributor, review and editing.

A. Mostafa, M. Edwards, T. Górecki, "Optimization aspects of comprehensive two-dimensional gas chromatography," *Journal of Chromatography A*, vol. 1255, pp. 38-55, 2012.

Author contributions include original concept, secondary manuscript contributor, review and editing.

example that demonstrates the limitations of single column separation was provided by Berger in 1996 [10]. Using a column measuring 450 metres in length, a separation of gasoline was performed. The analysis lasted 11 hours and the column was calculated to have 1.3×10^6 theoretical plates and a peak capacity of 1000. Although these values represent a highly efficient system, the separation was deemed inadequate as numerous coelutions and an elevated baseline were observed. While this column setup may be adequate for less complex samples, factors such as onerous analysis times and inlet pressures exceeding 100 psi make the use of long columns impractical for most analyses. Liquid chromatography techniques also suffer from fundamental limitations stemming from the small particle size of stationary phases, which leads to excessive head pressures that currently prevent them from fully resolving complex mixtures [11].

With the theoretical limits of 1D separations well understood, multidimensional (MD) separations were theorized as an alternative means to achieve gains in peak capacity. A MD separation is commonly defined as one in which a sample is subjected to two or more independent separation mechanisms, and separation achieved in prior dimensions is maintained throughout subsequent ones [12, 13]. The MD separation can be referred to as comprehensive multidimensional separation (CMD) when the entire sample is subjected to all separation dimensions. This definition is derived from the work of Giddings in the 1980s [12, 13]. For a separation utilizing two columns offering different selectivities with peak capacities of n_1 and n_2, respectively, the theoretical total peak capacity then is the product of these values, $n_1 \bullet n_2$. Theoretically, CMD separations utilizing two separation dimensions can provide peak capacity values an order of magnitude greater than that of conventional 1D techniques. In practice, technical hurdles, challenging samples and underutilization of the separation space make achieving these theoretical peak capacity values difficult. Several excellent reviews and book

chapters have been published that discuss the theory and function of multidimensional separations in great detail [14-26].

Although almost all CMD techniques utilize two independent separation mechanisms, three-dimensional systems have been attempted and may hold promise for some future applications. Therefore, the term CMD will be used throughout to describe all techniques using multiple separation dimensions comprehensively. Furthermore, the CMD systems described herein utilize some form of chromatography column to facilitate the separation. Multidimensional separation systems have been designed without the use of chromatography columns. They include such techniques as two-dimensional polyacrylamide gel electrophoresis (2D-PAGE) and two-dimensional thin-layer chromatography (2D-TLC) [27-31] . The focus of this thesis is dedicated to GC×GC and separation systems with chromatography columns playing a critical role, therefore other gel or plate-based techniques will not be reviewed.

Today, CMD separation technologies can be classified into several different categories. The first is comprehensive two-dimensional gas chromatography (GC×GC). This technique is used for the separation of complex volatile and semi-volatile chemical mixtures such as petrochemicals, flavours and fragrances, and environmental samples. GC×GC utilizes two capillary columns connected serially through a modulating interface. The large number of available stationary phases allows for numerous column combinations, but sets based on contrasting polarities remain the standard. The degree to which column chemistries differ from each other is often referred to as column set orthogonality. For example, a column combination featuring a non-polar column with 100 % polydimethylsiloxane (PDMS) in the first dimension (^{1}D) and a polar wax-type column in the second dimension (^{2}D) would be considered highly orthogonal. Column sets with similar column chemistries or polarities would be considered

poorly orthogonal. High degree of orthogonality is frequently desired when designing column sets as to maximize the peak capacity and the selectivity of the separation system.

1.2 Comprehensive two-dimensional gas chromatography (GC×GC)

First introduced in 1991 by Phillips and Liu at Southern Illinois University, GC×GC has seen considerable development and adoption in recent years [32]. To describe this technique in general terms, GC×GC utilizes two capillary columns of differing selectivities connected to each other through a modulating interface. The objective of the modulator is to trap or sample the primary column effluent and reinject the collected fraction into the secondary column for further separation. It is mandatory that each compound eluting from the primary column should be sampled between 3-4 times to maintain the integrity of the primary column separation [33]. Since capillary columns will be featured extensively in this thesis, the common terms by which they are described should be defined. Column length is described in metres (m), column internal diameter (id) in millimetres (mm) and the stationary phase coating thickness (d_f) in micrometers (µm). Although column lengths and diameters vary considerably depending on the application, a generic GC×GC system would likely have a non-polar primary column such an a Rxi-1 (e.g. 30 m x 0.25 mm id x 0.25 µm d_f) interfaced with a polar secondary column such as a Stabilwax (e.g. 1.5 m x 0.18 mm id x 0.18 µm d_f), or a mid-polarity column such as an a Rxi-17Sil MS (e.g. 1.5 m x 0.18 mm id x 0.18 µm d_f). The modulation period (P_M) is both the primary column sampling period and the time that is allowed for analytes to become separated in the secondary column. It can typically range from 1 to 10 seconds, depending on the modulation system and application. If the modulator allows some of the trapped primary column effluent to enter the secondary column before the end of the P_M, analyte breakthrough is said to have occurred. Substantial efforts have been made by those designing GC×GC systems to prevent breakthrough

from occurring as it compromises the integrity of the two-dimensional chromatogram. However, when analyzing samples containing compounds at high concentrations (> 100 ng/µl), performing splitless injections, or injecting large volumes of solvent, breakthrough is very challenging to prevent.

Another often encountered phenomenon when performing a GC×GC analysis is peak wraparound. This arises when the retention time of an analyte in the ^{2}D column exceeds the length of the P_M. In the aforementioned generic non-polar/polar GC×GC system, analytes would be separated in the secondary column according to their polarity. Compounds such as alkanes would elute quickly, esters more slowly, and alcohols even more slowly. The elution order of these compounds along the y-axis of a two-dimensional chromatogram would reflect the relative strength of their interactions with the stationary phase from weak to strong. Modulation periods shorter than the retention time of a strongly retained analyte cause this analyte to elute during the next period. After processing, this analyte then appears at a misleading position along the y-axis. Fortunately, peak wraparound can be identified in a GC×GC chromatogram relatively easily. Since separation in the secondary column is a virtually isothermal process, the longer the compounds are retained, the greater is the effect of band broadening phenomena such as longitudinal diffusion. Peaks eluting early along the y-axis, but significantly wider than those of other analytes with similar second dimension retention times, are likely to be wrapped around. Although most GC×GC methods strive to reduce peak wraparound, an understanding of this condition can allow the user to use more of the two-dimensional separation space and further optimize their separation. To eliminate wraparound, the analyst can increase the length of the P_M, increase the flow rate, increase the oven temperature programming rate (to increase the elution temperature), or use a secondary oven. These variables often have an effect on other GC×GC

parameters, of which there are many, increasing the skill required to properly optimize a GC×GC separation [34].

1.2.1 The GC×GC Interface

The modulator is often referred to as the 'heart' of the GC×GC instrument, as it plays a crucial role in the successful completion of a GC×GC analysis. In the absence of a modulating device intermittently sampling the first dimension, chromatographic peaks that were previously separated on the primary column may co-elute at the outlet of the 2nd dimension. This would compromise the integrity of the ^{1}D separation, thereby violating a key GC×GC requirement (Figure 1.1). Since the Phillips modulator was introduced in 1991, there have been significant advancements in modulation technology. Modulators can be classified as either thermal or valve-based devices.

1.2.2 Thermal Modulation Systems

Heater-based interfaces trap primary column effluent at or above oven temperatures, usually with the help of thick stationary phases. Cryogenic interfaces trap primary column effluent below oven temperatures with the use of various cooling mechanisms. The two-stage thermal desorption modulator (TDM) was designed and implemented by John Phillips in 1991 and has the distinction of being the interface that allowed Phillips to perform the first truly comprehensive two-dimensional gas chromatography separation that same year. First designed as a single stage sample introduction device in multiplex and high-speed gas chromatography, this simple apparatus was applied to GC×GC with very little alteration to its original design other than the use of two trapping stages [35, 36].

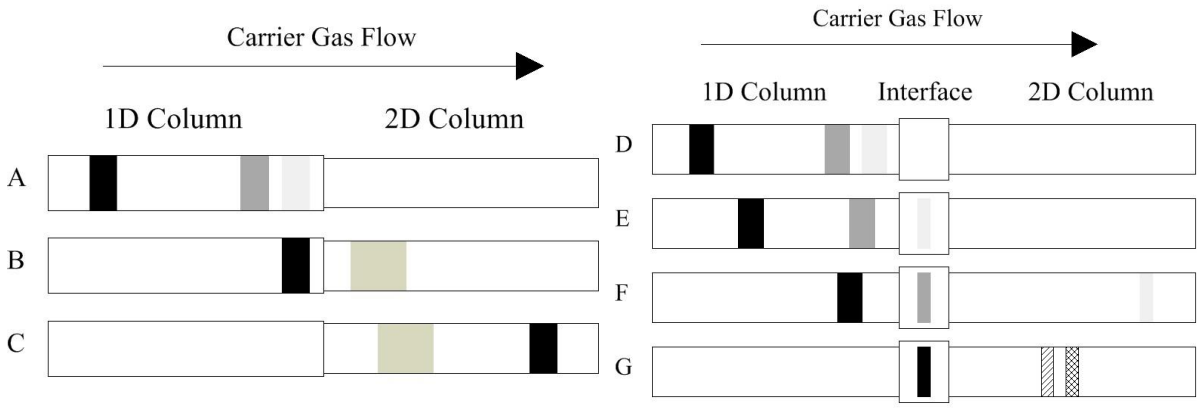

Figure 1.1 When a modulator is absent between the primary and secondary columns, analytes with close retention times at the outlet of the first dimension (A) may coalesce into a single band (B) in the secondary column and co-elute. Analytes retained more strongly in the primary column might catch up or even overtake earlier eluters in the secondary column (C). In a GC×GC setup, the first of two closely eluting bands is trapped in the modulator (E). It is then focused and injected into the secondary column as a narrow focused band (F), while the following band is trapped by the modulator, thus preventing the co-elution. Due to the difference in selectivity between the stationary phases, analytes co-eluting at the outlet of the primary column might become separated when injected into the secondary column (G).

The GC×GC system used by Phillips utilized a 250 µm id, 21 m long open tubular primary column with 0.25 µm Supelcowax-10 stationary phase, and a 100 µm id, 1 m long open tubular secondary column with 0.5 µm methyl silicone stationary phase from Quadrex Corporation. The two columns were joined together by shrinkable Teflon tubing along with a small splitter to adjust the flow rate through the second column. Electrically conductive gold paint was applied to a segment at the beginning of the second column, which was looped outside the oven and maintained at room temperature. The electrical resistance of the film was calculated after each coat of paint until a desired resistance was achieved. The total length of the modulating section was 15 cm. Electrical leads connected to the column provided current from a 40 V DC power supply to either end of the interface. Schematic diagram of the interface is shown in Figure 1.2

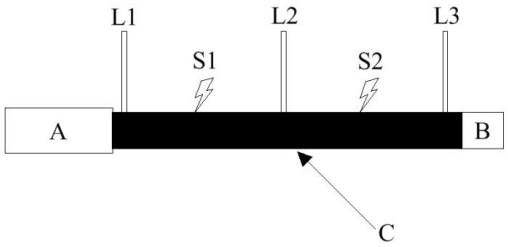

Figure 1.2 Schematic diagram of the original TDM, based on reference [32]. The primary column (A) is connected to the secondary column (B). Gold paint (C) is applied to the beginning segment of the secondary column. Electrical leads (L1, L2, L3) allow current to flow alternately between stage one (S1) and stage two (S2) during modulation.

As effluent from the primary column (A) entered the second column (B), it would become trapped and focused by the stationary phase coating kept below the oven temperature. Electrical current was then applied to first stage of the trap (S1) through leads L1 and L2. This caused rapid heating of the gold paint layer (C), forcing analytes trapped within the capillary to partition into the carrier gas. Once in the mobile phase, the effluent was swept to the second stage (S2) of the capillary, where it became trapped once again. At this time, the first stage of the modulator had cooled and would continue its trapping function, as the second stage was pulsed through the leads L2 and L3, injecting the trapped components as a narrow band to the secondary column. The pulses were applied to each stage 100 ms apart for a duration of 20 ms. Modulation occurred every 2 s. The experimental results collected were acceptable but left much to be desired. Wider than preferred injection pulses and component overlap were the main problems. These issues were recognized by Phillips and the dual-stage TDM was modified by increasing the length of the first trapping stage, as well as increasing the time between electrical pulses. It was shown that by making these modifications, sample breakthrough in the first stage was minimized, while the shorter second stage provided satisfactory focusing and injection of compounds into the second

column [37-39]. Although the TDM was vital in achieving the first fully comprehensive GC×GC separation, the gold-painted capillaries were not very robust and often required replacement [40].

An attempt was made at improving Phillips design by de Geus *et al*. in 1997 by evaluating a single stage version of the TDM [41]. The focus of this group was to increase the longevity and improve the modulation function of the TDM by experimenting with different electrically conductive materials applied to the outside of the capillary, as well as optimization of parameters such as voltage, pulse length and pulse interval. Some of the electrically conductive materials tested included an acryl resin-based coating containing metallic silver, pure metal silver and aluminum that were applied through a metal evaporation technique, and copper wire that was tightly coiled onto the capillary surface. The authors found that pure aluminum- and silver-plated modulators outperformed their metallic painted counterparts, but were inferior to the copper coiled interface, which proved to be the most robust. Unfortunately, this design suffered from high power requirements due to its large thermal mass. The authors also showed that pulsed heating prevented the modulator from reaching undesirably high temperatures and was a good alternative to constant heating.

Although the TDM was made more reliable, Phillips and his group had begun devising a new mechanical version of the resistively heated modulator referred to as the rotating thermal modulator (RTM). Development of resistively heated modulators did not stop here, however, as the benefit of no moving parts, as well as simplicity of resistive heating were very attractive features that drew the attention of some researchers to this method of modulation. In 2000, Lee *et al*. compared various modulating interface technologies and sought to use a new type of interface material, stainless steel capillary [42]. These capillaries were coated internally with 3 μm of PDMS and used in the same fashion as the previously described two-stage TDM. When

compared to metal paint-coated fused silica modulators, the stainless-steel interface produced significantly broader peaks, although the superior mechanical properties of the material improved the robustness of the device.

An interface designed by Burger *et al*. utilized a stainless steel capillary jacket in which a thick film fused silica capillary was housed [43]. Attached to the jacket through spot welds were a series of stainless steel connectors. Electrical current could be supplied to each of these connectors individually through copper leads and an electrical sequencing system, thereby heating small sections of the capillary in sequence, and consequently shuffling analytes down the modulator. The authors used this system successfully for three years without any modulator burn-out and obtained pulsed widths at half height on the order of 145 ms, a result comparable with other TDM systems. Stainless steel capillary columns helped improve the performance of resistively heated modulators, but also signaled the end of improvements that would be made to this style of interface for some time.

The development of alternative methods of thermal modulation began shortly after the TDM was proven as a functional GC×GC interface. First introduced in 1996, Phillips described the theory behind a rotating thermal modulator (RTM), also known as the ‘sweeper’, as well as its potential to improve field-portable gas chromatography (GC) instruments [44]. It was not until early 1999 when its construction was described in detail along with two years of prototype performance results [45]. The RTM had four main functions: accumulate (A), cut (B), focus (C) and launch (D) [45] (Figure 1.3).

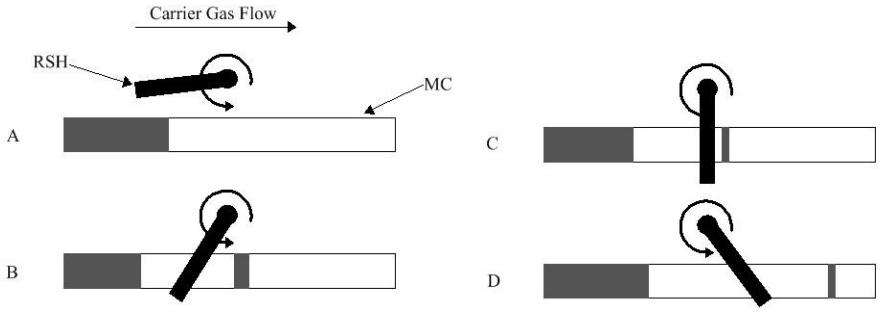

Figure 1.3 Schematic diagram of RTM, based on reference [45]. The rotating slotted heater (RSH) periodically passes over the modulating capillary (MC) as four main functions occur: accumulate (A), cut (B), focus (C) and launch (D).

As components exited the primary column, they would start to accumulate in the thick stationary phase of the modulator capillary (MC) (A). The RTM cycle would be engaged via computer control, causing the slotted heater (RSH), which was kept at around 100 °C above the GC oven temperature, to begin to rotate. The heater would move over the upstream portion of the capillary, rapidly heating a zone that moved along the tube at the speed of the heater's rotation, in the direction of the carrier gas flow, provided the linear velocity of the carrier gas was higher than the linear velocity of the heater along the MC. Analytes trapped in the capillary were instantly mobilized into the carrier gas by the moving hot zone, resulting in the creation of a thin "slice" of accumulated components (B). Flowing with the carrier gas, this fraction would not migrate far before becoming trapped and focused once again into a section of the capillary not yet exposed to the slotted heater (C). As the heater continued its rotation, the moving hot zone propelled the focused analyte band, ultimately launching it out of the capillary, into a short section of uncoated capillary and onto the secondary column (D). Trap cooling time was reduced by applying forced air cooling to the interface. The RTM prototype initially worked quite well in two of the five laboratories in which it was first tested [45]. Apart from its early success, the

RTM experienced several technical issues related to keeping the capillary aligned between the slotted heater and preventing mounting hardware from experiencing thermal expansion at high oven temperatures. A temperature differential of about 100 °C was also required for proper launching of the analyte bands, meaning that compounds with higher boiling points often had to be excluded from the analysis [40]. Even with some significant technical issues, the RTM became the first modulator to be commercially available and successfully functioned in many applications such as analysis of chlorinated biphenyls and toxaphene [46], semi-volatile aromatics [47] as well as other complex organic samples [48-53]. Dalluge reported that ca. 30 % of all papers published in GC×GC before the year 2003 used the RTM [54]. Its applicability to a wide range of samples, particularly those with very low or very high boiling points, was questioned by those experimenting and reviewing a new type of thermal modulator, the longitudinally modulated cryogenic system (LMCS) [54-58]. This was disputed by other researchers who were intimately involved with the RTM and had demonstrated its applicability in many analyses, albeit with a fair amount of customization [52, 59-63]. The RTM is today considered inferior compared to other methods of modulation and is no longer commercially available.

As Phillips was developing thermal methods of modulation, Marriott and coworkers were engineering a new kind of thermal modulator that utilized a cryogenic agent to trap analytes. Whereas both TDM and RTM trapped analytes at oven temperature and injected them at higher temperatures, cryogenic modulators trap analytes at temperatures significantly lower than that of the oven and inject compounds into the second dimension at or close to the oven temperature. Marriott's first design of the LMCS operated on this principle [64]. This design was based on the group's previous work on cryogenic trapping of solutes as a means of narrowing the

chromatographic bands before the detector to provide sharper elution profiles in GC [65]. Their first cryogenic trap was constructed from two concentric steel tubes of differing lengths and inside diameters that formed a cavity to which cryogen could be pumped in and out. The analytical GC column was placed within this trap approximately 40 cm from the detector. Liquid CO_2 was pumped through the trap while peaks of interest were eluting. The flow of the cryogen was then shut off, allowing the cooled capillary segment to return to oven temperature, thereby releasing any trapped analytes as focused bands into the detector. It was found that a GC analysis of *n*-alkanes (C_{13} – C_{16}) utilizing this trap produced greater sensitivity and lower detection limits than conventional GC. The main disadvantage was the time required for the capillary to reach temperatures high enough for effective desorption of trapped analytes. Their solution to this problem was to expose the portion of the capillary where components were trapped to the elevated temperatures of the GC oven, allowing for desorption of analytes to occur while trapping continued upstream of the desorbed peak. In this way, the LMCS was born (Figure 1.4) [64]. Modulation with this device was accomplished by moving the cryogenic trap longitudinally along the column towards the detector to trap components (A), or away from the detector to release them (B). The LMCS was applied to GC×GC for the first time in 1998, and the separation of a commercially available kerosene sample was briefly described by Marriott and Kinghorn in a short communication [66]. Little modification from the original design was made and the authors demonstrated that LMCS was a viable alternative to the RTM, if not a superior method of modulation. Some of the benefits highlighted included no need for a separate modulator capillary, the independence of oven temperature and modulator temperature (a major issue with the RTM), and the use of a single column connection. The LMCS proved to be applicable to other GC applications as well [67, 68]. After several years of use, the design of the

LMCS was improved to deal with several operational issues such as trap-column freezing, temperature control, and inconsistent functionality during extended use [69].

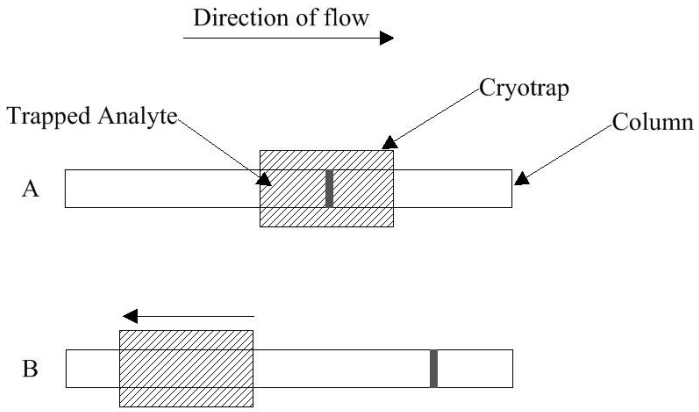

Figure 1.4 Schematic diagram of LMCS, based on reference [64]. Modulation with this device was accomplished by moving the cryogenic trap longitudinally along the column towards the detector to trap components (A) or away from the detector to release them (B).

A high speed, electrically controlled, pneumatic ram that quickly moved the trap away from the cold zone of the column in less than 10-ms was installed. This exposed the cooled portion of the column much faster than in previous LMCS systems and allowed for rapid heating of the column. The trap was modified to include a port for gaseous N_2 and was secured to control guides within the oven to ensure precise movement along the capillary column. The addition of gaseous N_2 helped prevent ice buildup within the trap. It was also reduced in size from 5 cm to 2.8 cm. The overall performance of the system was improved by utilizing a digital timer, controlled by computer software, to direct trap movement and control CO_2 valve operation. The authors studied the effect of this device on solute trapping and injection with great detail, evaluating the distribution of solute within the trap, the speed and time of remobilization of peaks, as well as its applicability to various GC×GC problems. The LMCS was arguably the

biggest innovation in modulation technology since the RTM developed by Phillips. The LMCS was used extensively by the authors, as well as other scientists, to improve the quality of GC×GC separations, thereby bringing attention to this still new and relatively obscure method for separation of complex mixtures [70-72]. It was estimated that by 2004, cryogenic modulators had likely replaced almost all of the thermal desorption modulators in use [73].

Although the LMCS was a significant improvement over thermal modulators, it was only able to cool the trap to a temperature of approximately -50 °C, which was insufficient for trapping many volatile organic compounds (VOCs). It also utilized a series of moving parts, an undesirable feature for long-term, maintenance-free use. Thus, the next stage in the evolution of cryogenic modulators was to utilize more effective cryogens and minimize the use of moving parts. One such device was developed by Ledford in 2000. It utilized two liquid CO_2 cold jets and two hot gas jets [74]. This design was based on Ledford's earlier work using RTM that was cooled between sweeps by a jet of liquid N_2-cooled gas [75]. As analytes exited the primary column, they were trapped in a cold spot created by the first (upstream) cryojet of the modulator. The first stage hot jet and second stage cold jet would then be engaged simultaneously, transferring trapped analytes to the second focusing stage of the modulator. To inject the focused chromatographic bands, the second hot jet was engaged and desorption of trapped analytes occurred. To prevent breakthrough while the second stage was hot, the first cryojet was engaged as injection occurred. Cryogenic modulation would evolve once again with Beens *et al*. developing a system that utilized two liquid CO_2 cryojets for trapping and ambient oven heat for analyte desorption and injection [76]. This was a simplified version of Ledford's four-jet model and proved to be one of the most effective modulators at the time. This design would be modified further by the same group by using a single liquid CO_2 cryojet to accomplish single

stage modulation [77]. As component breakthrough has been recognized as the main issue with single stage modulation systems, the authors evaluated this problem by studying the characteristics of the 2nd dimension peak as a function of the CO_2 valve switching times. Peaks of quality almost identical to the dual-cryojet system were achieved, and the single jet/single stage system was deemed a success [77]. Another interface, developed by Górecki and Harynuk, utilized Silcosteel capillaries contained within a cryochamber, cooled with liquid N_2, to trap and freeze analytes eluting from the primary column [78]. Reinjection was completed by resistively heating the Silcosteel capillaries, in single-stage or dual-stage modes. This modulator was effective in trapping VOCs and provided precise control over injection timing. The main drawback of this system was that liquid N_2 leaks often developed at the capillary entrance and exit locations in the cryochamber. This issue led to cold spots along the trap and as a consequence band broadening occurred.

Ledford *et al.* designed an alternative version of the single cryojet system that exploited a looped capillary to enable dual stage modulation by cooling two segments of the same loop [79]. This system was investigated in detail by Gaines and Frysinger [80] and was also made commercially available [81]. As analytes travelled out of the first column, they would become trapped at the upstream cooled position on the capillary. The cryojet would be shut off and the hot jet engaged, allowing the fraction, along with some breakthrough, to travel through the loop. The cryojet would then be turned back on, allowing further trapping of components arriving from the first column. The same jet would also serve to focus the analytes traveling through the loop that had arrived at the second cooled section. Turning the cryojet off and the hot jet on would allow another fraction to be flushed into the loop, while the focused analytes from the previous modulation would be injected into the second column for further separation.

Further innovation in cryojet modulation technology would come from Hyötyläinen , Kallio and coworkers in the form of rotating cryojet modulation. Their first design included two cryojets aligned on a single liquid CO_2 supply tube that would rotate alternately to spray the modulating capillary, effectively trapping analytes in two separate trapping zones [58]. The two zones were also fitted with a heating wire that could heat the area rapidly. The modulation cycle would proceed with the first cryojet trapping analytes arriving from the primary column. The CO_2 supply tube would rotate to expose the second cryojet to the modulator capillary as the first cryojet was moved away and the first cold stage desorbed by the coiled wire heater. Analytes which were now trapped at the second cooled stage would be desorbed by the second coiled heater as the cryojet moved back to its original position, no longer exposing the capillary to liquid CO_2. Their second design, referred to as the semi-rotating cryogenic modulator, used one rotating CO_2 cryojet instead of two. It also dispensed with the wire heaters, as the authors believed that oven temperature was sufficiently high to release the trapped analytes [82]. Both designs were successful and provided results similar in quality to other cryogenic modulators utilizing liquid CO_2 cryojets. This design has been modified to include a new modulator control program unit, increasing retention time reproducibility. The authors successfully used the modified system to analyze a sample of forest aerosols [83].

Although some great advancement had been made in cryogenic modulation through the use of liquid CO_2 cryojets and intelligent designs, some difficulty was still being experienced with trapping VOCs. The next stage in cryogenic modulation saw the expanded use of liquid N_2 as a means of trapping analytes in the modulation capillary. Górecki and Harynuk developed a cryogenic modulation system, based on the previous work of Ledford [79], which utilized a single cryojet interface with a delay loop for effective dual stage modulation (Figure 1.5) [84].

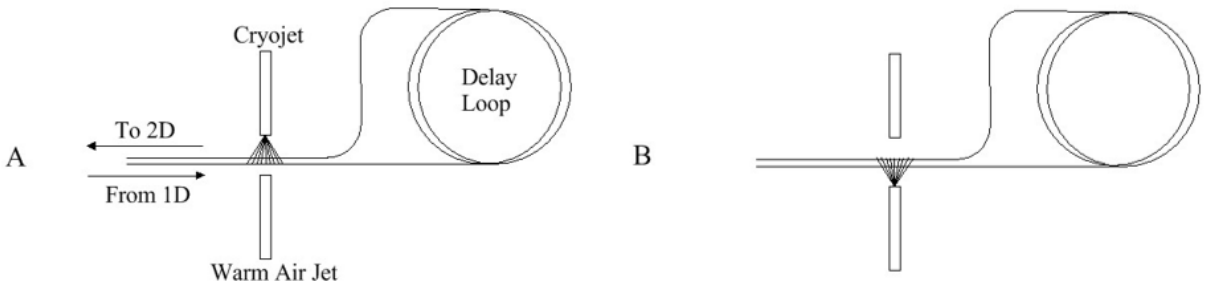

Figure 1.5 Schematic diagram of single jet delay loop modulator, based on references [79]. With the cryojet activated (A) analytes would be trapped and focused until the warm air jet was activacted (B), volatilizing them into the carrier gas and through the delay loop. Analytes would be trapped and released again into the second column after a secondary pass through the cryo/warm air jets (A).

A Dewar filled with liquid N_2 was used to cool in-house pressurized N_2 gas to just below its boiling point. This was done by passing the pressurized N_2 gas first through a heat exchanger and then through a length of coiled copper tubing that was immersed in the liquid N_2 vessel. Once cooled sufficiently, the now near boiling N_2 was directed to a phase separator which prevented gaseous N_2 from entering the cryojets. The liquid N_2 entered a custom-made low volume T-fitting with the cryojet connected to the perpendicular port and an insulated N_2 recycling line connected to the opposite port. A set of solenoid valves worked in alternative fashion to direct the liquid nitrogen either to the cryojet, or back to the Dewar via the recycling line. Trapping (Figure 1.5 A) and launching (Figure 1.5 B) occurred within a deactivated fused silica capillary with alternating hot and cold jets functioning in the same fashion as the previously described cryojet system by Ledford [79]. Effective trapping of a propane sample for one minute was observed with no component breakthrough occurring [84]. A mixture of *n*-alkanes in CS_2 and a commercially available unleaded gasoline sample were analyzed as well with no tailing or

breakthrough occurring [84]. Day-to-day reproducibility was also very good. This system has been used successfully for other analyses as well [85].

Pursch *et al*. designed a similar system that utilized liquid nitrogen directly from the Dewar, a second cryojet, and the beginning segment of the secondary column as the modulator capillary [86]. This system was also successful and provided quality separations of diesel and odour components in polymer coatings, as well as other samples [87]. Liquid N_2 interfaces proved to be the modulator of choice for the analysis of VOCs, as significantly lower trapping temperatures could be achieved with these devices. Although Górecki and Harynuk were able to minimize liquid N_2 consumption to about 30 L/day, the use of this cryogen proved to be expensive, thus the search for a GC×GC interface capable of trapping volatile compounds (C_3 – C_6) without the use of expensive consumables is an important task.

Mostafa and Gorecki designed a single-stage cryogenic modulation system which for the first time demonstrated the ability to trap solvents and ultra-volatile species using a cryogenic system [88]. The authors used a specially designed trapping capillary interfaced between the ^{1}D and ^{2}D columns that featured a plug of glass wool and quarts fiber filter at the center of a 10 cm x 0.32 mm id deactivated fused silica (DFS) capillary. The presence of this glass wool plug served two purposes. The first was to increase the surface area analytes were exposed to as they passed through the trapping capillary without significantly increasing the capillary's thermal mass. This would increase trapping efficiency and reduce the likelihood of breakthrough as the exposure to the cryogenically cooled surface would be increased. The second advantage the plug provided was its impact to carrier gas flow when the trap was at non-trapping temperatures. Due to the increased viscosity of gases at higher temperatures, carrier gas flow through the trapping capillary would be reduced in the period when the trap was being heated or at non-trapping

temperatures. This increased gas viscosity within the plug prevented breakthrough of analytes from the ^{1}D column through the trap in the period in which it was moving from a heated state to a cooled state. Trap cooling was provided by a specially designed liquid nitrogen (LN_2) delivery system that sprayed LN_2 from a jet directly on to the trapping capillary instead of cooling N_2 gas. Heating of the capillary was provided by in-house compressed air that was heated using a resistively heated rope heater wound around the warm air jet coil. It was noted that the LN_2 delivery system used in this study reduced cryogen usage to approximately 30 L/day, a significant decrease from the industry average of approximately 100 L/day. Samples of gasoline and diesel were evaluated with excellent results. The most impressive feature was this modulators trapping capacity and ability to modulate solvents without breakthrough. The authors demonstrated this by modulating CS_2, a accomplishment yet to be achieved by any commercially available cryogenic modulation system. Several cryogenic modulators are commercially available today through various instrument manufacturers.

Trapping in the modulator capillary assisted by compressed or cooled air has also been explored. A single-stage modulator was brought forward by Libardoni *et al.* which utilized a resistively heated stainless steel trapping capillary, with cooling assisted by a continuous flow of cold air [89]. An aluminum block was fashioned to accommodate the trapping capillary, as well as entry and exit points for the cold air. A two-stage refrigeration unit served to cool a heat exchanger in which air was circulated at a rate of 35 L/min. This air would move from the heat exchanger, at a temperature of -45° C, into the aluminum block, and cool the modulator to a temperature between -32° C and -20° C, depending on the status of the chromatographic analysis. The modulator was used to successfully analyze a sample of gasoline and a 40-component test mixture spanning a range of volatilities [89]. However, component breakthrough

was recognized for more volatile compounds. The authors attributed this to a relatively high trapping temperature compared to cryogenic devices, as well as a slow modulator cooling rate. This allowed components to evade trapping, and escape into the second column in the time immediately after the electrical pulse had been delivered and before the trap had fully cooled. The device was later modified to use circulating ethylene glycol in place of cooled air [90].The design was altered once again in later years to become a dual-stage modulator with circulated air cooling [91].

Jover *et al*. created an interface that employed two compressed air jets to trap analytes in a segment of the secondary column, and ambient oven heat for reinjection [92]. Pizzuti *et al.* developed a very similar system with a more robust construction [93]. Both designs were successful in producing good separations of lipids and pesticide residues. The downside to these instruments was their incapacity to trap alkanes below *n*-C_{14}.

Forced air cooling has also been successfully used recently in a modulator designed by our group for the purpose of in-situ analysis of the semi-volatile fraction of organic aerosols [94]. The device featured a uniquely flattened deactivated stainless-steel capillary coated internally with PDMS at two individual trapping sections measuring 3 cm in length. The 15 cm capillary was looped outside the oven and exposed to a cooling blower or a Vortex cooler, depending on the application. Two-stage thermal desorption of components trapped within the flattened capillary was accomplished using a custom-built capacitive discharge power supply. This modulator was successfully used in the thermal desorption aerosol comprehensive two-dimensional gas chromatography-mass spectrometry system (2D-TAG) developed by Goldstein *et al.* [95].

Additional advancements in thermal modulation technology have come in the form of miniaturising the device. Kim *et al*. reported the micro-fabrication of a dual-stage, thermoelectrically cooled modulator for use in µGC×µGC [96]. The authors utilized a boron doping process to create micro-channels in an oxide layer that was thermally grown on a wafer. A more detailed description of the fabrication process can be found in the article. These micro-channels were coated with PDMS and measured 4.2 cm and 2.8 cm in length for the first and second stages, respectively. Inside dimensions were 250 µm × 140 µm with a wall thickness of 30 µm. The heating of each stage was completed by providing voltage to micro heaters attached to the top portion of the micro-channels. Rapid cooling was accomplished by a thermoelectric cooler (TEC) secured to the bottom of the two stages. As analytes arrived at the first stage, they would become trapped in the first cooled micro-channel. The micro-heater would be engaged briefly to allow transfer of the analytes to the second cold trapping stage, where further focusing would occur. Once the first stage had sufficiently cooled, the second stage would be heated and the analytes injected as a focused band to the second column. The TEC would remain operational throughout the whole analysis to prevent breakthrough while desorption of the analytes occurred. The authors could operate the modulator within the range of -30 to 250 °C and effectively trap less volatile VOCs. This novel technique represented a move towards chip based GC×GC interfaces and showcased reasonable VOC trapping capabilities at relatively low temperatures without the use of expensive consumables [96-101].

Moving forward to 2016, a new consumable-free modulation system was described that borrowed a page from the past and shared some design characteristics with the LMCS introduced by Marriott and colleagues in 2002. The device was referred to as the thermal independent modulator (TIM) and featured a ‘modulation column’ that interfaced between the first and

second dimension separation columns. To facilitate trapping of analytes from the first column, a TEC device was staged in between two entry and exit heating zones. The modulation column would physically move in to and out of these hot and cold zones, periodically trapping and releasing analytes from the modulation column in to the second dimension column. The first iteration of the system featured a porous layer open tubular (PLOT) column as the modulation column to help trap volatile species that were difficult to retain. The system was first described by Luong and coworkers [102]. In this publication, the authors noted that injection bands produced by the device were wider than those produced by commercially available modulators of the time. This was attributed to the use of 0.25 mm id fused silica for the modulation column which produced a larger volume of vapour when analytes were mobilized into the second dimension relative to other modulators which used narrower column widths for modulation. Further, an additional length of capillary column in the exit hot zone facilitated band broadening before the analytes could reach the stationary phase of the ^{2}D column. Although injection peak widths were noted to be unconventionally wide, good separations of hydrocarbon standards and a winter diesel were achieved. Retention time standard deviations (RSD) were observed to be of acceptable levels at 0.009 % in the ^{1}D and 0.008 % in the ^{2}D. Peak area RSD was reported to be under 5 % for a series of aromatic species analyzed. The ultimate limitation of this device was the limited volatility range of the modulation column. PLOT columns are useful for trapping VOCs, but performance suffers for less volatile compounds as they are too strongly retained and require more heating events to be effectively mobilized into the second column. Alternatively, wall coated open tubular (WCOT) columns offered good performance for trapping semi-volatile organic compounds (SVOC) but were ineffective at trapping VOCs. The impact of modulation column internal coating thickness and internal diameter has recently been evaluated by Giocastro

and co-workers [103]. Although the device offers a limited effective range of volatility, it has been successfully applied to the study of bitumen samples [104], organic aerosols [105], VOCs [106], and monoterpenes in various citrus species leaf oils [107]. The modulator has also been commercialized under the name Solid State Modulator (SSM) by J&X Technologies (Shanghai, China).

The last contribution in this chapter describes a system that was inspired by the chip based thermal modulation systems described herein and the consumable-free thermal modulator system described in subsequent chapters. Coined as the thermal desorption modulator (TDM), this do-it-yourself design was proposed to address the perceived complication and cost of other consumable-free thermal modulation systems [108]. The design interfaced 1 m of MXT-5 0.25 mm id, 0.50 µm d_f metallic column between the ^{1}D and ^{2}D columns. The first and last 20 cm of this metallic column served as the first and second modulation stages, while the 60 cm central portion served as the modulation loop. Electrical connections at both ends of the 20 cm segments allowed current to be passed along these sections, facilitating rapid resistive heating and subsequent volatilization of analytes from the sorbent contained in these sections. Metallic columns of wider bore were initially tested but rejected due to their larger thermal mass and therefore longer required cooling periods before the next modulation event. Once thermally desorbed from the first modulation stage through a 355 to 500 ms heating pulse, analytes travelled along the 60 cm modulation loop until they encountered the second 20 cm modulation stage. Additional desorption events volatilized the analytes absorbed within the second stage into the carrier gas and along to the secondary column. The entire apparatus was contained within the GC oven and was kept at oven temperature by circulating oven air. The authors experimented with various lengths of modulation stages and modulation loops before determining that 20 cm

for the trapping stage and 60 cm for the modulation loop offered the best performance. The authors demonstrated the modulator's capability with separations of hop oils and petroleum distillate blends and reported run to run peak retention time reproducibility under 5 %. Although a novel proof of concept and certainly more cost effective than a commercially available system, this modulator provided poor chromatographic performance.

Thus far the GC×GC modulation devices described herein have used temperature differentials to trap and inject primary column effluent components into the secondary column. During the period when Phillips was evaluating the RTM, a new style of modulator exploiting valve-based technology and pressure differentials was being developed that would eventually expand into its own category of modulation interfaces that today come very close to matching the sensitivity and separation ability of their thermally modulating cousins [109].

1.2.3 Valve and Flow Differential Based Modulation Systems

Unlike thermal modulators which trap effluent from the primary column using temperature differentials, valve-based systems utilize pneumatic means to accomplish modulation of the primary column effluent. There is one exception which utilizes both cryogens and valves to modulate chromatographic peaks.

The diaphragm valve modulator (DVM) was the first valve-based interface to be successfully applied to GC×GC (Figure 1.6 A). Bruckner *et al.* first described their design in 1998 and suggested it may be used in place of thermal modulation, especially in the analysis of VOCs [110]. The system utilized a wide bore, PDMS-coated primary column and a narrow bore, polyethylene glycol-coated secondary column. A six-port diaphragm valve with low dead volume fittings, was interfaced between the two columns within the oven. Actuation of the valve

was completed with nitrogen gas controlled by a three-port normally closed solenoid valve. The nitrogen delivery system was modified to include a 1-L pressurized reservoir and large diameter gas lines connected to the solenoid valve to ensure no drop in pressure would be experienced during actuation. Makeup helium was provided to the diaphragm valve, as was a vent line. Overall, four of the 6 ports were used. The flows of helium and the vented effluent were controlled using a low-flow controller and fine metering valve, respectively. Gas flow was split between the second column and a 0.5-m length of fused silica capillary column to decrease the flow rate in the second dimension. The excess carrier gas was vented to the atmosphere. The diaphragm valve was actuated twice per second for a very short time, allowing a small portion of the first column effluent to enter the second column (Figure 1.6 A). As separation was occurring in the second dimension, all effluent from the first dimension would be vented to the atmosphere (Figure 1.6 B). Bruckner used the system to successfully analyze a sample of white gas (camping fuel) spiked with toluene, ethylbenzene, m-xylene, propylbenzene and o-xylene [110]. Good repeatability between GC×GC runs was observed, but modulator performance was not studied in great detail. The same system was also used to analyze aromatic isomers in jet fuel [111], as well as aromatics in naphtha [112]. Although rapid actuation allowed very narrow peaks of effluent to enter the second column, only about 10 % of the primary column effluent was sampled and reinjected, leading to significant analyte mass loss and the inapplicability of this system to trace analysis. Another issue was derived from the thermal limitations of the diaphragm valve. The valve could only be operated up to a maximum temperature of 175 °C, restricting analysis to VOCs, thereby limiting this system's applicability. Flow disturbances during valve actuation were also seen as a potential detriment to the system.

Seeley *et al*. first introduced differential flow modulation (DFM) in 2000 [113]. The design and function were based upon the recently invented DVM by Bruckner [110]. Unsatisfied with poor sample transfer between the first and the second columns, Seeley devised an interface capable of transferring significantly more of the primary column effluent into the second column. The design utilized a 6-port diaphragm valve with a similar configuration as the aforementioned authors, but featured the addition of a sample loop, thus making use of all six valve ports. The interface was kept outside of the oven and its temperature was maintained at 125 °C by block heaters. Effluent was transferred into and out of the interface by deactivated fused silica capillaries that were connected to the primary and secondary columns with fused silica unions. The modulator had two main stages: collection and injection. During the collection stage, effluent from the primary column entered the valve and was directed to a deactivated stainless steel sample loop measuring 10 cm long by 0.51 mm id. Effluent would be collected in this loop and be vented to the atmosphere once maximum volume had been exceeded. During the inject stage, the valve would be actuated, allowing a secondary flow of carrier gas to enter the sample loop and effectively sweep away the collected fraction into the secondary column. The flow rate in the secondary column was 20 times higher than in the primary column in order to produce compressed injection bands and allow fast separation. For a 1 s modulation cycle, the collection stage would last 0.8 s, and the injection stage 0.2 s.

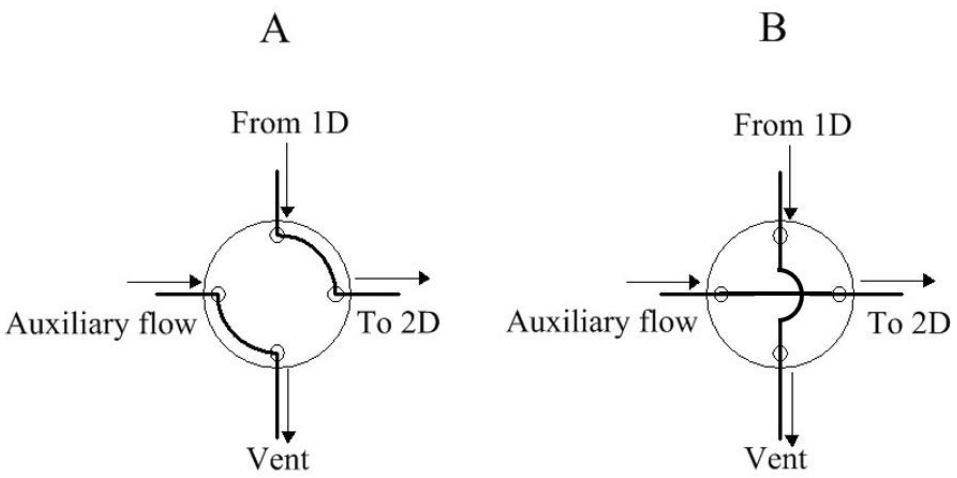

Figure 1.6 A general scheme of Bruckner's diaphragm valve modulator (DVM) based on reference [110]. During phase (A), effluent from the first-dimension column is directed to the second-dimension column. Auxiliary gas is vented to the atmosphere. During phase (B), first-dimension effluent is vented to the atmosphere as the auxiliary flow is directed to the second dimension column.

This improved version of Bruckner's DVM increased transfer efficiency of the effluent to the second column from ~10 % to ~80 %. The system proved to be robust but was still restricted by the maximum operating temperature of the diaphragm valve [114]. High flow rates in the second column also eliminated the possibility of using micro-bore columns, as very high head pressures would be required [115]. Recognizing the temperature limitations of the diaphragm valve design, steps were taken to increase its functionality at higher temperatures. Synovec *et al*. established that the valve temperature limitations were due to polymeric o-rings contained within the valve. Their solution was to mount the valve in such a way as to keep the o-rings outside of the oven, while the diaphragm and sample loop were kept inside [116, 117]. With the oven programmed to 250 °C, the sample loop was found to reach 247 °C, while the portion of the valve containing the o-rings maintained a temperature of ~80 °C. With the diaphragm valve components exposed to

effluent now capable of reaching higher temperatures, the range of compounds this interface could effectively modulate had increased to include semi-volatiles [116].

Although differential flow modulators had been improved, valve-based interfaces were still inapplicable to the analysis of complex samples containing higher boiling point compounds (> ~200 °C). These limitations would not plague those in the field for much longer, as Seeley was developing a novel system that would see the removal of the diaphragm valve from the flow path. Seeley *et al*. devised a flow-switching system that featured no valves within the GC×GC oven and used materials capable of handling a much wider range of temperatures than the problematic valve [118] (Figure 1.7). Attached to the exit of the primary column was a T-union (T1) that allowed carrier gas to travel either left or right through deactivated fused silica tubing to two additional T-unions (T2, T3). T2 and T3 were both connected to an auxiliary gas supply at their top port, and to a sample loop at their bottom port. All connections between unions were made with deactivated fused silica tubing. The auxiliary gas supply was controlled by a three-port solenoid valve (SV) capable of directing gas flow to either T2 or T3. Both sample loops were connected at the bottom of the apparatus with another T-union (T5), whose bottom outlet was connected to the secondary column. Effluent from the primary column would be directed to either the fill or flush sample loop, depending on the direction of the auxiliary flow. This would allow one sample loop to fill with the effluent, while the other was flushed with auxiliary gas. As the sample loop reached its effluent capacity, the solenoid valve would be activated, switching flow to the opposite side of the interface, allowing the auxiliary gas to inject the contents of the recently filled sample loop into the secondary column, while the now flushed sample loop functioned as an effluent collector. The auxiliary gas flow valve would be switched at regular intervals to achieve consistent modulation throughout the chromatographic run. Differential flow

was also featured in this design, with the ratio between the primary and secondary column flows ranging between 25 and 30, depending of the analysis. The authors successfully used the flow-switching system to analyze a mixture of VOCs, diesel fuel, and aromatics in gasoline [118, 119]. Narrow injection bands were observed throughout the chromatographic run. Placement of the switching valve outside of the oven and all components in contact with the effluent within the oven allowed this interface to expand the range of analytes to include less volatile species. Another advantage of this interface was the removal of a primary column effluent vent.

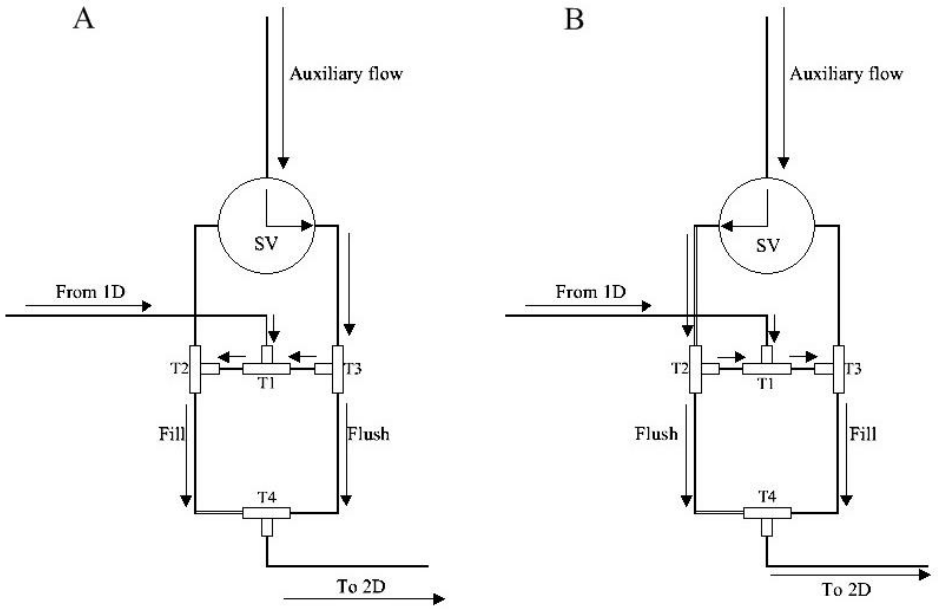

Figure 1.7 Schematic diagram of the flow switching modulator based on reference [121]. During phase A, the capillary attached to T2 is filled with first dimension effluent, while the contents of the capillary attached to T3 is flushed to the 2nd dimension column. In phase B, auxiliary flow is switched by the solenoid valve (SV) and the recently filled capillary is flushed into the second dimension, allowing the alternate capillary to fill with the 1st dimension eluate. Arrows indicate direction of gas flow.

This ensured 100 % mass transfer from the first column to the second column, a significant improvement from the ~10 % to ~80 % mass transfer of the previously introduced valve-based modulators [110, 120]. The disadvantages of this system were mainly derived from its inflexibility [121]. Balancing gas flow rate with sample loop volume and modulation timing was a careful operation. If any single parameter was altered, the whole pneumatic system would have to be re-evaluated and re-optimized, a rather tedious exercise. Modulation periods were also limited to around 2 s, thereby forcing separations in the second dimension to be very fast and perhaps not as effective as longer second dimension separations.

The next innovation in flow modulation would see the improvement of both the first and second dimension separations through employing an interface that combined valve-based techniques in combination with cryogens. To preserve the first dimension separation, multiple samples of the primary column effluent should be taken and injected into the secondary column. As previously mentioned, each fraction eluting from the primary column should be sampled at least three or four times [33]. With the need to sample the primary column so often, short modulation periods are often required, therefore fast and sometimes less resolved separations in the second dimension can occur. The concept of stop-flow modulation was first introduced by Harynuk and Górecki in attempt to remedy this well-known compromise between first dimension resolution and second dimension separation time [122]. The authors designed a system whereby flow in the first dimension could be stopped to allow the separation of primary column effluent in the second dimension to progress to completion (Figure 1.8). The design utilized an air actuated, high temperature, low dead-volume 6-port valve capable of withstanding up to 300 °C. Three of the 6 ports were blocked. Connected to one port was the primary analytical column. Connected to a second port was a second column with the same pneumatic resistance as the

primary column. This bypass column was connected to the primary gas supply using a Swagelok T union at a location just before the injector. This was done to make certain that equivalent gas pressure was supplied to the inlet of both columns, and to prevent accidental transfer of sample components into the bypass column. Connected to the third port was a section of deactivated fused silica tubing which was connected to the second analytical column. The segment of deactivated fused silica tubing served as a trapping capillary when cooled with a previously described liquid nitrogen cryojet interface [123]. After injection, the sample would make its way through the primary column, becoming separated. As the first components began to elute, the valve was in the sample position, and the eluate migrated through the valve to the deactivated silica capillary where it was trapped and focused by the liquid N_2 cryojet. After a predetermined trapping time had passed, the valve was actuated and moved into the stop position, while the cryojet was halted and the warm jet was activated. With the valve in the stop position, no carrier gas flowed in the primary column. Carrier gas was now delivered instead through the bypass column, into the valve, and through the deactivated fused silica capillary, flushing the focused analytes into the secondary analytical column. Once separation was complete in the second dimension, the cryojet was engaged and the valve actuated. The primary column separation resumed once again, as did trapping of the effluent in the cryojet interface. Periodic stopping of the flow in the primary analytical column allowed each second dimension separation to proceed independently of the length of the trapping stage (which determines the P_M in standard modulators), permitting the adjustment of individual parameters, such as column length and stationary phase, to create optimal separation conditions. This interface was compared to conventional GC×GC systems and proved to be superior by providing better resolution for early eluting peaks. It also allowed the use of long, efficient secondary dimension columns (up to 6 m

x 0.15 mm id), and consequently an increase the separation power of the system (albeit at the expense of longer separation time). Wrap around peaks were also eliminated, as enough time was permitted for a full separation on the secondary column to occur [124].

The design was altered in later years with the removal of the 6-port valve from the effluent path, and the inclusion of a pneumatic system to stop the flow in the first column [125]. A diesel fuel sample was successfully analyzed using this method and the authors also saw better overall performance. The main disadvantages of stop-flow GC×GC are its somewhat complicated setup and long analysis times.

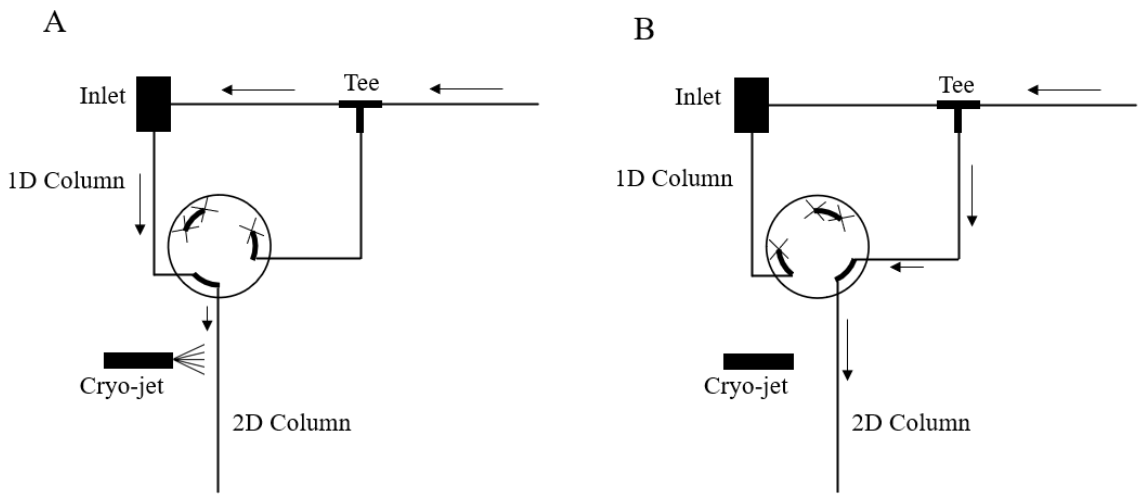

Figure 1.8 Schematic diagram of the stop flow modulator based on reference [122]. During sample phase A, one dimensional eluate proceeds along the ^{1}D column, through the 6-port solenoid valve. A piece of fused silica connects the valve and ^{2}D column where the cryo-jet focuses peaks exiting the ^{1}D column. During stop-flow phase B, the valve is actuated and flow from the ^{1}D column is stopped due the terminus of the ^{1}D column now being a blocked port of the valve. Flow now proceeds through the tee and onwards towards the secondary column. The cryo-jet is off in phase B allowing the mobilization of the analytes along the ^{2}D column for further separation while the ^{1}D column flow remains stopped. The X markers indicate a plugged valve port.

Seeley would later introduce an alternative form of the flow switching modulator called the simple fluidic modulator [126]. This interface featured the primary and secondary columns connected with two T-unions, and a deactivated fused silica capillary in between. An auxiliary gas flow of 20 ml/min was introduced to the remaining port of the T-unions. Control of the auxiliary flow was accomplished by a three-port solenoid valve. A short segment of deactivated fused silica tubing was used to join the solenoid valve and the primary column, while the secondary column was joined with a long segment. The modulator operated in two stages, fill and flush. During the fill stage, effluent from the primary column would enter the sample loop for a desired time, while auxiliary gas flow moved through the secondary column T-union and into the second dimension. The second stage began when the solenoid valve was actuated, forcing auxiliary gas flow in the opposite direction through the primary column T-union. The significantly higher flow rate of the auxiliary gas temporarily stopped the flow of effluent from the primary column, and quickly flushed the sample loop into the second dimension. Each stage would alternate to effectively sample first dimension peaks. Seeley used this modulator to analyze a sample of gasoline and obtained results of the same quality as those achieved by the previously described flow-switching interfaces [126]. This modulator can be seen in Figure 1.9. Seeley's design would be commercialized in 2006 by Agilent Technologies using their Capillary Flow Technology (CFT), which is based on a monolithically constructed manifold with integrated microfluidic channels [127]. In later years, this method would be investigated and modified further by Amirav *et al*. to become what is now known as the pulsed flow modulator [128, 129].

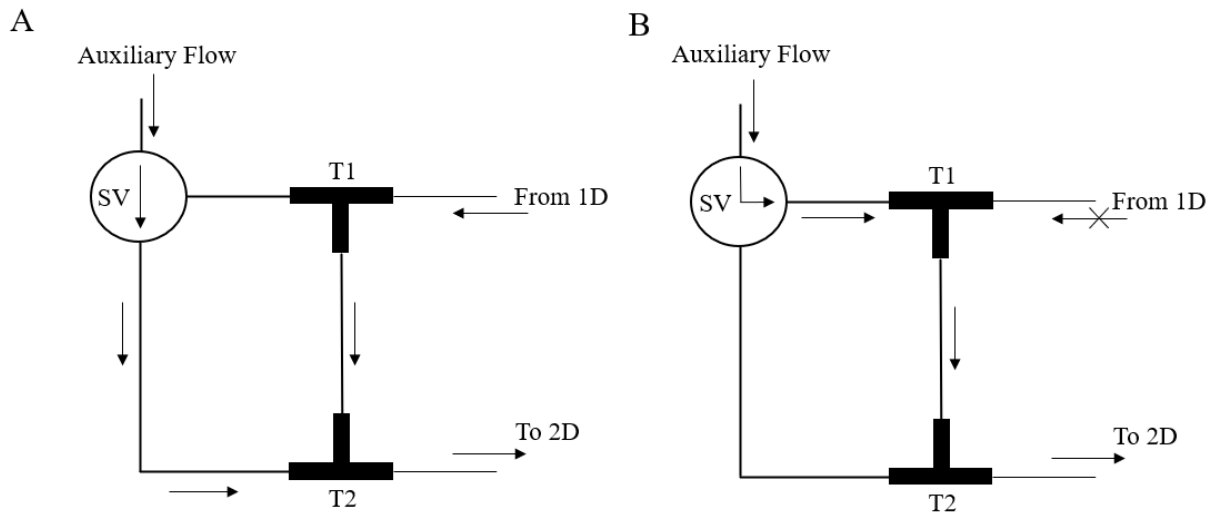

Figure 1.9 Schematic diagram of the simple fluidic modulator based on reference [126]. During fill phase A, the sample loop interfaced between T1 and T2 was filled with first dimension effluent, while the auxiliary flow was directed to T2 onwards to the secondary column. In flush phase B, auxiliary flow was redirected via the solenoid valve (SV) to T1, which quickly flushed the contents of the sample loop onto the head of the secondary column. The system quickly reverted back to fill phase A, which allowed the sample loop to refill while the eluate injected into the ^{2}D column became separated prior to detection. Arrows indicate direction of gas flow.

Seeley *et al*. once again introduced an alternative approach to modulation featuring a microfluidic Deans switch [130]. Their design resembled previously described differential flow modulators with a few modifications. The switch was designed to include Agilent's CFT plates with five ports and a three-way solenoid valve. Two ports of the CFT manifold were connected to the three-way solenoid valve, which directed the flow of auxiliary gas to one of the two ports. One of these two ports was connected with a T-union to the 2nd column and the 1st column, while the other port was connected to a flow restricting column and the primary column. Primary column flow was split with a T-section that was connected to both of the previously described unions.

The CFT manifold portion of the switch remained in the oven, while the solenoid was kept outside. The Deans switch operated in two stages, bypass and inject [130]. The bypass stage involved the solenoid directing an auxiliary flow of gas in such a way that effluent from the primary column was directed away from the secondary column and towards the flow restricting column. No separation occurred on this column, as it was made of deactivated fused silica and functioned only to maintain gas pressure within the system and to vent non-sampled effluent. During the inject stage, the direction of auxiliary gas flow was reversed, and primary column effluent was directed towards the secondary analytical column. The switch remained in the inject state for only 5-10 % of the P_M, thereby producing sharp injection bands into the 2^{nd} column. The Deans switch permitted a greater range of oven temperatures to be used, extending its use to semi-volatile compounds. The greatest disadvantage of the Deans switch modulator, similarly to that of the first diaphragm valve interface, was that only a small portion of the primary column effluent was directed to the secondary analytical column, greatly reducing sensitivity. Consequently, this interface is not suitable for trace analysis.

An additional development in valve-based modulation was introduced by Wang. It utilized two four-port, two-position switching valves that were actuated electronically [131]. The interface operated in two stages, referred to as X and Y by the author (Figure 1.10). In stage X, effluent from the primary column entered the first valve (V1) and traveled down a transfer line to the second valve (V2). Effluent would be vented to the atmosphere if the transfer line volume was exceeded. During this stage, auxiliary gas flow entered the second valve (V2) and swept through the opposite transfer line, flushing it into the secondary column. The Y-stage began when the valves were actuated into their second position. First dimension eluate that had filled the transfer line was now flushed into the secondary column by the auxiliary gas flow. Eluate

leaving the primary column would now fill the opposite transfer line, with excess being vented once maximum volume was exceeded. The valves (V1, V2) were actuated between these two stages to achieve modulation. Wang tested this device by analyzing samples of naptha, diesel, fatty acid methyl esters and PCBs [131]. According to the author, performance equivalent to thermal modulators was observed. Complete transfer of the effluent from the primary column to the secondary column was accomplished. The valves used were capable of withstanding temperatures of up to 350 °C, allowing for a wider range of analyses to be performed with this device. Wang utilized high flow rates and a wide bore column for second dimension separation, an attractive feature as a greater variety of stationary phase coatings are available for use in this type of column [132]. Swapping the two four-port, two position valves used in the study for one twelve-port, two position valve or one eight-port, two position valve was described as a simple alternative. Wang's differential flow modulator helped expand the range of analyses performed by valve-based modulation.

Mondello and coworkers explored a low-pressure flow modulation setup based on Seeley's earlier work [126, 133-136] . The modulator utilized a high volume external sampling loop and a wide bore secondary column. This flow modulation setup had greatly reduced flows in the secondary column allowing MS to be paired with the device. The authors also reported no loss in sensitivity relative to other flow modulators since splitting of the secondary column effluent was not necessary. However, the lower ^{2}D flows combined with wide bore columns reduced the separation capacity of the second dimension significantly relative to thermal modulation devices.

Lewis and coworkers explored their own version of the flow modulator based on Synovec's earlier designs that utilized a flexible sample loop and a 6-port, two-position

diaphragm valve [137-139]. Although the diaphragm valve limited the operating temperature of the GC×GC system, the modulator was shown to be a low cost, effective solution for the analysis of volatile samples. Moving forward to 2012, a group of scientists from the Dow Chemical Company in the United States, Canada and the Netherlands advanced Seeley's differential flow design. Led by J. Griffith, the reversed-flow differential flow modulator, or the reversed fill-flush (RFF) modulator, was developed to alleviate some of the more challenging operational aspects of the column connection system used to recreate Seeley's original design in an industrial setting [140]. Creating leak free and low dead-volume column connections with Valco Tees was not trivial and would often impact the performance of the device should they not be precisely set by the operator. Again utilizing Agilent's CFT microfluidic plate system, the authors were able to devise a system of channels and connections that was leak free and minimized dead volumes throughout. In Seeley's original design, the authors point out that analytes are flushed out of the collection channel in to the primary column in the same direction they are collected. During this flush state, primary column eluate continues to elute into the collection channel and those analytes eluting late in the cycle can enter the secondary column more slowly causing tailing peaks. By reversing the flow direction during the flush phase, the collection channel can be fully evacuated with a plug of analyte-free auxiliary carrier gas separating subsequent injection bands. This reduces tailing and allows for a complete return to baseline even for highly concentrated peaks. The modulator was built using a three port CFT purged splitter and a three port CFT unpurged splitter. On the purged three port plate, port one received the primary column, port two interfaced a collection loop of stainless steel capillary column to the unpurged three port plate, and port three connected the secondary column.

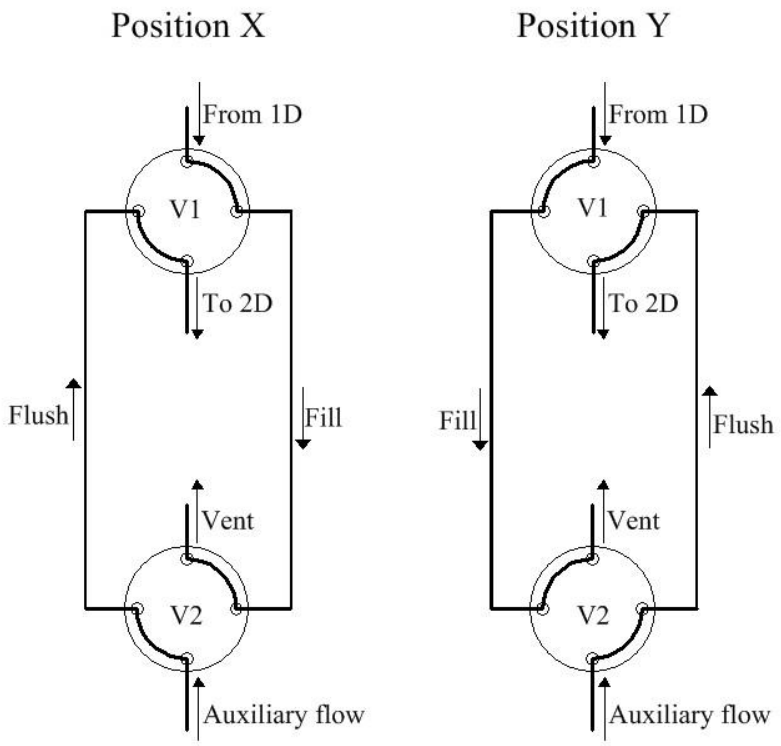

Figure 1.10 A general scheme of Wang's differential flow modulator based on reference [131]. Valves V1 and V2 would be actuated at the same time to either fill or flush the transfer lines into the ^{2}D column.

The purged line provided auxiliary flow from a secondary flow source directed by a three-way solenoid valve in the normally on or 'fill' position. On the unpurged three port plate, port one received the end of the steel collection loop, port two was connected to the auxiliary flow line connected to the valves normally closed position, and finally the third port included a bleed line that served as a flow restrictor (Figure 1.11). This modulator had two modes of operation, fill and flush. In fill mode, eluate from the primary column would enter the purged CFT plate. It would be directed to the collection loop, over to the unpurged CFT plate and out the bleed line, which was usually some length of 0.100 mm id deactivated fused silica. This bleed line could be connected to a monitoring detector such as a flame ionization detector (FID). Auxiliary flow

provided by a pneumatic control module (PCM) would be diverted through the normally open port of the solenoid valve to deliver flow to the secondary column. Proper balancing of the flow differentials between the primary column flow rate and the secondary column flow via the PCM was necessary to ensure analytes did not break through the internally etched channel connecting the primary and secondary columns. When optimized correctly, analytes would proceed from the primary column to the collection loop as auxiliary flow passed into the secondary column without interference. In the flush mode, the solenoid valve would be actuated and direct auxiliary flow for between 50 and 500 ms through the normally-closed port of the three-way valve. The flow would be split in the unpurged three-way splitter between the narrow bore bleed line and the wide bore collection loop. The flow of gas through the collection loop in flush mode was in the reverse direction of the fill mode, hence the term reverse fill-flush modulator. After the flushing step was complete, the auxiliary flow returned to the normally-open port of the three-way valve, and the content of the collection loop which was injected onto the head of the secondary column began to transit the secondary column. There are some unique features of this modulator that merit description. The bleed line length and diameter are critical to the successful operation of this device. The bleed line must provide enough impedance to the CFT splitter to force the flushing gas through the collection loop and onto the head of the secondary column. If the impedance of the bleed line is too low, flushing gas would naturally divert through the bleed line and provide ineffective flushing of the collection loop. If the impedance of the bleed line is too high, it creates pressure problems for the primary column flow source, the inlet of the GC, by requiring high column head pressures which can be unsustainable at hot GC oven temperatures. Collection loop volume is another important factor to consider. To ensure complete transfer of

the analytes from the primary column to the secondary column, the loop should be flushed before it fills to capacity.

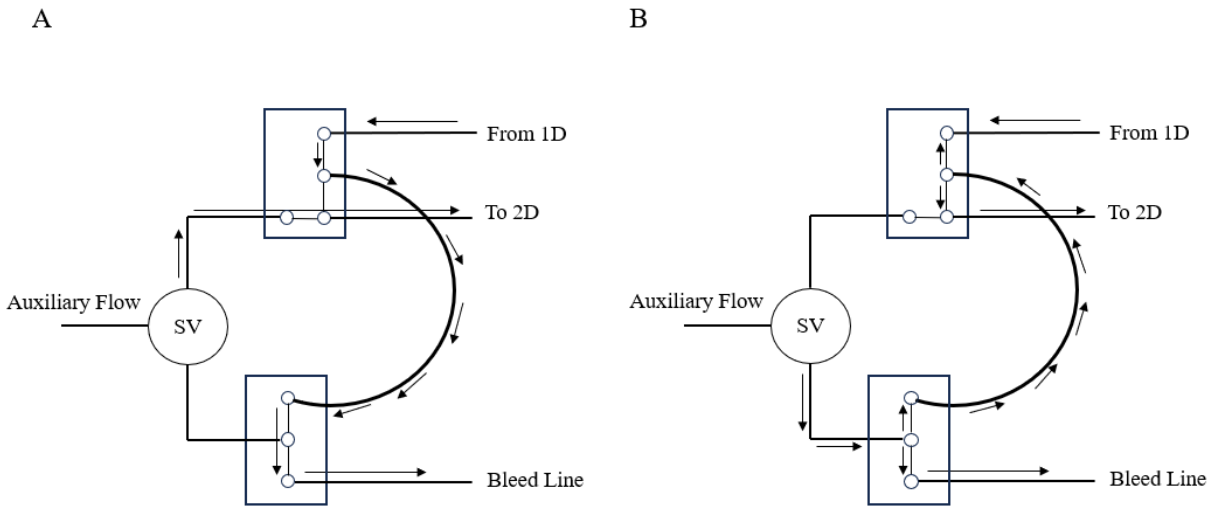

Figure 1.11 The RFF modulator developed by Griffiths and co-workers [140]. In fill mode A, ^{1}D column effluent enters the first CFT plate, transits through the collection loop to the second CFT plate and exits out the bleed line if no valve actuation occurs. Auxiliary gas flows through the first CFT plate and provides a separate source of ^{2}D carrier gas. In flush mode B, the solenoid valve is actuated and auxiliary carrier gas is sent to the second CFT plate where the majority of flow is diverted through the collection loop, sending its contents towards the head of the ^{2}D column. Pressure from the ^{1}D column impedes the flow of collection loop contents into the ^{1}D column forcing their diversion to the lower impedance ^{2}D column. This step happens for 100 ms to 500 ms depending on the loop volume before returning to fill stage A.

This means the P_M used in a complete transfer system, where all ^{1}D eluate is transferred to the ^{2}D column, is a function of primary column flow rate and collection loop volume. Furthermore, the width of the injection band loaded onto the second column during the modulation is impacted by the rate at which it is flushed, related to the secondary column flow rate. Ideally, the secondary column separation is complete or nearly complete before the next band is introduced. The relationship between ^{1}D flow, ^{2}D flow, collection loop volume and bleed line impedance must be

considered and optimized for this RFF modulator to work correctly. The ratio of flows between the ^{1}D and ^{2}D columns is also important to maximize the resolution on both columns. A particularly impactful feature of this device is the ability to modulate the solvent peak, which greatly improves the quality of chromatography for samples including large volumes of solvent or peaks that elute near the solvent peak. Overall improvements in peak shape, breakthrough reduction and system flexibility were achieved with this design relative to previous flow modulation systems.

The RFF modulation design by Griffith *et al*. would prove impactful for the expanded use of flow modulation, as commercial versions of the device became available approximately 5 years after their publication. Agilent released their own RFF design which operated in fundamentally the same way as the Griffith's design, with the exception that the collection loop, which was an externally connected segment of 0.53 mm id stainless steel capillary in the original RFF design, was now etched within a single CFT plate offering an internal collection channel for ^{1}D column effluent [141]. All necessary connections for auxiliary flows, ^{1}D, ^{2}D and bleed line were also included on this single CFT plate. Krupčík *et al.* compared their take on Griffith's RFF design to Agilent's FFF unit. They concluded that performance was similar when evaluating mixtures with low or equal concentrations of analytes like petroleum mixtures, but the RFF system outperformed the FFF system when evaluating mixtures with wide concentration ranges of analytes such as essential oils. Giardina *et al.* would later expand on the design by developing a pneumatic model to describe how the Agilent RFF modulator operated and could be optimized [142]. One key difference between the Griffith's design and the Agilent RFF is the collection loop being etched internally within the CFT plate, which restricts the P_M the analyst can practically use during their experiments. Since P_M in these RFF systems is related to ^{1}D flow rate

and collection channel volume, extended modulation periods of 4 seconds or greater would only be possible with very low ^{1}D flow rates. This can be problematic if the ^{1}D column is operated at a lower than ideal linear velocity, sacrificing ^{1}D resolution and therefore overall resolution. The analyst may decide to use a narrow bore column which can be operated at optimal linear velocity at lower flow rates; however, the trade-off is high head pressure at the ^{1}D inlet and lower sample loading capacity compared to a conventional 30 m x 0.25 mm id x 0.25 mm d_f analytical column. Whereas the designs of the Agilent RFF and Griffith's modulator are similar, the Griffith's design offers greater method development design flexibility to the analyst. The Agilent RFF design has been used for a wide variety of applications, recently including alcoholic beverage [143, 144] and fingerprint residue analysis [145].

A different RFF modulator was made available around the same time from SepSolve Analytical and was named the INSIGHT modulator [146]. Similar to the RFF modulator released by Agilent, this device was based on the Griffith's design, but offered some unique features. The modulator itself was designed on a single microfluidic plate, allowing all connections for auxiliary gasses and columns to be made on a single microfluidic unit. Similar to the Griffith's device, the INSIGHT modulator supported an external collection loop made from 0.53 mm id stainless steel capillary, which the analyst could shorten or lengthen to suit the desired modulation period, column flow rates and application at hand. A schematic of the device is shown in Figure 1.12. Since its release, the INSIGHT modulator has found commercial success globally and has been used in applications such as breath analysis [147], organic pollutants in electronic waste dust [148] and the aroma profiles of beer [149].

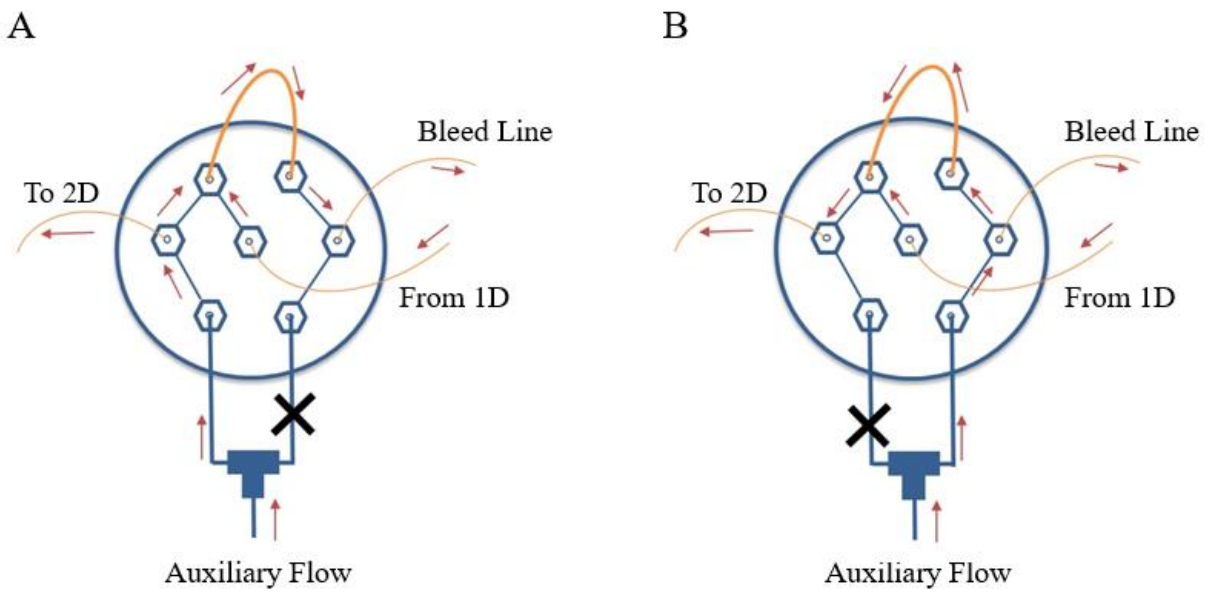

Figure 1.12 The INSIGHT modulator developed by SepSolve (based on reference [149]). The operational principle is fundamentally the same as that of the Griffith's modulator [143], except that all connections are made on a single microfluidic chip.

The most recent flow modulator to be made commercially available is the FLUX diverting flow modulator from LECO Corporation [150]. This design is based on the work of the Seeley group referred to as the multi-mode modulator (MMM) [151].This simple modulator is built using a four-way cross fitting connected to a tee through a section of tubing at its center. The primary and secondary columns are inserted into the cross and tee fittings, respectively, opposite each other, until the point where each column reaches the crimp in the central tubing. Auxiliary carrier gas is supplied to either the cross fitting or the tee, depending on the actuation state of the in-line solenoid valve. The final port of the cross leads to a waste line. This modulator has two modes of operation, divert and inject. In the divert mode, carrier gas is supplied to the tee fitting, which in turn supplies carrier gas to the ^{2}D column and diverts the ^{1}D effluent to waste. In the inject mode, the valve is actuated on the auxiliary gas line and flow

moves to the cross fitting, which injects the contents of the primary column effluent contained within the cross and connecting tubing sections towards the ^{2}D column. This injection period is brief at approximately 30 ms to 80 ms, after which the system returns to the divert mode sending ^{1}D effluent to waste as the recently injected analytes are separated on the ^{2}D column. This system is characterized by narrow injection bandwidths onto the head of the ^{2}D column owing to the short duration of the injection pulse. This can subsequently generate separations with good resolution. However, with the majority of ^{1}D column contents being diverted to waste, the duty cycle is low and reminicant of early flow modulators. What does remain true is that this modulator and the other flow modulators described herein have undoubtedly expanded the use of GC×GC globally by making the technique more accessible to laboratories with lower budgets and those seeking a retrofit solution for their GC instead of a new capital expenditure.

Since Phillips introduced the first GC×GC modulator design in 1991, scientists seeking greater peak capacity for their separations have never had more modulator options available to them than now. Technology has advanced to such a point that there are little differences in performance between thermal and valve-based devices [152]. When selecting a modulator, the analyst should consider several factors such as their need for sensitivity, repeatability of retention times and peak areas, cost of consumables used to operate the modulator, space within the laboratory to host modulator peripherals, purchasing budget, level of expertise within the laboratory to operate the device, optimization flexibility, and several more. It is no longer a question of thermal versus flow, but which modulator best suits the application and laboratory in which it will be used.

1.2.4 Optimization aspects of two-dimensional gas chromatography

In previous sections, GC×GC fundamentals and modulator designs throughout the years have been described. This section is dedicated to the discussion of optimization parameters used to generate high quality GC×GC chromatograms. Method optimization in GC×GC is more complicated than in 1D-GC as there are many more parameters to consider. In a commonly used column set for GC×GC, the ^{1}D column is non-polar, e.g. a 30 m × 0.25 mm id column with a film thickness of 0.25-1.0 μm, producing relatively broad peaks. Historically, a ^{2}D narrow bore (0.1 mm id), short (0.5 – 2.0 m), and polar column with film thickness of 0.1 μm was commonly used to allow fast and efficient separations in this dimension within approximately one modulation period. The trend now is towards selecting column sets with the same or similar internal diameters to reduce overall column train impedance and allow higher analyte loading of the ^{2}D column stationary phase compared to narrow bore columns. The next step is to select a temperature program, carrier gas flow rate and modulation period that allow all peaks to be sampled at least 2.5 – 3 times [33, 153]. In this conventional approach to optimization, the two dimensions are treated somewhat independently (as long as the ^{2}D column is kept in a separate oven). Though this approach has been popular with GC×GC users for a long time, it is not a standardized procedure and the conditions do not always provide the optimum GC×GC separation. Harynuk and Górecki pointed that the outcomes of separations optimized using this non-standardized procedure often seemed far from optimal [154]. For example, when chromatograms obtained using a 0.1 mm id column in the ^{2}D were compared with those obtained using a 0.25 mm id column, the ^{2}D peak widths for major components were often significantly larger when using the 0.1 mm column, with the remaining conditions being similar [154]. The authors attributed this to overloading of the narrow-bore column in the ^{2}D with the very narrow

peaks created by the modulator. It is clear, therefore, that GC×GC method optimization is not straightforward, which is probably one of the reasons for the still somewhat limited usage of the technique. Method optimization in GC×GC is mainly devoted to maximizing separation power and sensitivity. The main operational conditions that must be optimized are the modulation parameters, stationary phase chemistries, column dimensions, carrier gas flow, temperature programs and detector settings. Modulation parameters have been covered in Section 1.1.1.

1.2.4.1 Column combinations

Although the modulator is the key to successful GC×GC separations, the chromatographic columns play the most significant role in any GC separation. Simply installing the modulator between two columns does not guarantee a good GC×GC separation. Consequently, column combination optimization, including stationary phase chemistry, column dimensions and film thickness, is required to accomplish efficient GC×GC separations.

The most important aim of an optimized GC×GC separation is the maximum use of the ^{2}D separation space. The structured order separation is important only when analyzing samples that contain structurally related compounds such as homologues or isomers (e.g. petrochemical or fatty acid methyl ester (FAME) samples). Nevertheless, many of the published GC×GC chromatograms showed low exploitation of the separation space. The majority of applications in GC×GC have used a non-polar ^{1}D column (100 % dimethyl polysiloxane or 5 % diphenyl/95 % dimethyl polysiloxane) connected to a more polar ^{2}D column (e.g. polyethylene glycol, 50 % phenyl/50 % methyl polysiloxane) [155]. With such column combinations, analytes are separated primarily according to their vapor pressures in ^{1}D (especially the non-polar ones), and according to their polarity in ^{2}D. This means that two different separation mechanisms are involved, which is referred to as “orthogonality” of the separation process [156, 157]. There are, however,

numerous applications in which the columns are used in the reverse order, where a more polar column is used in the ^{1}D, and a less polar one in ^{2}D [158, 159]. Higher levels of orthogonality between the ^{1}D and ^{2}D columns can generate better separations [73, 160]. However, consequences such as increased wraparound may be increased. It should be emphasized that orthogonality is not a goal in itself. The success or failure of any separation is always decided by sufficient separation of the target analytes and overall utilization of the separation space. Since the inception of GC×GC, dozens of GC×GC stationary phase combinations have been evaluated. Representative examples of the combinations are presented in Table 1.1

Ryan *et al.* [161] studied how selectivity tuning of the ^{1}D column polarity affected the separation achieved. This study was mainly aimed at predicting GC×GC peak positions in the 2D separation space. The ^{1}D column polarity was systematically varied by combining different lengths of polar and low polarity columns while keeping the total column length constant. The resulting ^{1}D column was then coupled to both polar and non-polar ^{2}D columns. Figures 1.13 and 1.14 show the GC×GC contour plots of a 17-component standard mixture obtained from coupling of columns A-E (Table 1.2) with the polar polyethylene glycol phase and low-polarity 5 % phenyl methyl polysilphenylene siloxane phase ^{2}D columns, BP20 and BPX5, respectively. Maximum use of the ^{2}D separation space was achieved when the two columns were the most disparate (Figure 1.13A and 1.14E). As the polarity of the ^{1}D column approached that of the ^{2}D column in Figure 1.13, the separation space utilization was significantly reduced until nearly all analytes were arranged diagonally in the separation space (Figure 1.13E), indicating almost complete lack of two-dimensional separation. This occurred when the ^{1}D column was 100 % BP20, i.e. the same as the ^{2}D column.

Table 1.1: Representative examples of GC×GC column combinations

^{1}D (length m × id µm)	^{2}D (length m × id µm)	Analyte/sample	Reference examples
Poly(ethylene glycol) (21 m × 250 µm)	100 % Polydimethylsiloxane (PDMS) (1 m × 100 µm)	A hydrocarbon mixture and a coal liquids sample	[32]
(SolGel + poly(ethylene glycol)) composite phase (SolGel-WAX (30 m × 250 µm)	5 % Phenyl polysilphenylene siloxane (1 m × 100 µm)	Roasted coffee bean volatiles	[162]
Poly(ethylene glycol) (30 m × 250 µm)	5 % Phenyl polysilphenylene siloxane (1 m × 100 µm)	Lipids and roasted coffee bean volatiles	[163, 164]
Polyethylene glycol (TPA-treated) (30 m × 250 µm)	35 % Phenyl-polysilphenylenesiloxane (1 m × 100 µm)	Food analysis	[165]
(5 %-Phenyl)(1 %-Vinyl)-methylpolysiloxane (2 m × 100 µm)	14 % Cyanopropylphenyl) methylpolysiloxane (0.5 m × 100 µm)	Test mixtures	[49]
100 % PDMS (30 m × 250 µm)	(SolGel + Poly(ethylene glycol)) composite phase (SolGel-WAX (1.5 m × 250 µm)	Volatile components of Pinotage wines	[166]
100 % PDMS (50 m × 530 µm)	50 % Phenyl-polysilphenylene siloxane (2.2 m × 150 µm)	Volatile organic compounds in urban air	[167]
100 % Cyclodextrin directly bonded to PDMS (10 m × 100 µm)	(50 % Liquid crystal / 50 % dimethyl) siloxane column (1 m × 100 µm)	PCBs in environmental samples	[168]
100 % PDMS (1 m × 100 µm)	14 % Cyanopropylphenyl) methylpolysiloxane (2 m × 100 µm)	Essential oils	[169]
Polyethylene glycol (60 m × 250 µm)	(14 %-Cyanopropyl-phenyl)-methylpolysiloxane (3 m × 100 µm)	Cigarette smoke condensates	[170]

Poly(5 %-phenyl–95 %-methyl)siloxane phase (40 m × 100 µm)	1,12-Di (tripropylphosphonium) dodecane bis (trifluoromethanesulfonyl) imide (3 m × 100 µm)	PCBs	[171]
Poly(methyltrifluoropropyl siloxane) (30 m × 250 µm)	Poly(dimethyldiphenylsiloxane) (5 m × 250 µm)	Trace biodiesel in petroleum-based fuel	[172]

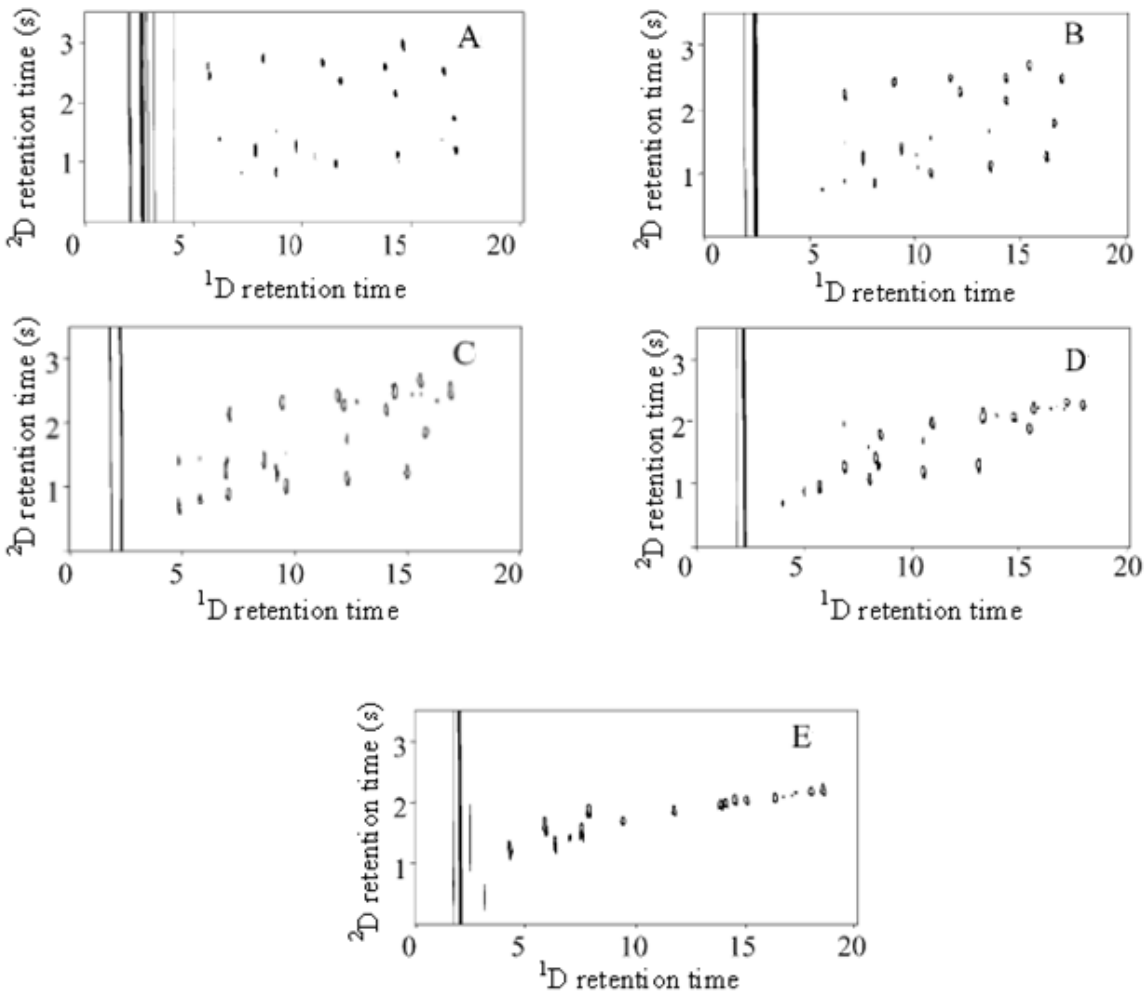

Figure 1.13 GC×GC contour plots for different ^{1}D columns coupled with a BP20 ^{2}D column. Panels (A – E) correspond to column designations according to ^{1}D columns shown in Table 1.2. Reproduced from reference [161].

The same result was obtained when a 100 % BPX5 column A was coupled to the same column in the second dimension (Figure 1.14A). A similar study was performed by Cordero *et al.*, but in that case the influence of selectivity tuning of the ^{2}D column on the GC×GC separation was studied [173].

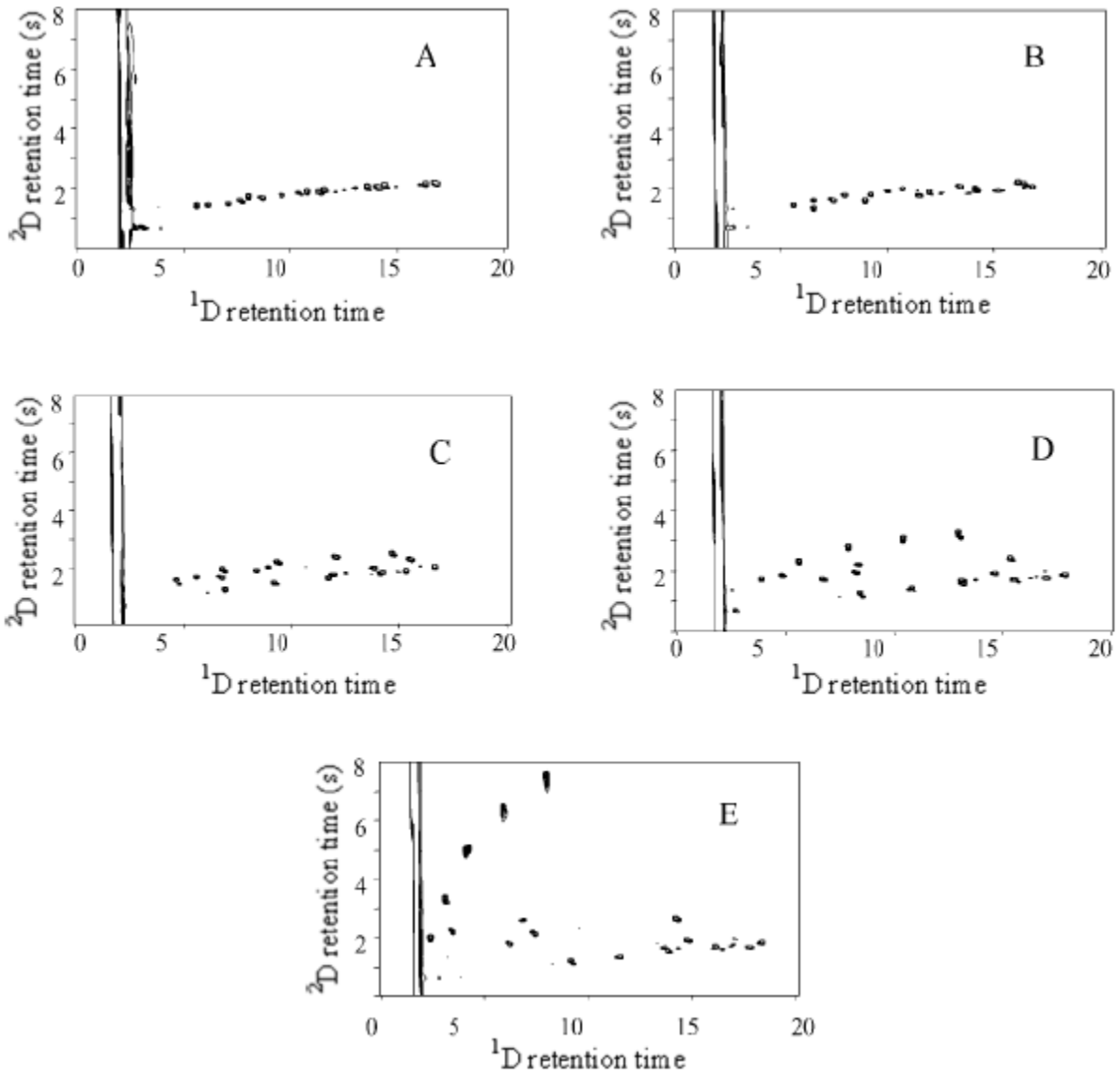

Figure 1.14 GC×GC contour plots for different ^{1}D columns coupled with a BPX5 ^{2}D column. Panels (A – E) correspond to column designations according to ^{1}D columns shown in Table 1.2. Reproduced from reference [161].

Table 1.2: Combined-polarity columns used in the ^{1}D [161].

^{1}D	Length of BPX5 column*	Length of BP20 column*
A	20	0
B	15	5
C	10	10
D	5	15
E	0	20

* each column is 0.25 mm id and 0.25 µm d_f.

The results showed that using a non-polar stationary phase in the ^{1}D provided the most orthogonal systems. Using a polar stationary phase in ^{1}D tends to decrease the separation space even when a proper orthogonal phase is used in the ^{2}D.

Ionic liquids (ILs) stationary phases can be tailored to have different degrees of polarity. They have the following characteristics: (1) high affinity towards dipolar solutes and solutes that can serve as hydrogen bond acids [174], (2) unique selectivity towards non-polar solutes such as alkanes and alkenes, similar to low-polarity stationary phases such as dimethylsiloxanes [175, 176], and (3) high temperature stability. For example, partially cross linked ILs can withstand up to 350 ºC, compared to majority of conventional polar stationary phases which cannot be used above 280 ºC. Breitbach and Armstrong used a high temperature phosphonium IL column in ^{1}D in combination with a conventional non-polar (5 % diphenyl / 95 % dimethyl siloxane) ^{2}D column [177]. The selectivity of IL column was compared with selectivities of polyethylene glycol and 50 % phenyl / 50 % methyl polysiloxane. The IL stationary phase tested showed strong interactions with hydrogen bonding and dipolar compounds. In addition, it displayed a unique selectivity towards low polarity hydrocarbons such as acyclic and cyclic alkanes and monounsaturated alkenes. In another study, a triflate (trifluoromethylsolfonate) IL column was used in the ^{2}D of a non-polar × IL setup and evaluated in the separation of 32 compounds

exemplifying varying chemical properties [178]. In particular, focus was placed on the separation of four phosphorus-oxygen containing compounds found in the 32 component mixture. The performance of this setup was compared to a setup containing a conventional polyethylene glycol column in the ^{2}D. The authors found the triflate IL column demonstrated superior selectivity towards phosphorus-oxygen containing compounds compared to the polyethylene glycol column.

In general, the ^{1}D column is usually long with typical dimensions of 15 to 30 m × 0.25 mm id, and a film thickness of 0.25-1.0 µm. The separation in the ^{2}D column has to be fast so that it can be finished in a time shorter than the modulation period to prevent wraparound. In thermal modulation, short, narrow-bore columns are commonly used in the ^{2}D; typically 0.5-1.5 m × 0.1–0.25 mm id and a film thickness of 0.1-0.25 µm [70, 179-182]. Flow modulators will frequently use longer, regular bore columns; typically 3-8 m x 0.25 mm id and a film thickness of 0.1-0.25 µm [150-152]. Adahchour *et al.* reported the use of a 0.5 m × 0.05 mm id column with a film thickness of 0.05 µm in the ^{2}D instead of the more usual 0.1 mm id columns with film thickness of 0.1 µm [183]. The design provided ultra-fast ^{2}D separation, i.e. the analysis time was reduced by more than three-fold without sacrificing resolution. However, the column was very prone to overloading, and such columns are not easily available.

In theory, short, narrow bore columns with thin films of stationary phase should always provide the most efficient separation. In GC×GC, however, problems arise when the ^{2}D column becomes overloaded, which occurs quite frequently with thermal modulators due to the zone compression during trapping. The concentration effect of the focused ^{1}D band may lead to overloading of the ^{2}D column even when the ^{1}D column is not overloaded [70]. This results in the deterioration of the peak capacity in the ^{2}D due to the large widths of overloaded peaks,

which might consume a significant portion of the limited ^{2}D separation space. Harynuk *et al.* studied the influence the ^{2}D column internal diameter on the ^{2}D peak widths [184]. The authors used a series of 1 m length ^{2}D columns with diameters ranging from 0.1 to 0.32 mm. The columns' phase ratio was maintained constant. A 30 m × 0.25 mm × 0.25 µm d_f non-polar column was used in ^{1}D. Different *n*-alkanes ($C_5 - C_{13}$) were injected at several concentration levels under the same volumetric flow rate and temperature programing conditions. Figure 1.15 illustrates a comparison of the GC×GC peaks eluting from the 0.1 and 0.25 mm ^{2}D columns. Both dimensions were overloaded when a mixture of pure compounds was injected, but the consequences were much more severe for the 0.1 mm ^{2}D column (Figure 1.15 A and C). When the columns were not overloaded at lower analyte concentrations, the 0.1 mm column provided slightly better performance than the 0.25 mm column. The authors concluded that using narrow-bore columns in the ^{2}D might not provide as great advantages as is commonly thought. The same group also studied the effect of the ^{1}D column film thickness on the GC×GC separation [185]. Four 30 m × 0.25 mm non-polar ^{1}D columns with film thicknesses of 0.1, 0.25, 0.5 and 1 µm were tested. Two polar columns (1 m × 0.1 mm × 0.1 µm d_f and 1 m × 0.25 mm × 0.15 µm d_f) were used as the ^{2}D columns. The authors concluded that when speed of the separation is prioritized over high resolution, thin-film ^{1}D columns and narrow-bore ^{2}D columns might be optimal. However, when high resolution is desired, thicker film (i.e. 0.25 or 0.5 µm) ^{1}D columns and larger diameter (i.e. 150 µm id) ^{2}D columns could be a better combination. Additional discussion relating to the chromatographic effects of overloading can be found elsewhere [186].

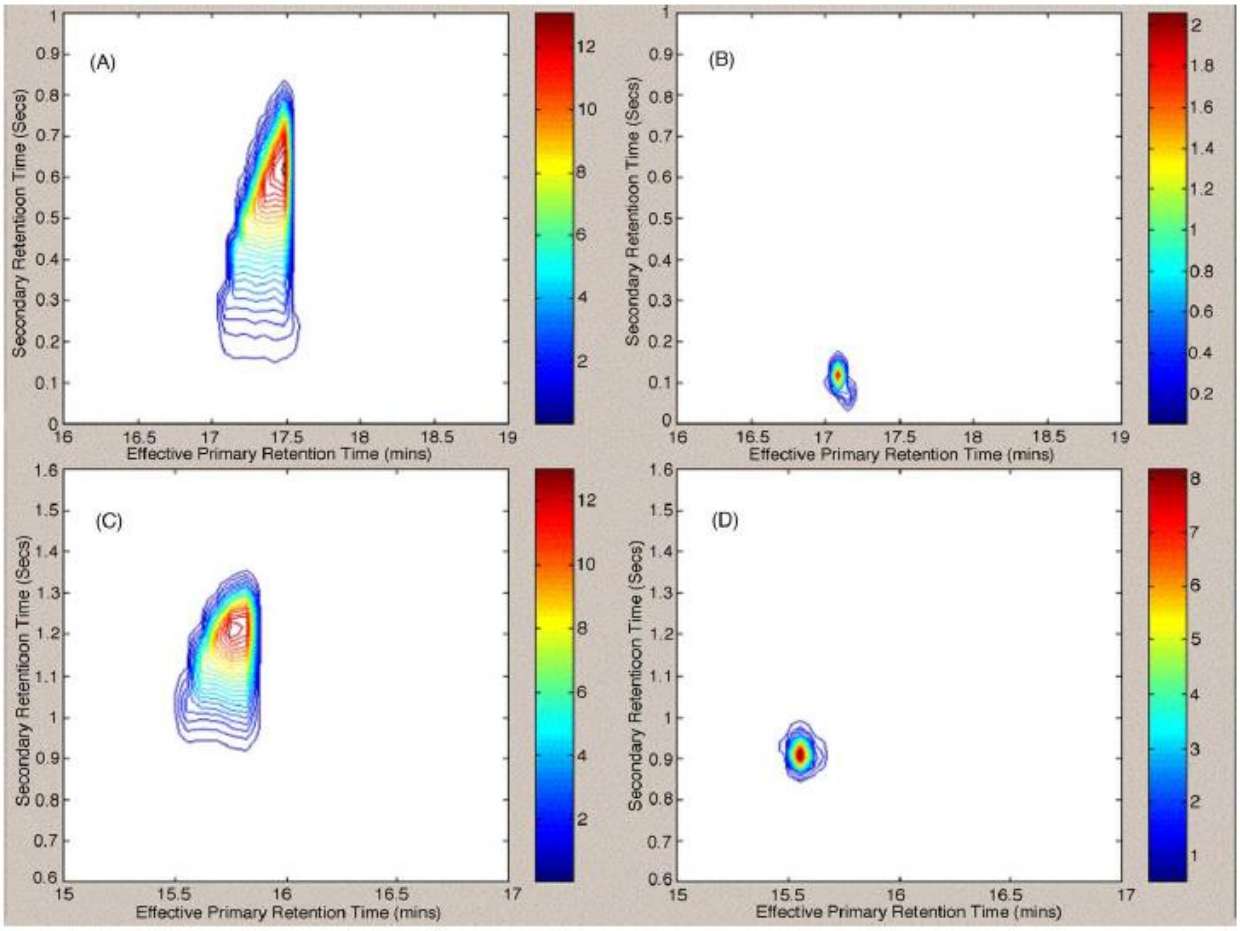

Figure 1.15 Undecane peaks from the mixture of pure compounds (A, C) and the 1000× dilution (B, D) run on the 100 µm id ^{2}D column (A, B) and the 250 µm id ^{2}D column (C, D). Reproduced from reference [184]

1.2.4.2 Carrier gas linear velocities

The majority of GC×GC separations in the literature are derived from previously optimized 1D-GC methods, especially with respect to the carrier gas flow rates. However, when the internal diameter of the ^{2}D column is smaller than that of the ^{1}D column, carrier gas pressure in the latter is considerably higher than in 1D-GC separations. As a result, the diffusion coefficients, and consequently the optimum velocity in the ^{1}D column are far lower than in 1D-GC. Beens *et al.* illustrated this and developed software to assist in the optimization of carrier

gas flow rates and column dimensions selection [187]. The software developed was used to calculate the separation parameters of two column combinations, one with a narrow bore (0.1 mm id) ^{2}D column and one with a wider bore (0.18 mm id) ^{2}D column. The result of this study was the conclusion that: (1) the optima for both dimensions are at widely different linear velocities, (2) the optimum of the ^{1}D is at a relatively low linear velocity, and (3), the wide-bore column combination provides more separation at the same analysis time. The authors concluded that when optimizing the GC×GC separation, it is advisable to operate both dimensions close to their optimum linear gas velocities, which can be mainly achieved by using two columns with the same internal diameter. Based on both this study and the Harynuk *et al.* study of overloading [188], the use of narrow bore ^{2}D columns might be far from optimal unless special precautions are taken.

Most GC×GC separations using columns in ^{2}D that have smaller id than the ^{1}D column are carried out at carrier gas velocities that are optimum or close to optimum in the first dimension, but much higher than optimum in the second dimension [187, 189-191]. Tranchida *et al.* in 2007 [192] presented various options for carrier gas velocity optimization in GC×GC: (1) to reduce the head pressure, thus the linear velocities in both dimensions; this causes retention times to increase, ^{1}D resolution to decrease and elution temperatures to increase; (2) to use a longer ^{2}D column; this increases the ^{2}D retention times and leads to degradation of the separation obtained in the ^{1}D column because of the need to use longer modulation periods; and (3) to use a wider-bore (0.15 - 0.18 mm id) ^{2}D column; this might enable the operation of both dimensions under near-optimal velocities. An alternative option described in detail by the authors was the use of a flow splitter prior to the modulator, which can be called “split flow” GC×GC. The idea of splitting the flow was originally used by Phillips [32, 37], where a T-union was used to

connect the two analytical columns, thus enabling the diversion of about a third of the ^{1}D column flow. The split flow GC×GC system by Tranchida *et al.* enabled independent adjustment of the carrier gas linear velocities in both dimensions [191]. A 30 m × 0.25 mm id ^{1}D column was connected to a 1 m × 0.10 mm id ^{2}D column and a 0.3 m × 0.10 mm id uncoated capillary segment through a Y press-fit. The ^{2}D column was passed through the cryogenic modulator, while the uncoated capillary was connected to a manual split valve. This design enabled optimization of the ^{2}D gas flow simply by adjusting the split valve. The design was tested in the analysis of cod liver oil FAMEs and the results were compared to the results obtained from a conventional GC×GC system under the same temperature program and at an average ^{1}D linear velocity of ~ 35 cm/s. This group also used a split flow GC×GC design for the optimization of ^{2}D separation using a 50 µm id column in ^{2}D and a twin-oven for the analysis of some complex samples such as roasted Arabica coffee volatiles [193] and a diesel sample [192].

Another approach to optimized linear velocities in both dimensions was based on stop-flow GC×GC, a modulator previously described in Section 1.2.3 [122]. The benefit of this design was that it allowed the stoppage of the ^{1}D flow which facilitated a longer separation in the ^{2}D. This was done without the need to increase the length of the modulation period in ^{1}D, thus preserving the separation accomplished in the first dimension. In this system, the ^{1}D and ^{2}D columns could be operated simultaneously under optimal flow conditions, and the ^{2}D column did not necessarily have to be short and/or narrow.

1.2.4.3 Temperature programming

Temperature program optimization is an important factor that influences any GC×GC separation. The occupation of the 2D separation space can be increased by tuning and optimizing the temperature programming rate [191, 194]. Figure 1.16 A shows the distribution of the analytes

around a diagonal when both dimensions are operated isothermally. In this case analyte volatility is the main determinant of retention, thus the retention times in both dimensions are correlated. Keeping the ^{1}D isothermal while increasing the ^{2}D temperature linearly causes the low-boiling point analytes eluting early from the ^{1}D to be launched into the ^{2}D column at lower ^{2}D temperature. On the contrary, high-boiling point analytes are launched into the ^{2}D column at higher ^{2}D temperature. Therefore, the ^{2}D temperature increase compensates for the decrease in analyte volatility during the run. This rotates the diagonal pattern in Figure 1.16 A into a horizontal one in Figure 1.16 B. In Figure 1.16 C, the ^{1}D temperature is increased linearly, while ^{2}D is kept isothermal. The diagonal pattern from Figure 1.16 A is curved upward. By increasing the temperature linearly in both dimensions, the retention times in both dimensions become reduced. Thus the peaks are well distributed within a smaller area (Figure 1.16 D). This simulation was close to the practical results obtained by Venkatramani *et al.* [194]. It is important to mention that GC×GC designs use either a single oven or two independent ovens. The latter increases the flexibility of the system. Using a single oven has two main limitations: (1) the maximum operating temperature is limited by the maximum temperature of the less thermally stable column, and (2) the ^{2}D analysis temperatures are dependent on the ^{1}D elution temperature [195]. Generally, the temperature-programming rate in GC×GC should be rather slow, i.e. 1 – 5 ^{o}C/min, to produce relatively broad peaks in the ^{1}D thus allowing the required 2.5 – 3 fold modulation of each peak. However, excessively slow temperature rates can adversely affect sensitivity and/or cause wraparound [195]. When two independent ovens are used, the ^{2}D column is usually programmed at the same rate, but with 20 – 30 ^{o}C offset from the ^{1}D rate.

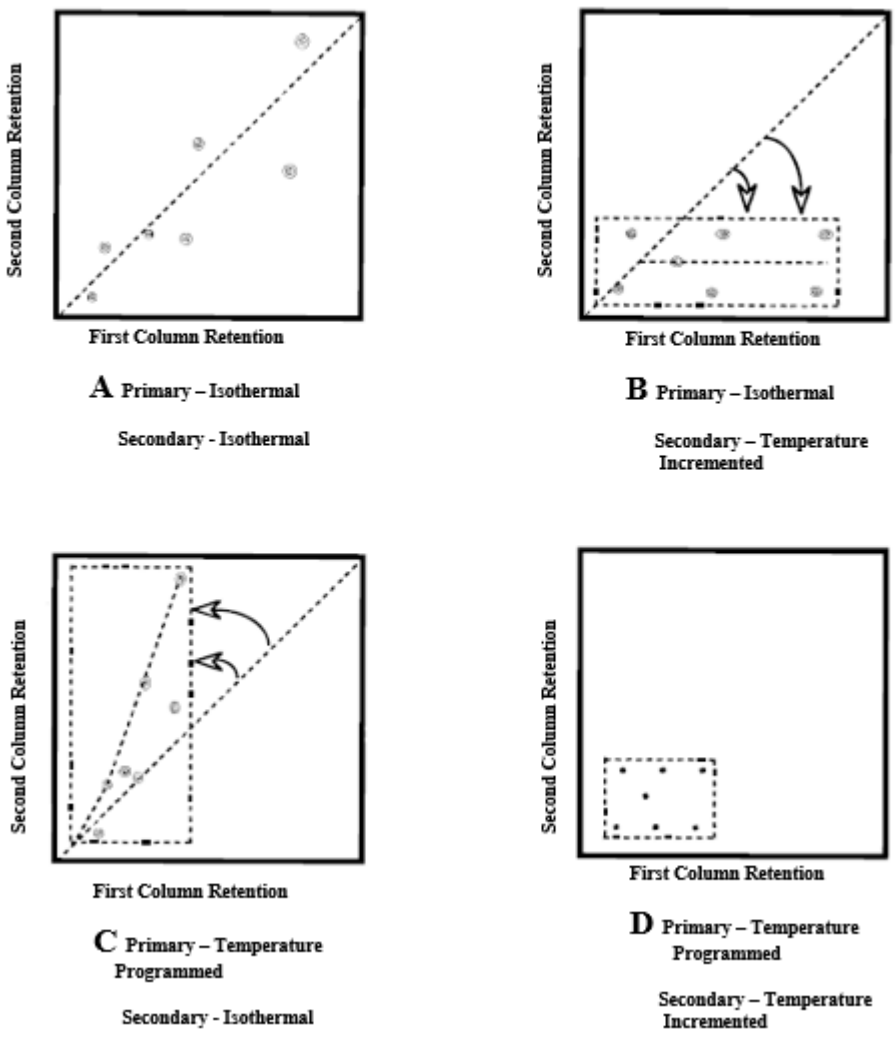

Figure 1.16 Simulated GC × GC chromatogram showing the influence of temperature on sample retention. Reproduced from reference [194].

More recently Chow and Gorecki devised a device for independent temperature programming of the ^{2}D column [196-199]. The system is based on direct resistive heating of a commercially available metallic secondary column. The column would be rapidly heated and cooled within the span of a modulation period across the entire GC run. The authors refined this design by integrating sophisticated temperature and timing control electronics which allowed precise

measurement of capillary and oven temperatures whilst ensuring applied heating was always in sync with the P_M across the GC run. This system was validated with both thermal and flow-based GC×GC systems and demonstrated excellent retention time and peak area repeatability. The use of a temperature programmed ^{2}D column gives the analyst more flexibility when optimizing their separation and offers greater peak capacity potential relative to conventional isothermal ^{2}D oven temperature offsets.

1.2.4.4 Detection systems for GC×GC

There are a number of detectors available for use in GC×GC to suit various application demands. With GC×GC providing separations in the second column on the order of 1 to 10 seconds long, peaks eluting into the detector are often numerous and very narrow. Typical peak widths at half height range from 40 to 120 ms. With at least 10 data points along the peak needing to be acquired for accurate peak area calculation, a general rule is that detectors for GC×GC should have data acquisition rates of at least 100 Hz [200]. For this reason, the most popular detector used with GC×GC is the flame ionization detector (FID). The FID is a small, robust detector characterized by fast acquisition speeds, low internal volume and wide dynamic range [201]. Its main disadvantage is its lack of selectivity. For the analysis of organohalogens, the micro electron capture detector (μ-ECD) has proven to be well suited for GC×GC [202, 203]. However, consideration should be given to the relatively large internal volume of the detector, which broadens second dimension peaks considerably at low make-up flow values. Other detectors such as the nitrogen-phosphorous detector (NPD), sulphur chemiluminescence detector (SCD), atomic emission detector (AED), and miniaturized pulsed discharge detectors (MPDD) have been used as well [204-213].

In 2014 a new detector technology for GC was commercialized by VUV Analytics Inc. of Austin, TX, and introduced as the Vacuum Ultraviolet (VUV) Detector. The VUV detector was first described by Schug *et al.* [214]. It is unique amongst detectors used with GC in that it exploits the absorption of ultraviolet light by analytes in the 115-185 nm range. Suitably high acquisition frequencies permit its use with GC×GC as described in studies looking at human breath [215] and fuels [216].

With accurate quantitation, targeted and non-targeted screening and structural elucidation being necessary attributes of many analytical methodologies, mass spectrometry (MS) and GC×GC have become an extremely useful pairing. Of the numerous MS detectors available, the time-of-flight (TOF) MS remains the most practically useful. In principle, TOF MS has the ability to scan at up to 500 Hz rate and provide < 10 parts per million (ppm) mass accuracy, as well as the largest mass range of any MS detector, although increased mass ranges require lower scanning rates and subsequently provide poorer mass resolution. When paired with GC or GC×GC, the TOF MS uses electron ionization (EI) allowing for NIST library searchable spectra to be produced. The combination of TOF MS and GC×GC helped resolve and identify analytes in some extremely challenging applications [217]. Several manufacturers provide standalone TOF MS systems, as well as complete GC×GC TOF MS packages. In recent years, several advances have been made in TOF MS technology, including the availability of high resolution TOF MS (HR TOF MS). These instruments are offered from Vendors such as LECO, JOEL, Agilent and Thermo Scientific. Waters Corporation offers a quadrupole time-of-flight (qTOF) instrument with an atmospheric pressure ionization source, which has shown to be an effective pairing with GC×GC to increase sensitivity of conventional GC separations [218]. The HR TOF MS detectors can provide mass accuracy at sub-ppm levels and scan at rates sufficient to

facilitate adequate peak reconstruction. These detectors are being used for accurate mass determination and identification of analytes in highly complex samples [219-223]. Although these HR TOF MS detectors are very powerful, they have limitations related to the dynamic range and the large amount of data produced.

Another development in the TOF MS area is the variable ionization system Markes has introduced for their Bench-TOF detectors. The user can adjust the EI source energy from 10 to 70 eV. At lower ionization energies the system can produce NIST searchable EI spectra with more pronounced molecular ions and a larger abundance of high mass fragments. This has been shown to be especially useful in differentiating challenging isomeric compounds [224].

Quadrupole MS (qMS) has been paired with GC×GC in the past and remains fairly popular due to the ease of use and relative availability compared to TOF MS detectors. These detectors can provide adequate sampling frequency for GC×GC, but only for very narrow mass ranges [225]. The mass range can be increased if second dimension peaks are intentionally made wide to allow for enough data points to be acquired. GC×GC with qMS is often used in selective ion monitoring (SIM) mode in target analysis. Significant efforts have been made by Mondello *et al*. to pair GC×GC with qMS detection [134, 135, 226-230]. The same group also utilized tandem mass spectrometry (MS/MS) in both scan and multiple reaction monitoring (MRM) modes to perform semi-quantitation of benzothiophene, dibenzothiophene and benzonaphthothiophene chemical classes [226]. More recently, GC×GC with qMS has been utilized to evaluate wine volatiles [231], atmospheric volatile organic compounds (VOCs) [232] and VOCs derived from Kava root extracts [233]

1.2.4.5 Summary

Today, GC×GC can be considered a mature technique. It offers many advantages over conventional 1D-GC separations. However, careful optimization is required to reach the full potential of the technique. GC×GC separation optimization is not as simple as in conventional 1D-GC. This complexity comes from the fact that two different columns are linked together, thus any changes to the ^{1}D column, flow rate, modulation, oven temperature programming rate, etc., will affect the separation not only in that dimension, but in the ^{2}D as well. For example, increasing the oven temperature programming rate while keeping other parameters constant will generally result in narrower ^{1}D peaks. This may increase the chance of overloading in the second dimension, leading to ^{2}D peak broadening and loss of resolution and 2D separation space. On the other hand, when the temperature programming rate is increased, the analyte elution temperature from the ^{1}D also increases. Consequently, separation will be performed at higher temperature in the ^{2}D. As a result, the chances of ^{2}D overloading are decreased due to the higher column sample capacity at higher temperature. In addition, narrower ^{1}D peaks may require shorter modulation periods to get a sufficient number of samples across the ^{1}D peaks. Table 1.3 illustrates the effects of the main chromatographic parameters on GC×GC separation outcome [234]. Careful consideration of all parameters and their interactions is needed for optimum results. However, once the complex interplay of the parameters is understood, GC×GC can reward the user with unparalleled separation power.

Table 1.3: Effects of changing GC×GC parameters on other aspects of the system. When parameter A in the Parameter column is increased, it will affect parameter B in the Effect column. If B increases with A, then (+) is indicated in the Direction column. If B decreases, (–) is indicated, and if the effect is uncertain, (±) is indicated.

Parameter (A)	Effect (B)	Direction
Oven programming rate	T_e	+
	${}^1w_h$; analysis time	-
${}^1d_c$	Capacity of ^{1}D	+
	${}^1\Delta p$; ${}^1u$	-
${}^2d_c$	Capacity of ^{2}D	+
	${}^2\Delta p$; ${}^2u$	-
${}^1d_f$	T_e; Capacity of ^{1}D	+
	${}^1w_h$; Mass per modulation	-
${}^2d_f$	Allowed/Required ^{2}D space; Capacity of ^{2}D; ^{2}D retention	+
${}^1l$	${}^1\Delta p$; ${}^1R_S$; T_e; ${}^1w_h$; Analysis Time	+
	${}^1u$	-
${}^2l$	${}^2\Delta p$; ${}^2R_S$; Allowed/Required ^{2}D space	+
	${}^2u$	-
Inlet Pressure	${}^1u$; ${}^2u$	+
	T_e; Analysis Time	-
P_M	Allowed/Required ^{2}D space; Chance of ^{2}D overloading	+
	${}^1R_S$	-
Capacity of ^{1}D	Chance of ^{1}D overloading	-
Capacity of ^{2}D	Chance of ^{2}D overloading	-
T_e	^{2}D retention; ${}^2w_h$; Chance of ^{2}D overloading	-
${}^1u$	${}^1R_S$	+/-
	T_e; Analysis Time	-
${}^2u$	${}^2R_S$	+/-
	Allowed/Required ^{2}D space	-
${}^1w_h$	P_M	+
	Mass per Modulation; ${}^1R_S$	-
${}^2w_h$	Allowed/Required ^{2}D space	+
	${}^2R_S$	-
${}^1\Delta p$	${}^1\Delta p/\Delta p_T$	+
${}^2\Delta p$	${}^1\Delta p/\Delta p_T$	-
${}^1\Delta p/\Delta p_T$	${}^1u_{opt}$	-
${}^1u_{opt}$	Analysis Time	-
Mass per modulation	Chance of ^{2}D overloading	+

T_e: elution temperature; ${}^1w_h$: ^{1}D peak width; ${}^1d_c$: ^{1}D column diameter; ${}^1\Delta p$: pressure drop in the ^{1}D; ${}^1u$: ^{1}D column linear velocity; ${}^2d_c$: ^{2}D column diameter; ${}^2\Delta p$: pressure drop in the ^{2}D; ^{2}u: ^{2}D column linear velocity; ${}^1d_f$: ^{1}D column film thickness; ${}^2d_f$: ^{2}D column film thickness; ${}^1l$: ^{1}D column length; ${}^1R_S$:^{1}D resolution; ${}^2l$: ^{2}D column length; ${}^2R_S$:^{2}D resolution; ${}^2w_h$: ^{2}D peak width; ${}^1\Delta p/\Delta p_T$: pressure drop in the ^{1}D compared to the total pressure drop; ${}^1u_{opt}$: ^{1}D column optimal linear velocity.

1.2.5 Applications of GC×GC

The majority of GC×GC practitioners have for some time now moved away from developing modulation technologies and focused on implementing the technique. Applications using GC×GC have continuously grown since its introduction over 30 years ago and in more recent years have focused on more routine application of the technique [235]. GC×GC is typically utilized in fields where complex volatile and semi-volatile samples are common. Selected recent examples of GC×GC applications in popular areas of study are reviewed below.

Petroleum and petroleum products are some of the most complex samples commonly analyzed by GC techniques. It is not uncommon to encounter thousands of unique compounds within many different chemical classes. The extra dimension of selectivity offered by GC×GC has been used for many years in the petroleum industry and some of the earliest applications described involve samples of gasoline, diesel, or crude oil. Today's petroleum chemists are faced with new challenges such detailed oil reservoir characterization or the analysis of biogenic based fuel precursors and pyrolysis oils [236-238].

One example is the analysis of vacuum residue oils and heavy fuel oils. These fuels are popular due to their low cost but pose a significant risk to the environment when burned in industrial boilers and especially marine vessels [239]. A global decrease in light crude resources has placed more focus on utilizing these low value oils and methods to derive more environmentally friendly derivatives through processes such as gasification and pyrolysis are currently under investigation. GC×GC is an excellent tool to understand the complex nature of the products before and after the pyrolysis process. Colleoni *et al.* used GC×GC to study the volatiles released during the pyrolysis of residual oils [240]. Their apparatus used pyrolysis for sample introduction, a thermal modulator for GC×GC separation, and FID, sulfur

chemiluminescence detection (SCD) and TOF MS in tandem for analyte detection and characterization. The column set used was a popular non-polar to mid-polar combination consisting of a HP-5ms 30 m x 0.25 mm x 0.25 µm in the ^{1}D and a BPX-50 2 m x 0.100 µm x 0.10 µm column in the ^{2}D. The authors developed their own algorithm to process the raw data acquired from the three detectors used in the analytical system. The algorithm was designed to select pyrolysis products and classify the molecules based on functional groups and elemental composition. The results were validated using a series of known mass fragments from chemical classes commonly found in petroleum products such as alkanes, alkylbenzenes and phenanthrenes. Using this method and additional data from the FID and SCD detectors, the authors were able to identify 26 separate molecular classes within the pyrolysate samples and deemed the pyrolysis-GC×GC-TOF MS/FID/SCD method an excellent technique for characterizing their complex samples.

Recently there have been efforts at ASTM International to introduce another routine GC×GC method for the group type quantification of hydrocarbons between boiling points of 36 °C and 343 °C [241]. This method has been designated D8396 and at the time of writing has been published with an inter-laboratory study ongoing.

Characterization of the volatile composition of foods, flavours and fragrances is of vital importance for quality control and regulatory purposes. Essential oils, food aromas and perfume products are highly complex samples containing many individual compounds across a variety of chemical classes [242]. GC×GC is being used extensively in this field for such tasks as elucidation of sensory-active components in wines and verification of the allergenic compounds in cosmetic products [243, 244]. One such example is the analysis of essential oils derived from various strains of *Lippia alba*, an aromatic shrub native to Brazil and other regions of South and

Central America [245]. This plant has been subjected to a genetic breeding program to identify strains with strong genetic variability that offer both resistance to environmental vulnerabilities and high levels of chemical constituents with commercial value. Gimenes and co-workers used hydrodistillation to extract the essential oil from eight varieties of *L.alba*, which were further diluted in ethyl acetate. The analytical system used consisted of a RFF modulator combined with qMS detection. The column set consisted of the popular non-polar to mid-polar combination with a HP-5MS 30 m x 0.25 mm x 0.25 µm in the ^{1}D and a HP-50+ 5 m x 0.100 µm x 0.10 µm column in the ^{2}D. The ^{2}D flow was split between qMS and FID detectors for dual detection capabilities. Multivariate statistical analysis of the results was utilized with principal component analysis (PCA) and hierarchical clustering analysis (HCA) being performed. The authors were able to classify the eight varieties into four main groups based on the presence of primarily terpene species that differentiated them. Overall, 73 individual metabolites were identified across the eight cultivars using GC×GC-qMS, the first time this technique had been applied to study this botanical. The authors demonstrated that GC×GC-qMS is a useful alternative to more expensive techniques utilizing thermal modulation combined with HRMS.

Monitoring contaminants in the environment is vitally important for human health and evaluating the impact humans are having on our planet. Environmental samples including soils, water and air are complex chemical mixtures without the introduction of anthropogenic contamination. Pollutants such as polychlorinated biphenyls (PCBs) which have 209 isomers or short chain chlorinated paraffins (SCCPs) which have thousands of isomers would be incredibly difficult to separate and characterize using conventional 1D techniques and would benefit from the application of GC×GC [202, 246, 247]. A recent example of GC×GC being applied to understand a complex environmental sample involves the analysis of organic pollutants in

drinking water [248]. In this study Murtada *et al.* used thin-film microextraction (TF-SPME) as a sample preparation technique to pre-concentrate trace level pollutants from various water sources in Waterloo, ON. Once the TF-SPME fibers had equilibrated within the 2.5 L water samples, they were subjected to thermal desorption (TD) and subsequently GC×GC-TOF MS analysis. Flow modulation with a column set consisting of a BP5 20 m x 0.18 mm x 0.18 µm in the ^{1}D and a BPX50 5 m x 0.25 mm x 0.25 µm column in the ^{2}D was utilized for separation. Many observable differences were found between the raw, soft and drinking water samples, but to further identify key differentiators, a tile-based approach was used to identify the top 50 factors that made the samples different [249]. This non-targeted comparison method separates the chromatogram into small regions or tiles, and spectral information from each tile is binned and compared with the other tiles in the dataset. The software functions to identify features which are regions of high variance based on the spectral data in the data set. These top 50 features were then used to inform a PCA plot comparing the three water sample types. The resulting data analysis revealed the gradual reduction of organic pollutants in water as it proceeded from a raw state through the softening process to further filtration to become drinking water. The authors concluded that the TF-SPME-GC×GC-TOF MS method deployed in the study was very well suited for the untargeted screening of organic pollutants in water sources.

Applications of GC×GC are extensive and beyond the scope of this work to summarize them exhaustively. For more thorough reading, a selection of recent reviews are listed in Table 1.4.

Table 1.4 Selection of recent reviews covering important application areas of GC×GC.

Application Area	Reference
Wine	[250]
Environmental contaminants	[251]
Clinical metabolomics	[252]
Seed and vegetable oils	[253]
Minerial Oils in food	[254]
Recycled plastics	[255]
Food-omics	[256]
Anti-doping	[257]
Pesticide residues	[258]
Food contact materials	[259]
Bio-wastes	[260]

1.3 Prior work

Previous contributions made by past members of the Górecki group have laid down the foundation for the research described herein. Former member Ognjen Panič established methods for thermally treating and reducing the internal diameter of trapping capillaries used in both single and dual-stage modulator designs. These methods are described in his Masters Thesis [261]. The procedure for internal diameter reduction involved placing the stainless steel capillary between two stainless steel shims and securing it in place with a piece of masking tape. The length and height of the shim was varied depending on the type of modulator being used. Once secured, two steel parallels were placed on either side of the shims and the assembly was placed within the jaws of a vice. The vice was tightened and the steel capillary secured within the apparatus was flattened to a height equivalent to that of the shims placed beside it. The length of capillary which was flattened was equivalent to the length of the steel parallels used in the assembly. Several sizes of shims and parallels were made available to customize the geometry of the trapping capillary. Panič also refined a procedure for the selective removal of stationary

phase from within the trapping capillary. This was initially explored to alleviate the issue of cold spots along the dual stage modulator design. Sections of the trapping capillary where electrical conduits had been welded would take longer to heat up and cool down due to their increased thermal mass. To reduce the impact of chromatographic tailing from these regions, stationary phase within these regions was selectively removed using this thermal treatment procedure. This was completed by applying high pressure air through the capillary while passing electrical current in pulses through sections of capillary where the stationary phase was desired to be removed. Through many subsequent heating events in which the steel capillary glowed red, the air passing through the capillary served to oxidize the stationary phase and remove it from the internal surfaces. These innovations were applied to a dual-stage modulator design which featured a 15 cm flattened capillary looped outside the GC oven which was cooled by an external blower (Figure 1.17). This modulator was successfully applied to the analysis of atmospheric organic aerosols in Berkley, California [95]. It was also demonstrated to be useful in the separation of PCBs in transformer oils, diesel and gasoline samples [262].

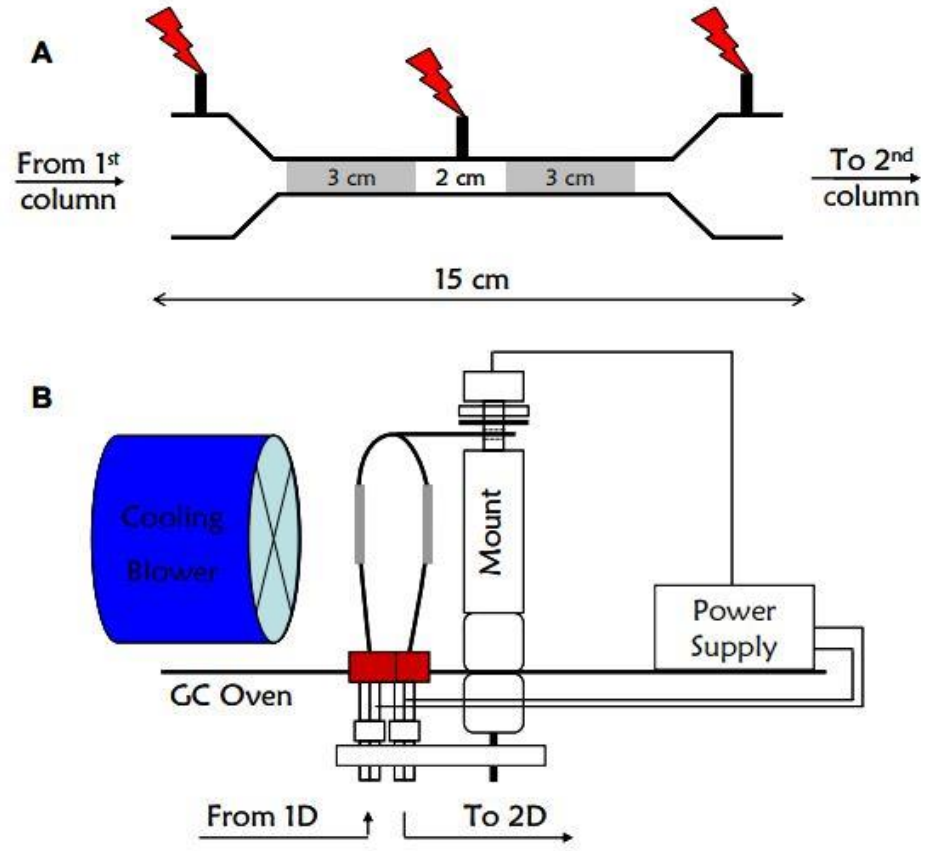

Figure 1.17 A diagrammatic representation of the modulator designed and described by Panič [261].

Christopher McNeish was next to improve on the work completed by Panič which resulted in the conversion of the dual-stage device into a single-stage modulator. The central electrical contact welded to the 15 cm flattened capillary was often the first component to fail after repeated capacitive discharge events. McNeish removed this contact and applied heating to the entire length of the capillary. Chromatographic performance on par to the previous dual-stage design was observed, and removal of the central contact point allowed longer continued use of the modulator. McNeish observed that analyte breakthrough in this design was very low or not observed, which was counterintuitive given single-stage designs commonly underperformed

dual-stage designs on this metric. The reason for this advantage was due to the impedance to primary carrier gas flow that was created by this trapping capillary during a modulation event. The viscosity of gasses increases with temperature and during a modulation event the gas contained within the trapping capillary is raised to temperatures well above oven temperatures. This feature, in addition to an observed pressure pulse, served to temporarily impede the flow of primary column eluate into the trap during a modulation event, preventing breakthrough. Another development by McNeish was the addition of a vortex cooling system to provide sub-ambient cooled air to the trapping capillary. A ceramic mount was created, inside of which the trapping capillary could be electrically isolated and cold air passed through. By cycling the compressed air source for the vortex cooler through the GC oven first, McNeish was able to gradually increase the temperature of the cooling air as the oven became hotter. This effectively created a passive temperature programmed cooling system. The work by McNeish demonstrated that single-stage designs had merit due to similar performance to relevant dual-stage designs and improved robustness.

1.4 Scope of the Thesis

This work was originally completed between the years of 2010 and 2015. The author of this work departed the graduate program at the University of Waterloo in 2015 for an employment opportunity focused on the development of GC×GC modulation technology. With the permission of the University of Waterloo, the author enrolled back into the PhD program in May 2023 to complete the requirements of the program. In the following chapters, the results of research on the development of a new consumable free GC×GC modulation technology and other technical solutions to improve GC separations will be presented. The development of a consumable-free modulation system for GC×GC will be discussed first, followed by the

development of an inlet backflush system for improvement of GC and GC×GC separations. Additional chapters present implementations of these technologies to several challenging applications facing users in fields of study such as petroleum, fragrances, environmental and forensics.

Chapter 2. Design and optimization of a consumable-free thermal modulation system

2.1 Tools, procedures and visualizations used in this work

2.1.1 Introduction

The following sections describe in order the sequence of modulator designs and modifications undertaken prior to reaching the final design which was named the Waterloo Modulator. All design work was carried out by the author using AutoCAD products made available for free online to registered students. All machine work required to build each modulator including the use of drill presses, lathes, mills and other heavy tools was undertaken by the author.

2.1.2 Experimental

2.1.2.1 Trapping capillary assembly

The basic procedure for trapping capillary manufacture was established by Panič and McNeish in previous works and was largely unmodified throughout the modulator development process [261, 262]. A section of metal capillary would be cut from a longer segment using a ceramic wafer. The length of this section would differ depending on the experiments being conducted. The most commonly used column for trap manufacture was an MXT-1 column with 1 µm of PDMS stationary phase coating. After the desired length of 0.28 mm MXT-1 column was cut, it would undergo the compression process described by Panič [262]. Flattening of the capillary reduced the distance in the vertical axis between the internal walls from 280 µm to approximately 100 µm as shown in Figure 2.1. Distance between walls in the horizontal axis was slightly increased.

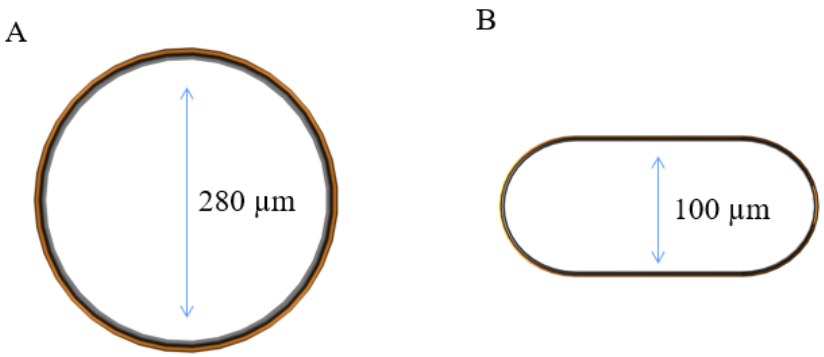

Figure 2.1 Diagram showing cross sectional capillary geometry and internal dimensions before (A) and after compression (B).

The outside dimension of the flattened capillary was checked with a metric micrometer (Mitutoyo, Japan) along its length to ensure equal compression had been applied and a uniform outside thickness of 0.36 mm had been achieved. Any deviations greater than 0.01 mm in outer wall-to-wall distance measured in the traps resulted in trap rejection. Several millimeters of the capillary were left unflattened at each end of the trap to facilitate connections. Once successfully flattened, one end of the capillary was connected to an in-house compressed air source through a Siltite stainless steel union (SGE, Austin, TX). The other end of the capillary was left open to the laboratory environment. Using a capacitive discharge power supply, electrical current was applied to a section of the capillary to momentarily increase the temperature along its length up to 800 °C. This was done by connecting electrical leads from the power supply to alligator clips which were then secured to the metal capillary. The section of capillary in between the clips would receive electrical discharge. The discharge was applied every 6 seconds for 100 pulses over a 10 minute treatment period. A diagram of the treatment setup is shown in Figure 2.2.

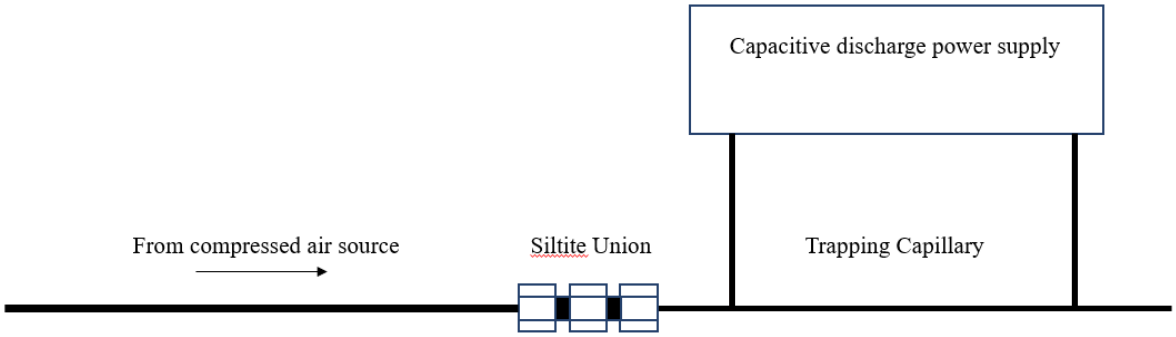

Figure 2.2 General setup for the thermal treatment procedure. A flattened trapping capillary would be connected to the compressed air source through a siltite union. Electrical leads would be attached to the trapping capillary using alligator clips, the distance between them being the section of capillary receiving thermal treatment. The air source would be turned on prior to applying capacitive discharge.

Once the MXT-1 capillary has received sufficient thermal treatment, the addition of ferrules to either end of the trap was required. Stainless steel Siltite ferrules (SGE, Austin, TX) measuring 0.25 mm were purchased in packs of 10 and manually bored to a greater internal diameter of 0.54 mm using a jewellery lathe in the Science Technical Services (STS) machine shop. The ferrules were then placed on the remaining cylindrical section of the capillary and swaged in place by compressing the ferrule within a Siltite union with a nut. The union was then loosened and removed, with the nut remaining on the capillary. Excess capillary outside of the swaged ferrule was trimmed using a ceramic wafer. This process was repeated for the other end, which resulted in a trapping capillary capable of being interfaced with two GC columns using the Siltite column connection system. Since the unions, nuts and ferrules were all stainless steel, the entire trap was electrically conductive allowing electrical current to be applied via alligator clips attached to the column connecting unions. A schematic of a completed trap can be seen in Figure 2.3.

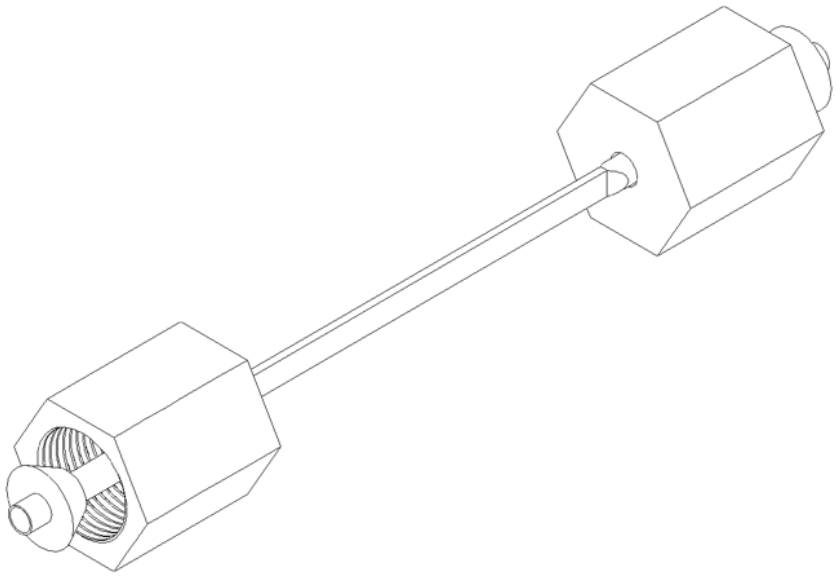

Figure 2.3 A completed trap assembly including connecting ferrules and nuts.

2.1.2.2 Temperature measurements

Throughout the modulator design and testing process, accurate temperature measurements of trap temperature during modulation, thermal treatment, cooldown periods and more were required. In addition, understanding the degree to which various cooling setups were impacting the trap desorption and cool down periods was also vital. To measure temperatures of the trapping capillary, a 50 µm Chromel/Alumel K-type thermocouple (Omega, Laval, QC) was spot welded to the center of the trap. The thermocouple was then connected to a custom-made amplifier (Science Technical Services, University of Waterloo) providing 100 x gain before being connected to a Hameg HM 605 60 MHz digital oscilloscope (Mainhausen, Germany). The oscilloscope was then adjusted such that each vertical division represented 0.1 V or 0.2 V, depending on the pulse strength. Upon collection of the signal, the divisions were converted to volts, divided by 100 to correct for the amplifier gain, and finally converted to millivolts (mV). To correlate the mV measurement to a temperature increase or decrease, a conversion formula

was derived from the NIST K-type thermocouple data table [263]. The result is as follows, where T is the corresponding temperature in °C and U is the mV recorded.

$$T = 24.596U - 0.2208$$

$$R^2 = 1$$

This equation was used to determine the temperatures reported herein.

2.1.2.3 Chromatographic conditions

The chromatographic system used in this work was an Agilent 6890 gas chromatograph (Agilent Technologies, Santa Clara, CA, USA) outfitted with a split/splitless (S/SL) inlet and an FID detector. The FID was operated at 300 ºC using 30 ml/min H_2, 300 ml/min of air and 30 ml/min of N_2 for make-up gas with an acquisition frequency of 200 Hz. Hydrogen carrier gas with a purity of 99.999 % (Praxair, Brantford, ON) was used and injections were carried out either manually or using a model 7683 Automatic Liquid Sampler (ALS). Various column configurations were used and will be specified as they are introduced.

2.1.2.4 Software

Chromatograms presented in this work were processed with one of the following software packages, depending on the instrument used and type of analysis: ChemStation (Agilent Technologies, Santa Clara, CA, USA), ChromSpace (Markes International, Bridgend, UK), GC Image (Lincoln, NE, USA) or ChromaTOF (LECO, St. Joseph, MI, USA).

2.2 Mark I design and evaluation

2.2.1 Introduction

Following on from the vortex cooled modulator design explored by McNeish, the main objectives were to improve on this device by expanding its effective volatility range and making

the modulator more reliable and easier to use. The initial Mark I (Mk I) design utilized the 15 cm long trapping capillary deployed by McNeish in his M.Sc. research. Experiments were designed to explore the trapping capability of the remaining stationary phase after thermal treatment. The vortex cooler utilized by McNeish was effective in supplying sub-ambient air to cool the trap after a desorption event, but was prone to ice buildup within the trap-containing ceramic channel. Trap cooldown times of 2 seconds or less were commonly observed with this modulator. Another goal of the Mk I design was to improve on these cooldown times and move away from vortex cooling. To this end, Peltier cooling was selected as an alternative technique offering electrically based cooling to temperatures as low at -20 °C. It was hypothesized that the use of Peltier coolers to compress the trapping capillary would improve cooling times after resistive heating and lower the potential for ice build up with the removal of compressed air. Reduced cooling times should in theory improve trapping capability, extending the volatility range of the compounds trapped by the modulator. The potential for breakthrough should also be reduced with more effective cooling. The vortex-cooled modulator required a skilled hand to place the trapping capillary within the ceramic slot and tighten the screws to secure it while also connecting it to electrical leads for the capacitive discharge power supply. A design that would make it easier for the end user to set this system up for analyses was desirable.

2.2.2 Experimental

2.2.2.1 Apparatus

Moving away from vortex cooling towards Peltier cooling necessitated a complete redesign of the modulator to enable the use of heatsinks and mount this new device atop the GC oven. Peltier cooling, also known as thermoelectric cooling (TEC), allows the transfer of heat from one side of an assembly to the other through the application of an electrical current to thermoelectric

materials. The assembly is created by alternating n-type and p-type semiconducting blocks connected electrically in series, but thermally in parallel. The n-type materials are negative charge carries, while p-type materials are positive charge carriers. When a DC (direct current) electrical current is applied to the circuit, both types of charge carriers are transferred away from the electrical junction, removing heat. If heat is applied to the junction, the carriers are mobilized and generate an electrical current. A diagram of a basic TEC setup is shown in Figure 2.4. TEC devices model number 12711-91-14C were acquired from Custom Thermoelectric (Bishopville, MD, USA). When operated at a maximum current of 14 A with highly efficient removal of heat from the hot side of the TEC, these devices are capable of generating a temperature differential between the cold side and the hot side of up to 67 °C. Power supply units (PSU) for the Peltier coolers were custom-made in the Electronics Shop of the Waterloo STS. The PSU allowed the power provided to the TEC unit to be adjusted, and therefore cooling to be stronger or weaker with the twist of a dial from a level of 0 to 10. The level of 10 provided 14 A, the maximum allowable current to the TEC units.

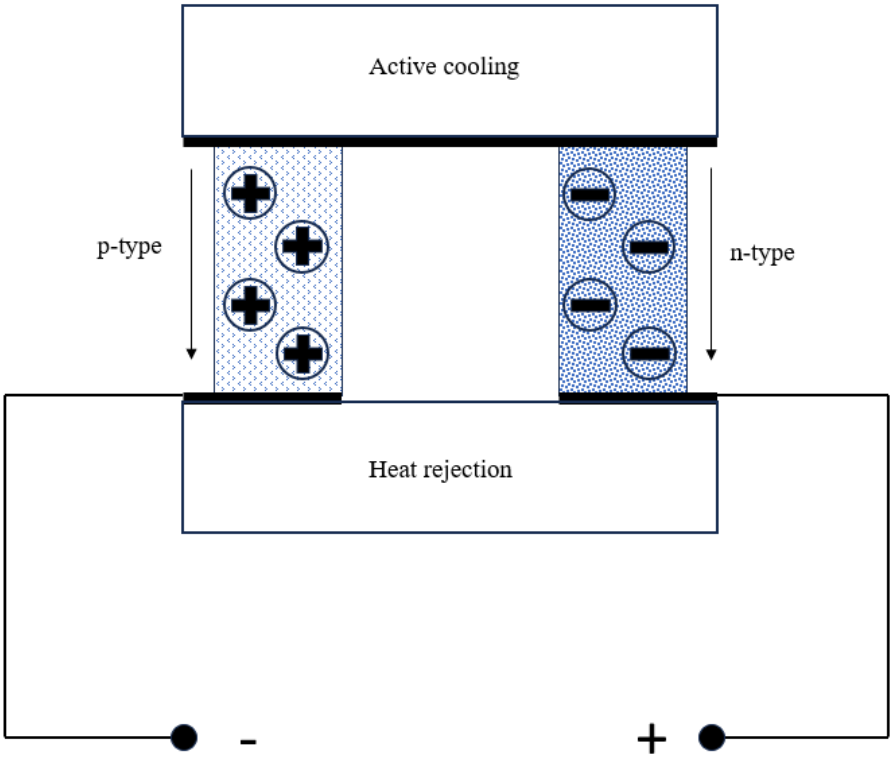

Figure 2.4 Schematic of a basic thermoelectric cooling device. When a DC voltage is applied across the p-type semiconductor the charge carriers (positive holes) move towards the negative pole of the circuit carrying heat with them. At the n-type semiconductor, the charge carriers are electrons which move towards the positive pole, carrying heat. When n-type and p-type semiconductors are connected serially by a conductor in an array, their charge carriers (positive holes and electrons), and consequently heat, will move in the same direction creating a hot junction and a cold junction. Heat is commonly removed from the hot junction using cooling fans and extruded metallic heat sinks.

Heat removal from the hot side of the TEC is critical to achieving the temperature differential, so appropriate heat sinks must be selected. Many types of computer central processing unit (CPU) coolers are commercially available and offer affordable and high performance heat removal. The heat sinks selected were the Hydro Series H55 Liquid CPU coolers (Corsair, Fremont, CA, USA). This model operates with a closed-loop coolant system in which the liquid is pumped

across a copper pad to remove heat from the source (normally a computer CPU). The heated liquid is then pumped upwards to an aluminum heat sink, which is cooled by two high speed fans. The cooled liquid is then returned to the copper pad to remove more heat from the CPU. The system used a three-pin 12 V connection which was made available on the STS-built PSUs. The TEC units were attached to the copper heatsink faces with Arctic Silver thermal paste (Arctic Silver, Visalia, CA, USA) which contained 99.9 % silver in a silicon based paste. This compound allowed good heat transfer between the TECs and the copper heatsinks. Although not an adhesive, the paste was also effective at securing the TECs to the copper face. An aluminum bracket was fabricated in the STS machine shop to allow the heatsink and TEC assembly to sit atop the GC oven. The bracket had two sides sat upon a grooved aluminum plate, which allowed them to be compressed against each other. Threaded rods were placed through holes in the bracket to allow the assembly to be securely tightened, compressing the TEC units against each other. The 15 cm trap used in the initial experiments would be bent to a semicircle form and inserted in between the TEC pads from below inside the GC oven. While holding the trapping capillary in the center between the TEC pads, the apparatus would be tightened by torquing the nuts affixed to the threaded rods of the bracket. Once snug, the trap would be compressed between the TEC pads and suspended from the top of the GC oven. A rendering and image on this setup can be seen in Figure 2.5.

A

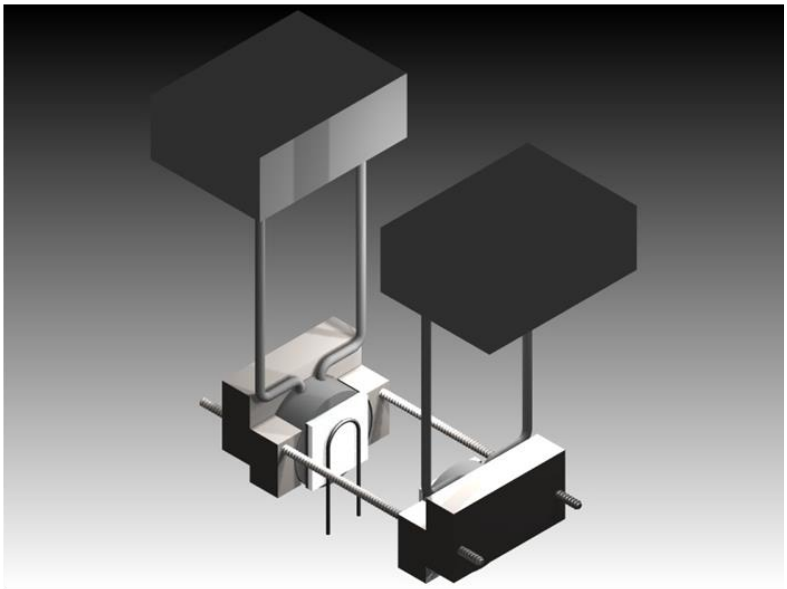

B

Figure 2.5 Rendering A is the conceptual design for the Mk I modulator with the trapping capillary looped up in between the TEC pads from the GC oven. The bracket was designed to securely hold the heat sinks in place while separated and compressed against each other. Image B is a photograph of the apparatus in use. Electrical cables from the TEC devices can be seen drawn up from the center of the bracket away from the heat of the GC oven.

Once the trap was secured within the bracket, alligator clips with exposed copper wire were attached. The wires were connected to the capacitive discharge power supply, which was used to deliver bursts of electrical current to the trap, rapidly heating it. The wires supplying the discharge were required to be bare as oven temperatures commonly used in experiments led to the decomposition of the insulating material. All precautions were taken to ensure the wires were a safe distance from conducting surfaces within the GC oven, and the discharge unit was always unplugged while trap insertion and clip attachments were taking place. In addition, the voltages used never exceeded the safe level (48 V).

2.2.2.2 Trapping Capillary

Building on the success of the work completed by Panič and McNeish, a 15 cm trapping capillary was utilized in the Mk I design. The general trap manufacturing procedure has been described in Section 2.1.1. In this work several trap variants were evaluated. They varied by the amount of stationary phase left remaining in the centre of the trap. The column used in these experiments was an MXT-1 Silcosteel capillary (Restek, Bellefonte, PA, USA) with 3 µm of 100 % PDMS coated internally. The traps were constructed by cutting a 20 cm length of column and flattening the center 15 cm to an outside dimension of 0.36 mm, reducing the internal distance between the walls to approximately 100 µm. The traps were then thermally treated to remove the stationary phase from either side of the section of untreated PDMS at the center of the trap. This was completed by marking the desired length of stationary phase on the trap with a black permanent marker and thermally treating the capillary on either side of it (Figure 2.6). Thermal treatment was completed by attaching alligator clips to the section of the capillary where the stationary phase would be removed. After a compressed air supply had been connected to the capillary, voltage at the capacitive discharge power supply would be increased until the treated

capillary glowed red with each pulse, indicating a temperature of approximately 800 °C had been achieved. A pulse would be applied every 6 seconds until 90 pulses had been achieved. Thermal treatment therefore lasted approximately 9-10 minutes per side of the capillary and around 20 minutes in total.

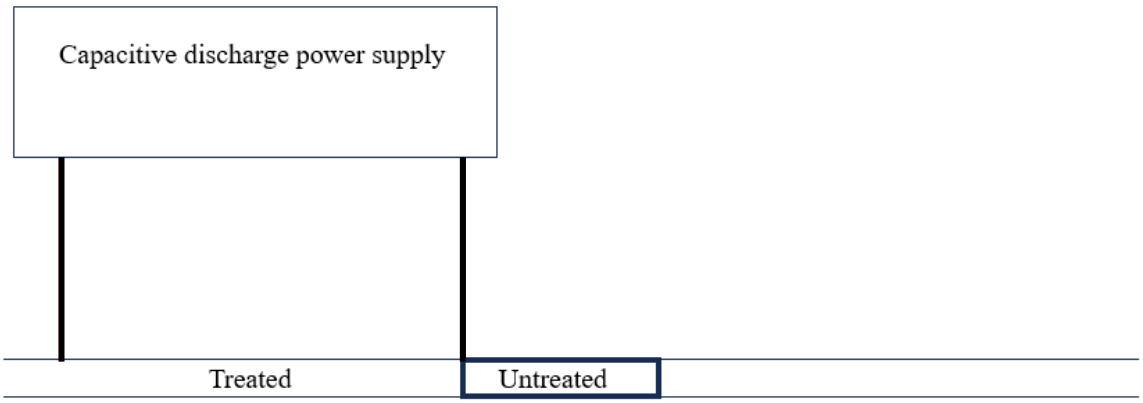

Figure 2.6 When manufacturing capillaries with sections of untreated PDMS, the area to be left untreated would first be measured and marked with a black permanent marker. Next, alligator clips connected to the capacitive discharge power supply would be attached to the capillary and current passed through the section of capillary to be thermally treated. The process would be repeated for the opposite side of the PDMS phase.

Three traps were evaluated that contained 4 cm, 5 cm and 6 cm of PDMS at the center of the capillary, with a total flattened length of 15 cm. All sections of the capillary except for the centre portion containing the stationary phase had received thermal treatment. Chromatographic experiments were completed to determine the ideal amount of stationary phase left in the trap to produce the best chromatographic performance.

2.2.2.3 Chromatographic conditions

A sample of gasoline was acquired from a local gas station and neat aliquots were dispensed into 2 ml GC vials. The column set used was a Rtx-1 30 m x 0.25 mm x 0.25 µm

(Restek, Bellefonte, PA, USA) in the ^{1}D and a SolGel-Wax 0.3 m x 0.25 mm x 0.25 µm (SGE, Sydney, Australia) in the ^{2}D. An oven temperature ramp of 40 °C for 3 minutes, 7 °C/min to 170 °C was applied. One microliter aliquot of the gasoline sample was injected with a split ratio of 100:1. A trap with 8 cm of PDMS coating was used with maximum capacitive discharge and maximum current to the TEC units being applied. A 6 second modulation period was used. A phase shift of -3.2 seconds has been used to display the chromatograms beginning with Figure 2.10.

2.2.3 Results and discussion

2.2.3.1 Capacitive discharge and cooling capabilities

To understand what voltage levels of the capacitive discharge power supply were required to sufficiently heat the trapping capillary, a k-type thermocouple was spot welded to the capillary midpoint and the trap was installed between the TEC devices and compressed. The TEC devices were also turned on and their voltages varied to determine the impact of cooling on trap heating and cool down times. A thermocouple was spot welded to the trapping capillary compressed between the TEC pads to determine its temperature. The procedure to measure temperatures using the thermocouple has been described in Section 2.1.2. Testing of the TEC units and corresponding PSUs revealed a temperature of -20 °C was achievable at the centre of the trapping capillary when maximum power was applied (Figure 2.7).

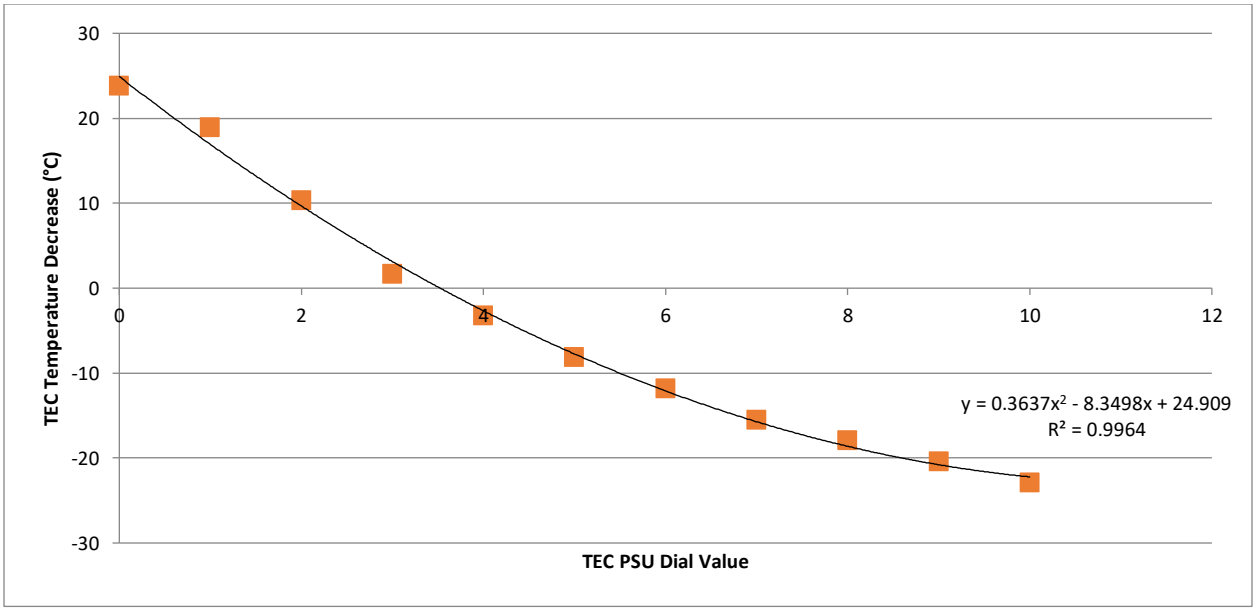

Figure 2.7 Measured temperature of the TEC with increase in current supplied. A dial on the TEC PSU could be set from a level of 0 to 10. A level of 10 supplied the maximum available current (14 A) to the TEC.

The capacitive discharge power supply was evaluated next to determine the voltage required to raise trap temperatures to approximately 350 °C. This temperature was selected as a target due to previous work that demonstrated it was hot enough to thermally desorb analytes from the trap without thermally degrading the stationary phase coating [261]. The 15 cm trap was centred between the TEC pads and capacitive discharge was gradually increased from zero to maximum values with no cooling and maximum cooling capacity being applied (Figure 2.8). The trap was allowed to cool fully before the next discharge pulse was delivered.

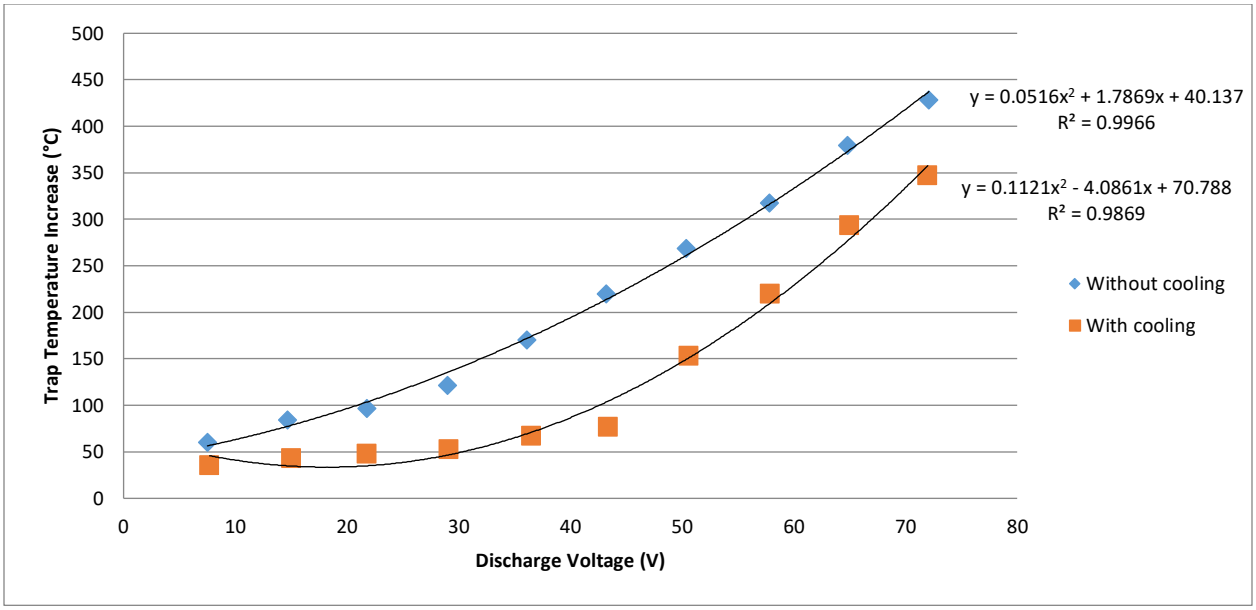

Figure 2.8 Measured increase in trap temperature as a function of discharge voltage with and without cooling being applied.

The results revealed that cooling of the TEC pads had a strong and direct impact on the maximum trap temperature achievable with the capacitive discharge power supply. The 350 °C target was reachable with maximum cooling capacity, but only at the maximum allowable voltage being applied to the trap. Cooldown times of the trap were also measured. Without active cooling used, the trap at all levels of discharge voltage applied would take more than 10 seconds to return to baseline temperature. With maximum cooling applied, the cooling time of the trap with maximum discharge voltage applied was consistently less than 3 seconds. With the thermal properties of the Mk I unit benchmarked, it was time to explore how well it operated as a GC×GC modulator.

2.2.3.2 Chromatographic performance

Initial separation conditions were adopted from a paper describing gasoline separation using a four jet, laboratory built cryogenic modulator [264]. Gasoline was selected as its readily

available locally and offers a challenging set of characteristics for the modulator. High ethanol content tests the modulator's availability to trap highly concentrated and volatile species. Narrow, gaussian-shaped peaks must be generated at the modulator to generate enough resolution in the ^{2}D column to separate the linear alkanes and saturated species from the one-ring and two-ring aromatic species. Pedroso et al. demonstrated an excellent separation of this sample and their chromatograms served as the blueprint for the separation the experiments were designed to achieve [264]. An example of their work can be found in Figure 2.9.

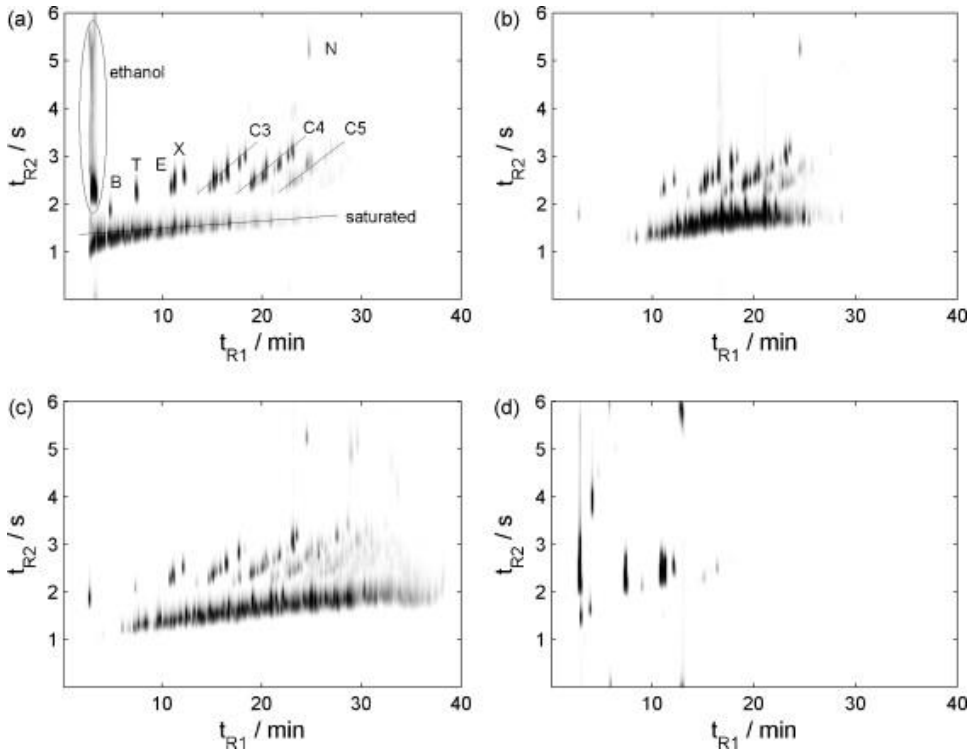

Figure 2.9 Separations of gasoline (A) by Pedroso *et al.*, 2008, which served as the model chromatogram. Also shown are separations of white spirit (B), kerosene (C) and thinner (D) [264].

The first chromatograms generated were very promising and to some extent somewhat expected given the success of Panič and McNeish using the 15 cm trapping capillary. Band broadening of

early eluters was observed, as well as significant wraparound for the aromatic components. Increasing the primary column flow rate reduced the wraparound and improved the resolution in the second dimension, but worsened breakthrough of the earliest eluting compounds (Figure 2.10). Chromatograms in the Figures below begin at time 0 unless otherwise noted.

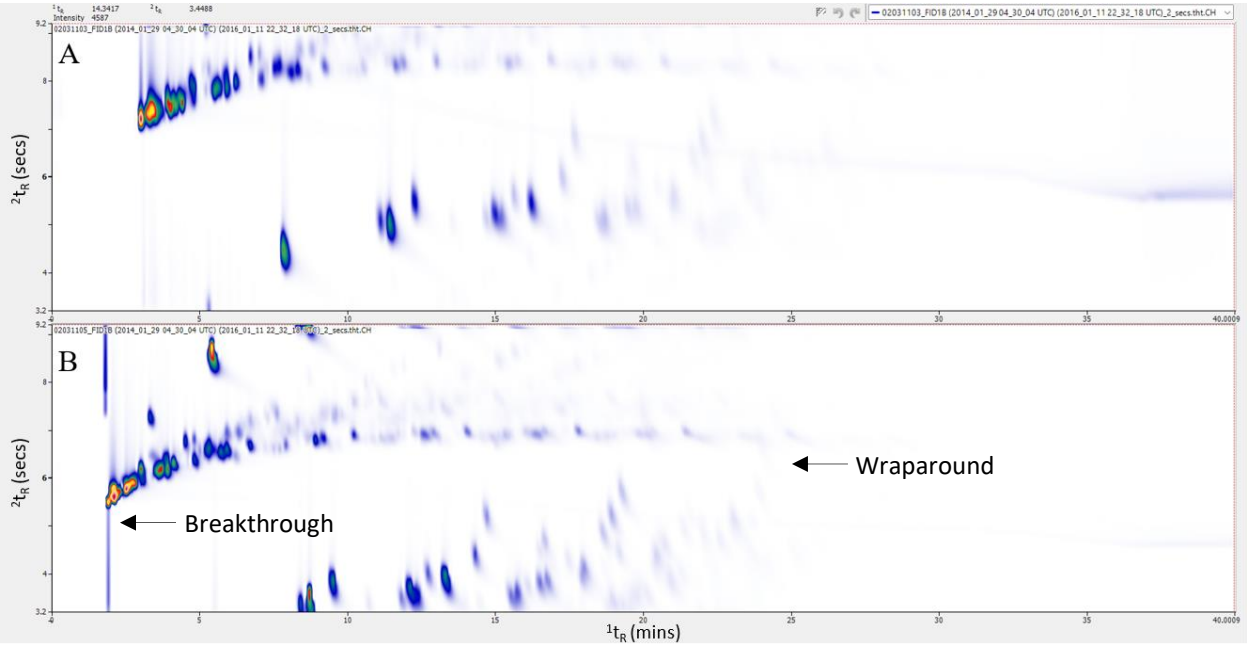

Figure 2.10 100:1 split injection of 1 µL neat gasoline sample with a primary column flow rate of 0.6 ml/min (A) and 1.0 ml/min (B).

The ^{2}D column was replaced with a DB-WAX 0.25 mm x 0.25 µm column of various lengths and a separation more similar to the work of Pedroso et al. was achieved (Figure 2.11).

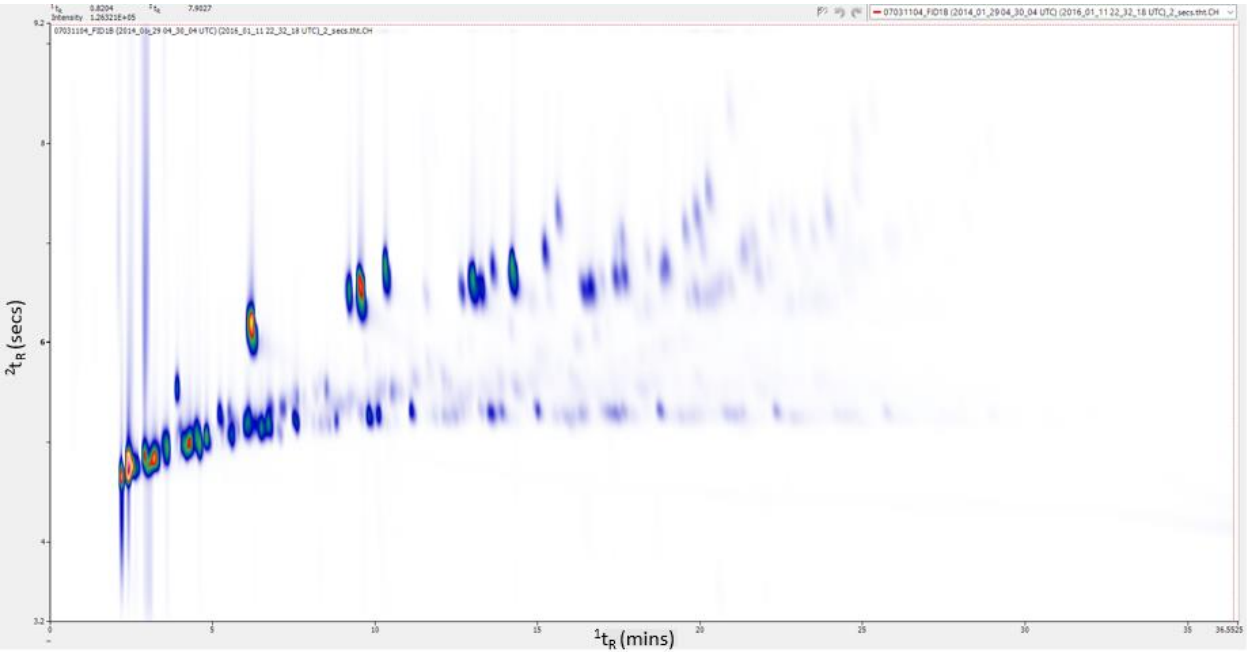

Figure 2.11 Separation of gasoline with a 40 cm x 0.25 mm wax column in the ^{2}D.

Accepting the separation conditions provided sufficiently good results with minimal breakthrough and narrow peak widths, the next component of the system to evaluate was the amount of stationary phase left within the trapping capillary. All experiments thus far had been completed using a trap with 8 cm of PDMS remaining at the centre. Traps were manufactured with 6 cm, 4 cm and 2 cm of material remaining and subjected to the same separation conditions. Peak widths of early eluting compounds were of particular interest to determine if the amount of stationary phase in the trap impacted its ability to trap these volatile species. The results of these tests were very surprising and almost counter intuitive. A visual comparison is shown in Figure 2.12. Peak widths of the earliest eluting compounds were the smallest and exhibited the least amount of breakthrough in experiments using traps with the least amount of the stationary phase remaining (results not shown). Peak widths for the earliest eluting compounds with an 8 cm PDMS trap were commonly around 450 milliseconds (ms) at half height. The 2 cm PDMS trap produced the same peaks with widths at half heights of 120 ms. At this point in the testing of the

Mk I modulator, failure of the heat sink assemblies occurred, which required a reassessment of the overall design. The trap stationary phase experiments were put on hold until this was completed.

2.2.4 Conclusions

The Mk I modulator represented a very good start to the design and evaluation process. The 15 cm trapping capillary designed by Panič and McNeish produced reasonable results immediately. Peltier cooling proved to be a very effective alternative to vortex cooling without the hassle of requiring a compressed air connection or managing ice build ups within the trapping capillary air channel. Separations of gasoline very close to those generated by Pedroso et al. [264] were generated by the Mk I design. For a consumable-free single-stage modulator, this was certainly an accomplishment. There were however some serious flaws with the modulator. Although performance for early eluting compounds was very good, analytes less volatile than n-C_{13} required many modulation events to remove them from the trapping capillary. The TEC devices provided the necessary cooling to trap early eluters, but caused the trap to be too retentive as heaver analytes made their way through the column (Figure 2.13). The level of cooling and heating one could apply to the system was fixed within each experiment and could not be altered throughout the run unless one manually reduced the cooling applied by gradually reducing power supplied to the TEC units. This could be done by turning the dial on the face of the PSU throughout the run. The system lacked temperature programming capabilities.

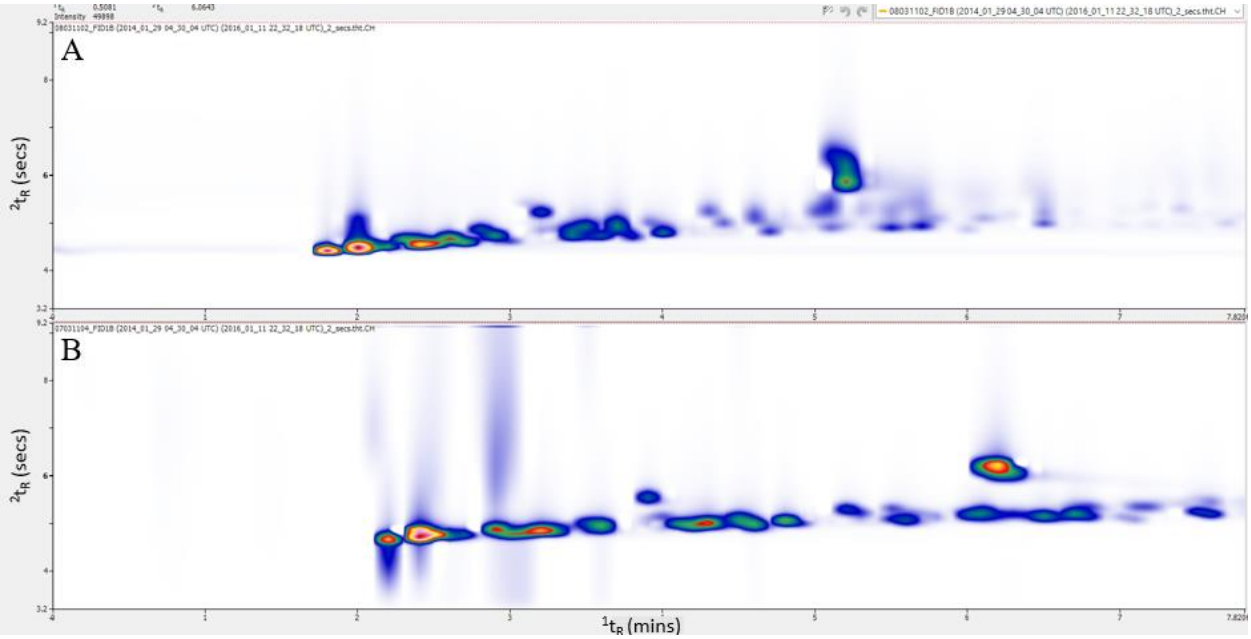

Figure 2.12 Gasoline separations with a 2 cm PDMS trap (A) showing narrower peak widths in the ^{2}D and less breakthrough than utilizing the 8 cm PDMS trap (B). Both experiments were completed under the same injection and chromatographic conditions. A close-up view of the early eluting compounds is shown for greater detail.

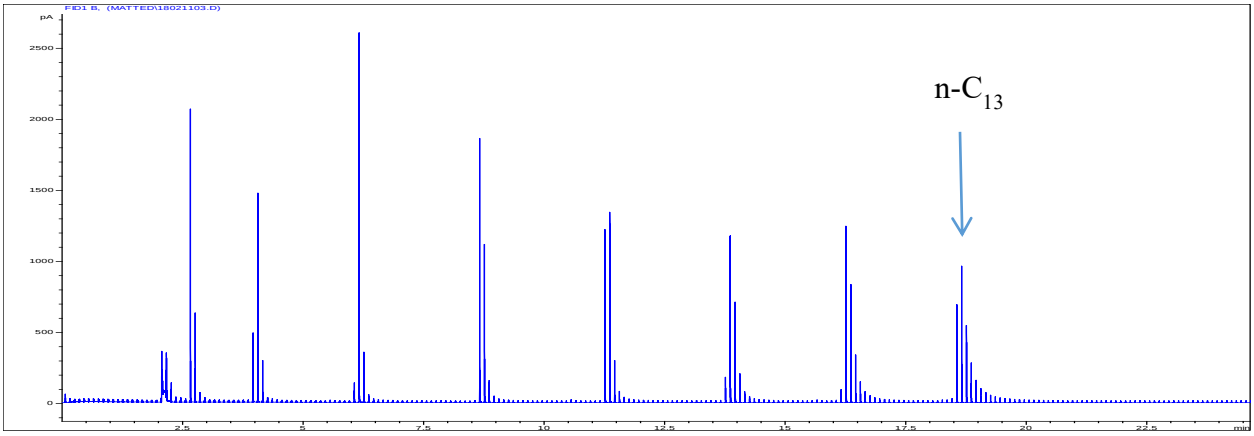

Figure 2.13 A series of linear alkanes shown in the ^{1}D view. An ideal number of modulations per peak (3 to 4) is seen for early eluters. Three to four samples per peak has been demonstrated to be sufficiently frequent to preserve the ^{1}D column separation [33]. The number of modulations per peak grows quickly as the alkanes become less volatile.

In the period of approximately three months since the modulator inception, the heat sink assemblies failed, which made the system no longer usable. The components of the heatsink held closest to the GC oven were made mostly of plastic and these parts failed and caused coolant to leak from behind the copper cooling pads due to continued exposure to the hot GC oven. The TEC devices cannot function properly without the transfer of heat from the hot side, which subsequently caused them to fail as well. This provided a good opportunity to rethink the design of the system and improve on some of the flaws observed.

2.3 Mark II design and evaluation

2.3.1 Introduction

During the first round of experiments the impact that stationary phase content within the trapping capillary had on breakthrough prevention and modulated peak performance was not entirely clear. In addition, premature failure of the CPU heatsinks exposed vulnerabilities in the bracket design which allowed aluminum exposed to hot GC oven air to make direct contact with the plastic CPU heat sink surface. Moving forward to the next iteration of the consumable-free modulator, key design changes would focus on better management of heat exposure from the GC oven to the heat sinks and trapping capillary design.

2.3.2 Experimental

2.3.2.1 Apparatus

With the destruction of the initial set of heat sinks, a new bracket was designed that would allow the insertion of insulation around the heatsink to better protect it from heat. A new heatsink model by Corsair called the H100 Liquid CPU cooler became available and provided a square heat transfer pad which was better suited to the TEC devices. The bracket was redesigned to

raise more of the TEC and heat sink assembly out of the GC oven in an attempt to reduce how hot the assembly would get during a GC run. It was thought that this would also help the heat sinks transfer more heat from the TEC surface as their temperature above the oven should be reduced. In both the rendering and image shown in Figure 2.14, the gap between the aluminum bracket and block can be seen. R20 insulation available in the laboratory from other cryogenic modulator projects was used to surround the heat sink component contained within the bracket. The new heatsinks conveniently provided a four-point surface mount which was used to insert M5 hex head screws into threaded holes within the surface of the bracket. All fabrication was completed by the author in the STS machine shop. An aluminum base plate was fabricated to allow the modulator assembly to fit snug atop the GC oven (Figure 2.15). Two slots were milled into the inner square of the base plate to allow easy access for electrical leads from the capacitive discharge power supply. No changes were made to the TEC devices or capacitive discharge power supply for the Mk II experiments.

2.3.2.2 Trapping Capillary

Later experiments using the MK I modulator implied that better analyte retention and peak shape may be possible with less stationary phase coating within the trapping capillary. It was also observed that to reach the desired discharge temperature of 350 °C, the maximum voltage of the capacitive discharge power supply was required. Another issue with the 15 cm trap was its orientation when compressed between the TEC pads. The flattened side of the trap would be positioned parallel to the direction of the compression such that the pads were touching the narrow side of the capillary. In this orientation the TEC pads were making physical contact with very little of the capillary surface. In addition, when compressing the TEC units against the trap, the capillary would have a tendency to deform and twist so the flattened surface of the capillary

was facing the TEC. This deformation could potentially damage the trap and interfere with the intended internal distance. With these considerations in mind, the decision was made to move away from the 15 cm capillary towards a shorter 7 cm trap. With less than half of the tubing being used, the trap offered significantly less electrical resistance, hence should have been able to be heated to much higher temperatures with less power required. This shorter trap would also allow horizontal orientation with the flat side facing the TEC pads. This would allow better heat transfer and more even compression of the TEC pads along the trap's length without risking physical deformation.

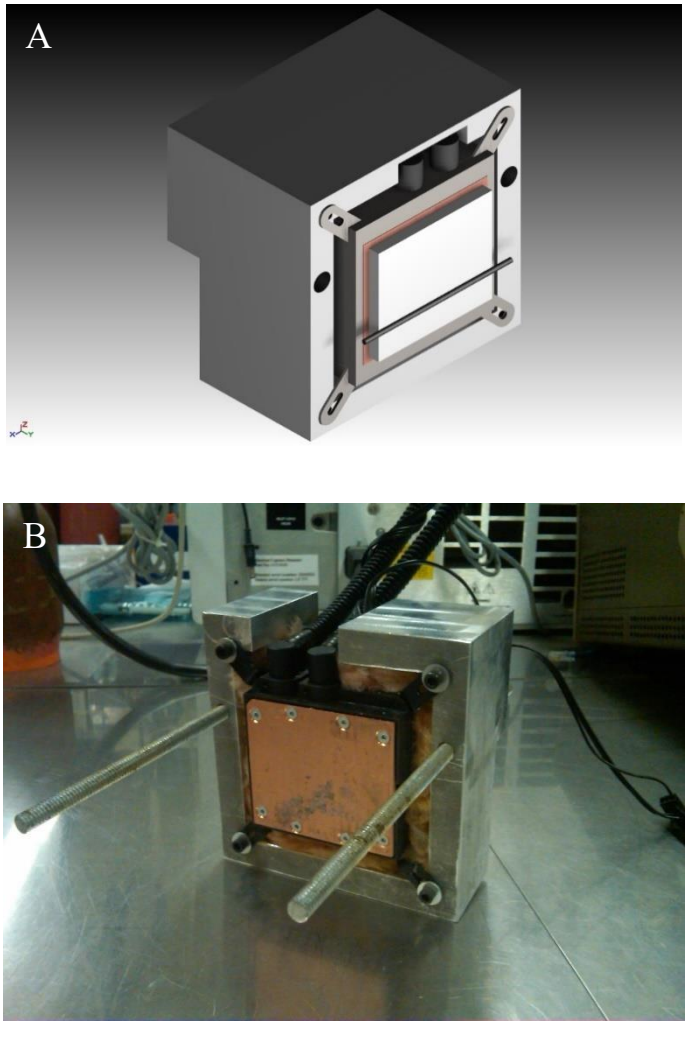

Figure 2.14 Rendering of the Mk II bracket design (A) and image of the finished product (B).

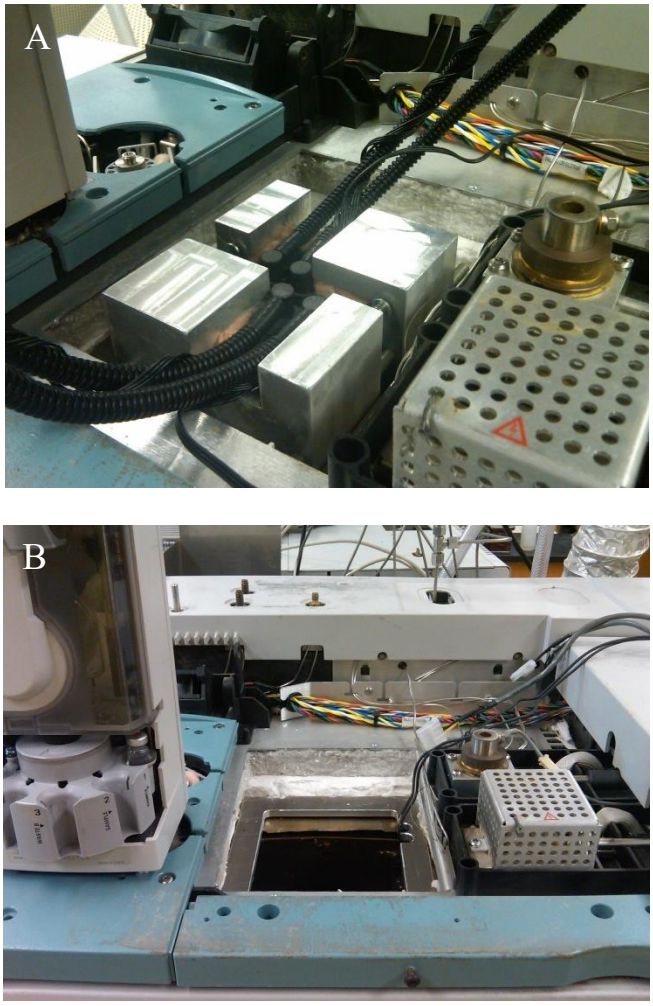

Figure 2.15 Images of the Mk II modulator installed on the Agilent 6890 GC (A) and the unoccupied baseplate that was fabricated to mount the modulation assembly (B).

New shims were manufactured in the STS machine shop to allow a length of 5 cm to be flattened using the previously described procedure. An additional 1 cm of unflattened capillary was left on either side of the 5 cm flattened section to allow nuts and ferrules to be connected. This trap will be referred to as the 7 cm trap herein. Since it had been shown previously that less stationary phase coating within the trap yielded narrower peaks, the decision was made to thermally condition the entire focusing trap and leave no untreated stationary phase behind. The

thermal treatment of the trap needed to be modified accordingly to ensure all phase was removed. Upon successful flattening, the 7 cm capillary was connected to compressed air line with in-line filters. Compressed air was turned on and electrical leads connected to the capacitive discharge power supplywere attached directly to the flattened capillary using alligator clips. The distance between the clips was 7 cm. Electrical current from the capacitive discharge power supply was then passed through the flattened section of the trap every 6 seconds for 10 minutes (100 pulses). The temperature reached at the outside of the capillary during each pulse was approximately 800 °C. This was determined experimentally using the temperature measurement procedure previously described in section 2.1.2.2. After 10 minutes the capillary was removed from the air supply and the clips removed. Stainless steel ferrules and nuts were then installed on the capillary as previously described in section 2.1.1. Once the ferrules and nuts were installed and excess capillary trimmed, the capillary was connected once again to the compressed air line and underwent two more thermal treatments, 5 minutes each. The clips were in this case connected to the fitting nuts. After the first 5 minute treatment, the trap was detached and the direction of air flow was reversed. The second 5 minute treatment was then applied. After the second 5 minute treatment was complete, the trap was removed from the air line and treatment deemed complete. This additional treatment step was devised to ensure that any remaining PDMS stationary phase would be removed before installing the trap in to the modulation system. This would be the first time a trap without any untreated PDMS coating would be evaluated.

2.3.2.3 Chromatographic conditions

For this series of performance evaluation experiments, samples of alkanes and diesel fuel were evaluated. A 600 ppm linear alkane standard with *n*-C_6 to *n*-C_{13} (Sigma Aldrich, Oakville, ON, Canada) was prepared in CS_2. The column set used was an Rtx-1 30 m x 0.25 mm x 0.25

µm (Restek, Bellefonte, PA, USA) in the ^{1}D and a SolGel-Wax 0.3 m x 0.25 mm x 0.25 µm (SGE, Sydney, Australia) in the ^{2}D. An oven temperature ramp of 40 °C for 3 minutes, 7 °C/min to 170 °C was applied. A flow rate of 1 ml/min was used. 1 µl of standard was injected with a split ratio of 75:1. This resulted in 8 ng of each analyte being injected on column. Maximum power was applied to the TEC devices with a trap desorption temperature of 350 °C. A 6 second modulation period was used. For the diesel fuel analysis, the sample was diluted 10:1 (v/v) in CS_2 and an increased split ratio of 100:1 was used. The oven temperature ramp was modified to 40 °C for 2 minutes, 5 °C/minute to 240 °C. Cooling was reduced to 20 % total capacity. The first run applied a trap desorption temperature of 400 °C, with the second run using a desorption temperature of 350 °C.

2.3.3 Results and discussion

2.3.3.1 Capacitive discharge and cooling capabilities

With the trap length shortened and orientation between the cooling pads changed, a new series of temperature tests was required to benchmark the new system. As with the Mk I design, the k-type thermocouple was spot welded to the centre of the trapping capillary and temperature measurements were carried out. For this round of experiments, the temperature of the trap was evaluated without any compression, compression with the TEC devices but without power applied, and temperature of the trap with 25 %, 50 %, 75 % and 100 % power applied to the TEC units. This corresponded to voltages applied to the TEC units of 3 V, 6 V, 9 V and 12 V, respectively. The results can be found in Figure 2.16.

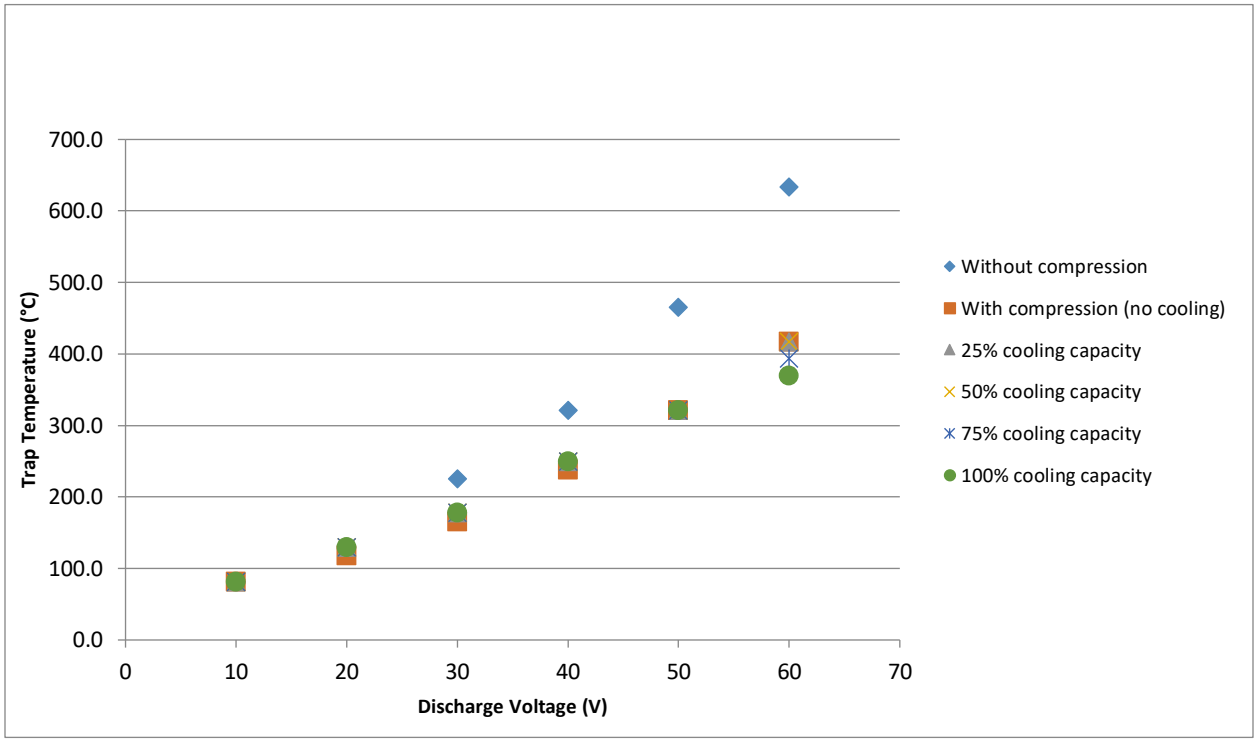

Figure 2.16 Measured increases in the 7 cm trapping capillary temperature at various capacitive discharge and applied cooling levels.

As expected, the temperature increase of the focusing trap at maximum capacitive discharge voltage was much higher with the 7 cm trap than with the 15 cm trap (compare with Figure 2.8). The most striking result was the impact on trap temperature increase that compressing the trap had without any cooling applied. Only at the highest discharge level did the cooling effect of the TEC devices have any real impact on the peak trap temperature. In previous experiments with the Mk I modulator, maximum discharge voltage was required to reach the desired 350 °C. Reduced discharge voltages would be required with this version to achieve that desorption temperature.

Cool down times of the trap were evaluated with the trap compressed and no cooling applied, as well as the trap compressed with various levels of cooling applied. Generating the fastest possible trap cool down times is desirable to prevent breakthrough of analytes into the ^{2}D column. These results are found in Figure 2.17.

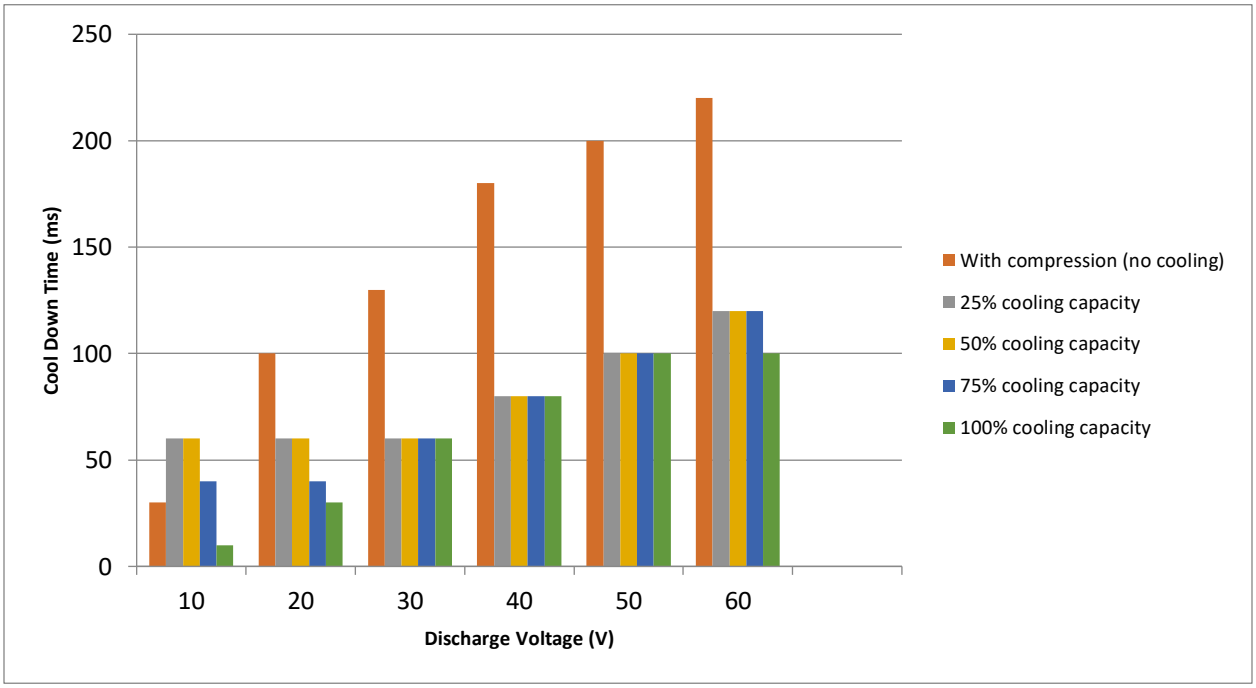

Figure 2.17 Trapping capillary cool down times after a discharge event at various levels of power applied to the TEC devices and capacitive discharge voltages. Experiments were completed at 10 V intervals.

Promising results were achieved with cool down times under 100 ms seen for the first time. These results also showed the meaningful impact that active cooling can have over just compressing the trap. At the highest discharge temperatures any level of applied cooling served to reduce cool down times of the trap. From a chromatographic perspective, fast cool down times are desired to trap analytes entering the trap after a modulation event. A trap remaining hot longer is more likely to allow those analytes to proceed from the ^{1}D column through the trap and

into the ^{2}D column, causing breakthrough. A trap returning to its resting cooled state more quickly is more likely to trap the analytes arriving from the ^{1}D column.

2.3.3.2 Chromatographic performance

The alkane mixture was analyzed and the resulting chromatogram is shown in Figure 2.18. The chromatogram revealed good modulation performance with narrow peaks and a good return to baseline with moderate peak tailing. The solvent (CS_2) suffered breakthrough, but hexane was effectively modulated. As the analytes became less volatile, it was clear that more modulation events were necessary to remove them from the trap. Heptane required four events for complete removal, while tridecane required 10 modulation events. This implied that the cooling effect imparted by the TEC devices, although effective for the early eluters, was too efficient for species above *n*-C_{10}.

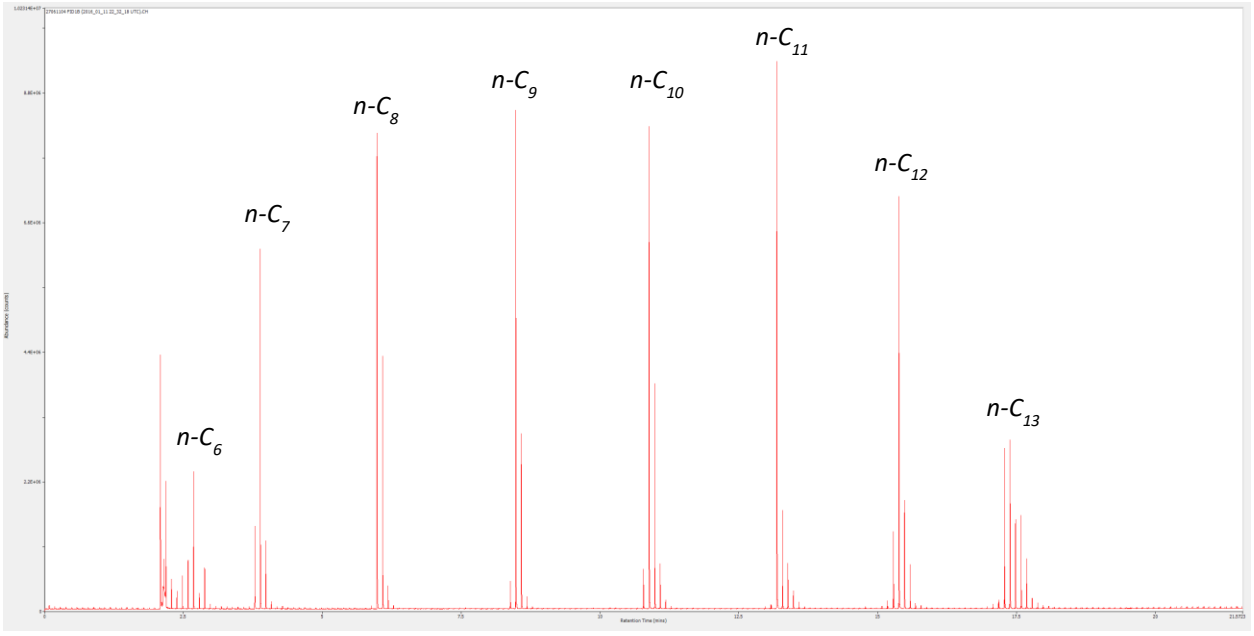

Figure 2.18 1D view of the separation of *n*-C_6 to *n*-C_{13} (8 ng on column).

With the ability to apply more power to the trapping capillary, the impact of raising the desorption temperature above the 350 °C setpoint was explored by evaluating some diesel

samples. Cooling was reduced to 20 % total capacity. The first run applied a trap desorption temperature of 400 °C, with the second run using a desorption temperature of 350 °C. The resulting chromatograms can be found in Figure 2.19. In both experiments, it was immediately clear that reducing the cooling effect was beneficial in liberating analytes with chain lengths greater than *n*-C_{10} from the trapping capillary, as fewer modulation events for these analytes were required. Another observation from the higher temperature desorption run was the presence of siloxanes earlier and in greater abundance in the run than when using the 350 °C temperature. This suggested that the trap material was decomposing more quickly with the higher applied temperature.

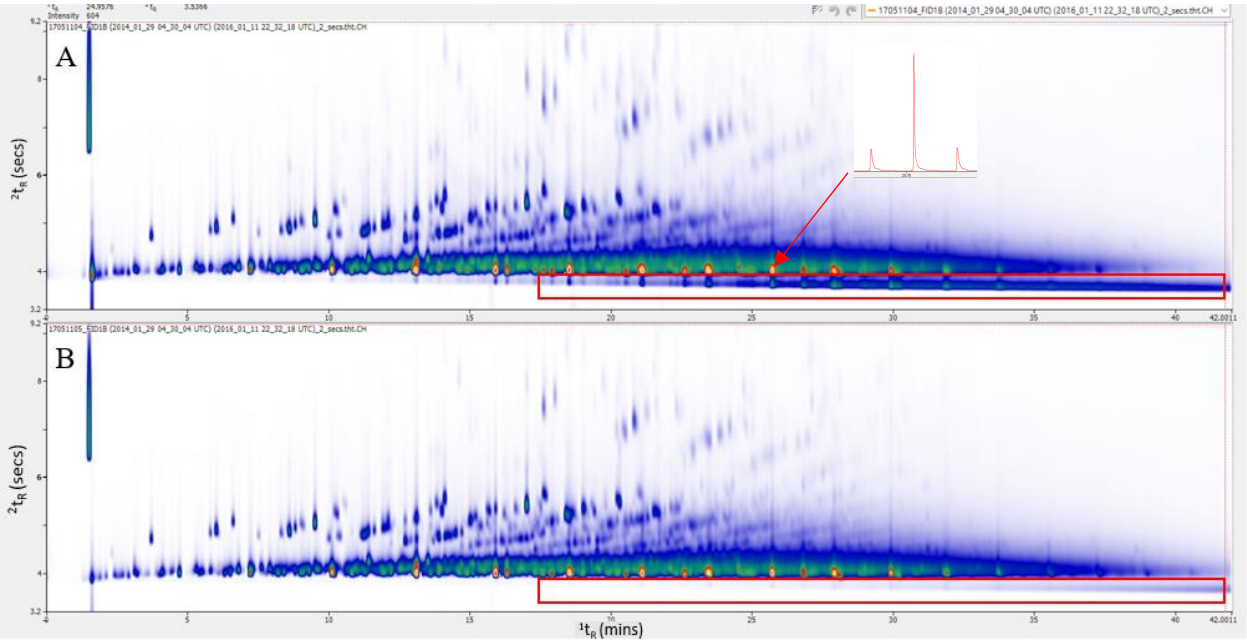

Figure 2.19 Separations of diesel fuel using a trap desorption temperature of 400 °C (A) and 350 °C (B). Siloxanes bleed from the ^{1}D column and trapping capillary is shown in the rectangular box. The ^{1}D profile of the *n*-C_{16} peak is shown in the inset in panel A to reveal that three modulation events were required, an improvement compared to previous results.

These experiments demonstrated that increasing trap desorption temperature had the advantage of producing narrower, therefore taller ^{2}D peaks, but came with the cost of introducing increased siloxane content on the ^{2}D column. Higher desorption temperature also put more mechanical stress on the trapping capillary, shortening trap lifetime. Overall better performance was observed when applied cooling was reduced, allowing the trapping capillary to reach higher temperatures later in the run without increased siloxanes and added mechanical stress. Acquired results suggested that a continuous increase in the trapping temperature maintained throughout the entire run would allow efficient modulation of both volatile and semi-volatile species.

The diesel chromatograms were of sufficiently high quality to proceed with a set of experiments to determine retention time and peak area repeatability of the system. Using the same column set and GC conditions, a sequence of 30 diesel injections was set up to run throughout the week. Although 30 runs had been added to the queue for this study, only 18 runs managed to get completed. The repeated oven ramping to 240 °C resulted in another heat sink failure at the copper cooling pad point, which subsequently let to the destruction of the TEC devices. The 18 runs that were successfully completed were processed in ChromSpace. Three peaks were selected from the chromatogram from different regions that were representative of many other peaks in number of modulations and area. Regions of interest were overlaid on top of the three peaks and their ^{1}D and ^{2}D retention times, as well as peak areas were calculated. A representative chromatogram and location of these peaks can be seen in Figure 2.20. The repeatability of retention times from the diesel replicate experiments was excellent, but peak area repeatability was poor (Table 2.1). Ideally, values closer to 10 % RSD for peak area would be achieved as they routinely are for conventional one-dimensional gas chromatography applications.

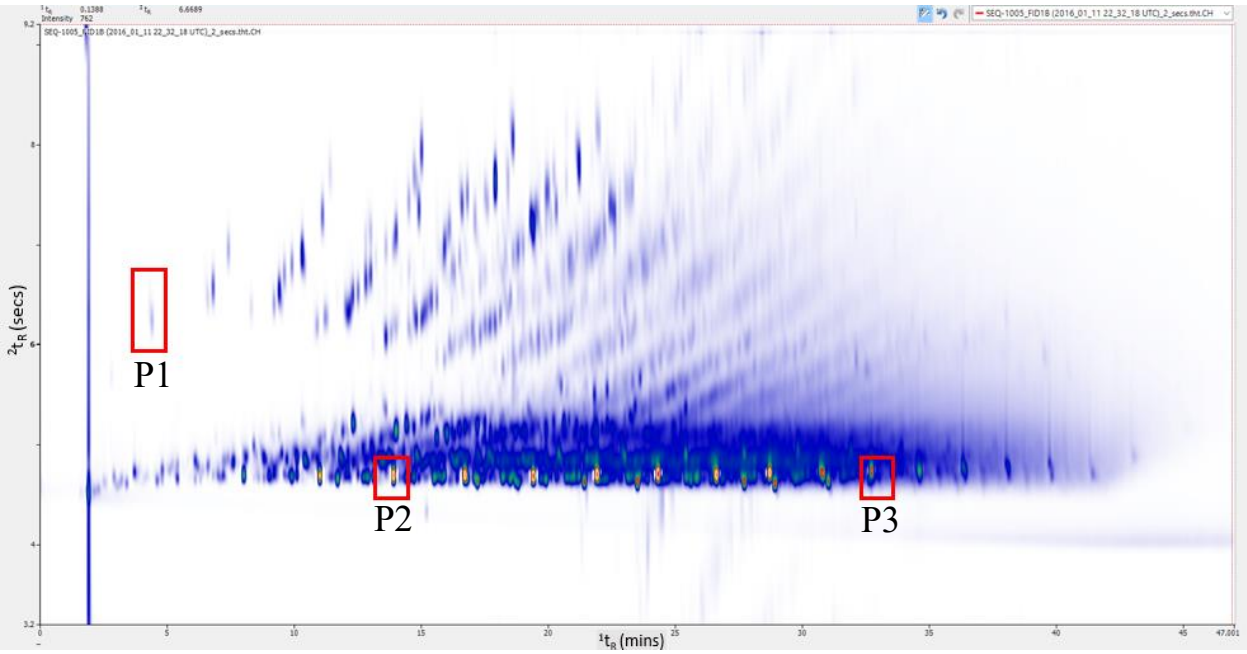

Figure 2.20 Three peaks (P1, P2 and P3) from the diesel separation were selected for closer inspection.

Retention times for the peaks were very reproducible. Integration and merging of GC×GC sub-peaks, which are individual modulated fractions of ^{1}D column eluate, can be challenging for software, especially without MS data to help validate that a sub-peak should be included in the total peak area due to spectral similarity with other sub-peaks. Inclusion or exclusion of sub-peaks during integration may have contributed to varying peak area results. Inconsistent injection volumes could have been a contributing factor. Varying laboratory temperatures also could have contributed to the issue. Insufficient cool down time between runs may have also contributed by not allowing the modulator to reach a baseline temperature before the next injection was made. Five replicates from the 18 run sequence are shown overlaid in Figure 2.21.

Table 2.1 ^{1}D and ^{2}D retention times from three peaks of a diesel separation. Peak areas from these peaks are also listed.

^{1D}	Average (min)	Std. Dev.	% RSD	Std. Dev. In Seconds
Peak 1	4.36	0.00	0.07	0.18
Peak 2	13.90	0.01	0.06	0.47
Peak 3	32.69	0.10	0.31	6.09

^{2D}	Average (s)	Std. Dev.	% RSD	Std. Dev. In Seconds
Peak 1	6.27	0.01	0.14	0.01
Peak 2	4.69	0.00	0.09	0.00
Peak 3	4.74	0.04	0.81	0.04

Peak Area	Average	Std. Dev.	% RSD
Peak 1	8862172.22	1731819.82	19.54
Peak 2	179703261.11	64627329.12	35.96
Peak 3	165087400.00	76465127.55	46.32

2.3.4 Conclusions

Although the lifetime of the Mk II design was short due to the failure of the heat sinks, some important observations were made to inform the design of the Mk III modulator. The most obvious conclusion was that the use of plastic components anywhere near the GC oven was going to eventually result in failure. The heat sinks used were not engineered to withstand the temperatures they were being exposed to, so their use was not sustainable. If the TEC devices were going to be used in the Mk III design, a more reliable method to remove heat would have to be explored. Temperature testing of the trapping capillary revealed that simply compressing the trap was almost as effective as providing active cooling. Given the issues and extra hardware required, was it necessary to provide active cooling at all? The Mk II design allowed a constant voltage to be applied to the TEC devices such that they would provide the same cooling level throughout a GC run. Experiments with linear alkanes revealed that the cooling effect was too strong past the early eluting species and less cooling would actually be beneficial as the GC oven

became hotter and less volatile species entered the modulator. The need for temperature programming of the trap was becoming apparent. Moving away from the 15 cm trap to the 7 cm trap provided more evenly distributed compression along its length and removed the need to operate the capacitive discharge power supply at maximum power. Finally, thermal treatment of the entire trapping capillary was very successful.

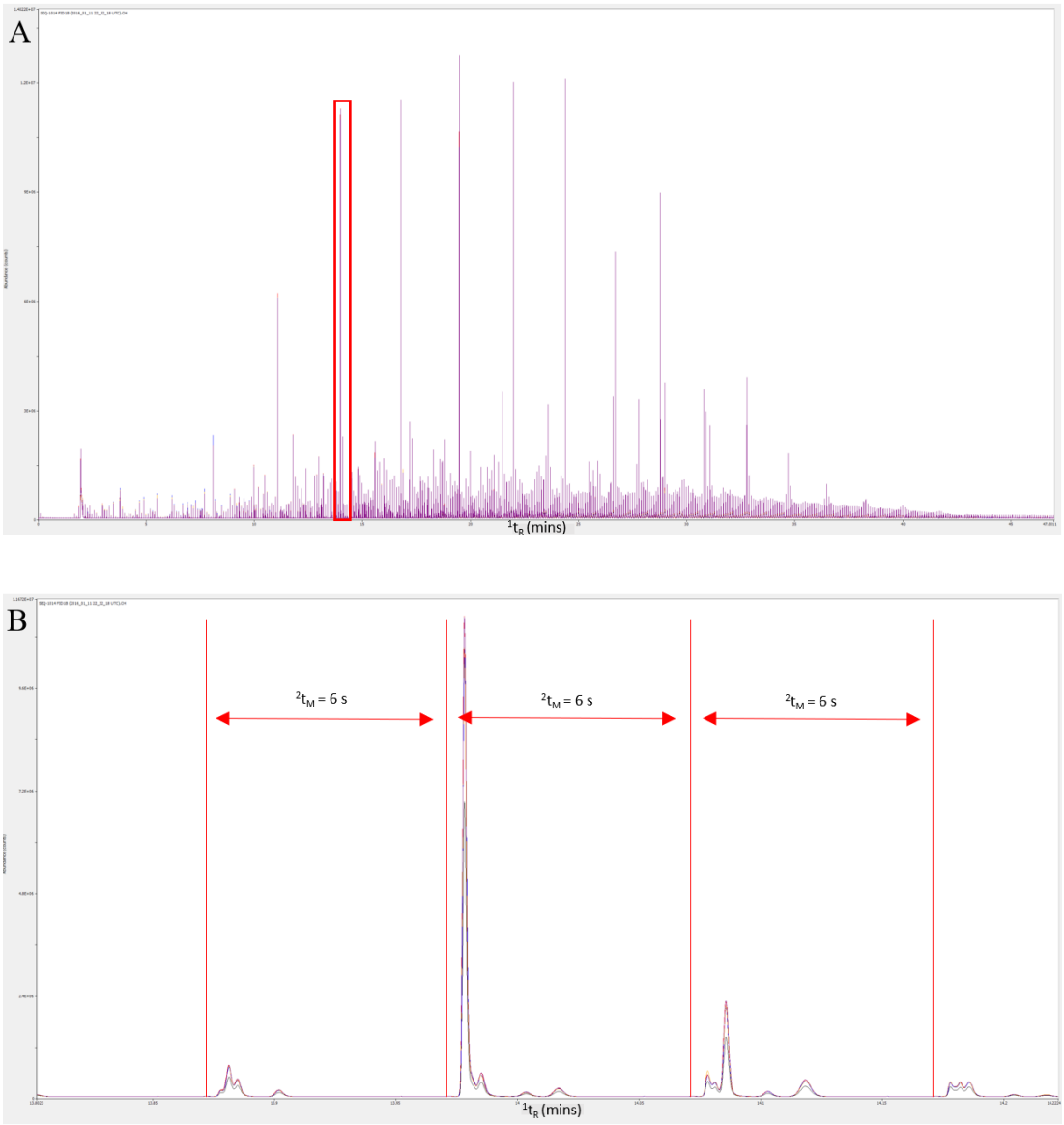

Figure 2.21 Five replicate diesel injections are shown overlaid (A). The red box is a selection of sub-peaks at 14 minutes shown in greater detail below (B).

How could a trap 10 cm shorter with no stationary phase coating perform better than previous designs? The improved cool down times were certainly helping to reduce breakthrough and improve trapping, but how was this possible with apparently no stationary phase coating left? The thermal treatment clearly had an important impact on the sorptive capabilities of the trap. The physical and chemical properties of the trap internal coating before and after thermal treatment would be investigated in detail at a later stage. Moving forward to the Mk III design, the 7 cm thermally treated trap would remain in use for all remaining experiments.

2.4 Mark III design and evaluation

2.4.1 Introduction

Following the second failure of the CPU heatsink assemblies, the decision was made to use more resilient materials for the construction of the Mk III modulator. Focus was also placed on integrating temperature programming capabilities for the cooling system in an attempt to reduce trapping temperatures for higher boiling species.

2.4.2 Experimental

2.4.2.1 Apparatus

Replacing the CPU heatsinks with a suitable alternative was not a simple task. The TEC devices needed to be oriented such that the trap could be compressed horizontally across the surface meaning any heatsink would need to fit behind the TEC, compressed to its hot side. The liquid cooled CPU heatsink units were well suited for this as the fan assembly was oriented away from the cooling copper plate and attached through flexible tubing. More commonly used CPU heatsinks are rigid extruded copper or aluminum structures with large footprints designed to fit within a desktop computer's hard shell. Needing compression as well, the heatsink would require

points where fasteners could be used to attach it to the aluminum bracket. Space is limited above the GC and most units that were reviewed were deemed unsuitable due to size or shape restrictions. An approximately 30 cm length of extruded aluminum heatsink material with a 5 cm wide face was sourced from the STS electronics shop and outfitted to the MK II aluminum bracket. Each half of the bracket was milled out to allow the heatsink, which was cut in half, to be mounted vertically. The bracket offered space between the extruded fins of the heatsink and the bracket itself, which allowed air from the GC oven to be directed over the fins and out to the laboratory atmosphere. While not as efficient as the liquid cooled CPU heatsinks, the new design transferred enough heat away from the TEC devices for them to generate a temperature of 18 °C at the cold side running at maximum capacity. This was a large increase in temperature from previously seen values of -20 °C or greater at the same cooling level. Images of the Mk III design are shown in Figure 2.22. Transfer of heat from the heat sinks to the cooler laboratory air would prove to be a key factor in the performance improvements seen with this iteration. No changes were made to the trapping capillary design or orientation for the Mk II modulator.

2.4.2.2 Chromatographic conditions

For this series of performance evaluation experiments, a 500 ppm linear alkane standard with *n*-C_6 to *n*-C_{40} (C_6, C_8, C_{10}, C_{12}, C_{18}, C_{20}, C_{24}, C_{28}, C_{32}, C_{36}, C_{40},), (Sigma Aldrich, Oakville, ON, Canada) was prepared in CS_2. The column set used was an RTX-1ms 30 m x 0.25 mm x 0.25 µm (Restek, Bellefonte, PA, USA) in the ^{1}D and a DFS column 0.4 m x 0.25 mm (Restek, Bellefonte, PA, USA) in the ^{2}D. An oven temperature of 40 °C, ramped at 6 °C/min to 320 °C, held for 12.33 minutes was applied. A flow rate of 1 ml/min was used. 1 µl of standard was injected with a split ratio of 10:1. This resulted in 50 ng of each analyte being injected on

column. No power was applied to the TEC devices and a trap desorption temperature of 295 °C was used. A 6 second modulation period was used.

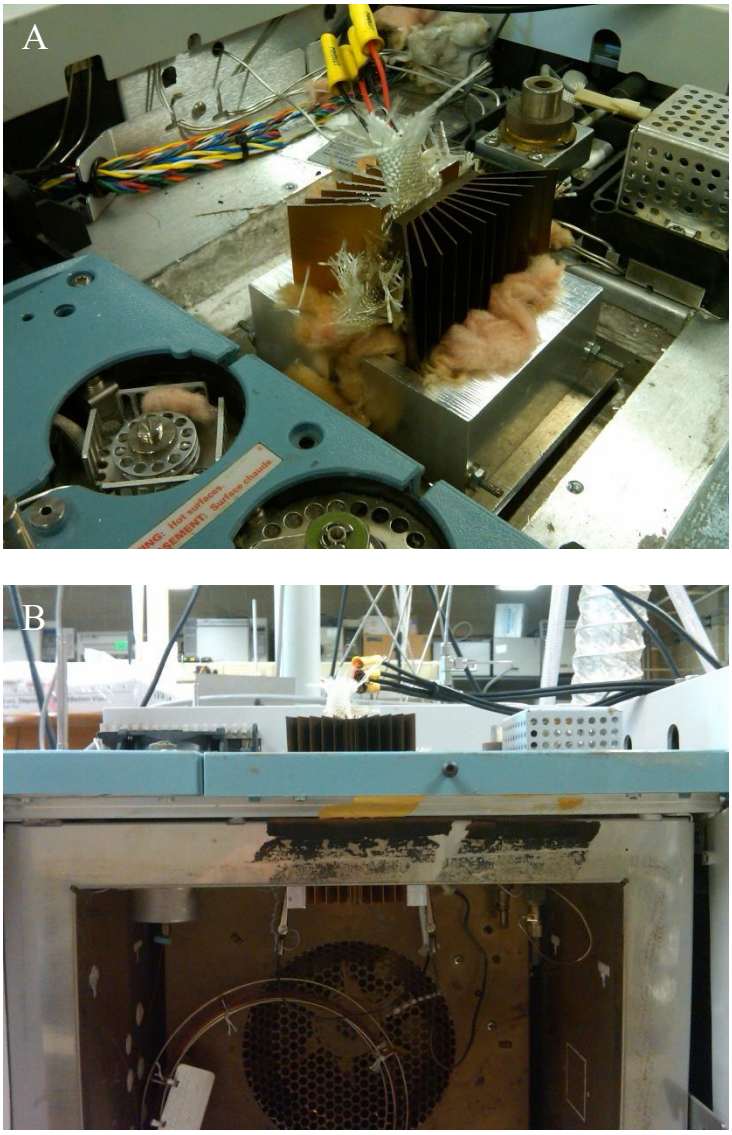

Figure 2.22 The Mk III design featuring the vertically oriented heat sink. Wires connecting the TEC devices can be seen leaving the centre of the assembly and R-20 insulation isolating the heatsink from the aluminum bracket (A). The bottom of the heatsink can be seen extending into the GC oven where oven air was allowed to escape up past the extruded fins into the laboratory (B).

To evaluate an equally complex but different set of samples than petroleum products, a selection of aromatic items were acquired for analysis with the Mk III modulator. Flavour and fragrance samples contain many chemical classes with varying degrees of polarity and concentrations, which makes them a suitable subset of samples to evaluate modulator performance. Preparation of the commercially available Speyside whisky was completed by diluting the whisky with deionized water to a 20 % (v/v) alcohol level. Sodium Chloride was added to obtain a 30 % (w/w) concentration in the solution. From this stock, 12 ml was added to a 20 ml headspace vial and sealed. A 100 µm PDMS SPME fiber (Supelco, Bellefonte, PA, USA) was exposed to the headspace for 10 minutes with constant stirring. A chromatographic system outfitted with a 0.75 mm SPME inlet liner held at 280 °C and column set using a Rtx-1 30 m x 0.25 mm x 0.25 µm (Restek, Bellefonte, PA, USA) in the ^{1}D and a ZB-50 40 cm x 0.25 mm x 0.25 µm in the ^{2}D were used. The oven temperature program was 40 °C with a 5 minute hold, 5 °C/minute to 260 °C, held for 10 minutes. Carrier gas flow rate of 1.8 ml/min was used. Fibers were desorbed in the inlet for 1 minute. No power was applied to the TEC units and capacitive discharge level of 36 V was used. This voltage level would raise the temperature of the trap approximately 140 °C above its resting temperature throughout the GC run. This lower desorption temperature was used due to the absence of late eluting, high boiling point analytes that would have require a higher desorption temperature for effective removal from the trap. The modulation period used was 6 seconds.

The ground coffee sample was removed from a new, sealed package, and a 20 ml headspace vial with 3 grams of sample then sealed. A 100 µm PDMS SPME fiber was exposed to the headspace for 30 minutes with constant but slow stirring of the grains using a magnetic stir bar at room temperature. The cigar was removed fresh from its packaging and split down the

middle with a clean razor blade. Tobacco was not cut or processed in any way before placing it into a 20 ml headspace vial filling it with 3 grams of sample. A 100 µm PDMS SPME fiber was exposed to the headspace for 30 minutes at room temperature. The chromatographic conditions were the same as with the whisky sample except for the oven temperature program which used a starting temperature of 40 °C with a 2 minute hold, 6 °C/minute to 200 °C, hold for 10 minutes. Carrier gas flow rate of 1.8 ml/min was used. Approximately 20 % of available PSU power was applied to the TEC devices and a capacitive discharge level of 36 V was used. This voltage level would raise the temperature of the trap approximately 140 °C above its initial temperature throughout the GC run. The modulation period used was 6 seconds.

2.4.3 Results and discussion

2.4.3.1 Capacitive discharge and cooling capabilities

Testing was conducted to evaluate how this new cooling system performed when cooling the trap throughout a GC run (Figure 2.23). Temperature measurements were taken at the trap as done previously with the TEC devices at full power and receiving no power at all. The trap was compressed between the TEC devices for all measurements. A 5 °C/min oven temperature ramp was used. Oven temperatures were not measured and assumed to be accurate on the digital oven temperature readout of the GC. The experiments revealed that the trap would always lag behind the temperature of the oven. Active cooling with the TECs at full power proved to be far more effective at cooling the trap throughout the run compared to passive cooling. At the final ramp temperature of 300 °C, the trap remained approximately 100 °C cooler with passive cooling and approximately 200 °C cooler with active cooling. The most surprising result was how large of a temperature differential was created between the oven and the trap with no power applied to the TEC devices.

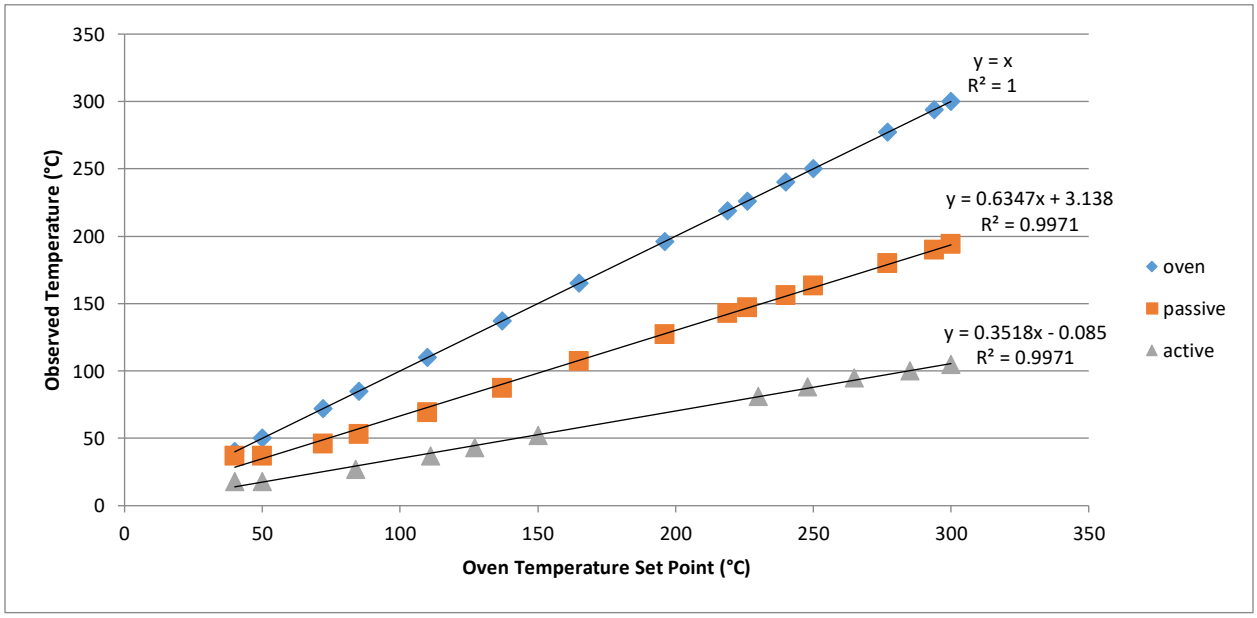

Figure 2.23 Observed temperature of a compressed trapping capillary with passive and active cooling applied at increasing GC oven temperatures.

There appeared to be excellent heat transfer from the heatsink fins to the laboratory air likely due to convection currents generated by the elevated heatsink temperature. The Mk III system was in effect a passively temperature programmed setup. In previous iterations, the TEC devices functioned to keep the trapping capillary at the same temperature throughout the run. Exposing the heatsinks to gradually higher temperatures from the GC oven allowed the trap to become hotter throughout the run, facilitating desorption of later eluting, less volatile compounds. This development was expected to help expand the volatility range of the modulator further into the semi-volatile range.

2.4.3.2 Chromatographic performance

With passive temperature programming looking feasible, a series of experiments were developed to challenge the MK III modulator. One concern with the transition to the new heat sink design was how the unit would perform with low boiling point compounds. Even with the active cooling at full power, the temperature of the trap at 40 °C oven temperature was approximately 23 °C. The Mk II held the trap at -20 °C at this oven temperature. To evaluate the effective volatility range, a 500 ppm solution of linear alkanes *n*-C_6 to *n*-C_{40} (C_6, C_8, C_{10}, C_{12}, C_{18}, C_{20}, C_{24}, C_{28}, C_{32}, C_{36}, C_{40}) was prepared in CS_2. The resulting chromatogram is shown in Figure 2.24.

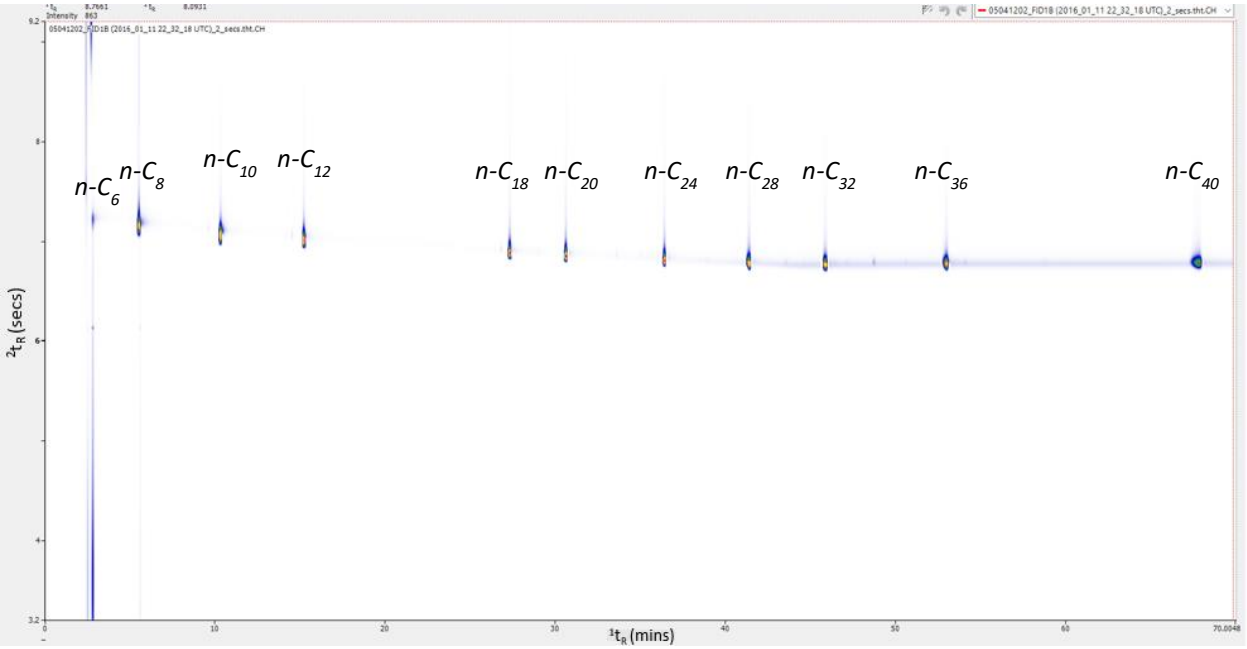

Figure 2.24 A series of linear alkanes ranging from *n*-C_6 to *n*-C_{40}.

To understand the true peak shape eluting from the modulator, a deactivated fused silica transfer line was substituted for a ^{2}D column containing stationary phase. Without any stationary phase interactions, any tailing or other peak deformations could be directly attributed to the

modulator. Peak broadening as a function of diffusion in the carrier gas in the ^{2}D column could have played a role as a contributing factor to ^{2}D peak shape, but since time spent by the analytes in the ^{2}D column was very short (1 second), this likely was not significant. The resulting chromatogram revealed a small degree of tailing in the transfer line. There was minimal observed tailing in the ^{1}D, and each peak was observed to be sampled and modulated the recommended three to four times as described by Murphy et al. [33]. The peak of the latest eluting compound, tetracontane, was wider because it eluted during the oven temperature final hold period. No separation between the siloxane bleed from the first column and the alkanes was observed because no stationary phase was present in the ^{2}D. Previous separations with cooling applied prevented analytes with boiling points higher than that of *n*-C_{20} from being released from the trap effectively. However, with the passive temperature programming, peaks eluting during the oven temperature ramp were released from the trap in 3-4 modulation events. Even the late eluting tetracontane, which was considerably broader due to eluting in the isothermal period at the end of the GC run, required only 6-7 modulation events to be fully released from the trapping capillary. This result was very encouraging and meant that the reduction in cooling together with the new temperature programmed design allowed the volatility range of the modulator to be expanded greatly. As expected, the modulator had difficulty trapping the solvent, hexane and octane without active cooling applied. Perhaps this was a sacrifice that would need to be made if modulation of analytes up to *n*-C_{40} was desired. The 50 ng injection could be considered a relatively large amount of analyte to be injected on column, so perhaps breakthrough at this concentration was to be expected. The same standard was run again with 5 ng injected on column. No breakthrough of hexane or octane was observed (Figure 2.25).

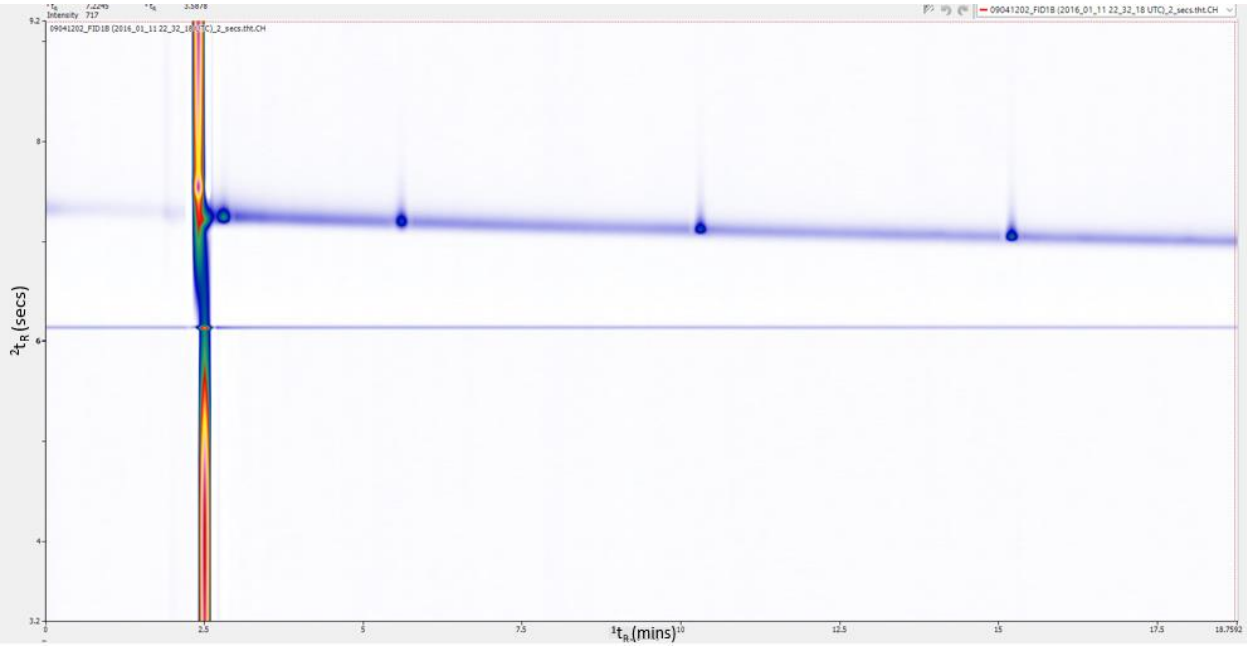

Figure 2.25 Fragment of a chromatogram showing CS_2 breaking through the trap, but subsequent analytes being trapped and injected into the deactivated fused silica transfer line without issue.

This result was encouraging as it implied that samples in the low ppm range of concentration and a volatility range from *n*-C_6 up to *n*-C_{40} could be effectively analyzed with this modulator. That qualified the device for a vast number of petroleum separations. At the time of these experiments, standards and real samples with analytes beyond *n*-C_{40} were not available in the laboratory. Ideally a crude oil sample would have been a good specimen to look at.

With the volatility range now confirmed to be expanded with the Mk III modulator, it was time to test its ability to evaluate some more complex flavour and fragrance samples. A series of experiments were devised to evaluate the aromas of Scottish Whisky, coffee, and cigar tobacco. Using solid-phase microextraction (SPME), aroma collected from the headspace of these complex flavour and fragrance type samples was preconcentrated and injected into the system.

Scotch whisky is a complex sample offering up to 1000 individual components across several chemical classes in the headspace to deliver unique aroma profiles [265]. As such, the headspace of this sample presents a suitably complex sample to challenge the modulator's ability to focus and inject both trace level and highly concentrated species across a wide range of polarities. The resulting chromatogram revealed the complex nature of the headspace, with over 600 individual peaks being detected (Figure 2.26). Breakthrough was observed at the beginning of the chromatogram for highly concentrated, polar volatile components such as ethanol. Overall, though, the separation was acceptable, with only moderate tailing in the ^{2}D column from concentrated analytes such as the (likely) ethyl esters eluting as a series through the middle of the ^{2}D space across the chromatogram. Late eluting analytes appeared to have no issue with modulation.

The next samples to be evaluated were ground coffee from a popular local coffee shop and tobacco from a popular Cuban cigar brand. The resulting coffee chromatogram can be seen in Figure 2.27, and the tobacco chromatogram in Figure 2.28.

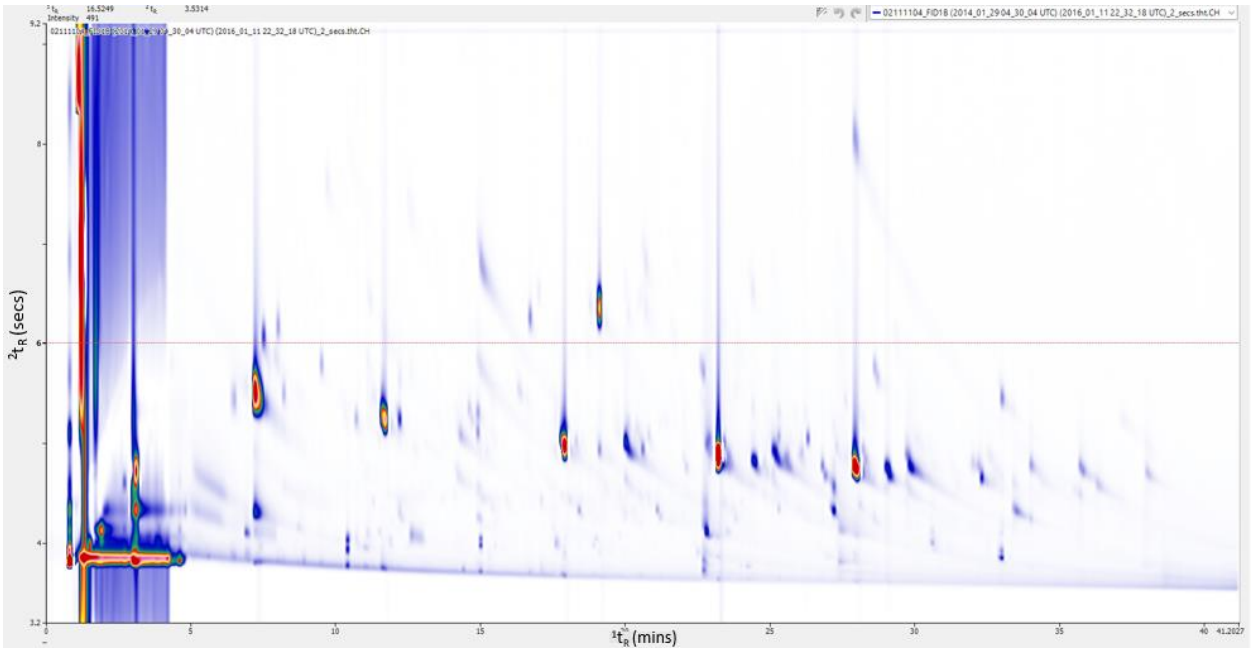

Figure 2.26 A chromatogram of Scotch whisky headspace revealing its complex aroma profile.

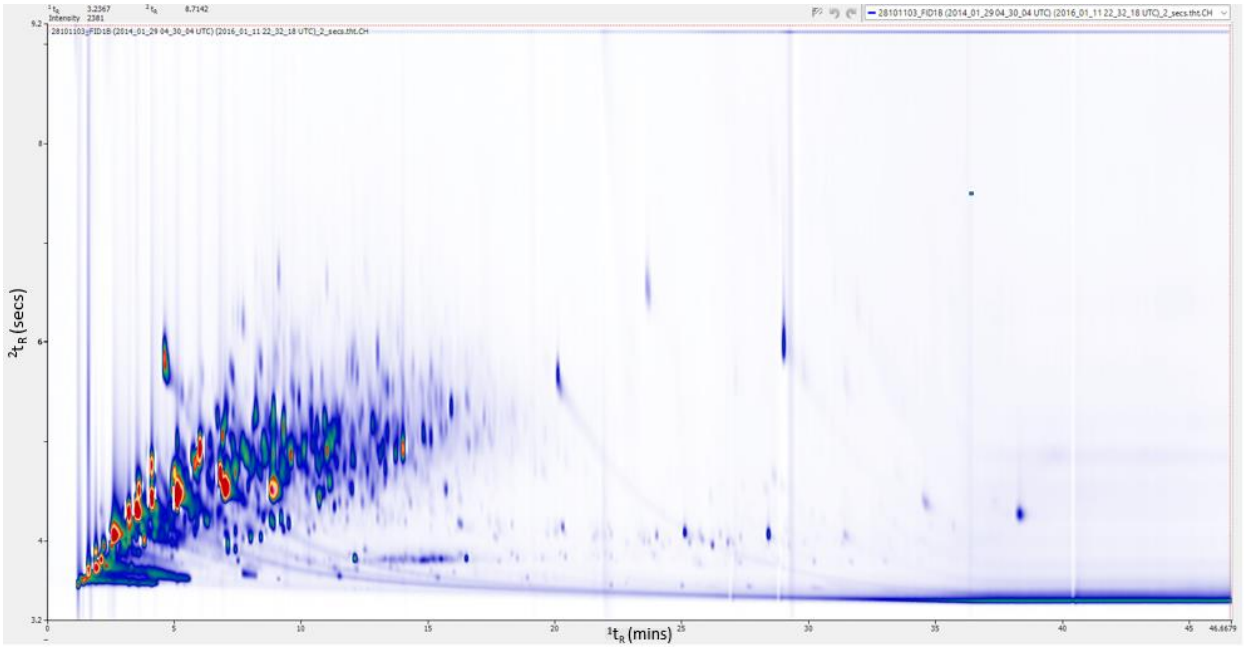

Figure 2.27 A chromatogram generated from the headspace of a fresh ground coffee sample.

Like whisky, coffee offers another complex aroma profile with over 1000 compounds in chemical classes such as ketones, aldehydes, pyrazines, furans and many more [266]. The coffee headspace revealed a highly complex chromatogram with heavier weighting towards the volatile compounds with little semi-volatile content. With this observed in preliminary experiments, the decision was made to apply cooling from the TEC devices to assist with the trapping of volatile analytes. It was excellent to see very limited breakthrough of these compounds even though many of them appeared to be fairly concentrated. A slower temperature ramp and use of a more polar column in the ^{2}D would likely have been beneficial to generate a better separation and utilize more of the two-dimensional space.

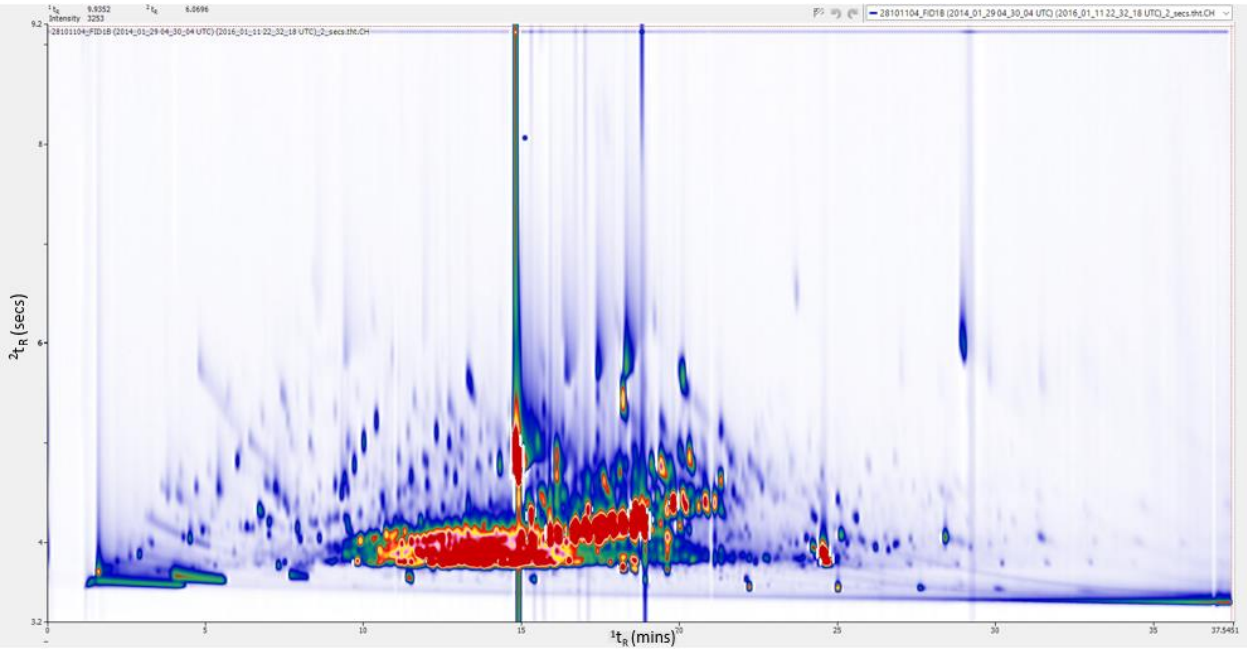

Figure 2.28 A chromatogram generated from the headspace of Cuban cigar tobacco.

Finally, the headspace of a cigar was evaluated, which similarly to the previous two samples offered hundreds of potential VOCs to separate [267]. The resulting chromatogram was very interesting with a greater proportion of semi-volatile content relative to the coffee sample

and fewer concentrated peaks. One particular peak showed significant breakthrough, while the majority of the chromatogram was well modulated. This is another case where a slower oven temperature ramp and longer ^{2}D column would have induced more analyte interactions with the ^{2}D column thereby resulting in an improved second dimension separation. Alternatively, a more polar column such as polyethylene glycol in the ^{2}D would have facilitated many more interactions with the stationary phase and induced greater separation of the abundant polar compounds present. The goal of these experiments was to move away from exclusively injecting non-polar mixes and petrochemicals towards more complex samples in the flavour and fragrance world. A truly universal modulator should have the ability to analyze multiple sample types and chemical classes without much modification, and showing good quality chromatography through these experiments was an important step towards proving that with this modulator.

2.4.4 Conclusions

The Mk III design was the best performing modulator to date and implemented some important new features which made a large impact on the chromatographic separations. The replacement of the CPU heatsinks increased the reliability of the modulator. No breakdowns or malfunctions were experienced during the lifetime of the Mk III unit. Modifying the bracket to fit passive aluminum heatsinks that could be cooled by local convection currents of laboratory air allowed the apparatus to heat up as the GC oven proceeded along its temperature gradient. Enough heat was transferred using this method to keep the TEC devices functional throughout a GC run. Since the heat sinks gradually became warmer in tandem with the GC oven, the TECs warmed accordingly. In this way, passive temperature programming of the modulator had been introduced. The end user could now elect to define the level of cooling they desired for the trap without the consequence of the trap remaining at the same temperature throughout the entire GC

run. More important was the demonstration that using the TEC devices was not always necessary. If the sample was sufficiently dilute in the low ppm range, the Mk III modulator showed that compression of the trap between ceramic pads and a passive temperature program for the apparatus was sufficient to produce excellent quality chromatography. From the performance standpoint, the Mk III modulator was producing high quality chromatography and at this point in the development process it was hard to justify making any new significant changes to the overall design. The 7 cm trap, compression between TEC or ceramic pads, complete thermal treatment of the trapping capillary and passive temperature programming were the key components to this modulator and did not need to be changed significantly moving forward. That being said, the overall design of the unit left much to be desired. The use of threaded rods to tighten the apparatus against the trap was cumbersome and created the potential for uneven compression across the length of the trap. This was noticed when opening the oven after a GC run to reveal one side of the trapping capillary angled lower within the TEC pads. A new system to compress the trap evenly and allow easier installation by the end user was needed. In addition, the use of TECs to compress the trap was not sustainable. These devices were not engineered to receive compression forces and throughout the testing period several units were cracked and required replacement. A more suitable electrically insulative material was needed in the next design.

2.5 Mark IV design and evaluation

2.5.1 Introduction

Design efforts to this point had largely focused on implementing changes to improve sorptive capabilities, volatility range and temperature programming. The Mk III demonstrated very good chromatographic capabilities and the decision was made to not make any new

functional changes, but focus instead on improving the ease of use. The following sections describe the changes made to achieve this goal.

2.5.2 Experimental

2.5.2.1 Apparatus

Compression of the trap between the TECs had proven to be a successful approach, but the TEC ceramic faces were structurally weak and regularly suffered fractures making them unusable. Experiments showed that simply compressing the trap was sufficient to bring down cooling times after heating to low hundreds of milliseconds. Further experiments showed that applying power to the TECs was not necessary to achieve good chromatographic performance; rather, the ability for the trap to stay cooler than the oven throughout the analysis whilst tracking the oven's increasing temperature was the critical factor. The decision was undertaken to remove the TECs from the compressible section of the modulator and replace them with a new material called Macor which is a machinable glass ceramic (Corning, New York, USA) [268]. Macor was selected because it is both compressible and an electrical insulator. It is also able to withstand high temperatures and is easily machinable. Sections of Macor could be milled to the precise tolerances with threaded holes to secure them to metal supports. With an alternative compression material found, a new approach to securing the trapping capillary was needed. During the brainstorming process, the mechanical function of a wooden clothespin became an attractive design concept. Here you have a very simple machine that compresses at one end of the unit while maintaining tension at that point using two lengths of wood and a spring. If the Mk IV could adopt the same design concept, the end user would simply need to pinch the top of the assembly to open the compression section, slide in the trapping capillary and release the top of the modulator to compress the trap. This design would also allow even compression along the

length of the trap if tension could be applied evenly at the top of the modulator. With these factors in mind, a new design was conceptualized and drafted. The final rendering of the Mk IV design appears in Figure 2.29. This assembly consisted of two rectangular copper plates that served the same purpose as the wooden lengths from the clothespin. Copper was selected over aluminum as it provided better thermal conductivity. The Macor pads were affixed to the bottom of the copper plates equipped with heatsinks at the top. At its centre, a barrel and pin assembly was attached to connect both pieces of copper together in a hinge-like mechanism. Above this pivot point, springs were compressed and installed.

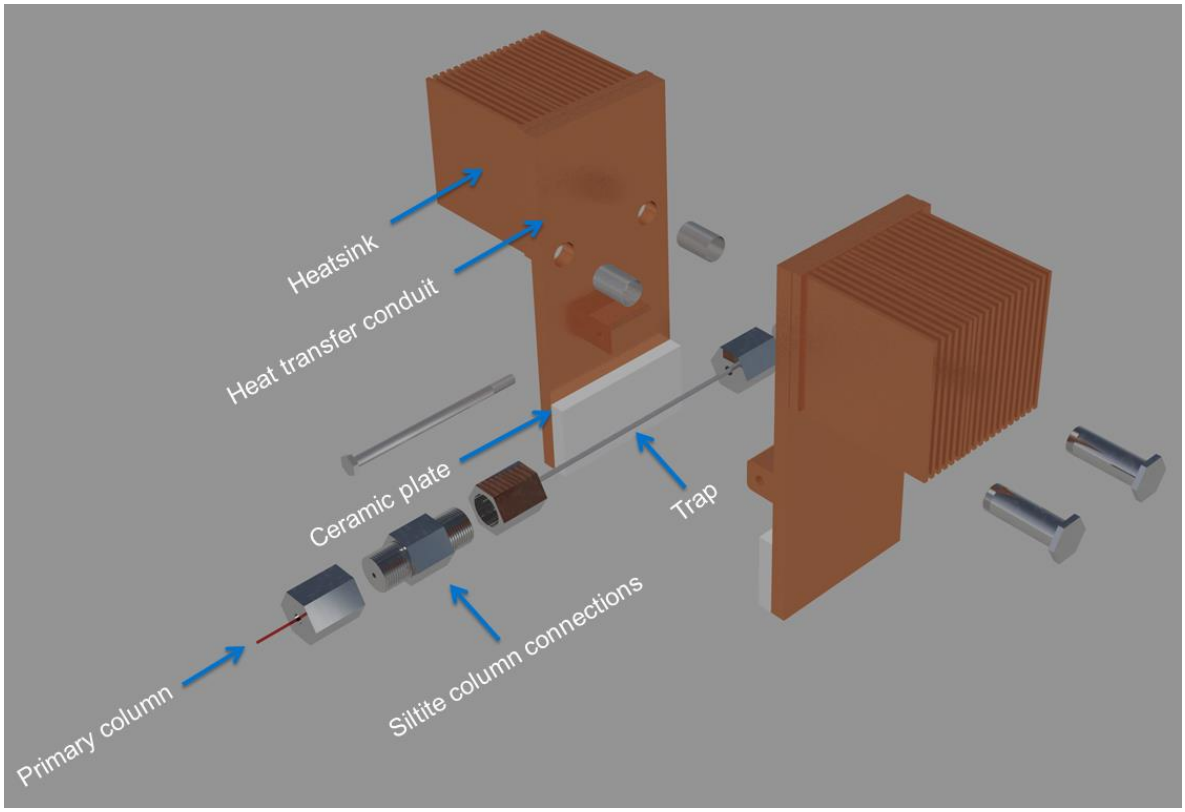

Figure 2.29 Rendering of the Mk IV modulator design showing where the Macor pads were located relative to the heat sinks.

Threaded holes in one of the copper plates allowed bolts to be secured inside the springs, while through holes in the other plate allowed that plate to move freely over the bolts when the modulator was pinched at its top. Images of the MK IV installed on a GC can be seen in Figure 2.30.

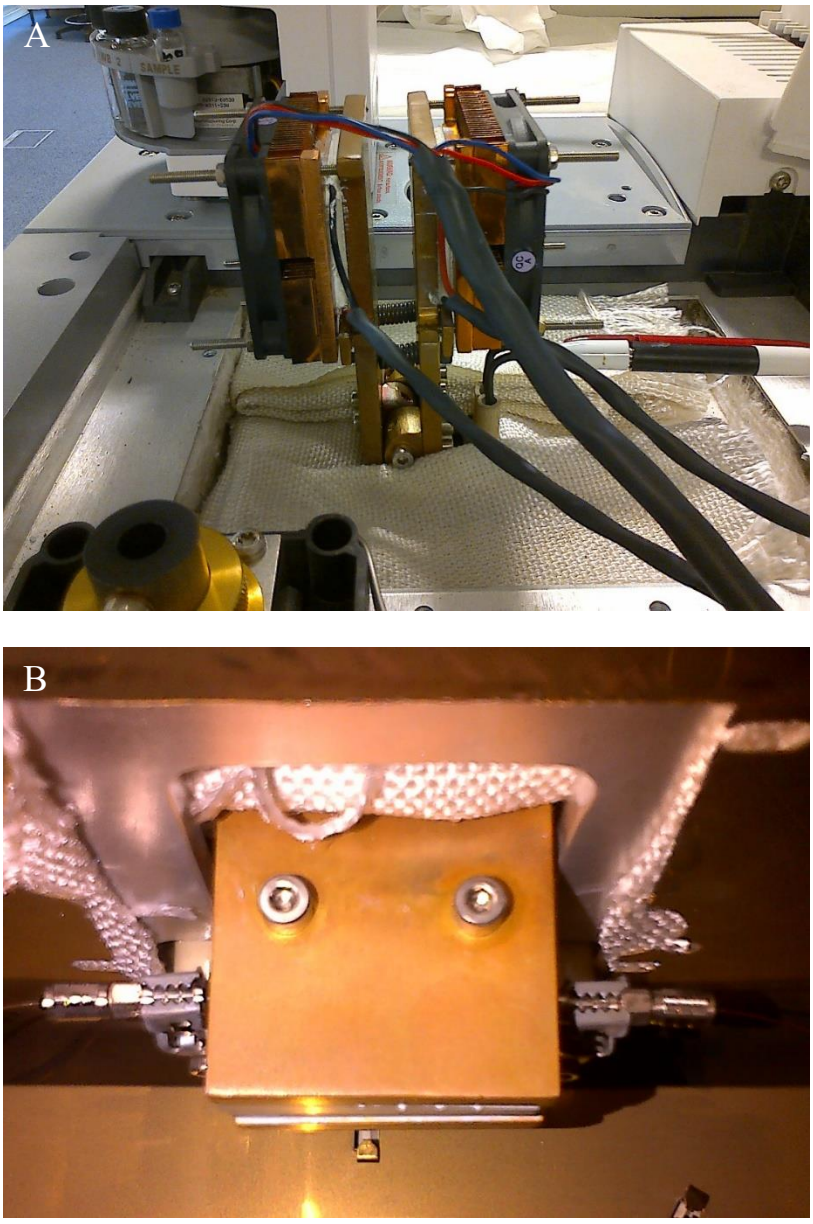

Figure 2.30 A side view of the Mk IV design as seen from the top of the GC oven (A) and a view from inside the GC oven showing the mounting bracket, Macor pads and alligator clips used to deliver current from the capacitive discharge PSU to the trap (B).

The TEC units were affixed to the top of the apparatus with active heat sinks. Although the heatsink fans were vulnerable to heat from the GC oven, they were located sufficiently far away to prevent heat damage. The use of TECs in this assembly created a cold finger effect where a thermal gradient was generated from the top of the copper plates to the bottom located in the GC oven. Heat would be drawn away from the Macor pads, but given that a third of the assembly was located inside the GC oven, the exposure to hot GC oven air would gradually heat the unit throughout the analytical run maintaining the passive temperature programming capability.

Further consideration was given to protecting the end user from coming into contact with any source of capacitive discharge or TEC power supply. All cables were contained within insulative sheaths and a banana connector system was devised to easily separate the capacitive discharge cables from the main assembly. Sturdy high gauge solid copper wiring was used within the oven where it attached to a pivot assembly which allowed the alligator clips to swivel 90 degrees for easy attachment to the stainless steel unions of the trapping capillary. Fiberglass mats were overlaid on the modulator assembly bracket protecting the end user from exposure to hot surfaces. The compressed springs provided sufficient tension to keep the trap in its place between the Macor pads for many subsequent runs. Even compression along the trap length was now assured. The Mk IV design integrated all necessary performance enhancing changes while keeping a focus on safety and ease of use. However, testing was needed to determine how it compared with the successful Mk III prototype.

2.5.3 Results and discussion

2.5.3.1 Capacitive discharge and cooling capabilities

Initial experiments focused on differences between the passive and active cooling capabilities of the modulator. As was done for the previous three prototypes, temperature

measurements taken from the centre of a compressed trapping capillary were collected. In this round, data was collected at three different temperature ramp rates of 3 °C/min, 6 °C/min and 9 °C/min. The data can be seen in Figures 2.31, 2.32 and 2.33, respectively. The relationship between oven temperature set point and observed temperature was linear as shown in the following Figures. The relationship between oven set point and observed temperature of the trapping capillary was best described by a line of best fit using polynomial equations, which are displayed in each Figure with their corresponding R-squared values.

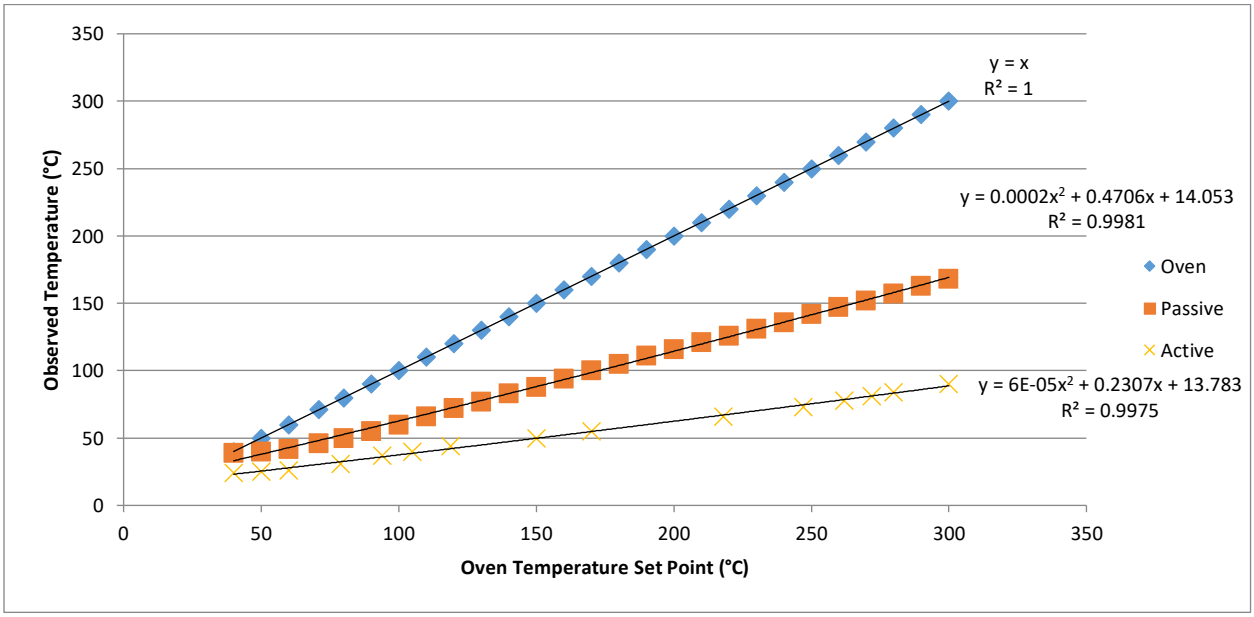

Figure 2.31 Observed temperature of a compressed trapping capillary with passive and active cooling applied at GC oven temperature increasing at 3 °C/minute.

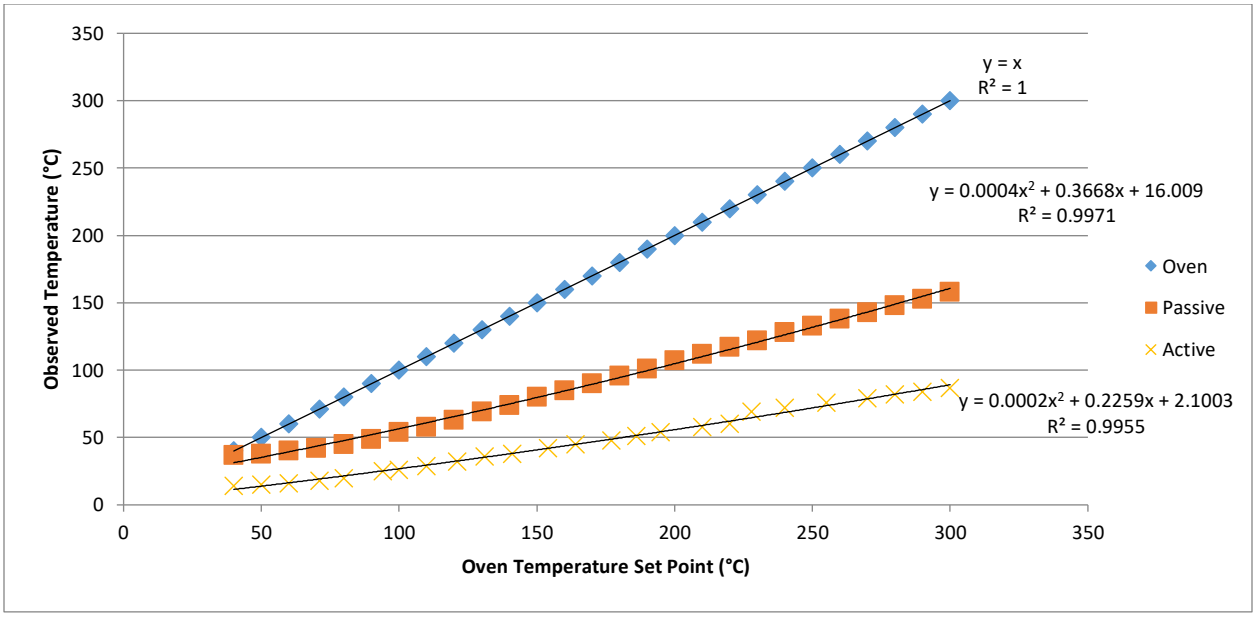

Figure 2.32 Observed temperature of a compressed trapping capillary with passive and active cooling applied at GC oven temperature increasing at 6 °C/minute.

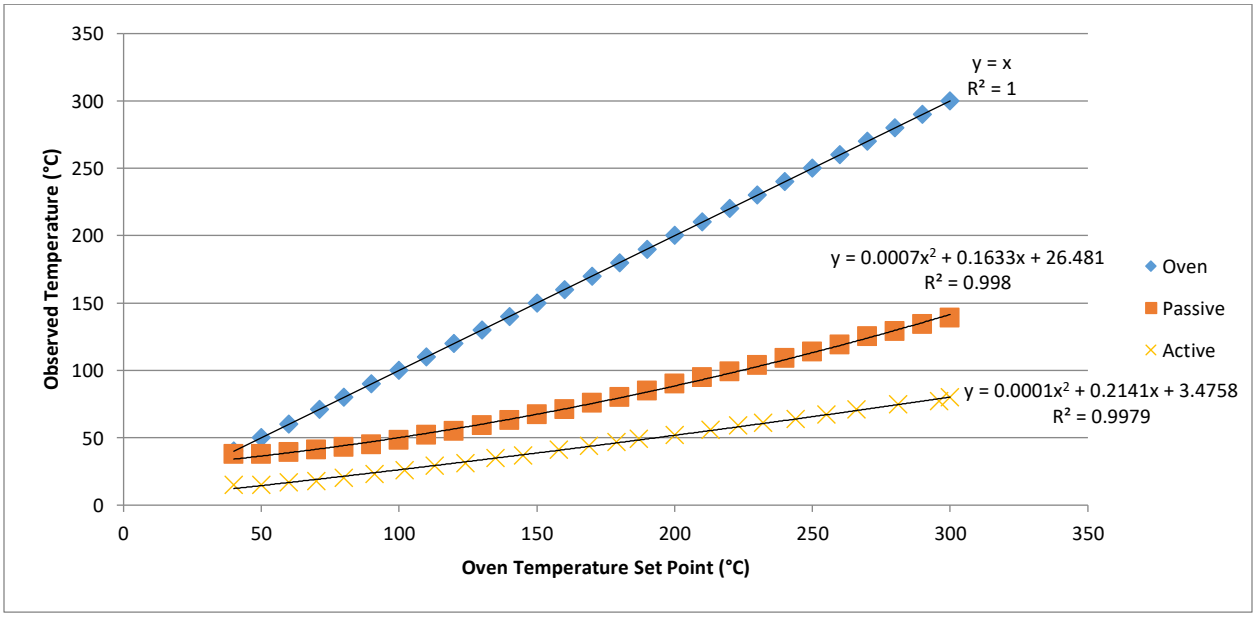

Figure 2.33 Observed temperature of a compressed trapping capillary with passive and active cooling applied at GC oven temperature increasing at 9 °C/minute.

When passive cooling was applied, the trap temperature difference between the 3 °C/min ramp and 9 °C/min ramp at the end of the GC run time was less than 30 °C. That margin was much smaller when the TEC units were activated and the trap temperature diverged less than 10 °C at the end of the run across the three temperature ramps. It was also clear that the addition of TEC units to the copper modulator plate was an effective method of cooling the Macor pads compared to passive cooling only. Another observation was that temperature programming was possible without the use of hot air passing through the heat sink body. Exposure of the copper plates to the oven was enough to gradually raise the modulator temperature during the GC run. In the interest of comparing the cooling performance of the Mk III to the Mk IV, temperature measurements from both modulators were plotted on the same chart. The comparison of each unit using passive cooling is shown in Figure 2.34, and using active cooling in Figure 2.35. The resulting comparison revealed that performance between the two modulators was very close, with the Mk IV slightly outperforming the Mk III in both passive and active cooling applications. A 34 °C difference was found between the Mk III and Mk IV units at the end of the 6 °C/min GC run. The difference was much smaller when looking at active cooling at just 18 °C. This was a good result as the Mk III performed very well and the goal of the Mk IV was not to improve or change its trap cooling behaviour, but to try and replicate it while improving safety and ease of use. These experiments suggested that this goal had been accomplished.

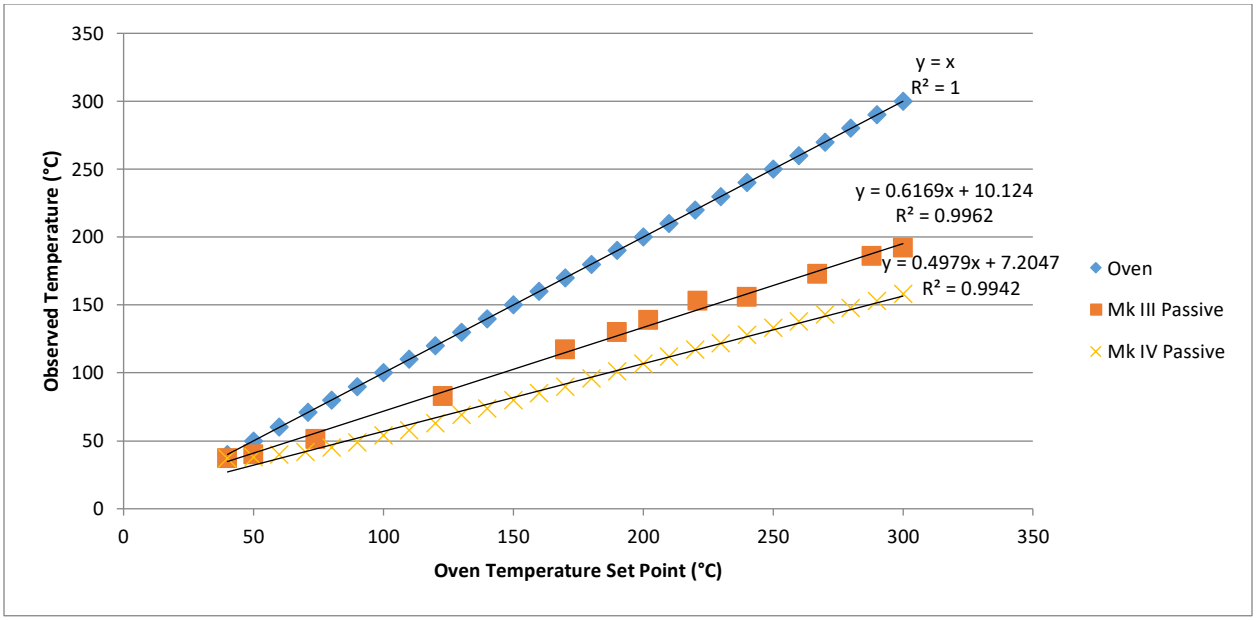

Figure 2.34 Comparison of the impact of passive cooling from the Mk III and Mk IV modulators on a compressed trapping capillary temperature at GC oven temperature increasing at 6 °C/minute.

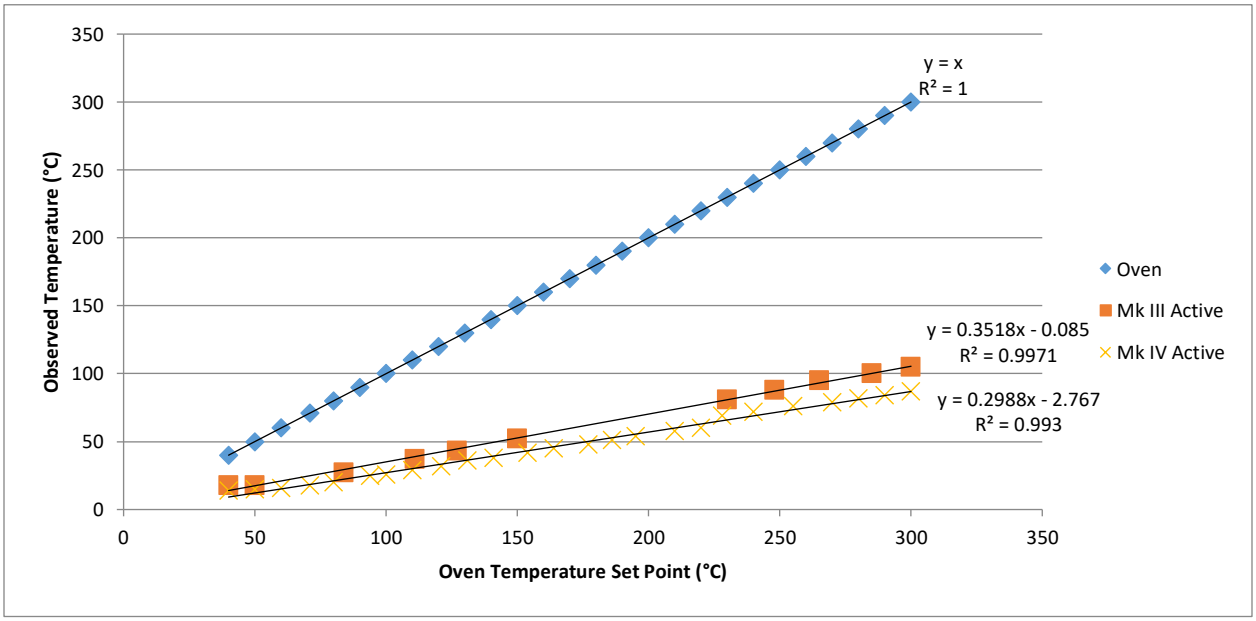

Figure 2.35 Comparison of the impact of active cooling from the Mk III and Mk IV modulators on a compressed trapping capillary temperature at GC oven temperature increasing at 6 °C/minute.

2.5.3.2 Chromatographic performance

The Mk IV modulator was not benchmarked chromatographically in the same way as the previous three iterations. Thermal testing suggested its performance was effectively the same or slightly better than the high performing Mk III unit. Instead, the opportunity to work closely with collaborators to test the device in real-world applications presented itself. The results of these experiments are described in detail in Chapter 4, which is dedicated to the applications of the modulator.

2.5.4 Conclusions

New features, designs and materials were introduced into the Mk IV design. The changes led to a more robust modulator with the smallest footprint yet. Simple mechanisms were integrated to ease trap installation and minimize exposure of the end user to electrical contacts. With volatility range expanded to *n*-C_6 to *n*-C_{40} and validation that performance was excellent for multiple chemical classes and sample complexities, the main goals that were set out at the beginning of the modulator design process had been accomplished. Chapter 2 has described design changes and thermal properties of the modulator. Chapter 3 will be dedicated to understanding the trapping capillary and its key role in the modulator's performance.

Chapter 3. Understanding the impact of trapping capillary thermal treatment

3.1 Introduction

Early in the design process it became clear that shorter trapping capillaries exposed to complete thermal treatment of the stationary phase provided superior trapping capabilities (Section 2.2). Shorter traps were also easier to heat and cooled more quickly. Initially, the trapping effect was confusing and counter-intuitive, with less stationary phase within the trapping capillary observed to be more sorptive and better performing than having more stationary phase. To understand the impact the thermal treatment was having on the trap's stationary phase chemistry, a series of experiments to look more closely at the phase itself were devised. Scanning electron microscopy (SEM) was deployed to visualize the effects of flattening and thermally treating the capillary. This technique scans the surface of a material with a focused beam of electrons and then detects electrons which have been emitted from the atoms of the material being scanned. Detailed images of the material with nanometre (nm) resolution can be generated. Energy-dispersive X-ray spectroscopy (EDS), a technique available within the SEM instrument, was used to determine the elemental composition of the stationary phase before and after thermal treatment. The EDS technique relies on the detection of X-rays being generated from the material after exposure to a high energy electron beam. The energy of the X-rays generated is specific to the elements present within the material. The X-rays are converted to an energy spectrum, which can be used to determine the relative abundance of elements within the material. Finally, X-ray photoelectron spectroscopy (XPS) was used to further determine the elemental composition of the stationary phase before and after thermal treatment. XPS is a technique used to analyze a material's surface chemistry by impacting the material with a beam of X-rays and measuring the energy of the emitted electrons. A photoelectron spectrum can be

generated by summing the emitted electrons at various kinetic energies. The technique is useful for characterizing the top 1-10 nm of a material's surface. In addition to studying the impact of thermal treatment on PDMS, other stationary phase coatings were also evaluated to determine if thermal treatment could be used to create additional sorptive phases. Capillary columns in the treated and untreated form were tested for their ability to serve as an effective trap for GC×GC modulation. In addition to PDMS, three different stationary phase chemistries were selected for further analysis. These coatings include MXT-1301 (6 %-cyanopropyl-phenyl)-dimethylpolysiloxane, MXT-35: (35 %-phenyl)-dimethylpolysiloxane and MXT-200 (35 %-trifluoropropyl)-dimethylpolysiloxane. Their chemical structures can be seen in Figure 3.1. Each of the thermally treated and untreated capillary columns were evaluated through the GC×GC separation of diesel fuel.

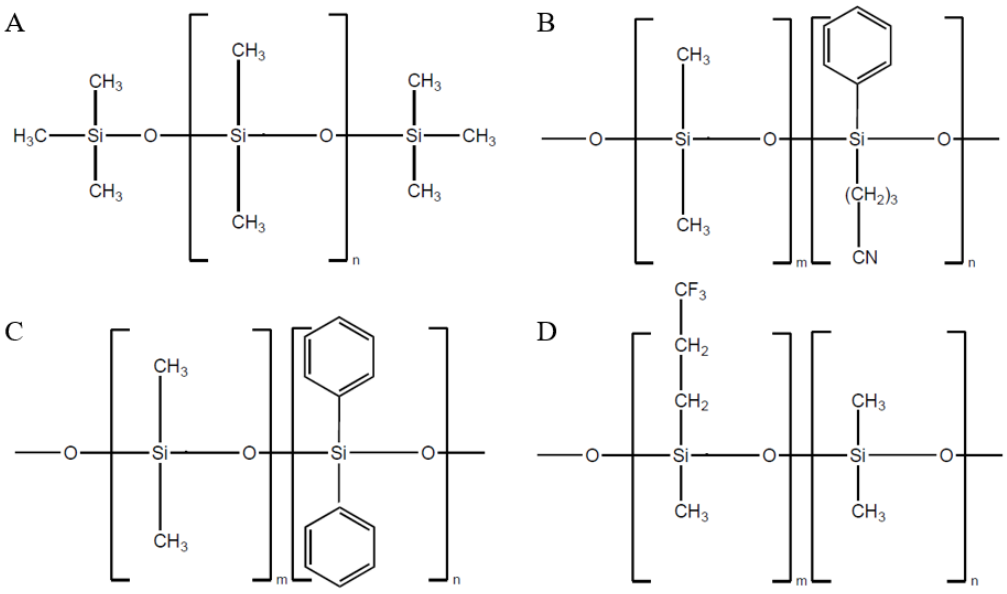

Figure 3.1 Chemical structure of the four stationary phase coatings evaluated. They include 100 % Dimethylpolysiloxane (A), (6 %-cyanopropyl-phenyl)-dimethylpolysiloxane (B), (35 %-phenyl)-dimethylpolysiloxane (C) and (35 %-trifluoropropyl)-dimethylpolysiloxane (D).

3.2 Experimental

3.2.1 Imaging and material characterization

SEM Imaging, EDS elemental analysis and XPS surface chemistry analysis were completed in the Waterloo Advanced Technology Laboratory (WATLab) using a Zeiss FESEM 1530 instrument (Oberkochen, Baden-Württemberg, Germany) and a Thermo VG ESCALab 250 XPS device (Thermo Fisher Scientific, Waltham, MA, USA). Chromatographic experiments were conducted on instruments previously described in section 2.1.3. The method for trap construction was described in section 2.1.1. A new thermal treatment method was established with the move from a 15 cm trap to a 7 cm trap (5 cm flattened) during the Mk II design phase described in section 2.3. Those procedures were maintained throughout these experiments.

3.2.2 Alternative trap coatings and chromatographic conditions

Six different commercially available metal capillary columns were acquired from Restek Corporation (Bellefonte PA, USA). They include 30 m x 0.28 mm x 1 µm MXT-1 (100 % polydimethylsiloxane), 30 m x 0.25 mm x 0.25 µm MXT-1 (100 % polydimethylsiloxane), 30 m x 0.25 mm x 0.1 µm MXT-1 (100 % polydimethylsiloxane), 30 m x 0.28 mm x 1.5 µm MXT-1301 (6 %-cyanopropyl-phenyl)-dimethylpolysiloxane, 30 m x 0.25 mm x 1 µm MXT-35 (35 %-phenyl)-dimethylpolysiloxane and 30 m x 0.25 mm x 1 µm MXT-200 (35 %-trifluoropropyl)-dimethylpolysiloxane. Thus far only 0.28 mm columns had been used to construct traps. The GC×GC-FID system consisted of an Agilent 6890 GC (Palo Alto, CA, USA) equipped with a split/spitless injector. A column combination consisting of a VF5ms 27 m x 0.25 mm x 0.15 µm (J&W Scientific, Folsom, CA, USA) in the ^{1}D and a SolGel Wax 0.5 m x 0.25 mm x 0.25 µm (SGE, Ringwood, Victoria, Australia) in the ^{2}D was used. The oven temperature began at 40 °C, increasing at 8 °C/min to 240 °C, then 20 °C/min to 260 °C with a 5 minute hold. A 1 µl sample

of diesel fuel acquired from a local gas station was injected using the split/splitless injector operated in split mode at a temperature of 300 ºC while using a 2 mm id gooseneck liner (Restek Corp.). The sample was split 300:1 during injection. Hydrogen carrier gas with a purity of 99.999 % was used at a 2.3 ml/min constant flow rate. An FID detector acquiring at 200 Hz was used for detection and Agilent Chemstation software was used for data acquisition. Data processing was completed in GC Image (Lincoln, NE, USA). A modulation period of 8 s was used for all experiments.

3.3 Results and discussion

3.3.1 SEM imaging of the capillary

To evaluate the inside of a steel capillary was not as easy as anticipated. Stainless steel is a very hard material and opening a capillary without destroying it was not an easy task. It was found that MXT-1 0.53 mm x 3 µm tubing was an easier material to work with, so it was used for the following experiments. To open the capillary, the surface of one side would first need to be sanded down to remove enough material to make the wall weak. A razor blade or a needle tip was then inserted into the open end of the tube and used to split the capillary along its length. Once a capillary was opened for analysis, it was not possible to use it again. Consequently, different capillaries were used in the comparison of treated and untreated traps. A new, untreated capillary having been split open is shown in Figure 3.2. A separate segment of MXT-1 capillary having undergone thermal treatment is shown in Figure 3.3. The difference between the capillaries before and after treatment was pronounced. The dark PDMS coating seen before thermal treatment at first appeared to be completely removed. Zooming in closer on the treated capillary using the SEM revealed a uniform undulating coating within the trap (Figure 3.4). Increasing the magnification level further revealed that the internal surface of the treated

capillary was coated with spherical nanoparticles measuring between 400 to 500 nm in diameter (Figures 3.5 and 3.6).

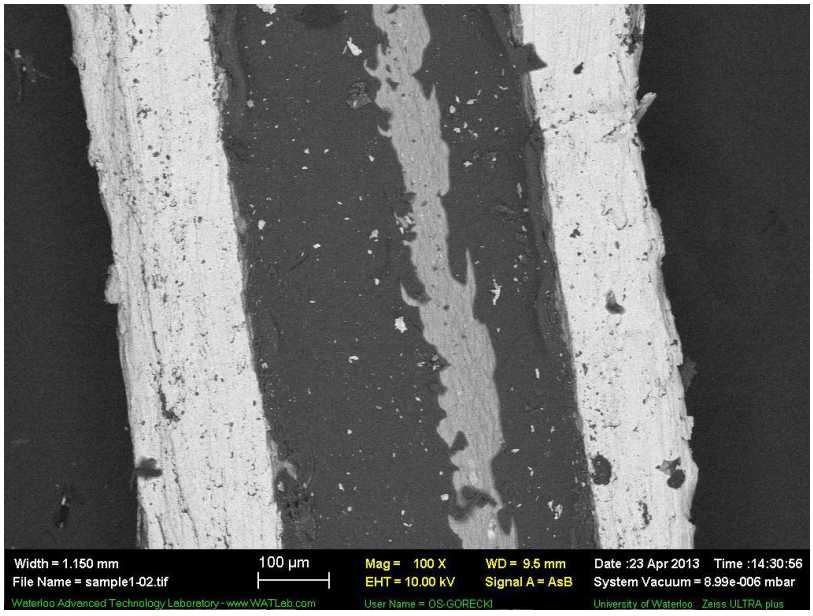

Figure 3.2 SEM image from the inside of the MXT-1 capillary before treatment. The light area shown is the capillary wall, and the dark material inside is the 100 % PDMS coating. The vertical scarring through the centre is the result of prying the capillary open.

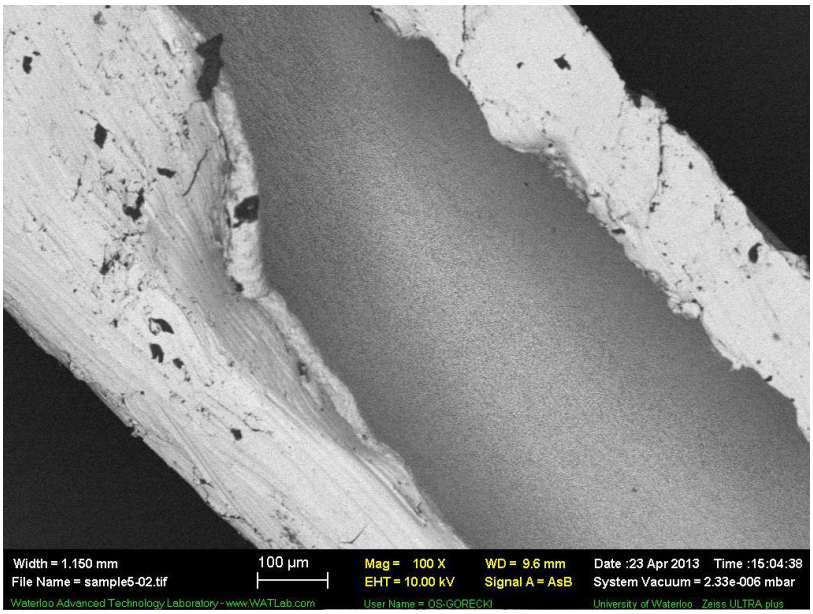

Figure 3.3 SEM image from the inside of the MXT-1 capillary after treatment. The light area shown is the capillary wall and the grey material inside is the new thermally treated sorptive coating.

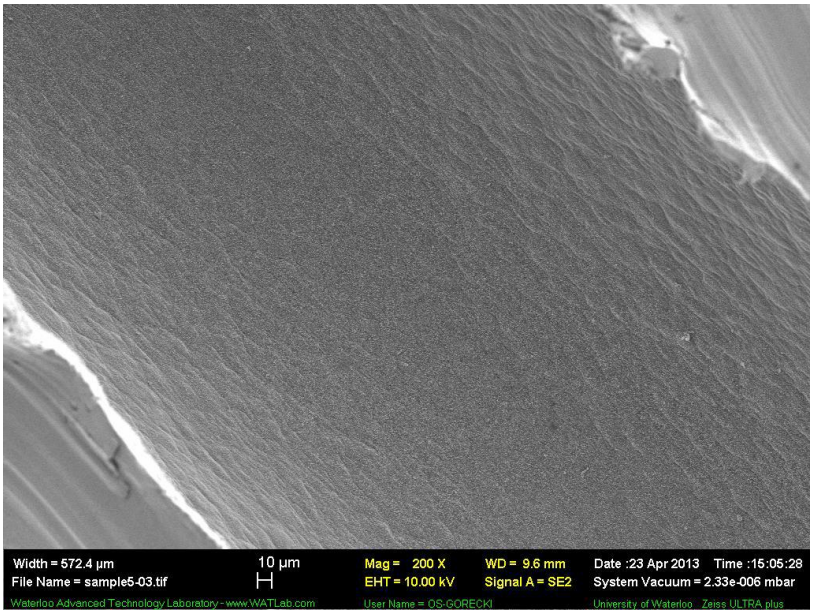

Figure 3.4 A higher zoom level of the internal coating of the thermally treated MXT-1 capillary.

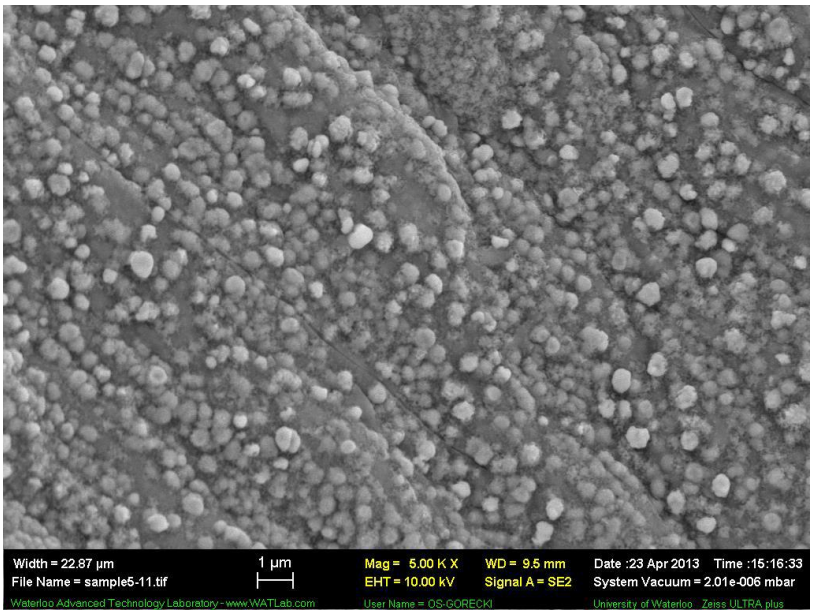

Figure 3.5 A further magnification of the treated MXT-1 capillary showed the surface coated with spherical nanoparticles.

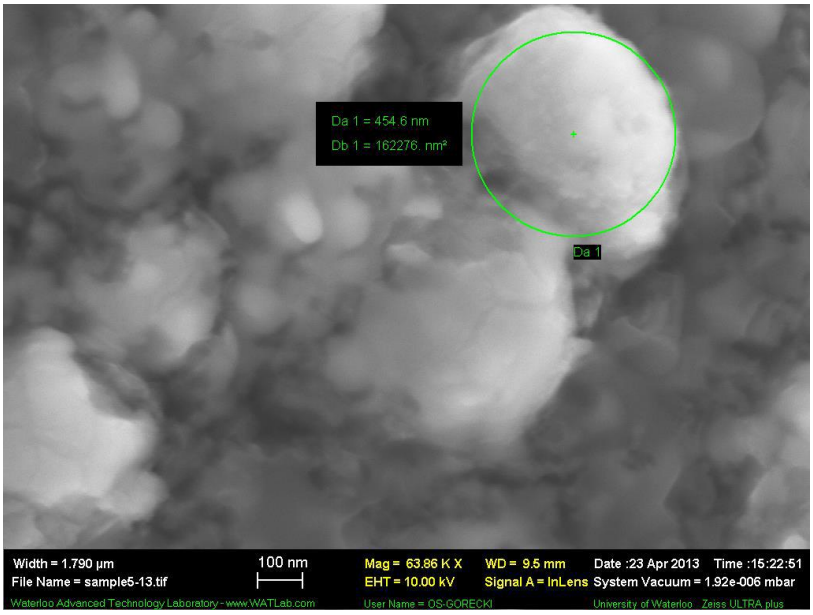

Figure 3.6 Additional magnification of the treated surface revealed that the spherical nanoparticles were approximately 400-500 nm in diameter.

Although the MXT-1 0.28 mm x 1 µm capillary could not be opened to investigate without destroying it, cross sectional images could be taken using the SEM. Figure 3.7 shows a flattened and thermally treated capillary with a high level of contrast to reveal the internal surface. The image reveals very well rounded sides with a flat top and bottom where compression had previously been applied. A uniform 100 µm distance from bottom to top appeared to be present, which confirmed the flattening procedure was working to generate the desired internal geometry of the capillary. The final SEM image taken focused further into the treated 0.28 mm capillary to reveal the anatomy of the treated surface (Figure 3.8). The result was a beautiful image showing the dynamic internal surface of the capillary coated with the spherical nanoparticles. Although the surface appeared to be fully coated, it was not flat and featured ridges and valleys not seen when observing the PDMS coating which was quite uniform. This suggested that through thermal treatment, the total surface area of the modified polymeric spherical coating was

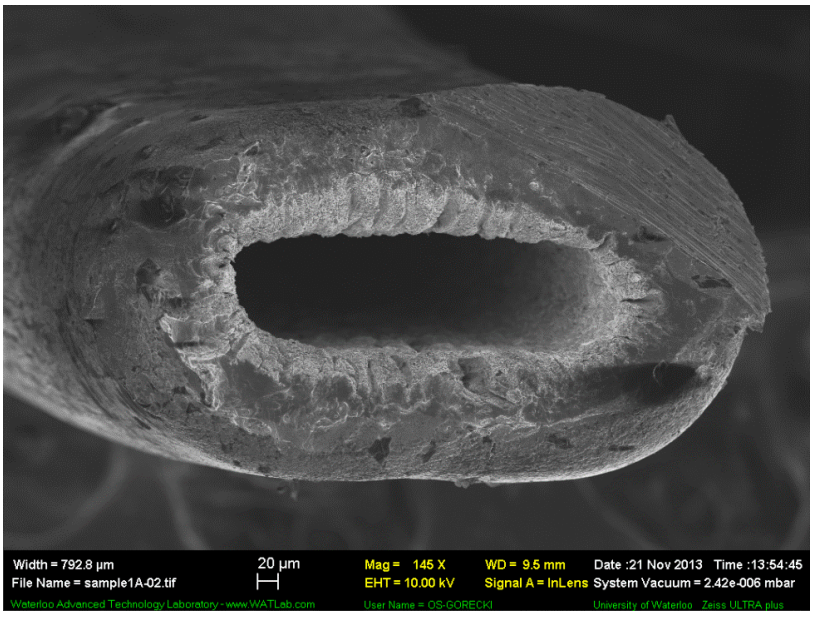

Figure 3.7 A cross sectional image of the flattened and treated MXT-1 0.28 mm x 1 µm capillary. The diagonal scarring pattern found at the top right of the capillary is from the ceramic wafer cutting action.

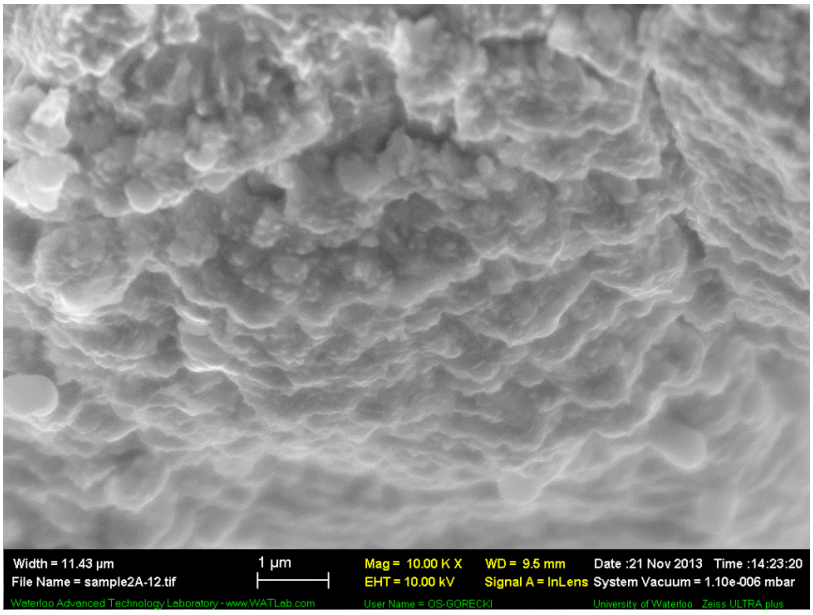

Figure 3.8 A highly focused SEM image of the thermally treated MXT-1 0.28 mm x 1 µm capillary revealing the undulating surface coated with spherical nanoparticles.

increased greatly. Increased surface area would result in more sites for adsorption, and likely a greater trapping capacity relative to an untreated capillary.

Thus far the SEM images confirmed that the PDMS layer had indeed been converted to a new material coating the internal surface of the capillary through thermal treatment. A spherical nanoparticle coating was left, but its elemental composition remained unknown. The images confirmed that the flattening process was producing a very uniform 100 µm wall-to-wall internal height. It was now time to move to elemental analysis to determine the chemical nature of the modified stationary phase.

3.3.2 EDS Analysis of the modified stationary phase coating

PDMS is a silicon-based polymer having the structure shown in Figure 3.9. PDMS is a popular stationary phase coating for gas chromatography columns and is known to be chemically inert under a wide range of conditions.

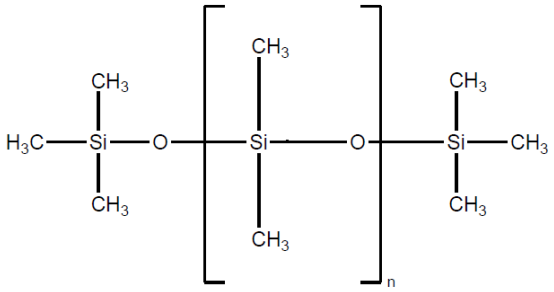

Figure 3.9 Chemical structure of PDMS

To determine how the chemical nature of the PDMS coating had changed during the thermal treatment, EDS analysis was conducted to reveal relative atomic percentages of carbon, silicon and oxygen. Analysis was performed on several sections of untreated PDMS contained within the MXT-1 column and on the internal coating of an MXT-1 column which had received thermal treatment for 10 minutes. Figure 3.10 shows the sections of capillary where the EDS measurements were taken. Figure 3.11 features the results of the EDS analysis.

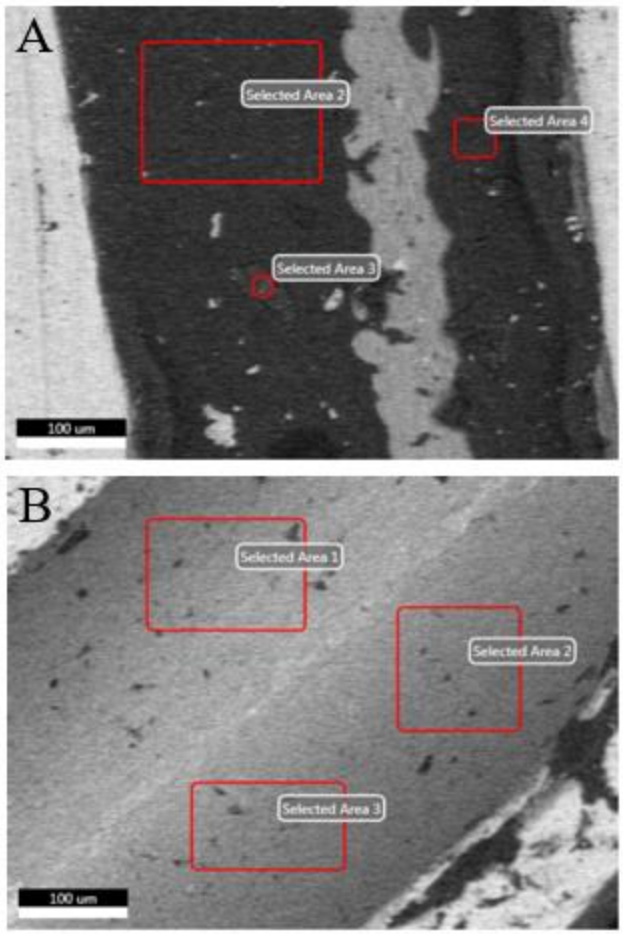

Figure 3.10 Areas where the EDS analysis was conducted on an untreated capillary (A) and a capillary thermally treated for 10 minutes (B).

Scans of the untreated PDMS showed percentages of carbon, silicon and oxygen that were closely in line with expected values with an average of 55.7 % for carbon, 27.8 % for oxygen and 21.3 % for silicon across the three scan areas. Moving to the capillary that had been treated for 10 minutes, the relative atomic percentages changed drastically. The atomic percentage of carbon was reduced from ~50 % to ~30 %. Removal of carbon in the form of CO_2 through the high temperature thermal treatment process was the likely cause of carbon % reduction. Oxygen was slightly lower at ~20 %, and silicon approximately doubled in atomic percentage moving to

~50 %. Thermal treatment appeared to have the effect of proportionally reducing carbon content whilst increasing the relative percentage of silicon present. The EDS analysis delivered some interesting results and provided some insight as to how the PDMS phase was changing through thermal treatment. The final step was to collect data with the XPS technique to shed light on the nature of the chemical bonds amongst the carbon, oxygen and silicon nanomaterial.

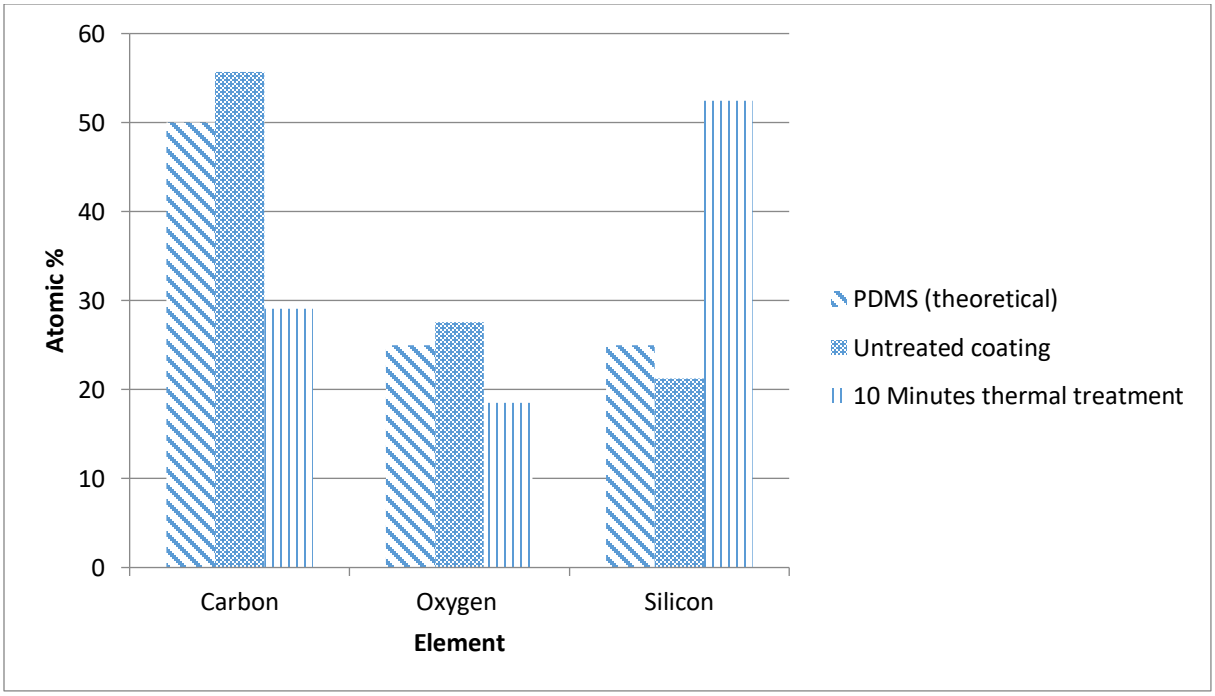

Figure 3.11 Relative atomic percentages of carbon, oxygen and silicon with and without thermal treatment. PDMS is shown with its predicted atomic percentage as a reference.

3.3.3 XPS analysis of the modified stationary phase

The samples used for the XPS analysis included MXT-1 0.53 mm x 3 µm capillaries that were untreated and thermally treated. The capillaries were cut open and the internal coating exposed to the X-ray source of the XPS instrument. Three locations within the untreated and

treated samples were selected for the XPS analysis. The first element studied was carbon, for which the C1*s* orbital electron bond intensity was investigated. The untreated samples revealed a peak at ~ 284.8 eV binding energy, which suggests sp^3 hybridised carbon binding. This result is in line with how carbon is bound within the PDMS polymeric lattice. Upon thermal treatment, the peak shifted to slightly lower binding energy of ~ 284 eV, which suggests somewhat less sp^3 binding of carbon and a greater presence of Si-C binding. However a difference of only 0.8 eV is likely not a meaningful shift in binding energy. The resulting spectra are shown in Figure 3.12. The next element for investigation was oxygen. In untreated PDMS, the O 1*s* XPS spectra revealed a singular peak at binding energy ~ 533 eV, which represents chains of Si-O-Si units, which are prevalent in PDMS. Upon thermal treatment the original peak at ~ 533 eV broadened greatly towards lower binding energy and was accompanied by a second peak with a binding energy of ~ 530 eV. This indicates that Si-O-Si chains remained present after thermal treatment, but were now accompanied by other species, potentially various metal carbonates and/or metal oxides. The resulting spectra are shown in Figure 3.13.

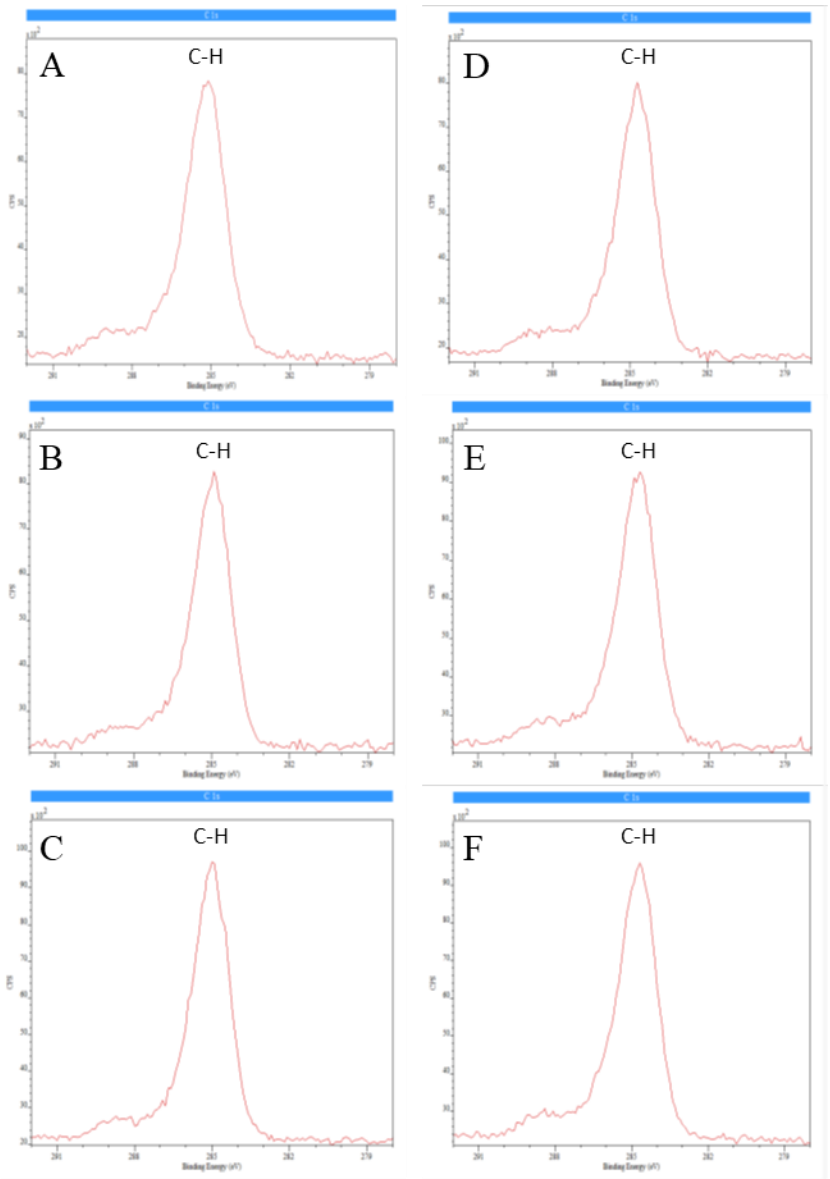

Figure 3.12 XPS binding energy spectra for C 1*s* from an untreated capillary (A, B, C) and 10 minute thermally treated capillary (D, E, F). Very little difference in the acquired spectra was observed after thermal treatment.

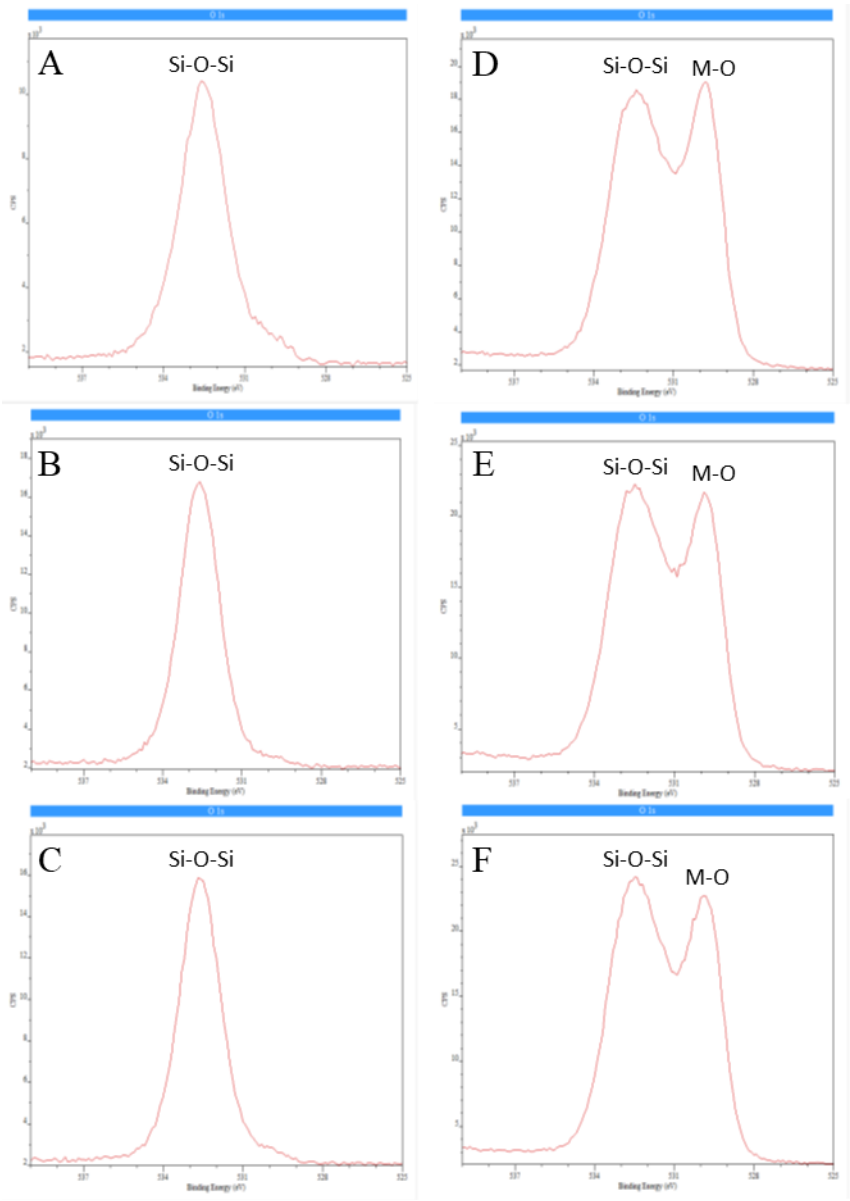

Figure 3.13 XPS binding energy spectra for O 1*s* from an untreated capillary (A, B ,C) and 10 minute thermally treated capillary (D, E, F). Si-O-Si bonds remained present post treatment with the inclusion of new metal oxide (M-O) bonding being observed.

The final element investigated was silicon. In untreated PDMS, the Si 2*p* XPS spectra revealed two peaks. The peak at the lower binding energy, ~ 99.4 eV, represented Si-Si bonding [269, 270]. This likely corresponded to the underlying passivation layer which was comprised of silicon. The peak at the higher binding energy, ~ 103.5 eV, represented Si-O-Si bonding. Upon

thermal treatment of the stationary phase, XPS spectra revealed one large peak at binding energy ~ 103.5 eV and a trace peak at ~ 99.4 eV, suggesting nearly all the silicon present were chains of O-Si-O units, supporting the result found in the C 1*s* analysis. The resulting spectra are shown in Figure 3.14.

The SEM, EDS and XPS results revealed important information about how the thermal treatment impacted the PDMS stationary phase. Through SEM it was shown that the PDMS was being converted to a highly porous, high surface area coating consisting of 400-500 nm wide nanoparticles. The flattening process was also confirmed to be working as intended with 100 µm wall to wall heights being observed inside the capillary. The EDS data suggested that thermal treatment reduced the amount of carbon present relative to the amount of silicon, with oxygen remaining relatively consistent. The XPS data revealed that carbon likely remained bound in the sp^3 configuration after thermal treatment, with a slight shift towards greater Si-C binding. For oxygen, post treatment it appeared present within chains of O-Si-O units. The Si 2*p* analysis confirmed this result and showed that after thermal treatment nearly all silicon present was confirmed to be in the O-Si-O state bound with oxygen. The presence of a peak at ~ 99.4 eV in the Si 2*p* likely corresponds to the silicon passivation later present in the column. Overall, the results of these experiment suggested that the thermal treatment process converted PDMS into carbon-doped, highly oxygen-rich silica-based nanoparticles. These nanoparticles are highly effective when used as a trapping medium for GC×GC.

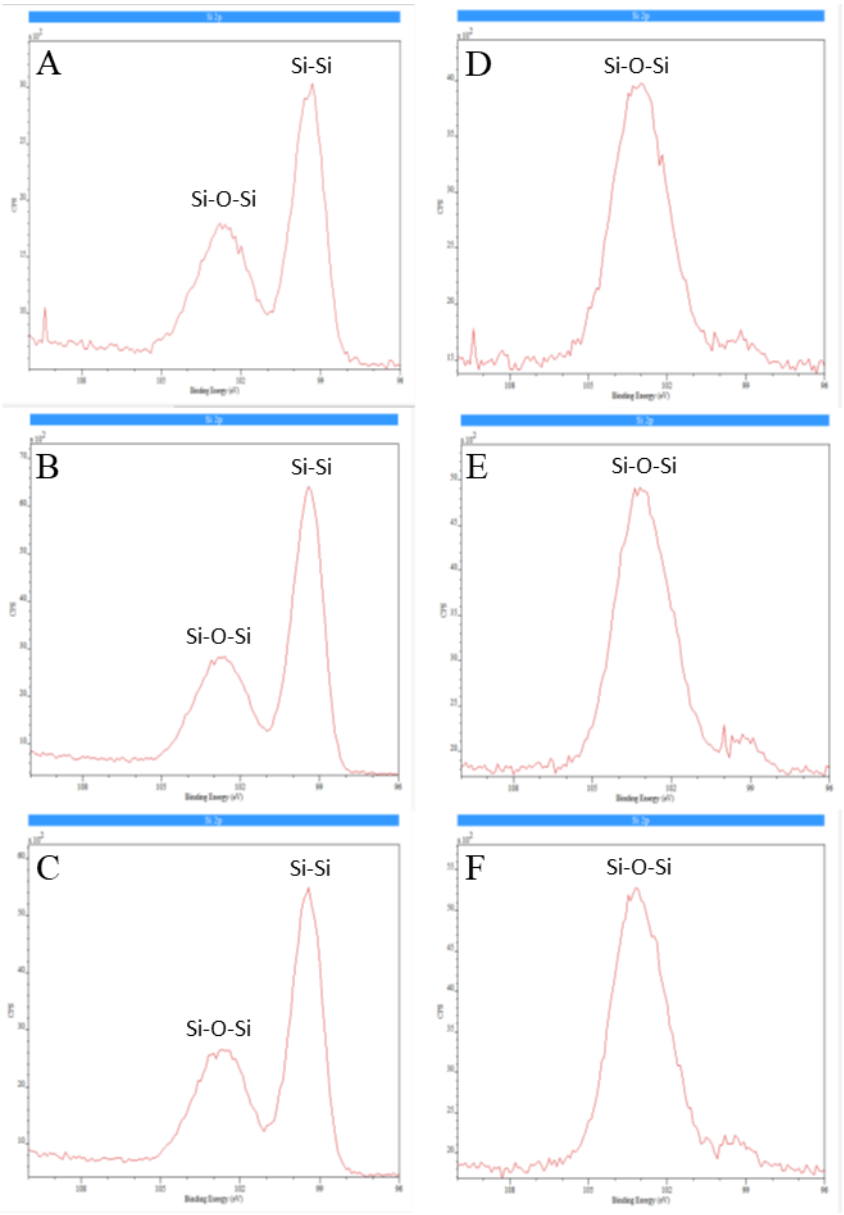

Figure 3.14 XPS binding energy spectra for Si 2*p* from an untreated capillary (A, B, C) and 10 minute thermally treated capillary (D, E, F).

3.3.4 Evaluation of other stationary phase coatings as suitable trapping materials

Thus far only 0.28 mm columns had been used to construct the traps. With the exception of the MXT-1301 column, the phases selected for testing were not available in a column diameter of 0.28 mm. A column diameter of 0.25 mm was available, so the trap construction

method and thermal treatment regime described in section 2.3.2 were modified in attempt to produce a trap similar in construction to those used throughout this work. Attempts to flatten the capillary using shims and compression often led to the complete collapse of the capillary wall making the trap unusable. The steel capillary wall thickness was clearly thinner and weaker than the equivalent 0.28 mm steel column. A consistent method for flattening the 0.25 mm columns was unfortunately not developed. It was also found that when the 0.25 mm metal columns were compressed between the ceramic pads of the modulator, the material would often deform due to the pressure applied. Some traps were constructed using these 0.25 mm columns and tests carried out. However, given the inconsistency in the traps, the results of those experiments were disappointing and will not described. In addition, comparing traps made from columns of differing internal diameters would not have delivered a like-for-like comparison. This left the MXT-1301 0.28 mm column as the only available option with an alternative stationary phase to 100 % PDMS that could proceed through the flattening and thermal treatment methods described in section 2.3.2.

The diesel sample was run first with an MXT-1 0.28 mm x 1 µm thermally treated trap to set a baseline for performance. The chromatogram of this separation is shown in Figure 3.15. The separation using this trap was of good quality, with no visible breakthrough and good separation between the monoaromatic, diaromatic and triaromatic groups. A trap was then installed using the same column material which had not undergone the thermal treatment. This separation is shown in Figure 3.16. The most noticeable difference between the separations is the breakthrough of early eluting compounds in the separation using the non-thermally treated trap.

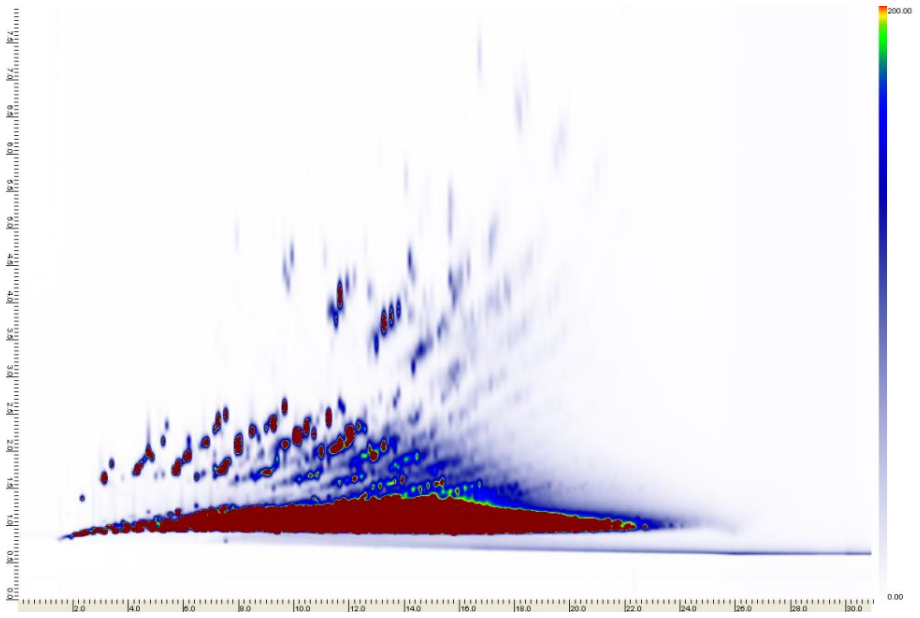

Figure 3.15 A GC×GC chromatogram of diesel using the MXT-1 0.28 mm x 1 µm thermally treated trap.

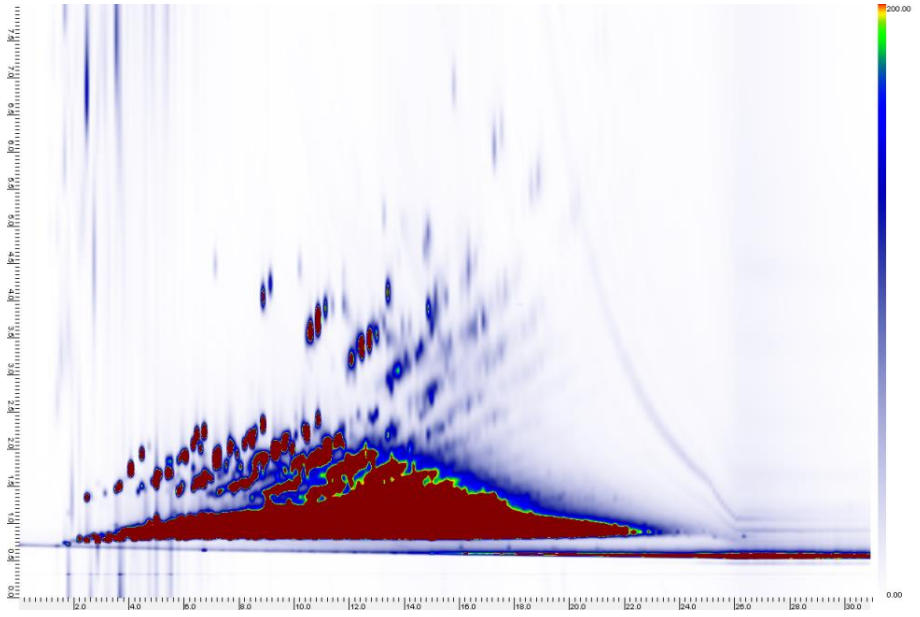

Figure 3.16 A GC×GC chromatogram of diesel using the MXT-1 0.28 mm x 1 µm trap with no thermal treatment.

There is also an overall loss of chromatographic resolution, especially noticeable in the later eluting compounds of the monoaromatic region. Siloxane bleed is also more pronounced for the untreated trap. This simple comparison shows thermal treatment is an effective way to increase the sorptive capabilities of the trapping capillary.

The next trap to be tested was made with the MXT-1301 0.28 mm x 1.5 µm column. The thermally treated trap was evaluated first and the resulting chromatogram is shown in Figure 3.17. Compared to the separation achieved using the MXT-1, 1 µm trap, the performance was very similar. The MXT-1301 trap separation had less resolution in the monoaromatic region and appeared to be suffering from a greater level of column bleed. No changes in the ^{1}D column were made during the experiments, so it is plausible that the source of the additional siloxanes was from the incomplete thermal treatment of the thicker 1.5 µm 6 %-cyanopropyl-phenyl)-dimethylpolysiloxane coating. If the thermal treatment program was optimized to take into account the additional stationary phase coating the MXT-1301 column, this column would likely be a suitable alternative trap material to the MXT-1 column.

The next trap to be installed was the untreated MXT-1301 trap. The resulting chromatogram is shown in Figure 3.18. As seen with the MXT-1 untreated trap, breakthrough of early eluting compounds and a reduction in resolution were observed relative to the thermally treated traps.

3.4 Conclusions

Advanced tools were deployed to better understand the composition of the stationary phase coating after the thermal treatment. SEM provided visual confirmation that the PDMS coating was being removed and converted in to a new, highly sorptive material coating the inner walls of the trapping capillary. The material was spherical in shape, approximately several hundred nm in diameter and evenly distributed across the inner surface of the capillary.

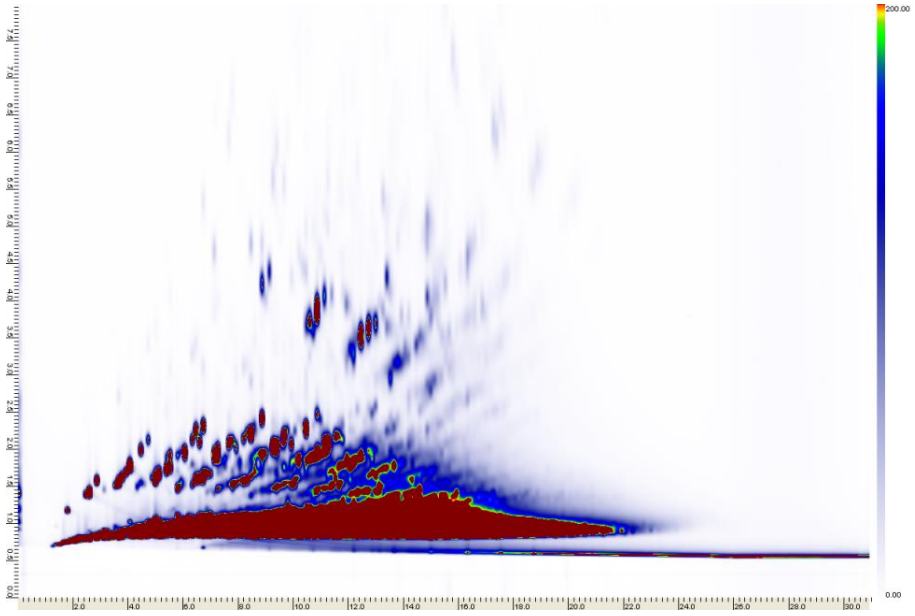

Figure 3.17 A GC×GC chromatogram of diesel using the MXT-1301 0.28 mm x 1.5 µm thermally treated trap.

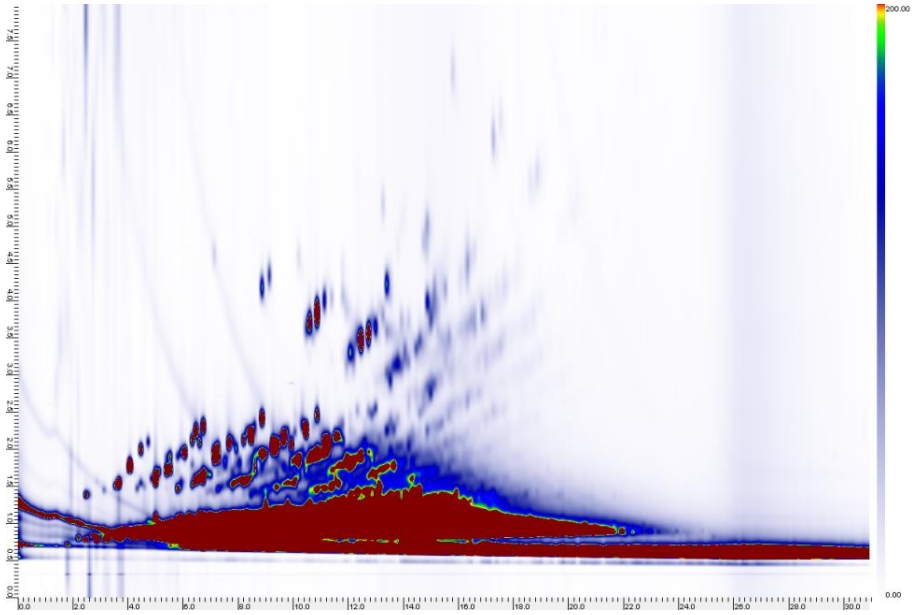

Figure 3.18 A GC×GC chromatogram of diesel using the MXT-1301 0.28 mm x 1.5 µm trap with no thermal treatment.

EDS and XPS analysis suggested that these spherical nanoparticles were silica-based and highly oxidized. Chromatographic testing of treated and untreated traps revealed that the thermally treated material provided advantages in the adsorption of volatile early eluting compounds and generation of greater ^{2}D resolution through the injection of more focused chromatographic bands from the modulator. The new material generated through thermal treatment was shown to be a highly effective trapping medium for use in GC×GC.

Chapter 4. Application of the Waterloo Modulator to real world analytical challenges

4.1 Analysis of honeybush tea (*Cyclopia* spp.) volatiles[2]

4.1.1 Introduction

Comprehensive two-dimensional gas chromatography (GC×GC) has found widespread application in the analysis of complex mixtures of volatile and semi-volatile compounds in for example petrochemical, natural product, environmental and food and beverage samples [200, 271]. Currently, the majority of commercial GC×GC systems utilise cryogenic modulation, which provide excellent performance for most analytes, but they are expensive to operate due to the high demand for cryogenic agents. On the other hand, failure of heater-based modulators to effectively trap highly volatile compounds and the limited volatility range of these systems have hampered their more widespread use [195]. Górecki and co-workers have developed a novel single-stage thermal modulator that offers consumable-free operation and efficient modulation [203]. In this study, the application of this single-stage modulator for the analysis of honeybush tea volatile compounds was explored.

"Fermented" honeybush (*Cyclopia* spp.) is an indigenous herbal tea from South Africa [272] which is well known for its characteristic aroma, recently extensively profiled to identify

[2] This section is based on the following publication:

G. Ntlhokwe, A.G.J. Tredoux, T. Górecki, M. Edwards, J. Vestner, M. Muller, L. Erasmus, E. Joubert, J. Christel Cronje, A. de Villiers, "Analysis of honeybush tea (Cyclopia spp.) volatiles by comprehensive two-dimensional gas chromatography using a single-stage thermal modulator," *Analytical and Bioanalytical Chemistry*, vol. 409, pp. 4127-4138, 2017.

Author contributions include design and manufacture of the Mk III modulator, remote technical, operational and chromatographic support, secondary manuscript contributor, review and editing.

major aroma attributes, i.e. “floral”, “sweet-associated”, “fruity”, “plant-like” and “woody” [273]. The popularity of honeybush tea stems not only from its taste and aroma, but also from its reputation as a healthy beverage, primarily associated with its content of flavonoids and xanthones [274]. Honeybush tea has traditionally been produced from the leaves and stems of several *Cyclopia* species harvested in the wild. Of commercial importance are the cultivated species, *Cyclopia subternata* and *Cyclopia genistoides.* Cultivation of *C. maculata* is being explored for honeybush tea production to meet the growing demand [272].

Taste and aroma are the important sensory characteristics used to evaluate the quality of beverages such as tea [275]. The aroma characteristics are primarily determined by the composition of volatile compounds [276]. The volatile composition of honeybush tea has been studied extensively by Le Roux et al. [277-279] by means of gas chromatography-olfactometry (GC-O) and gas chromatography-mass spectrometry (GC-MS). In total, 255 volatile compounds were identified in hot water infusions of unfermented and fermented wild-harvested *C. intermedia and C. sessiliflora*, as well as the cultivated *C. subternata* and *C. genistoides*, with terpenoids being the major chemical class. Forty-six of the identified compounds were established as being odour-active by GC-O [279]. Honeybush tea thus represents a complex sample ideally amenable to GC×GC separation. In the current work, the volatile composition of honeybush tea produced from three *Cyclopia* species with prominent differences in their sensory aroma profiles [280] were analysed by GC×GC using the single-stage thermal modulator.

4.1.2 Experimental

4.1.2.1 Chemicals and materials

Fermented plant material (tea bag fraction 12 < mesh < 40) of *C. genistoides* prepared by the Post-Harvest Division of ARC Infruitec-Nietvooribij, Stellenbosch, was used for method optimisation. Solid phase micro-extraction (SPME) fibres (100 µm PDMS, 65 µm PDMS/divinylbenzene (PDMS/DVB), 50/30 µm PDMS/CAR (Carboxen), 50/30 µm PDMS/CAR/DVB, 85 µm CAR/PDMS, 85 µm polyacrylate (PA) and 60 µm polyethylene glycol (PEG)) and the SPME manual holder were purchased from Supelco (Bellefonte, PA, USA). Sodium chloride (NaCl) and a mixture of C_7-C_{40} linear hydrocarbons were purchased from Sigma-Aldrich (St. Louis, MO, USA). Ascorbic acid was purchased from Hopkin & William (Johannesburg, SA) and reference standards (Table 4.1) were purchased from Fluka or Sigma-Aldrich, or synthesised as detailed elsewhere [279] and were kindly provided by Prof. B.V. Burger and Dr. M. Le Roux (Lecus, Stellenbosch University). A standard solution containing all reference standards at varying concentrations (4.00 – 24.0 mg/L) in dichloromethane (Sigma-Aldrich) was stored at -4 °C and analysed within 2 weeks [279]. Deionised water was obtained from a Milli-Q water purification system (Millipore, Milford, MA, USA). Five batches of plant material of each of the cultivated species, *C. genistoides, C. subternata* and *C. maculata*, were harvested in 2013 from plantations located in the Western Cape. Samples of each species were harvested from the same plantation, with the plantations for *C. genistoides, C. maculata* and *C. subternata* situated at Bredasdorp, Bereaville and Stellenbosch, respectively. All plant material was fermented at 90 °C for 16 h as described elsewhere [280]. The infusions were subjected to descriptive sensory analysis.

4.1.2.2. Sample preparation

The same fermented plant material was used for all method optimisation experiments. Boiled deionised water (100 ml) was added to 1.25 g plant material in a flask. The flask was covered with aluminium foil and the tea was infused for 5 min with occasional (manual) swirling. The hot infusion was then filtered through a pre-washed (with 100 ml boiled deionised water) filter paper directly into a flask containing 90 mg ascorbic acid. The filtrate was allowed to cool to room temperature before SPME extraction. A fresh infusion was prepared for each set of optimisation experiments.

4.1.2.3. Headspace SPME extraction procedure

SPME fibres were conditioned as recommended by the manufacturer prior to use. Six fibres with different coatings were evaluated. 10 ml of each infusion was transferred to a 20 ml vial containing 2 g NaCl (previously heated to 100 °C and cooled to room temperature to remove moisture) and a PTFE stir bar. The vials were capped immediately and the fibre was exposed to the headspace of the sample. Extraction was performed at room temperature (21 ± 2 °C) at a stirring rate of 1000 rpm for 30 min. Fibres were pre-conditioned at 250 °C in a GC injection port for 30 min each day, and blank analyses were performed daily to verify that the system and the fibre remained contaminant-free. The final method utilised the PDMS/DVB fibre with the same conditions as outlined above.

4.1.2.4. Instrumentation

All analyses were performed on an in-house built GC×GC system consisting of an Agilent 6890 GC (Agilent Technologies, Palo Alto, CA, USA) equipped with an FID and a programmed temperature vaporizing (PTV) injector (Gerstel, Mulheim a/d Ruhr, Germany). The

instrument was retrofitted with the Mk III single-stage thermal modulator previously described in section 2.3.

4.1.2.5. Instrumental conditions

Hydrogen (99.999 % purity, Air Products, Cape Town, SA) was used as carrier gas. The following conditions were used for the initial experiments: initial flow rate 2.06 ml/min at a constant inlet pressure of 151.7 kPa; initial oven temperature 40 °C, held for 2 min, followed by a temperature ramp at 5.5 °C/min to 240 °C, held for 5 min. Analytes were desorbed in the injector at 240 °C for 5 min in splitless mode (splitless time 1.5 min). The PTV was used as a standard split/splitless injector, heated to 240 °C prior to injection. The FID temperature was set to 250 °C (air = 450 ml/min, H_2 = 40 ml/min, make up gas N_2 = 45 ml/min) and an acquisition rate of 100 Hz was used. Two second dimension columns with different polarities, 50 % phenyl/50 % PDMS (Rxi-17Sil MS, 0.6 m × 0.15 mm × 0.15 µm, Restek) and trifluoropropyl methyl polysiloxane (Rtx-200, 0.6 m × 0.15 mm × 0.15 µm, Restek) were also evaluated for the non-polar × polar configuration. For evaluation of a polar × non-polar column combination, a 30 m × 0.25 mm × 0.25 µm DB-WAXetr column (J&W Scientific) was used in ^{1}D and a 0.6 m × 0.15 mm × 0.15 µm Rxi-5ms column (Restek) in ^{2}D. For the optimal column combination (HP-5MS × Stabilwax), the optimisation of carrier gas flow was evaluated at head pressures of 75, 100 and 151.7 kPa. Oven temperature ramping rates of 2, 3 and 5.5 °C/min were evaluated. The modulation discharge voltage was evaluated at 20 V and 30 V. The optimal column combination comprised 30 m × 0.25 mm × 0.50 µm HP-5MS (J&W Scientific) and 0.6 m × 0.15 mm × 0.15 µm Stabilwax (Restek) columns in ^{1}D and ^{2}D, respectively. Analyses were performed at a constant column head pressure of 100 kPa. The modulation period was 5 s, and the discharge voltage 30 V. Analytes were desorbed in splitless mode (splitless time 1.5 min) for 2 min in the

GC inlet at 240 °C. The oven was held at 40 °C for 2 min, ramped at 3 °C/min to 240 °C and held for 5 min at the final temperature.

4.1.2.6. Data processing

GC×GC-FID raw chromatograms were exported from MSD ChemStation software (Agilent) as .CSV (comma-separated values) files. Contour plots were then created in MATLAB (R2008a, The MathWorks Inc., Natick, MA, USA) using built-in functions.

4.1.3. Results and discussion

4.1.3.1. Method development

To verify the effective operation of the modulator used here, a thermocouple was mounted between the ceramic plates during a temperature programmed analysis to measure their temperature relative to that of the oven. These measurements confirmed that the temperature between the plates was consistently lower than the oven temperature throughout the analysis, reaching a maximum difference of 64.5 °C when the oven first reached its maximum value (Figure 4.1). This difference should be sufficient to trap analytes effectively in the absence of overloading effects. Indeed, this is confirmed by the results for honeybush tea samples, where the earliest eluting compounds are effectively trapped (e.g. 1-pentanol, see further). It is also relevant to note from this experiment that cooling of the modulator to its initial temperature takes approximately 15 min. This is the minimum equilibration time that should be allowed between injections. Re-mobilisation of trapped analytes is achieved by using capacitive discharge at a pre-set voltage. The voltage bears a direct relationship with temperature and therefore determines the efficiency of re-mobilisation. Discharge voltages of 20 and 30 V were evaluated. Some peak splitting for alcohols was observed at high discharge voltage, although the reason for this is not clear. Nevertheless, since a discharge voltage of 30 V provided better peaks shapes, and no peak

splitting for the majority of honeybush volatiles, this voltage was used in subsequent analyses (Figure 4.2).

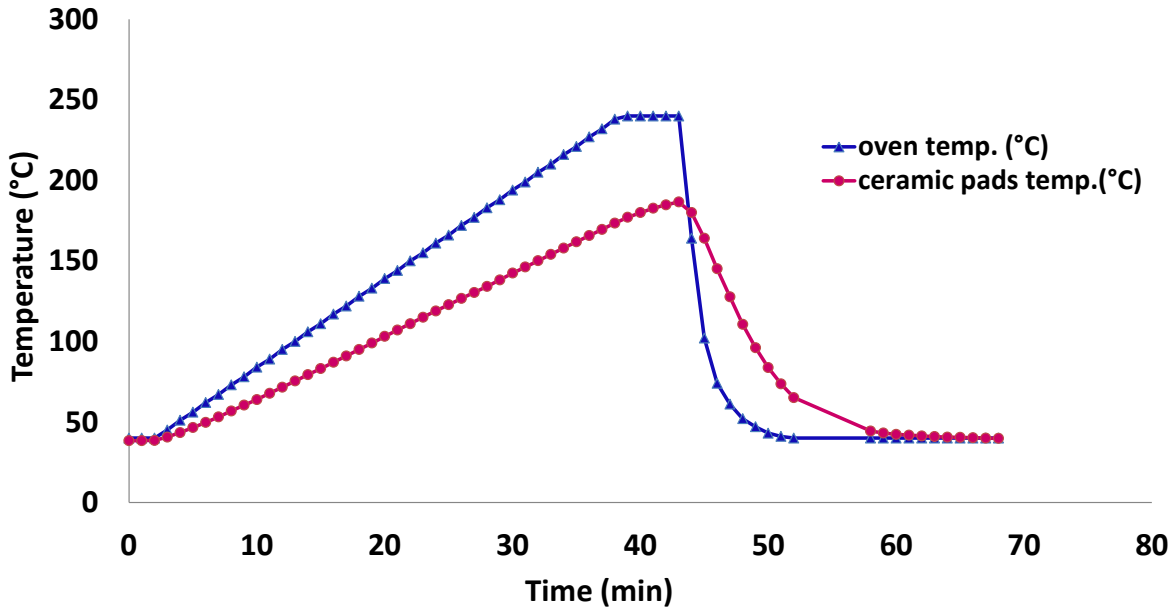

Figure 4.1 Temperature difference between the modulator's ceramic plates (as measured using a thermocouple placed between them) and the oven temperature (according to the GC), determined at an oven temperature ramping rate of 5.5 °C/min from 40 °C to 240 °C.

Both non-polar × polar and polar × non-polar column combinations have been used with success in GC×GC, with the optimal configuration depending on the compounds of interest [195, 281]. Both types of column sets were therefore evaluated as a first step in method development for honeybush tea volatiles. The non-polar × polar column combination showed better utilisation of the two-dimensional separation space, as well as less breakthrough from the trap, as is evident from less 'streaking'. This is likely due to the fact that more polar compounds, which are weakly retained on the non-polar trapping phase, elute from the ^{1}D polar column at higher temperatures. Subsequent method optimisation was therefore performed using the non-polar × polar column set.

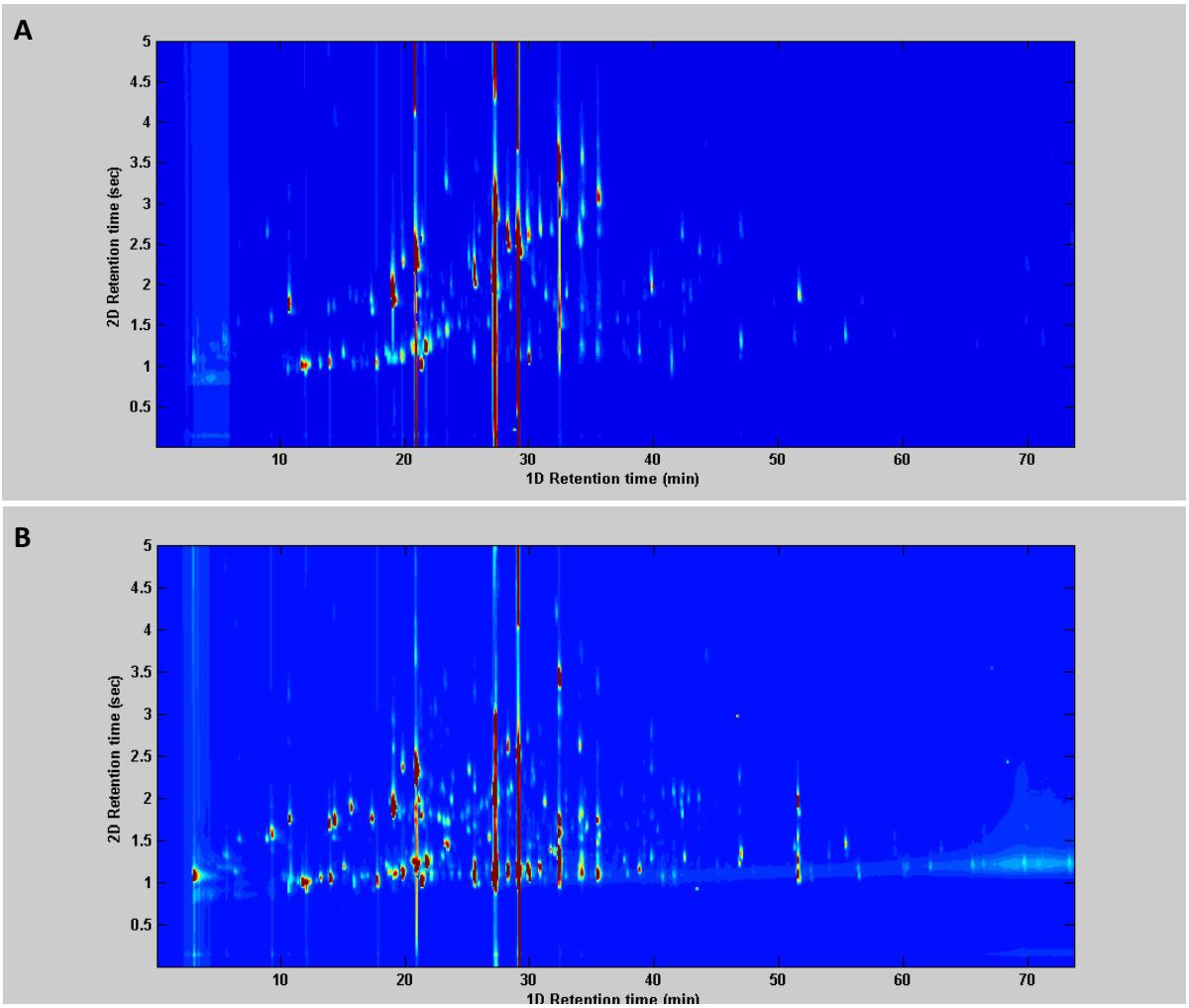

Figure 4.2 Illustration of the effect of the modulator discharge voltage on the GC×GC separation of honeybush tea volatile compounds: (A) 20 V and (B) 30 V discharge voltages. Analyses were performed using the optimised conditions (Section 4.1.2.5).

For the more polar honeybush volatiles, wrap-around (where highly retained analytes elute in subsequent modulation period(s)) was observed. In an attempt to reduce wraparound, alternative ^{2}D columns of lower polarity (trifluoropropyl methyl polysiloxane and 50 % phenyl/50 % PDMS) were evaluated. With the least polar ^{2}D column (Rxi-17Sil MS) wraparound was significantly reduced. However, the lower retention of the majority of honeybush volatiles on this column also resulted in much worse overall separation. The PDMS × Stabilwax column

combination was therefore chosen for further method optimisation. Note that although increasing the modulation period is an obvious choice to reduce wraparound, this is associated with a loss of ^{1}D resolution due to insufficient sampling of first-dimension peaks.

One of the challenges in GC×GC method optimisation is that most experimental parameters are interrelated [282]. Slow ramping rates generate relatively broad first dimension peaks, which facilitate achieving sufficient sampling of first-dimension peaks to satisfy sampling requirements [33]. For the thermal modulator used here, broader ^{1}D peaks are also beneficial since the amount of analyte trapped during each modulation step is reduced, which minimises the risk of breakthrough. On the other hand, a very slow ramp increases the analysis time significantly, and may produce broader ^{2}D peaks. The oven temperature ramping rate was evaluated between 2 °C/min and 5.5 °C/min. At 5.5 °C/min, separation in the first dimension was clearly compromised due to both decreased resolution and increased under-sampling. A ramping rate of 3 °C/min was chosen as a compromise to maintain good resolution for acceptable analysis times (in agreement with literature reference [195]). Since the column head-pressure determines the carrier gas flow rates in both columns, GC×GC analyses are typically carried out at carrier gas velocities close to the optimum for the ^{1}D column, but considerably above the optimal velocity in the ^{2}D column [283]. Acceptable linear velocities for hydrogen in ^{1}D and ^{2}D columns have been suggested to be approximately 20 and 100-130 cm/sec, respectively [195]. Optimisation of the carrier gas flow rate was performed using constant column head pressures of 151.7, 100 and 75 kPa, corresponding to initial flow rates of 2.06, 1.06 and 0.81 ml/min, respectively. The average linear velocities in both dimensions were calculated according to Shellie et al. [190]. At high flow rates, resolution in ^{1}D was compromised, whereas at a low flow rate resolution in ^{2}D decreased since the analytes eluted at higher temperatures. An intermediate

flow rate of 1.06 ml/min was therefore selected as optimal, resulting in a carrier gas linear velocity in ^{2}D within the range 100-130 cm/sec. Using these conditions, the modulation period of 5 s used in initial experiments was long enough to minimise wraparound, but short enough to minimise first dimension under-sampling, and was therefore used for all subsequent analyses.

4.1.3.2. Identification of honeybush tea volatiles

A set of 15 samples, containing five samples each of *C. genistoides*, *C. maculata* and *C. subternata* from the 2013 harvest season was subjected to GC×GC-FID analysis. All samples were analysed in duplicate. Tentative identification of compounds was based on comparison of retention times with reference standards and ^{1}D retention index values compared to NIST and PHEROBASE databases. A total of 84 compounds were identified in the tea samples in this manner (Table 4.1). These included 5-methylfurfural (12), and butyl benzoate (70), identified here for the first time in honeybush tea using reference standards. Figure 4.3 shows the GC×GC-FID contour plot obtained for the analysis of the reference standards and Figure 4.4 shows representative contour plots obtained for each of the three *Cyclopia* spp. Most compounds were common to all three species, with differences observed primarily in terms of their relative amounts. Figure 4.4 illustrates on the one hand the complexity of the honeybush tea volatiles, and on the other the performance of the single-stage thermal modulator for their comprehensive analysis. Some overloading was observed for high-level and polar compounds, yet overall excellent resolution was obtained and good utilisation of the two-dimensional separation space was evident. The benefit of the two-dimensional separation is clear from Figure 4.5, which shows the raw FID data depicting six consecutive ^{2}D chromatograms and the corresponding part of the contour plot.

Table 4.1 Volatile compounds identified in Cyclopia species by GC×GC-FID using reference standards. Differences between calculated and literature retention indices of under 30 are generally accepted.

Peak no.	Compound name	Retention index		*Cyclopia* species		
		[a]RI_{cal}	[a]RI_{Lit}	GEN	MAC	SUB
1	1-pentanol	766	779	Y	Y	Y
2	(*Z*)-2-penten-1-ol	772	783	Y	Y	Y
3	hexanal	803	800	Y	Y	Y
4	(*E*)-2-hexenal	854	854	Y	Y	Y
5	(*Z*)-3-hexen-1-ol	859	857	Y	Y	Y
6	3-methylbutanoic acid	870	877	Y	Y	Y
7	(*Z*)-4-heptenal	903	899	Y	Y	Y
8	γ-butyrolactone	919	922	Y	Y	Y
9	α-pinene	957	939	Y	Y	Y
10	6-methyl-2-heptanone	958	956	Y	Y	Y
11	benzaldehyde	966	969	Y	Y	Y
12	5-methylfurfural	969	978	Y	Y	Y
13	1-octen-3-ol	981	983	Y	Y	Y
14	(6*Z*)-2,6-dimethyl-2,6-octadiene[b]	990	981	Y	Y	Y
15	6-methyl-5-hepten-2-one	994	995	Y	Y	Y
16	decane	1002	1000	Y	Y	Y
17	octanal	1005	1007	Y	Y	Y
18	2-formyl-1-methylpyrrole	1011	1010	Y	Y	Y
19	(*E*,*E*)-2,4-heptadienal	1014	1017	Y	Y	Y
20	(*Z*)-β-ocimene	1029	1037	Y	Y	Y
21	limonene	1033	1033	Y	Y	Y
22	2,2,6- trimethylcyclohexanone	1041	1036	Y	Y	Y
23	4-hexanolide	1061	1056	Y	Y	Y
24	γ-terpinene	1064	1063	Y	Y	Y
25	2,6,6-trimethylcyclohexen-2-one	1065	1054	Y	Y	Y
26	1-octanol	1073	1074	Y	Y	Y
27	acetophenone	1073	1078	Y	Y	Y
28	*trans*-linalool oxide (furanoid)	1079	1076	Y	Y	Y
29	2-nonanone	1094	1093	Y	Y	Y
30	terpinolene	1095	1089	Y	Y	Y
31	nonanal	1108	1109	Y	Y	Y
32	2-phenylethanol	1123	1127	Y	Y	Y
33	methyl octanoate	1127	1128	Y	Y	Y

34	isophorone	1128	1030	Y	Y	Y
35	4-acetyl-1-methyl-cyclohexene	1138	1144	Y	Y	Y
36	(*E*)-3-nonen-2-one	1144	1144	Y	Y	Y
37	4-ketoisophorone	1150	1152	Y	Y	Y
38	(*E*,*Z*)-2,6,-nonadienal	1158	1159	Y	Y	Y
39	4-vinylanisole	1159	1158	Y	N	N
40	(*E*)-2-nonenal	1164	1165	Y	Y	Y
41	isoborneol	1169	1169	Y	Y	Y
42	benzyl acetate	1177	1172	Y	Y	Y
43	4-terpinenol	1186	1181	Y	Y	Y
44	p-cymen-8-ol	1192	1191	Y	Y	Y
45	α-terpineol	1198	1203	Y	Y	Y
46	dodecane	1202	1200	Y	Y	Y
47	decanal	1208	1210	Y	Y	Y
48	methyl nonanoate	1227	1227	Y	Y	Y
49	β-cyclocitral	1230	1234	Y	Y	Y
50	nerol	1235	1236	Y	Y	Y
51	(*Z*)-3-hexenyl-2-methyl butanoate	1235	1231	Y	Y	Y
52	(*Z*)-3-hexenyl isovalerate	1240	1240	Y	Y	Y
53	neral	1248	1248	Y	Y	Y
54	geraniol	1265	1260	N	N	N
55	p-anisaldehyde	1272	1270	N	N	N
56	geranial	1277	1277	Y	Y	Y
57	geranyl formate	1307	1305	Y	Y	Y
58	theaspirane isomer 1	1312	1313	Y	Y	Y
59	(*E*,*E*)-2,4-decadienal	1323	1319	Y	Y	Y
60	methyl decanoate	1323	1326	Y	Y	Y
61	*cis*-3-hexenyl-(*E*)-2-methyl-2-butenoate[b]	1328	1312	Y	Y	Y
62	theaspirane isomer 2	1330	1331	Y	Y	Y
63	hexyl tiglate	1335	1337	Y	Y	Y
64	α-cubebene	1361	1362	Y	Y	Y
65	eugenol	1370	1373	Y	Y	Y
66	(*E*)-2-undecenal	1370	1371	Y	Y	Y
67	4-nonanolide	1372	1377	Y	Y	Y
68	butyl benzoate	1382	1389	Y	Y	Y
69	geranyl acetate	1388	1381	Y	Y	Y
70	α-copaene	1391	1393	Y	Y	Y
71	(*E*)-β-damascenone	1396	1400	Y	Y	Y
72	tetradecane	1402	1400	Y	Y	Y
73	6,10-dimethyl-2-undecanone	1409	1410	Y	Y	Y

74	dodecanal	1413	1414	Y	Y	Y
75	2,6-dimethylnaphthalene	1419	1416	Y	Y	Y
76	(*E*)-β-damascone	1428	1409	Y	Y	Y
77	(*E*)-caryophyllene	1439	1419	Y	Y	Y
78	α-lonone	1441	1426	Y	Y	Y
79	α-humulene	1474	1477	Y	Y	Y
80	5,6-epoxy-β-ionone	1498	1484	Y	Y	Y
81	pentadecane	1502	1500	Y	Y	Y
82	5-decanolide	1508	1514	Y	Y	Y
83	methyl dodecanoate	1527	1528	Y	Y	Y
84	(*E*)-nerolidol	1573	1572	N	N	N
85	(*Z*)-3-hexenyl benzoate	1584	1588	N	N	N
86	hexyl benzoate	1590	1597	Y	Y	Y
87	isopropyl myristate	1827	1812	Y	Y	Y
88	hexahydrofarnesylacetone	1850	1838	Y	Y	Y

Y - identified compounds; N - not detected.

[a] – RI_{cal}- experimental retention index (note that the accuracy of this value is affected by the length of the modulation period and phasing of the modulation; the most abundant peak slice was used for each compound); RI_{Lit} - retention index from literature (NIST or PHEROBASE databases).

[b] – retention index obtained from reference [277].

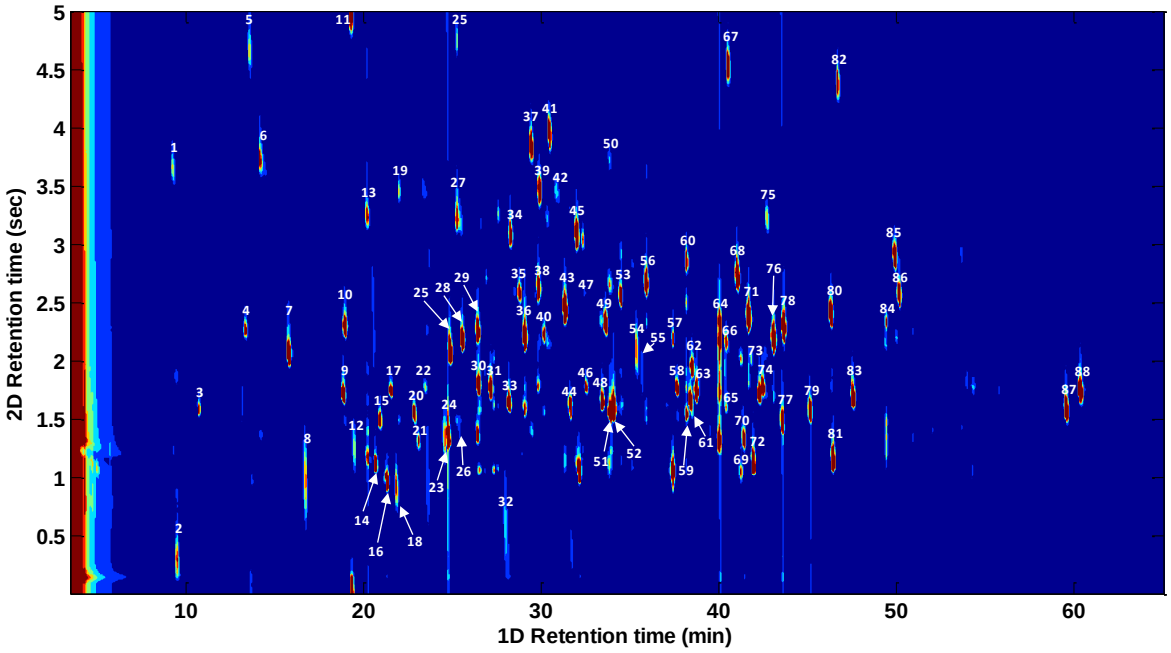

Figure 4.3 GC×GC-FID contour plot obtained for the separation of honeybush tea reference standards. The analysis was performed using optimized conditions (refer to Section 4.1.2.5). Peak numbers correspond to Table 4.1.

In these slices compounds labelled unknown 2 and unknown 3 co-elute perfectly in the first dimension, but are separated on the polar ^{2}D column, whilst the opposite is true for unknown 1 and (*Z*)-β-ocimene (20), which co-elute in the second dimension but are separated in the first. For accurate identification of compounds and for comparison of volatile profiles between samples, it is essential to achieve very stable retention times in both dimensions. In GC×GC, shifts in ^{1}D retention times are caused by irreproducible injection and/or small variations in temperature and carrier gas flow [34]**,** while shifts in ^{2}D are primarily caused by the modulator.

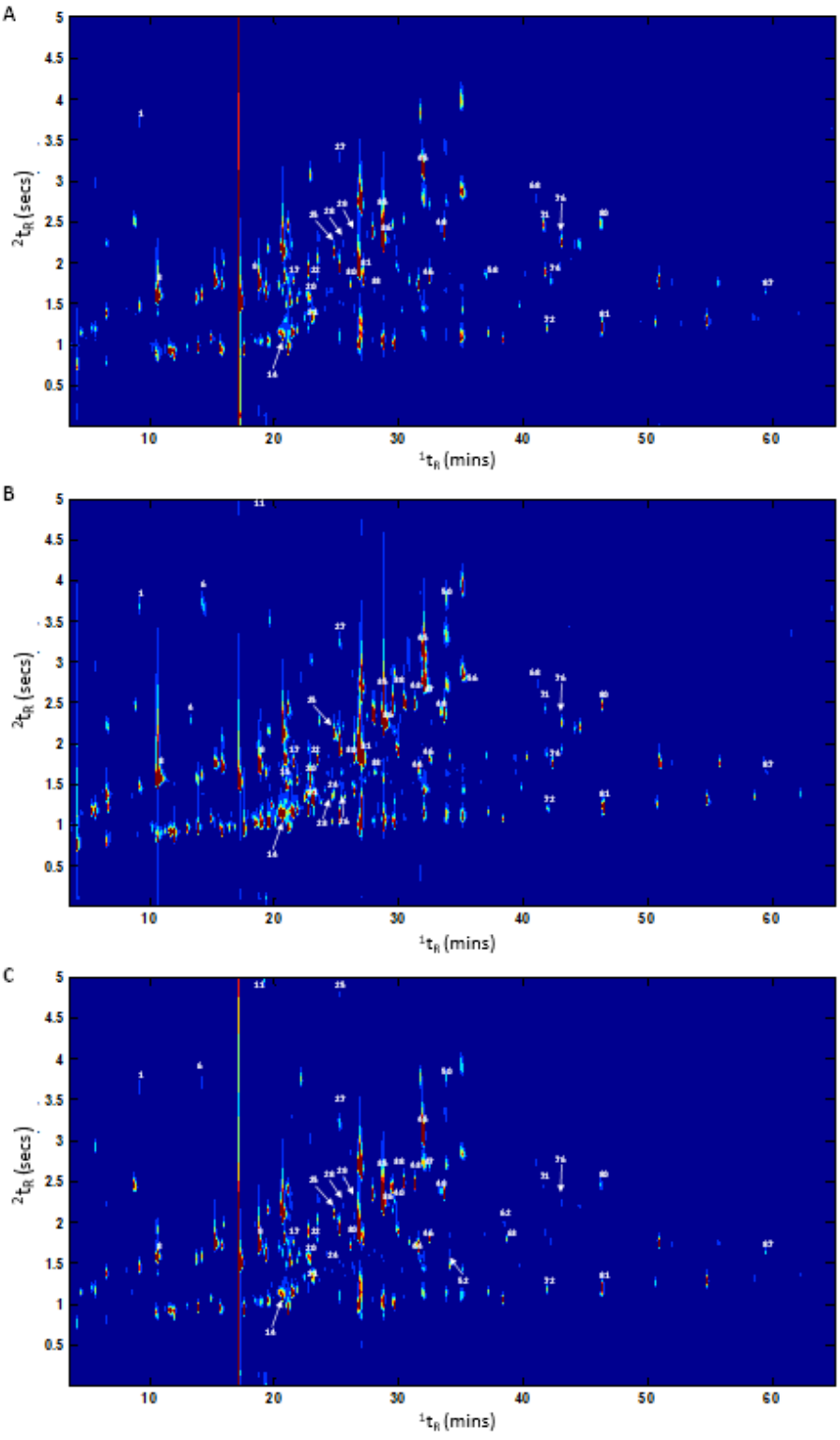

Figure 4.4 Representative GC×GC-FID contour plots obtained for the analyses of (A) *C. maculata*, (B) *C. subternata* and (C) *C. genistoides* samples. Analyses were performed using optimized conditions (Section 4.3.2.5). Peak numbers correspond to Table 4.1.

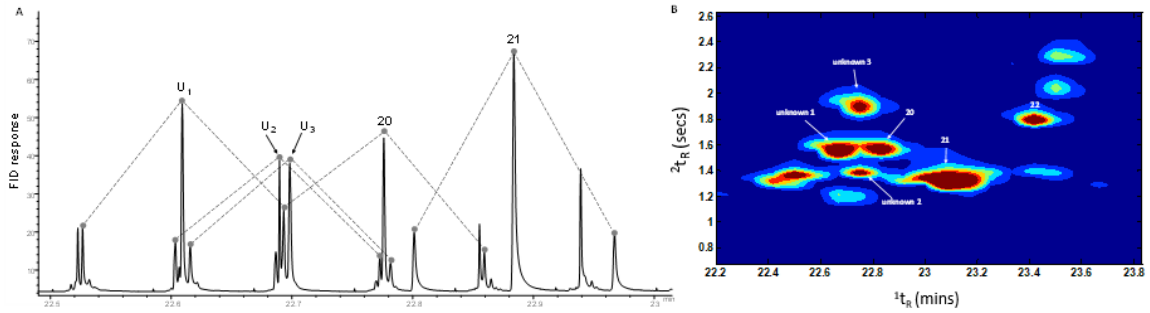

Figure 4.5 (A) Zoomed in region of the raw GC×GC-FID chromatogram of *C. maculata* corresponding to six consecutive ^{2}D chromatograms, and (B) corresponding part of the contour plot illustrating the resolution of the two-dimensional separation. Peak labels correspond to Table 4.1. U_x = unknown.

To evaluate the repeatability of the thermal modulator used in this work, a *C. maculata* sample was analysed six times each on two consecutive days to determine intraday and interday repeatability. Eight compounds covering a wide range of retention in both dimensions were selected for this purpose (Table 4.2). The average relative standard deviation (RSD) for ^{1}D and ^{2}D retention times were 0.07 % and 1.34 %, respectively. The shifts in ^{1}D corresponded to ± 1 modulation period and were mainly due to the fact that manual injection was used. This also influenced the ^{2}D retention times to some extent, as the analytes eluted at slightly different temperatures due to small discrepancies between the time of injection and starting each analysis. Despite this, however, the modulator showed excellent retention time reproducibility. See Appendix A for further information relating to these results.

Table 4.2: Summary of the repeatability of retention in both dimensions for the GC×GC separation of selected honeybush tea (*C. maculata*) volatiles using the optimized conditions (Section 4.1.2.5).

		First dimension repeatability			Second dimension repeatability			
Peak No.	Compounds	^1t_R (min)	Intra-day % RSD (n=6)	Inter-day % RSD (n=6)	^2t_R (s)	intra-day % RSD (n=6)	Inter-day % RSD (n=6)	$^2W_{1/2}$ (s)
1	1-pentanol	9.07	0.01	0.00	3.79	1.19	1.00	0.18
8	γ-butyrolactone	16.63	0.00	0.85	1.51	1.62	4.69	0.06
25	2,6,6-trimethyl cyclohexen-2-one	24.62	0.00	0.00	2.04	0.00	1.21	0.12
36	(E)-3-nonen-2-one	28.53	0.12	0.12	2.21	1.11	1.11	0.18
56	geranial	35.71	0.00	0.00	2.70	0.00	1.80	0.24
57	geranyl formate	37.45	0.00	0.00	1.74	0.00	1.93	0.12
76	(E)-β-damascone	42.87	0.00	0.00	2.08	1.49	1.59	0.18
80	5,6-epoxy-β-ionone	46.04	0.00	0.00	2.36	1.31	1.30	0.18

4.1.4. Conclusions

A consumable-free single-stage thermal modulator has successfully been applied for the GC×GC separation of honeybush tea (*Cyclopia* spp.) volatile constituents. Following method optimisation, good separation of honeybush volatiles was obtained. The modulator provides cost-effective operation and showed excellent performance in terms of retention time reproducibility, which proved beneficial in terms of multivariate analysis of the data. Limitations were observed for compounds present at high levels, where breakthrough due to trap overloading was observed. This is however a common problem in the analysis of natural products and beverages due to the large concentration range of compounds in such samples. Eighty four compounds were positively identified in three *Cyclopia* spp. using the developed method. Due in part to the limited number of available reference standards, only 5-methylfurfural and butyl benzoate were identified for the first time in honeybush tea. This work has illustrated the utility of GC×GC separation for honeybush tea analysis.

4.2 Analysis of polychlorinated biphenyls, organochlorine pesticides and chlorobenzenes[3]

4.2.1 Introduction

Analysis of persistent organic pollutants is a challenge for environmental laboratories for many reasons including a large number of compounds with varying chemical and physical properties present simultaneously in samples, concentration ranges varying from femtogram (fg) to microgram (µg) levels for different compound classes, many isomers for contaminant class, etc. Very large amounts of numerous Stockholm priority organic pollutants (POPs) (approximately 1 million tonnes of PCBs and 2 million tonnes of DDT alone) were manufactured during the last century and used in numerous industrial applications, and as pesticides and flame retardants [284]. Polychlorinated biphenyls (PCBs), organochlorine pesticides (OCs) and chlorobenzenes (CBs) are routinely analyzed in a variety of sample matrices including fish, fatty food, and environmental samples typically using one dimensional GC. There is currently no single GC column phase that can separate all 209 PCBs or 210 polychlorinated dibenzo-p-dioxins/polychlorinated dibenzofurans (PCDD/Fs), and consequently at least 2 columns must be used for accurate quantification of these types of pollutants [285].

PCBs, OCs and CBs can be routinely analysed using GC×GC for solid samples such as soil, sediment and sludge using the officially accredited GC×GC method developed at the Ontario Ministry of the Environment to reduce the number of sample preparation steps, improve data

[3] This section is based on the following publication:

A.M. Muscalu, M. Edwards, T. Gorecki, E.J. Reiner, "Evaluation of a single-stage consumable-free modulator for comprehensive two-dimensional gas chromatography: Analysis of polychlorinated biphenyls, organochlorine pesticides and chlorobenzenes," *Journal of Chromatography. A,* vol. 1391, pp. 93-101, 2015.

Author contributions include design and manufacture of the Mk IV modulator, on-site technical, operational and chromatographic analysis and support, secondary manuscript contributor, review and editing.

quality for these target classes of compounds and eliminate fractionation of the extracts, which is required with one dimensional analysis [286, 287]. This method has resulted in significant time- and analysis costs savings. The GC×GC system yields excellent within- and between-class separations and has replaced several conventional GC instruments. The GC×GC method developed has been shown previously to be both precise and accurate. The objective of this study was to evaluate the performance of a new single-stage consumable-free thermal modulator developed at the University of Waterloo versus the industry leading modulation system, the quad-jet liquid-nitrogen LN_2 modulator. The chromatographic separations, as well as the performance data were directly compared to the routine accredited method used for the analysis of PCBs, OCs and CBs in solid samples [286, 287].

4.2.2 Experimental

4.2.2.1 Standards and samples

PCB standards (BP-MS, BP-MS2, BP-MS3 – 82 compounds) were obtained from Wellington Laboratories (Guelph ON, Canada), while the chlorobenzenes (CB) and organochlorine pesticides (OC) standard mixtures, 15 and 23 compounds respectively, were acquired from Absolute Standards Inc. (Hamden, CT, USA). The multi-level calibration standard solutions containing PCB/OC/CB were prepared in iso-octane to produce a calibration series with concentrations ranging from 1 ng/ml to 500 ng/ml. 4,4'-Dibromo-octafluoro-biphenyl was added to each calibration solution at a concentration of 10 ng/ml as the internal standard for PCB congener quantification. Decachlorobiphenyl and 1,3,5-tribromobenzene (North Kingstown, RI, USA) were used as surrogates. A portion of an air-dried soil/sediment/sludge sample was extracted using accelerated solvent extraction (ASE, Dionex™ ASE™ 350, Thermo Scientific, Bannockburn IL, USA). The ASE conditions were as follows: one cycle extraction at 100 °C, heat

time 5 min., purge time 90 s, flush volume 60 %, extraction solvent 25 % dichloromethane/75 % hexane (V/V). The resulting extract was then subjected to a single stage silica cartridge cleanup procedure prior to instrumental analysis. This simple and fast sample preparation method results in a significant reduction in sample handling and solvent requirements. No fractionation of extracts is required prior to instrumental analysis, which results in significant time- and analysis costs savings with definitive enhancement in data quality. Sediment reference material SRM1944 (Standard Reference Material SRM1944 - New York/New Jersey Waterway Sediment) from National Institute of Standards and Technology (NIST - Gaithersburg, MD, USA) and another soil sample (CALA proficiency testing for PCB Total) were used to test the performance of the new modulator. The "real" samples' test results obtained with the consumable-free modulator were compared to the performance data acquired with the industry standard LN_2 modulator using the accredited routine method.

4.2.2.2 GC×GC System

The GC×GC-μECD system used for this study consisted of an Agilent 6890 gas chromatograph equipped with a split/splitless injector and a μECD detector. The following chromatographic column combination was used: 30 m x 0.25 mm, x 0.25 μm film thickness DB-1 (100 % dimethylpolysiloxane) from J&W Scientific (Folsom, CA, USA) as the first dimension column, 1.6 m, 0.18 mm, 0.18 μm film thickness Rtx-PCB from Restek Corporation as the second dimension column, and a 0.3 m, 0.1 mm IP-Deact column (Restek Corp.) as the transfer line to the detector. The transfer line was used in the experiments only when the LECO modulator was used. One microlitre samples were injected using the split/splitless injector operated in splitless mode at a temperature of 250 ºC while using a 4 mm id gooseneck liner (Restek Corp.). Helium

gas with a purity of 99.999 % was used as carrier gas at 1.2 ml/min flow rate. The micro-ECD system was operated at 300 °C using data acquisition rate of 50 Hz, with 5 % methane in argon as the detector make-up gas at a flow-rate of 150 ml/min. ChromaTof software (LECO Corp.) was used for data acquisition and processing for all analyses performed for this study.

4.2.2.3 Modulation

The LECO LN_2 quad-jet dual-stage modulator initially installed on the GC×GC system was used to develop the routine method for the analysis of PCBs and other halogenated compounds. Details are presented elsewhere [22]. The new modulator prototype was installed on the same system in order to obtain directly comparable data. This single-stage thermal modulator for GC×GC required no consumables for operation and was developed to trap, focus and re-inject the analytes into the second column using a specially prepared coated stainless steel capillary trap. Focusing of the analytes within this trap is assisted through compression of the trap between two ceramic cooling blocks. Injection of focused chromatographic bands into the secondary column was accomplished using a capacitive discharge power supply to resistively heat the trap, while rapid cooling was accomplished by compressing the steel capillary between two passively or actively cooled ceramic pads. The details of the system are described in Chapter 2 and shown in Figure 2.29. Once all the columns/parts were installed and leak checked, the column flow was measured at the secondary column outlet and set to 1.2 ml/min. The outlet was then connected to the μECD. The timing of the modulation with the GC run was critical for data acquisition and to generate reproducible GC×GC chromatograms. For this purpose, the timing of the modulation was synchronized with the data acquisition clock of the FID electrometer, installed on the system but not used for the analysis purposes. The modulation period set for all the runs was 4 s, similar to

the quad-jet, dual-stage modulator. The secondary oven was not used for any experiments involving the new modulator.

4.2.3 Results and discussion

4.2.3.1 GC×GC separations

The evaluation of the chromatographic separations was first carried out using the consumable-free modulator with passively cooled ceramic plates. When this type of cooling was employed, breakthrough was observed for some analytes as the ceramic plates were not cooling efficiently enough when the GC oven was heating during the run and cooling down in-between analytical runs (Figure 4.6 A). Higher voltage was tested with the trap, but it had a deleterious effect on trap longevity making the system impractical for routine use (Figure 4.6 B).

To improve the modulator's performance, an active cooling system using thermoelectric coolers attached to the heat conduits to which the ceramic plates were mounted was installed, and the breakthrough was significantly reduced for most problem compounds (Figure 4.6 C). This set-up was used for all performance data presented in this paper. Two exceptions were observed for the more volatile non-aromatic compounds: hexachloro-ethane (HCE) and hexachloro-butadiene (HCBD). Different experiments were performed to minimize the breakthrough of these compounds and the best results were obtained when the oven temperature was programmed to start at 60 ºC instead of the 80 ºC used with the validated method. The outcome of the routine GC×GC analysis for PCBs/OCs/CBs when using the LECO system is presented in Figure 4.6 D showing that PCB congeners were separated according to their degree of chlorination, as well as their planar structure (more retained in the ^{2}D plane). Wrap-around was observed for both systems but did not affect the separation of any of the target compounds. The GC×GC-μECD routine method using the cryogenic modulator and targeting 118 compounds showed a total of eight co-elutions: 3

within-class (PCB4/PCB10, PCB90/PCB101, 1,2,3,5-tetrachlorobenzene (1,2,3,5-TCB)/1,2,4,5-tetrachlorobenzene (1,2,4,5-TCB) and 4 between-class (heptachlor-epoxide/PCB74, gamma-chlordane (γ-CHLA)/PCB60, cis-nonachlor/PCB114, and methoxychlor (DMDT)/ PCB171). Figures 4.7 A and B indicate that, without further optimization of the GC method when using the single stage thermal modulator, two of these co-elutions were resolved: heptachlor-epoxide/PCB74 and cis-nonachlor/PCB114, which was further confirmed by analyzing individual standards for each of the compounds. These separations were very important as PCB74 is one of the major congeners in Aroclor 1232, 1242 and 1248, and PCB114 is one of the twelve dioxin-like PCBs. On the other hand, two compounds that were separated with the quad-jet modulator were co-eluting with the new modulator tested: PCB99 (large contributor in Aroclors) and alpha-chlordane (ubiquitous in environmental samples). To assess if this co-elution was due to the modulator's performance and not to the slight difference in the column set-up, the experiments with the quad-jet modulator were repeated with the 30 cm transfer line to the detector removed. The experiments showed that these compounds also co-eluted with the quad-jet modulator when the transfer line was not used, hence it was concluded that both systems performed similar under comparable conditions.

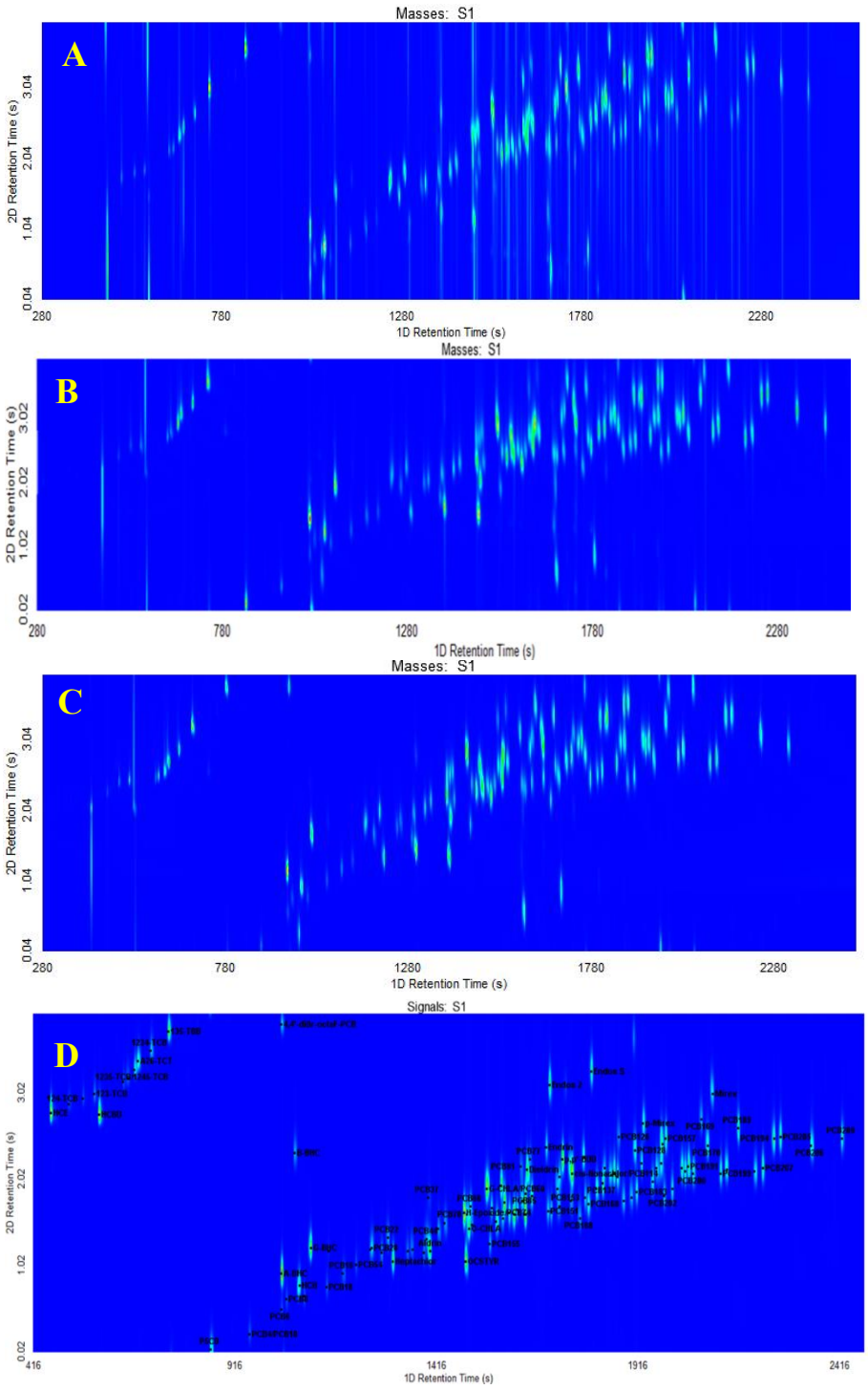

Figure 4.6 GC×GC-μECD contour plot of PCB/OC/CB standard mix (118 target compounds). (A) consumable-free modulator with passive cooling (22.4 discharge voltage) V; (B) consumable-free modulator with passive cooling at higher discharge voltage (24.4 V); (C) consumable-free modulator with active cooling for the ceramic plates (22.8 V discharge voltage); (D) LN_2 modulator.

4.2.3.2 Peak Characteristics

The peak widths in GC×GC are very small due to the modulation process: the first column eluent trapped in small fractions by thermal focusing during the modulation cycle is re-injected into the ^{2}D column resulting in very fast separation in the second dimension (peak width 50-600 ms). To evaluate the modulation's efficiency, the peak widths obtained with the single-stage thermal modulator were compared with the peak widths data from the accredited method. Table 4.3 and Figure 4.7 present the peak attributes, such as peak widths and heights, for selected target compounds for ten replicates analysed with each system (for the complete set of data for the target analytes see Appendix table S1) as obtained with both modulation types for a standard mix of 20 ng/ml. The data showed that peak widths ranged from 100 to 250 ms for LN_2 system and from 150 to 320 ms for the thermal modulator. When peak heights were compared, both systems produced similar results (Figure 4.8).

4.2.3.3 Thermal Modulator Performance: Quantification, Repeatability and Reproducibility

GC×GC calibration was performed using the PCB/OC/CB standard mixture at six different concentration levels ranging from 1 to 500 ng/ml to develop second order calibration curves used for quantification. External standard calibration method was used for the OC and CB, and internal standard calibration procedure was used for PCB quantification. Retention reference compounds and the internal standard were used to check retention time stability between runs. An initial assessment of the modulator was performed by evaluating the

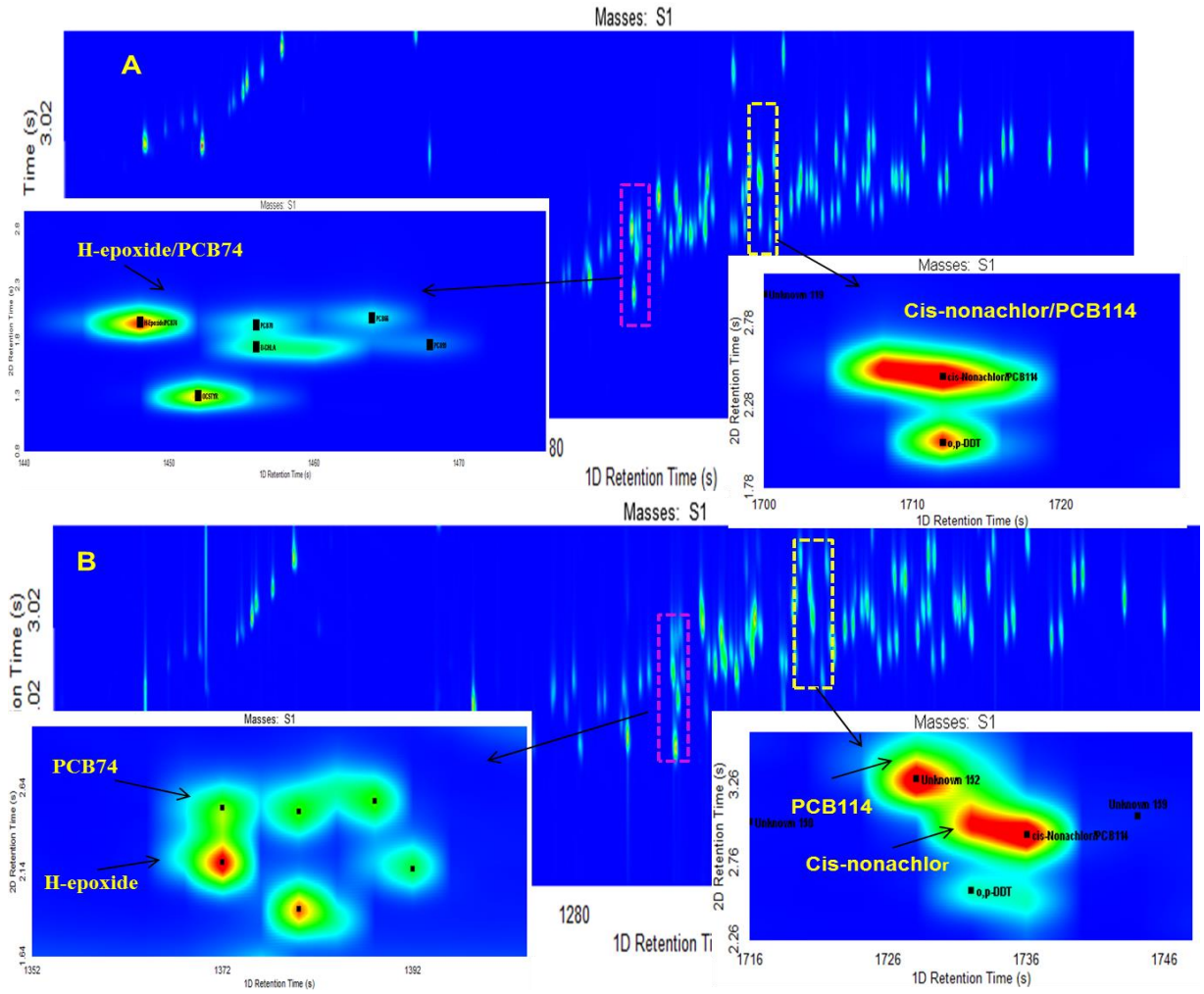

Figure 4.7 GC×GC- μECD contour plot of co-elutions with the GC set-ups using (A) the quad-jet LN_2 modulator and (B) the new consumable-free thermal modulator.

instrument detection limits (IDL) for each of the compounds. When using the consumable-free modulator, the IDLs ranged from 0.1 to 0.4 ng/ml, similar to the data obtained with the LN_2 modulator. Beside the IDLs, the data presented in Table 4.4 for selected compounds (see Appendix B for further information) showed that the instrument precision at the low level (1 ng/ml) expressed as relative standard deviation (% RSD) ranged from 1 to 14 % for PCBs, 1 to 4 % for CBs, and 1 to 9 % for OCs (with DDTs and heptachlor poorer performers, 17 % and 31 % respectively).

Table 4.3 Peak width attributes: Full Width at Half Height as obtained with both modulation systems

Name	Full Width at Half Height (ms) (N=10)	
	LN_2 Modulator	Consumable-free Modulator
PCB8	0.169	0.215
PCB18	0.172	0.223
PCB28/PCB31	0.189	0.268
PCB52	0.182	0.246
PCB66	0.209	0.273
PCB70	0.182	0.279
PCB74*	0.195	0.249
PCB90/PCB101	0.191	0.254
PCB114**	0.205	0.322
PCB118	0.206	0.288
PCB138	0.203	0.276
PCB153	0.199	0.269
PCB180	0.205	0.276
PCB206	0.218	0.288
PCB209	0.210	0.288
o,p-DDT	0.196	0.289
p,p'-DDD	0.206	0.290
p,p'-DDE	0.233	0.284
p,p'-DDT	0.208	0.285
Cis-nonachlor**	0.205	0.295
Heptachlor-epoxide*	0.195	0.295
Mirex	0.239	0.317
Oxy-chlordane	0.213	0.241
HCB	0.163	0.204
Octachlorostyrene	0.172	0.220

*Co-elution Heptachlor-epoxide/PCB74 - LN_2 system
**Co-elution Cis-nonachlor/PCB114 - LN_2 system

To assess the within-day quantitation repeatability, ten replicates of the 20 ng/ml standard were analysed and the data is presented in Table 4.5 (see Appendix B for further information). Experimental results showed % RSDs ranging from 2 to 11 % for PCBs (PCB114 – 21 % and

PCB85 – 13 %, poor performance, not baseline resolved), 4 to 8 % for CBs and 3 to 16 % for OCs (endrin – 24 %), very similar to the data obtained with the LN_2 modulator.

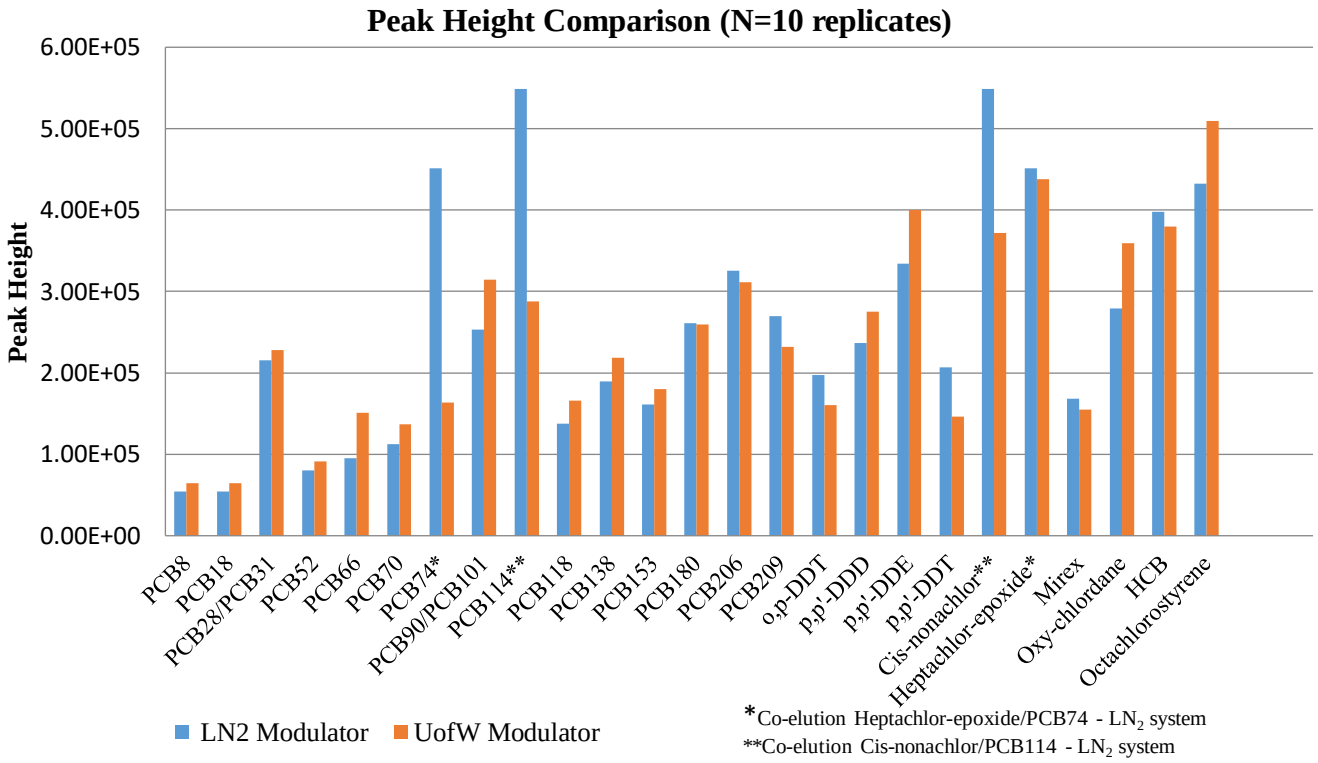

Figure 4.8 Peak height comparison for selected compounds analyzed with LN_2 modulator and the consumable-free thermal modulator (*co-elution Heptachlor-epoxide/PCB74for the LN_2 system, **co-elution Cis-nonachlor/PCB114 for the LN_2 system).

To further evaluate the instrument performance, between-run results of 5 replicates at 20 ng/ml were evaluated and the data showed % RSDs between 3 and 15 % for PCBs, 3 to 13 % for OCs (exceptions included endrin at 33 %, p,p'-DDT at 45 % and heptachlor at 51 %), and 6 to 12 % for CBs (see Appendix B for further information).

SRM1944, a NIST sediment standard reference sample, was one of the reference materials used to determine the efficiency of the extraction, clean-up and instrumental procedures and to

assess the accuracy of the GC×GC-μECD method prior to accreditation. One of these SRM1944 extracts, previously analyzed with the LN_2 system, was re-injected into the system using the new consumable-free modulator and the recoveries of the target analytes were determined. These analyses assessed the performance of the modulators when analysing real samples where numerous interferences were present. The results presented in Figure 4.9 A showed that the performance of both modulators was comparable. The error bars represent the standard deviations for the SRM1944 certified values. The target compounds were separated in the second dimension from the other classes of contaminants present, similar to the routine method's separation (Figure 4.9 B). In addition to accurately quantifying the target compounds, the analyses performed with the new modulator showed similar enhanced separations of the targets from matrix interferences and other classes of contaminants present in the sediment samples. The performance of the new modulator was also evaluated by analysing a soil sample, proficiency testing sample for PCB known to have many interferences present, and the final result expressed as PCB total (sum of all the PCBc with concentrations above method's detection limits) was compared to the data obtained from the routine method as well as the design value. The quantitative results were very comparable between the tests: 77.9 μg/g for the consumable-free modulator, 85.4 μg/g for the routine method compared to the design value of 99.36 μg/g.

Table 4.4. Instrument Detection Limits for the GC×GC-μECD systems with the two modulators

Name	Design (ng/ml)	LN_2 Commercial Modulator (N=9)			Consumable-free Modulator (N=5)		
		Avg.	% RSD	IDL	Avg.	% RSD	IDL
PCB8	1	0.95	5.77	0.16	0.81	11.33	0.28
PCB18	1	1.05	1.99	0.06	0.89	5.15	0.14
PCB28/PCB31	2	1.78	1.08	0.08	2.07	3.26	0.20
PCB52	1	0.94	12.50	0.35	1.04	6.56	0.20
PCB66	1	0.98	3.82	0.11	1.01	4.39	0.13
PCB70	1	0.98	7.17	0.21	0.96	5.37	0.16
PCB74*	2 (1)	1.96	1.81	0.10	1.17	1.15	0.04
PCB90/PCB101	2	2.04	5.40	0.33	2.12	1.31	0.08
PCB114**	2 (1)	1.89	3.26	0.17	0.12	0.35	0.00
PCB118	1	1.07	3.02	0.10	1.21	2.80	0.10
PCB138	1	1.12	2.36	0.08	0.93	4.30	0.12
PCB153	1	1.00	4.08	0.12	0.89	4.63	0.12
PCB180	1	1.07	3.67	0.12	0.94	2.76	0.08
PCB206	1	1.02	11.02	0.34	1.00	3.32	0.10
PCB209	1	1.05	2.06	0.07	1.13	1.45	0.05
o,p-DDT	1	1.31	4.02	0.12	0.99	17.05	0.51
p,p'-DDD	1	0.87	10.76	0.42	1.17	2.04	0.07
p,p'-DDE	1	1.02	4.17	0.11	1.23	2.42	0.09
p,p'-DDT	1	1.40	2.43	0.07	1.17	8.74	0.31
Cis-nonachlor**	1	1.89	3.26	0.17	1.02	12.09	0.37
Heptachlor-epoxide*	1	1.96	1.81	0.10	1.19	2.40	0.09
Mirex	1	0.82	3.50	0.15	1.08	8.39	0.27
Oxy-chlordane	1	1.03	2.05	0.07	1.05	7.65	0.24
HCB	1	0.83	3.24	0.08	1.11	1.76	0.06
Octachlorostyrene	1	0.86	2.03	0.05	1.15	3.10	0.11

*Co-elution Heptachlor-epoxide/PCB74 - LN_2 system

**Co-elution Cis-nonachlor/PCB114 - LN_2 system

4.2.3.4 Robustness: Between-run and between-trap system reproducibility

To test the system's robustness and assess its suitability for routine analysis, we evaluated the ^{1}D and ^{2}D retention time shifts in-between analytical runs. The results were very encouraging as negligible shifts in retention times were observed for both within-day and between-day

comparisons of the studied samples. For instance, the % RSD of the within-run retention time shifts calculated for the routine method's five reference compounds (1,3,5-tribromobenzene, p,p'-DDE, PCB52, PCB151 and PCB199), for ten replicates of the 20 ng/ml standard, ranged from 0.3 to 0.6 % in the first dimension and from 0.8 to 2 % s in the 2nd dimension.

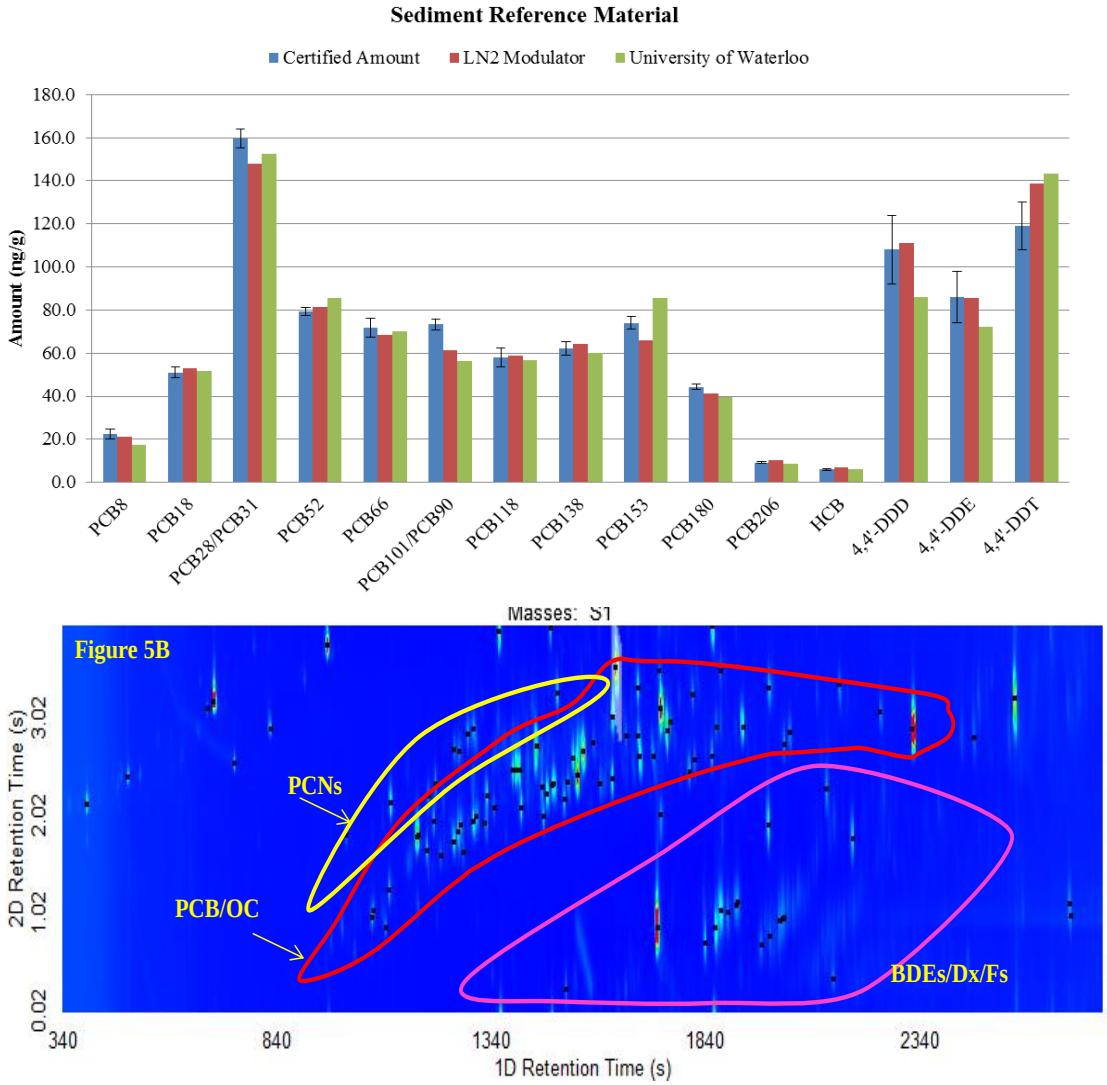

Figure 4.9 Sediment Reference Material (SRM1944) comparison: (A) Certified values comparison as obtained from both systems. (B) Two-dimensional chromatograms showing the target compounds' separation from interferences present in the sediment sample when using the consumable-free single stage modulator. BDE – brominated diphenylethers; Dx – polychlorinated dioxins; Fs – polychlorinated furans; PCN – polychlorinated naphthalenes.

Beside the retention time shifts, it was very important to have reproducible chromatograms when the trap needed to be replaced. Changing the column set for the routine method (DB-1 x Rtx-PCB x transfer line) required very meticulous adjustments: it was critical to have a specific length of the ^{2}D column placed in the main oven upstream of the modulator and an exact length of the transfer line to the detector to obtain reproducible chromatograms. The consumable-free modulator was not using the secondary oven and the column lengths in the ^{2}D oven or transfer line were not variables in this case. For the tests, the trap used for the determination of the performance data presented in this thesis was switched for a new trap and tested by injecting three replicates of the calibration standard at 20 ng/ml. The retention times of the five reference compounds used to monitor the time shifts for the routine method (1,3,5-tribromobenzene, p,p'-DDE, PCB52, PCB151 and PCB199) were checked for the old and the new trap and negligible shifts were observed. All the retention time shifts fell in-between the ranges observed for the within-run retention time % RSDs presented above.

Table 4.5 Repeatability - within-run standards at 20 ng/ml: PCBs with different chlorination level, OCs and CBs

Compound Name		Expected amount (ng/ml)	**LN_2 Modulator (N=10)**		**Consumable-free Modulator (N=10)**	
			Average	**RSD (%)**	**Average**	**RSD (%)**
EU Indicator PCBs	# Chlorines					
PCB28/PCB31	2,4,4'-/2,4',5-Trichlorobiphenyl	40 (coelution)	41.8	3.8	38.8	2.6
PCB52	2,2',5,5'-Tetrachlorobiphenyl	20	20.5	0.7	20.1	3.4
PCB90/PCB101	2,2',3,4',5-/2,2',4,5,5'-Pentachlorobiphenyl	40 (coelution)	43.2	1.2	38.2	2.6
PCB118	2,3',4,4',5-Pentachlorobiphenyl	20	18.0	5.8	21.1	5.3
PCB138	2,2',3,4,4',5'-Hexachlorobiphenyl	20	20.2	2.9	18.8	4.8
PCB153	2,2',4,4',5,5'-Hexachlorobiphenyl	20	22.8	7.8	18.8	12.9
PCB180	2,2',3,4,4',5,5'-Heptachlorobiphenyl	20	21.7	4.6	19.0	6.9
Other PCBs	# Chlorines					
PCB8	2,4'-Dichlorobiphenyl	20	21.2	2.7	20.3	3.1
PCB18	2,2',5-Trichlorobiphenyl	20	20.4	2.9	21.1	2.3
PCB206	2,2',3,3',4,4',5,5',6-Nonachlorobiphenyl	20	21.8	7.9	18.8	3.1
PCB209*	2,2',3,3',4,4',5,5',6,6'-Decachlorobiphenyl	20	20.7	6.9	18.7	4.2
OCs						
p,p'-DDE		20	18.8	3.3	18.2	4.7
Mirex		20	18.1	7.7	18.5	2.3

Oxy-chlordane	20	19.1	7.9	19.7	6.5
Heptachlor-epoxide**	20	N/A	N/A	20.8	11.5
CBs					
HCB	20	22.3	3.4	19.8	5.8
Octachlorostyrene	20	20.0	7.9	19.5	6.2
1,3,5-tribromobenzene*	20	21.9	4.4	20.7	5.0

*Surrogates
**Co-elutes with
PCB74

4.2.4 Conclusions

Comprehensive two-dimensional gas chromatography coupled with a micro electron capture detector has been used as a sensitive and selective routine method for the determination of PCBs, OCs, and CBs in sediments, soils and sludges in a single analytical run for the last five years in the analytical laboratory of the Ontario ministry of the Environment and Climate Change. The method proved to be an excellent analytical tool in the assessment of the presence of other additional compounds and the initial identification and monitoring of new and emerging halogenated compounds present in sample extracts. The evaluation of the new consumable-free single stage thermal modulator was performed for the same target compounds as the accredited method and focused on the chromatographic separations and system's repeatability and reproducibility of the results. The performance of the consumable-free thermal modulation system proved to be comparable to the commercially available LN_2 modulator. The experimental data obtained was accurate and precise for the standards and reference material tested. Also, without any further optimization of the GC method and without using the secondary oven, two co-elutions found in the LN_2 method were resolved when the newly developed modulator was used. This very simple, consumable free and cost effective modulator was very easy to install and operate on any GC system making it a less expensive alternative for performing GC×GC separations.

Furthermore, its flexibility gives new opportunities of performing comprehensive two-dimensional GC with other detectors that are fast enough to handle the narrow peaks generated by GC×GC.

4.3 Evaluation of a miniaturized single-stage thermal modulator for comprehensive two-dimensional gas chromatography of petroleum contaminated soils[4]

4.3.1 Introduction

Modulation based on cryogenic focusing has proven to be very effective in GC×GC and has become the dominant modulation strategy [288]. The main limitation of this strategy is the need for a refrigeration unit or expensive liquid cryogen, which limits the adoption of this technique for routine and portable analysis [289]. Resistive heating has been shown to be very effective for providing temperature programmed GC analysis [289]] and this technique was used during the initial development the GC×GC technique [32]. Harynuk and Górecki used resistively heated stainless steel (SS) trapping capillaries (530 µm) packed with the macroporous organic polymer Tenax TA using both liquid nitrogen cryogen and air-cooling for solute focusing [290]. Capacitive discharge facilitated rapid mobilisation of trapped components with the application of electrical current to the SS capillary. Libardoni et al. later developed a single-stage thermal modulator with another SS capillary (180 µm) coated with a non-polar stationary phase (MXT-1, 0.2 µm), however this design was reliant on refrigerated air or cryogen for solute focusing [89,

[4] This section is based on the following publication:

M.R. Jacobs, M. Edwards, T. Górecki, P.N. Nesterenko, R.A. Shellie, "Evaluation of a miniaturised single-stage thermal modulator for comprehensive two-dimensional gas chromatography of petroleum contaminated soils," *Journal of Chromatography A*, vol. 1463, pp. 162-168, 2016.

Author contributions include design and manufacture of the miniature version of the Mk IV modulator, remote technical, operational and chromatographic support, secondary manuscript contributor, review and editing.

291]. Work done by Colin et al. highlighted how alternative modulator stationary phases could be beneficial for thermal modulator designs, compared to conventional stationary phase coatings [100].The use of a highly polar room temperature ionic liquid stationary phase coating within a micro-fabricated GC×GC modulator minimized stationary phase bleed from the modulator while temperature pulses were being applied compared to conventional PDMS-based coatings that have been utilized in the past as the basis of thermal modulators [101]. Muscalu et al. reported the development of novel thermally stable stationary phase coating for single-stage thermal GC×GC for the analysis of polychlorinated biphenyl compounds [203]. While dual-stage modulators are typically used to prevent solutes from passing through a modulator without being focused, several authors have demonstrated that optimisation of a single-stage modulator design can minimize the potential for breakthrough without recourse to an additional focusing stage [89, 203]. The aim of this study was to evaluate a miniaturized single-stage thermal modulator that incorporates an adsorptive stationary phase coating and high-speed resistive heating for comprehensive two-dimensional GC×GC modulation. This modulator was evaluated using a range of compounds and then applied to the analysis of petroleum hydrocarbon spills affecting a sub-Antarctic research station. The performance of this novel modulator is reported herein.

4.3.2 Experimental

4.3.2.1 Instruments

An Agilent 6850A Gas Chromatograph (Agilent Technologies, Wilmington, DE, USA) equipped with a S/SL injector, 7683B Series ALS (Agilent) and an FID was used for all analyses. The first-dimension column was a DB5-MS 25 m × 250 m × 0.25 m (Agilent) coated with a low-polarity silarylene-based stationary phase equivalent to 5 % diphenyl- 95 % dimethylpolysiloxane. The second-dimension column was an Rxi 17Sil MS 1 m × 100 µm × 0.1

µm (Restek, Bellefonte, PA, USA) coated with a mid-polarity silarylene stationary phase equivalent to 50 % diphenyl- 50 % dimethylpolysiloxane, which was selected due to its high efficiency and rapid separation speed. The modulator was constructed from a segment of SS capillary (4 cm long, 0.28 mm) coated with an adsorptive stationary phase coating prepared using a proprietary procedure [203]. The modulator was installed within the GC convection oven and connected to the first- and second-dimension columns using two SilTite mini unions (Trajan Scientific & Medical, Ringwood, Australia). The trapping capillary was compressed between a pair of ceramic pads mounted on a hinged device that was installed through the wall or roof of the GC convection oven as shown in Figure 4.10 B. The compression device served as a heat conduit, ensuring that the modulator was kept at sub-oven temperature. The device was made of

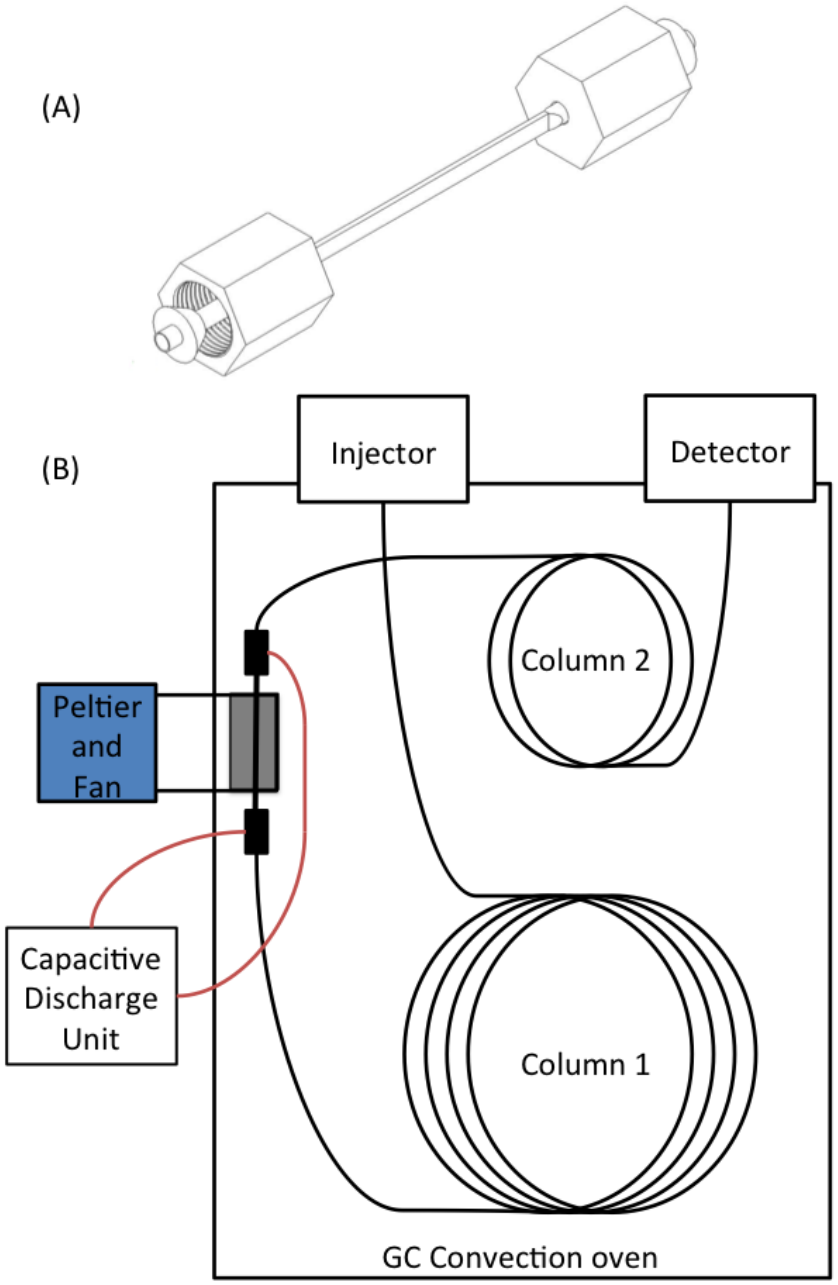

Figure 4.10 Schematic diagram of the trapping capillary used in the resistively heated single-stage modulator (A) and a diagram showing the modulator's installation in a GC convection oven (B).

copper and cooled using a pair of fans (12 V) and thermoelectric cooling pads (5 V, 2.6 A) that were mounted outside of the convection oven. The trap was connected to a programmable (0–40 V) capacitive discharge power supply (4 × 44,000 µF capacitor array) using two glass fiber braid-insulated copper wires.

4.3.2.2 Modulator performance testing

A test mixture containing a range of different compounds was injected (1 µL) into the S/SL inlet at a split ratio of 100:1 and all analytes were determined in triplicate. The inlet temperature was 250 °C and a 4 mm SGE split liner (Trajan) was used. The carrier gas was hydrogen, with a constant flow rate of 1.0 ml/min. The initial head pressure was 87.08 kPa at 30 °C. The GC temperature was initially 30 °C for 1 min and then temperature programed at a rate of 5 °C/min to 200 °C. The FID temperature was 250 °C and operated at a data sampling rate of 200 Hz to ensure adequate detection of the narrow peaks generated during modulation [292]. The capacitive discharge power supply was programmed to provide a modulation period of 3.0 s, with a discharge voltage of 21.0 V.

4.3.2.3 Petroleum spill analysis

Samples and standards were injected (1 µL) into a S/SL inlet with a split ratio of 20:1. The inlet temperature was 280 °C and a 4 mm SGE split liner was used. All samples were analyzed in triplicate while the facilitator sample (Section 4.2.2.4) was analyzed ten times throughout the analytical sequence. The carrier gas was hydrogen with a constant flow of 0.8 ml/min. The initial head pressure was 66.10 kPa at 40 °C. The GC temperature was initially 40 °C for 1 min and then the temperature was programed at a rate of 5 °C/min to 320 °C and held for 3 min. The FID temperature was 280 °C. FID data acquisition rate and capacitive discharge power supply parameters were as described in Section 4.2.2.2.

4.3.2.4. Standards and samples

Toluene, *n*-octane, ethylbenzene, 2-heptanone, pentylacetate, *n*-decane, 2-octanol, 2-nonanone, 1,6-hexanediol, *n*-docecane, 2-decanol, 4-chlorophenol and *n*-tetradecane were obtained from Sigma Aldrich (Castle Hill, Australia) and used to prepare a stock solution of a model mixture used for the performance testing of the modulator of 10,000 mg/kg in dichloromethane (Sigma Aldrich). This stock was diluted with dichloromethane to obtain a series of standards with concentration ranging from 100 to 0.5 mg/kg. Soil extracts were obtained from the Australian Antarctic Division (Kingston, Tasmania). Soil samples were prepared using the method described in ref. [293]. Each soil sample (10 g) was spiked with 1-bromoeicosane at 25 mg/kg (Sigma-Aldrich) and then extracted using *n*-hexane (Mallinckrodt Baker, USA). The extracts originated from two sites, indicated as the Fuel Farm (FF) and Main Power House (MPH) on Macquarie Island (see reference [294] for details on each sampling site). A sample of Special Antarctic Blend (SAB) diesel was obtained from the Macquarie Island research station. A series of SAB diesel dilutions were prepared ranging in concentration from 100 to 3000 mg/kg in *n*-hexane (Mallinckrodt Baker). Each SAB diesel sample was spiked with 1-bromoeicosane at 25 mg/kg (Sigma-Aldrich) for internal standardisation purposes. Two fuel spill sample extracts containing approximately 3000 mg/kg of petroleum hydrocarbons from the FF and MPH sites were combined in a 1:1 ratio and used as a facilitator sample as described by Furbo et al. [295]. A 10 mg/kg standard containing *n*-alkanes from *n*-octane to *n*-eicosane (Sigma Aldrich) and a range of polycyclic aromatic hydrocarbons (PAHs) including naphthalene, fluoranthene, acenaphthene, chrysene, benzo(k)fluoranthene, dibenz(a,h)anthracene, benzo(g,h,i)perylene, benzo(a)pyrene, anthracene, phenanthrene, indeno(1,2,3-c,d)pyrene, benzo(b)fluoranthene,

fluorene, pyrene, benz(a)anthracene, 2-methylnaphthalene and acenaphthylene (Restek, catalogue #31458) was prepared in *n*-hexane (Sigma Aldrich).

4.3.2.5. Data processing

Data were acquired using ChemStation Software B04.03(16) (Agilent, Santa Clara, CA, USA) and then imported into GC Image R2.5b4 software (GC Image LLC, Lincoln NE, USA). Baseline correction and peak detection were performed using GC Image with default settings. Peak areas, retention times and chromatograms were generated for the modulator performance testing mixture, which were then exported to Microsoft Excel for calibration and analysis. The Image Investigator feature of GC Image was used to generate a composite chromatogram that was constructed from ten replicate analyses of the facilitator sample. A peak template was then constructed based on this composite chromatogram. This peak template and the Image Investigator feature were used to analyze each of the GC×GC chromatograms and generate a peak summary report. All chromatograms were manually reviewed to ensure correct alignment of the peak template and all peak summary tables were exported in Excel format for further analysis.

4.3.3 Results and discussion

4.3.3.1 Modulator evaluation

The key to effective single stage modulation is to ensure that the mobilisation step is very rapid, and that the return to trapping temperatures is fast enough to prevent the breakthrough of solutes from the first-dimension column. A SS capillary (280 µm) was used as the basis for the present modulator, which is based on previous research by Górecki and co-workers [95, 203]. The capillary was rapidly heated using a capacitive discharge power supply to high temperature (>400 °C) in just a few milliseconds, with the final trap temperature depending on the charging

voltage selected with the power supply. Figure 4.10 shows the construction (A) and installation (B) of the single-stage GC×GC modulator. The modulator was installed within the GC convection oven using a Peltier-cooled heat-sink device as shown in Figure 4.10 B. This installation of the heat sink through the wall of the GC convection oven allowed the trap to track the temperature of the oven with a temperature differential to enhance the solute loading capabilities of the trap. For example, while the GC oven temperature was 40 °C, the initial modulator temperature was 15 °C cooler with respect to the oven. This temperature differential increased progressively throughout a temperature-programmed analysis to yield a 100 °C differential at an oven temperature of 300 °C. The present modulator differs from the Mk IV design, previously described in section 2.5, in a number of ways [203]. Specifically, the length of the trapping capillary has been reduced to just 4 cm long, and the total size of the heat conduits and heat sink used for trap cooling was reduced by more than 50 % while still providing modulation capabilities. The modulator was amenable towards field analysis with its small size and requirement of only electricity for operation. An image of the modulator can be seen in Figure 4.11.

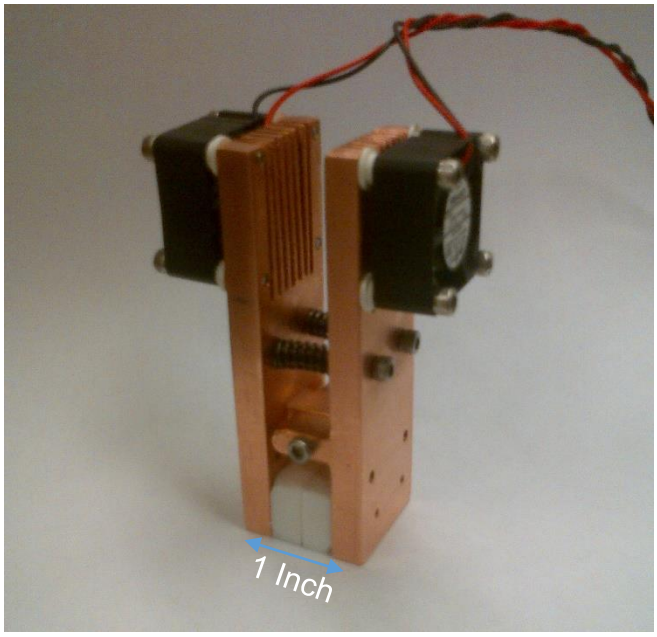

Figure 4.11 A photo of the portable version of the Mk IV design.

The ability of this modulator to trap and mobilize solutes was assessed by analysing a model mixture composed of 13 compounds with different chemical functionalities to determine whether any solute discrimination was occurring within the modulator. A range of concentrations (0.5–100 mg/kg) were analysed in triplicate to evaluate the solute loading capabilities of the trap, as well as determine its ability to focus solutes in a repeatable manner, with the results summarized in Table 4.6. A bi-logarithmic plot of peak area (Vp) versus solute mass (m_s) was used to assess the loss of solutes to breakthrough, where slopes of less than 1 represent solute losses [90, 91].

All solutes were well modulated with the exception of *n*-octane, which showed significant breakthrough with approximately 21 % of the mass passing through the trap without being focused. Interestingly, toluene was well focused by the modulator, suggesting that the stationary phase of the trap had enhanced solute loading capacity for aromatic compounds compared to volatile aliphatic compounds like *n*-octane.

Table 4.6 Summary of different resistively heated modulator designs including: the capillary type (SS = stainless steel, FS = fused silica), trap stationary phase, modulator cooling used.

Authors	Modulator construction	Trapping stationary phase	Trap cooling	Ref
Liu and Phillips	FS column, 100 µm, conductive paint, dual stage, 15 cm	PDMS 0.5 µm	GC oven only	[32]
de Geus *et al.*	FS column, 220 µm, conductive paint, 30 cm	CP-Sil8 CB (5 % phenyl, PDMS) 0.5 µm	Air cooling	[41]
Phillips *et al.*	FS column, 100 µm, rotating modulator, 10 cm	PDMS 3.5 µm	GC oven only	[45]
Harynuk and Górecki	SS tube, 530 µm, 2.0 cm	Micro packed TENAX TA	Liquid nitrogen	[78]
Burger *et al.*	SS tube, 530 µm, 11 cm; FS column 200 µm	DB-1 (PDMS) 3 µm	GC oven only	[43]
Libardoni *et al.*	SS column, 180 µm, single-stage, 5.5 cm	MXT-1 (PDMS) 0.2 µm	Refrigerated air	[89]
Libardoni *et al.*	SS column, 180 µm, single-stage, 5.5 cm	MXT-1 (PDMS) 0.2 µm	Refrigerated ethylene glycol	[291]
Goldstein *et al.*	SS column, 530 µm, dual stage, 15 cm	MXT-1 (PDMS) 3 µm	Air cooling	[95]
Libardoni *et al.*	SS column, 100 µm, dual stage, 5.5 and 2.2 cm	MXT-1 (PDMS) 0.2 µm	Refrigerated air	[91]
Panič *et al.*	SS column, 280 µm, dual stage, 15 cm	MXT-1 (PDMS) 1 µm	Air cooling	[94]
Muscalu *et al.*	SS column, 280 µm, flattened to 100 µm, 15 cm	Proprietary adsorptive coating	Air and thermoelectric cooling	[203]
Present modulator	SS column, 280 µm, flattened to 100 µm, 4 cm	Proprietary adsorptive coating	Air and thermoelectric cooling	N/A

Higher molecular weight *n*-alkanes (*n*-nonane onwards) did not exhibit this breakthrough effect, suggesting that the cooling of the trap might not have been sufficient for focusing high concentrations of the most volatile aliphatic hydrocarbons. A chromatogram of two representative compounds (*n*-decane and ethylbenzene) is shown in Figure 4.12. A number of test compounds also revealed log V_p− log m_s slopes greater than 1, which indicates that some

signal enhancement was occurring. Calibrations were linear across the concentration range of 5–1300 pg (mass on column) with an average LOD of 70 pg using FID. Average RSDs (%) of 9 × 10^{-5} and 2.7 were achieved for the first- ($^{1}t_R$) and second dimension ($^{2}t_R$) retention times, respectively, which compared favourably with other thermal and cryogenic modulators [32, 89, 90, 203]. An average peak area repeatability of 3 % RSD was obtained, which is sufficient for quantitative analysis. The second-dimension peak widths of each solute summarized in Table 4.7 showed average values on the order of 72 ± 3 ms measured at half height. Polar solutes were retained more strongly by the second-dimension column than aliphatic species, which caused greater peak broadening compared to non-polar analytes, as expected during GC×GC separations. Peak symmetry was used as an indicator of analyte sorption behaviour between the mobile and stationary phase. Peak symmetry was calculated using the following formula:

$$Peak\ symmetry = \frac{b}{a}$$

where *b* represents the distance from the peak midpoint to the trailing edge of the peak measured at 5% peak height, and *a* represents the distance from the leading edge to the midpoint measured at 5% peak height. Peak symmetry values less than 1 represent a fronting peak, and values greater than 1 represent a tailing peak. The peak symmetry factors for polar solutes were on average 1.9 ± 0.3, while non-polar solutes displayed greater asymmetry with a symmetry factor of 2.8 ± 0.5. The improved symmetry statistics for the polar solutes is likely due to the improved capacity of each of these solutes in the polar second-dimension column. The consumable free system provided performance competitive with cryogenic based and alternative thermally modulated GC×GC systems, which typically produce peaks with widths between 20 and 120 ms at half

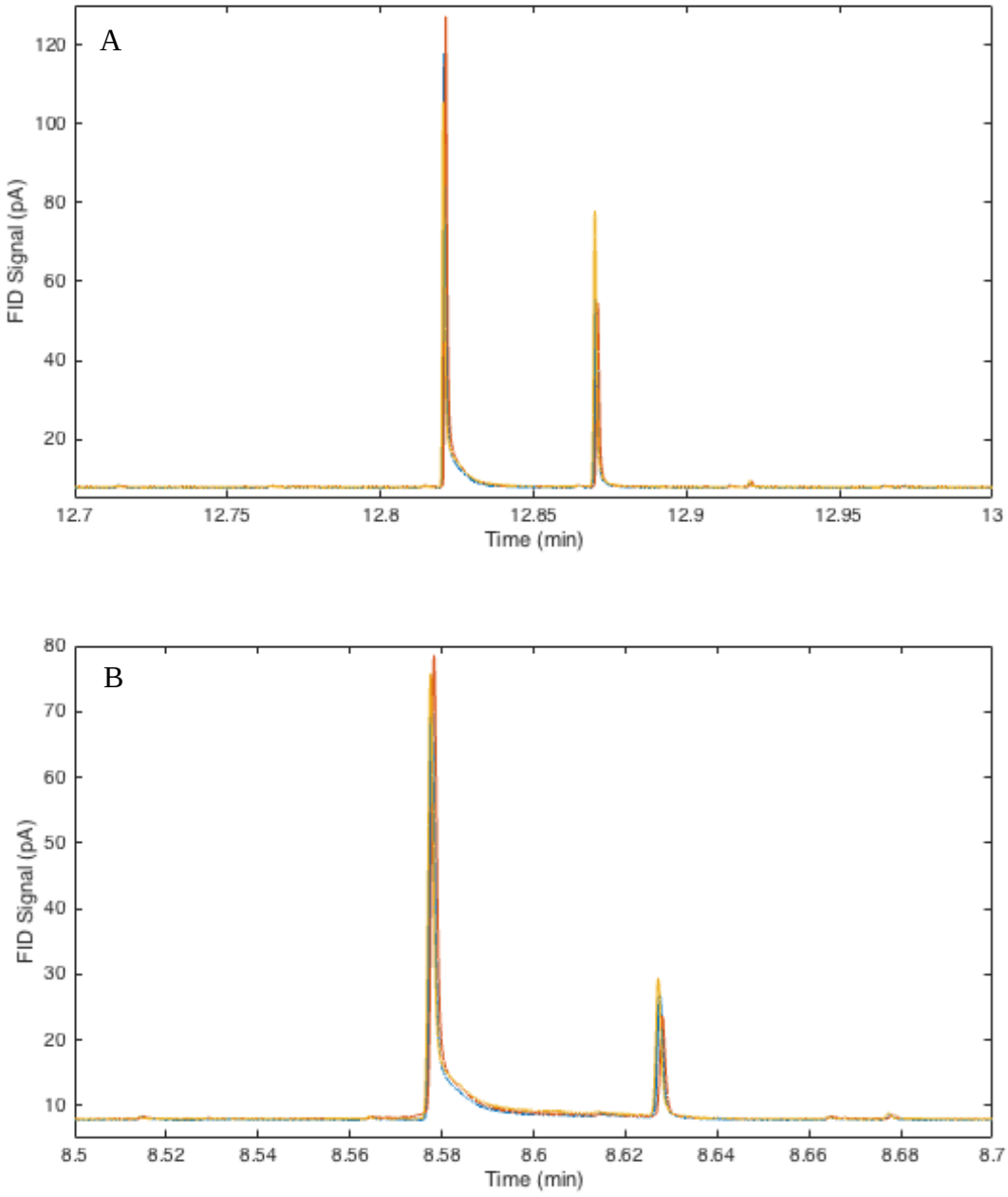

Figure 4.12 One-dimensional chromatograms for (A) *n*-decane solute and (B) ethylbenzene solutes, showing peak symmetry of the modulated solutes. Three chromatograms are overlaid, the on-column solute mass is 25 pg for both solutes.

height. Application of the capacitive discharge-based thermal modulator is more convenient to implement than present commercial cryogenic modulators, and easier to configure and optimize

than flow modulated GC×GC systems. Commercial cryogenic modulators require constant resupplying of cryogen, while the present modulator only requires electricity for operation. A discharge voltage is selected to ensure that focused solutes are eluted in a narrow injection band, similar to the programming of hot/cold jet timings of cryogenic modulators. It is important that the voltage selected is not so high so as to cause analytes to be pyrolyzed during desorption from the trap, or destruction of the metal capillary by overheating. The requirement of increasing the temperature of the SS capillary relative to the GC convection oven limits the ability of the modulator to mobilize high molecular weight solutes without damaging the SS capillary or stationary phase of the modulator. Effective modulation was demonstrated for the solute *n*-triacontane while using a low charging voltage of 21 V for the present research. Finally, it is important to ensure that the trapping capillary is carefully aligned between the two ceramic pads to ensure that it is satisfactorily cooled.

Table 4.7 Peak statistics for test compounds showing the retention time and peak area repeatability (n = 12); Log-Log slope and linearity test (n = 21, F_{crit} = 3.45); limit of detection (mass on column); the second-dimension peak widths at half peak height (150 pg solute mass on column, n = 3, α = 0.05); the symmetry factor (calculated using 150 pg solute mass on column, n = 3, α = 0.05).

Compound	^{1}D Retention time (RSD %)	^{2}D Retention time (RSD %)	Peak Area (RSD %)	Log-Log Slope (Peak area vs mass)	$F_{experimental}$	LOD (pg)	^{2}D Peak width (ms)	^{2}D Peak Symmetry
Toluene	1.7×10^{-4}	2.3	5.3	1.00 ± 0.02	2.61	132	93 ± 3	1.5 ± 0.2
n-octane	1.5×10^{-4}	3.4	3.0	0.79 ± 0.01	1.04	207	88 ± 3	1.7 ± 0.2
Ethylbenzene	1.2×10^{-4}	2.3	4.3	0.96 ± 0.01	1.80	113	88 ± 6	1.6 ± 0.3
2-heptanone	1.1×10^{-4}	2.6	3.9	1.06 ± 0.01	1.10	37	77 ± 3	2.5 ± 0.3
pentylacetate	1.0×10^{-4}	2.4	4.3	1.24 ± 0.03	2.51	43	110 ± 1	1.7 ± 0.7
n-decane	7.8×10^{-5}	3.1	0.9	1.03 ± 0.01	2.30	34	52 ± 3	3.3 ± 0.9
2-octanol	7.6×10^{-5}	2.3	1.9	1.19 ± 0.03	1.14	62	67 ± 3	1.6 ± 0.5
2-nonanone	6.5×10^{-5}	2.9	2.4	1.28 ± 0.02	3.05	29	55 ± 1	2.4 ± 0.3
1,6-hexanediol	6.3×10^{-5}	2.3	3.0	1.12 ± 0.01	2.45	19	72 ± 3	2.2 ± 0.1
n-dodecane	5.3×10^{-5}	3.2	1.7	1.02 ± 0.01	3.10	29	45 ± 1	3.4 ± 1.3
2-decanol	5.2×10^{-5}	2.3	1.9	1.18 ± 0.02	1.26	22	70 ± 1	2.0 ± 0.6
4-chlorophenol	1.5×10^{-4}	2.8	4.9	1.19 ± 0.03	1.38	160	72 ± 3	1.6 ± 0.3
n-tetradecane	4.1×10^{-5}	3.2	2.6	0.97 ± 0.01	1.17	21	47 ± 3	2.7 ± 0.4

4.3.3.2. Modulator application to petroleum spill analysis

Petroleum hydrocarbon contamination (PHC) of Antarctic and sub-Antarctic terrestrial environments is a significant problem arising from human polar exploration and research [296, 297]. Conventional single-dimensional GC is unable to adequately separate the components of these PHC-contaminated soils due to the complexity of petroleum and its degradation products. GC×GC can be used to enhance the separation of complex petroleum spills, by separating compounds in two temporal dimensions [200, 288]. Analysis of petroleum-based samples using GC×GC has been well established in a number of studies and offers benefits in terms of signal enhancement as well as simplifying the integration of peak areas, due to the constant presence of

a reliable baseline throughout the GC×GC chromatogram [298-304]. Furthermore, the two-dimensional chromatograms that are generated can be used for fuel source fingerprinting to determine the source of petroleum contamination [305].

The present GC×GC platform was applied to the separation of PHC present in contaminated soil sample extracts sourced from Macquarie Island, a small sub-Antarctic island located 1500 km southeast of Australia. It serves as a critical breeding location for seals and sea birds, and a permanent research station has been maintained there since 1948 for the purposes of studying sub-Antarctic wildlife, and as a resupply station for Antarctic operations. There have been a number of petroleum spill incidents with release volumes ranging from 100 to 10,000 L and remediation of these petroleum spills is ongoing [293]. The risk posed by PHC has been evaluated using microbial and invertebrate species which are indigenous to Macquarie Island, with total PHC levels in soil ranging from 50 to 200 mg/kg (of soil) posing significant risk to the health of the islands' ecosystem [294, 306].

Figure 4.13 shows a GC×GC separation of a SAB diesel sample obtained from Macquarie Island. A number of the more abundant components of the petroleum-based sample revealed a tailing peak asymmetry, which indicates that the modulator stationary phase capacity was exceeded for these solutes. This overloading and breakthrough occurs when a solute exceeds the capacity of the modulator stationary phase while the trap is cooling down from the hot state following a capacitive discharge event [89].

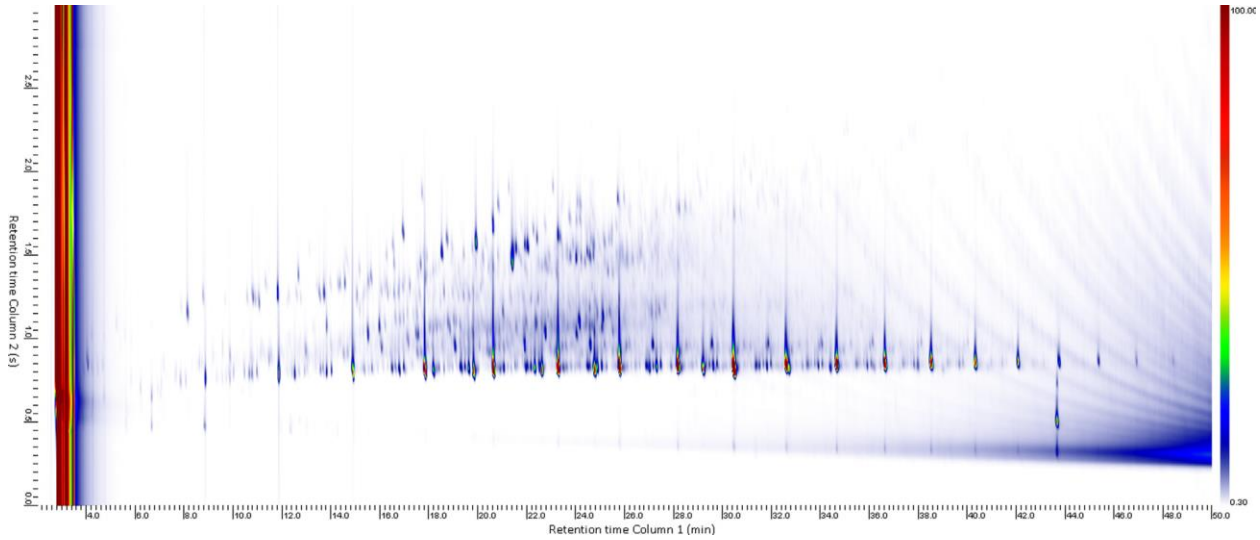

Figure 4.13 Two-dimensional chromatogram of Special Antarctic Blend (SAB) diesel (3000 mg/kg in *n*-hexane).

Dilution of the samples or the use of a higher split ratio would alleviate solute overloading issue and minimize peak tailing, but this would also reduce analytical sensitivity. However, the majority of peaks in the two-dimensional chromatogram exhibited good peak symmetry with minimal peak tailing or peak fronting, which confirmed that the stationary phase capacity of the second-dimension column was not being exceeded for these compounds.

An eight-level calibration was prepared using a series of SAB diesel standards spanning concentrations from blank to 3000 mg/kg. The integrated peak area of each of these SAB diesel standards was normalized using the 1-bromoeicosane internal standard used to construct a calibration graph to estimate the concentration of PHC-contaminated soil. LOD values for total PHCs were calculated using these peak area responses and the calibration procedure outlined in reference [307] (8 level calibration, n = 16, 2 replicates for each level, F_{exp} = 2.5, F_{crit} = 3.2, blank average 0.0017) and all LOD values were relative to the ability of the method to quantify known amounts of authentic SAB diesel. The LOD was 11 mg/kg, which compared favourably

to the 64 mg/kg LOD achieved using the previous 1D GC method [308]. This lower LOD was important for being able to quantify low levels of PHCs in samples to ensure that remediation efforts have been sufficient for the cleanup of petroleum spill sites as outlined by Mooney et al. [306]. The calibration was used to determine the amounts of PHC present at two sites on Macquarie Island, and the GC×GC determinations were found to be significantly different from one another. One-dimensional GC typically under-predicted the concentration of PHC at levels below 1500 mg/kg, which is likely due to the peak focusing effect provided by the modulator. Additionally, the average confidence intervals of determinations provided by the GC×GC system were 0.3 ± 0.2, compared to the 30 ± 36 mg/kg achieved using one-dimensional GC. The wider range of confidence intervals for the one-dimensional system resulted from uncertainties of the more heavily contaminated soil samples that were problematic to integrate due to the lack of a stable chromatographic baseline.

4.3.4 Conclusions

The resistively heated single-stage thermal modulator described herein reduces the complexity of hardware required for achieving GC×GC while delivering excellent performance. Access to electrical power is the only consumable presently needed for operation of this modulator, compared to other designs that require liquid cryogen. Additionally, the modulator and capacitive discharge power supply are compact and amenable to portable analysis unlike the refrigeration units that are used as alternatives for liquid cryogen. This modulator delivered retention time and peak area repeatability comparable or better than present commercially available modulators. Capacitive discharge facilitated rapid, repeatable mobilisation of trapped solutes in narrow reinjection bands (72 ± 3 ms average peak widths) as is required for GC×GC analysis. The present modulator is able to focus a wide range of chemically different solutes at

different concentrations (5–1300 pg on column mass) without the need for a secondary trapping stage, which simplifies system design. This modulator was applied for the separation of petroleum contaminated soil samples and found to be very effective for categorising petroleum spill sources and measuring low concentrations of petroleum when compared with one-dimensional GC analysis.

4.4 Evaluation of a commercial perfume sample by GC×GC-FID

4.4.1 Introduction

Flavours and fragrances are amongst the most studied application areas within GC×GC due to samples within this category featuring hundreds of unique compounds across a wide range of chemical classes. One sample that has received considerable attention in recent years are commercial fragrances and perfumes. In 2003, the European Union cosmetics directive decided to regulate 26 fragrance allergens in cosmetic products [309]. Later in 2009, the European cosmetics regulation moved to require customers of cosmetic products to be informed if these allergens were above 10 ppm in leave-on products, and 100 ppm in wash-off products [310]. This regulation required chemists to develop reliable methods to quantify this target list of allergens, which resulted in the development of the European standard method EN 16274, updated most recently in 2016 [311]. The GCMS method used two separate columns of differing polarity for the separation of the complex samples with MS being used for detection and quantitation. A logical alternative to this approach would be to use GC×GC as a separation mechanism instead, as the separation of such complex samples could be achieved in a single analysis instead of two as described in the EN 16274 method. Upon attending a meeting where the performance and application of the Mk IV modulator was being presented, an individual

employed by a major fragrance producer in Switzerland requested their samples be evaluated in Waterloo by GC×GC analysis. An experimental plan was developed and samples of a commercially available perfume were delivered to Waterloo. The purpose of the experiments was to evaluate the retention time and peak area repeatability of the Mk IV modulator in a preliminary test to determine its potential suitability for the GC×GC analysis of fragrance allergens.

4.4.2 Experimental

4.4.2.1 Chemicals and materials

Commercial perfume samples were delivered by the collaborator in 10 ml headspace vials sealed with screw top caps. A 1 ml aliquot of the fragrance sample was subsequently removed and placed in to a 2 ml GC vial. Samples were kept in a refrigerator when not in use. The wash solvent used with the liquid autosampler was ethyl acetate (Sigma Aldrich, Mississauga, Canada). No further dilution of the sample with solvent was required.

4.4.2.2. Instrumentation

The GC×GC-TOF MS system used for this study consisted of an Agilent 6890 GC (Palo Alto, CA, USA) equipped with a split/spitless injector. A column combination consisting of a DB-1 30 m x 0.25 mm x 0.25 µm (J&W Scientific, Folsom, CA, USA) was used in the ^{1}D and a DB-50 2 m x 0.18 mm x 0.18 µm (J&W Scientific, Folsom, CA, USA) was used as the ^{2}D column. The oven temperature program started at 30 °C, increasing at 4 °C/min until 310 °C. A 1 µl sample was injected using the split/splitless injector operated in split mode at a temperature of 300 ºC while using a 2 mm id gooseneck liner (Restek Corp.). The sample was split 50:1 during injection. Helium gas with a purity of 99.999 % was used as the carrier gas at 1.2 ml/min constant flow rate. A LECO Pegasus TOF MS detector (LECO, St. Joseph, MI, USA) was used for detection. The

transfer line and ion source were both held at 300 °C. A mass range of 35-400 atomic mass units (amu) was selected with the detector acquiring at 200 hertz (Hz) at a voltage of -1800 V. ChromaTof software (LECO, St. Joseph, MI, USA) was used for data acquisition and processing of the TOF MS data. The Mk IV modulator used in this study has been previously described in section 2.5. A modulation period of 4 s was used for all experiments.

4.4.3 Results and discussion

The initial review of the perfume sample revealed a highly complex chromatogram with a wide range of analyte concentrations. Both 1D and 2D chromatograms of the sample can be seen in Figure 4.14. Peak detection was performed and the acquired spectra were searched against a NIST library for compound identification. The prominent solvent peak revealed the perfume had been diluted in ethanol. Fortunately the solvent tail had reduced to such a level as not to interfere with the first compound of interest. Over 500 separate peaks were identified within the sample, the bulk of which eluted before the 50 minute mark of the temperature ramp which corresponded to an oven temperature of approximately 230 °C. Good peak shape overall was observed with some tailing seen in the ^{2}D for more concentrated species. The purpose of running this sample was to determine how the Mk IV performed in peak area and retention time repeatability. The sample was run 5 times a day over two days. Five peaks were selected from the chromatogram that ranged in ^{1}D retention times from 11 minutes to 60 minutes and had strong spectral matches to the NIST library. These peaks included α-pinene, limonene, α-phellandrene, benzyl acetate, ethyl vanillin and 4-methoxycinnamic acid. Overlaid sub-peaks for limonene and ethyl vanillin are shown in Figure 4.15. For all six peaks selected, the sub peaks from each replicate injection when overlaid on each other appeared to be well aligned. Each peak's area, ^{1}D and ^{2}D retention times were recorded and plotted in Excel.

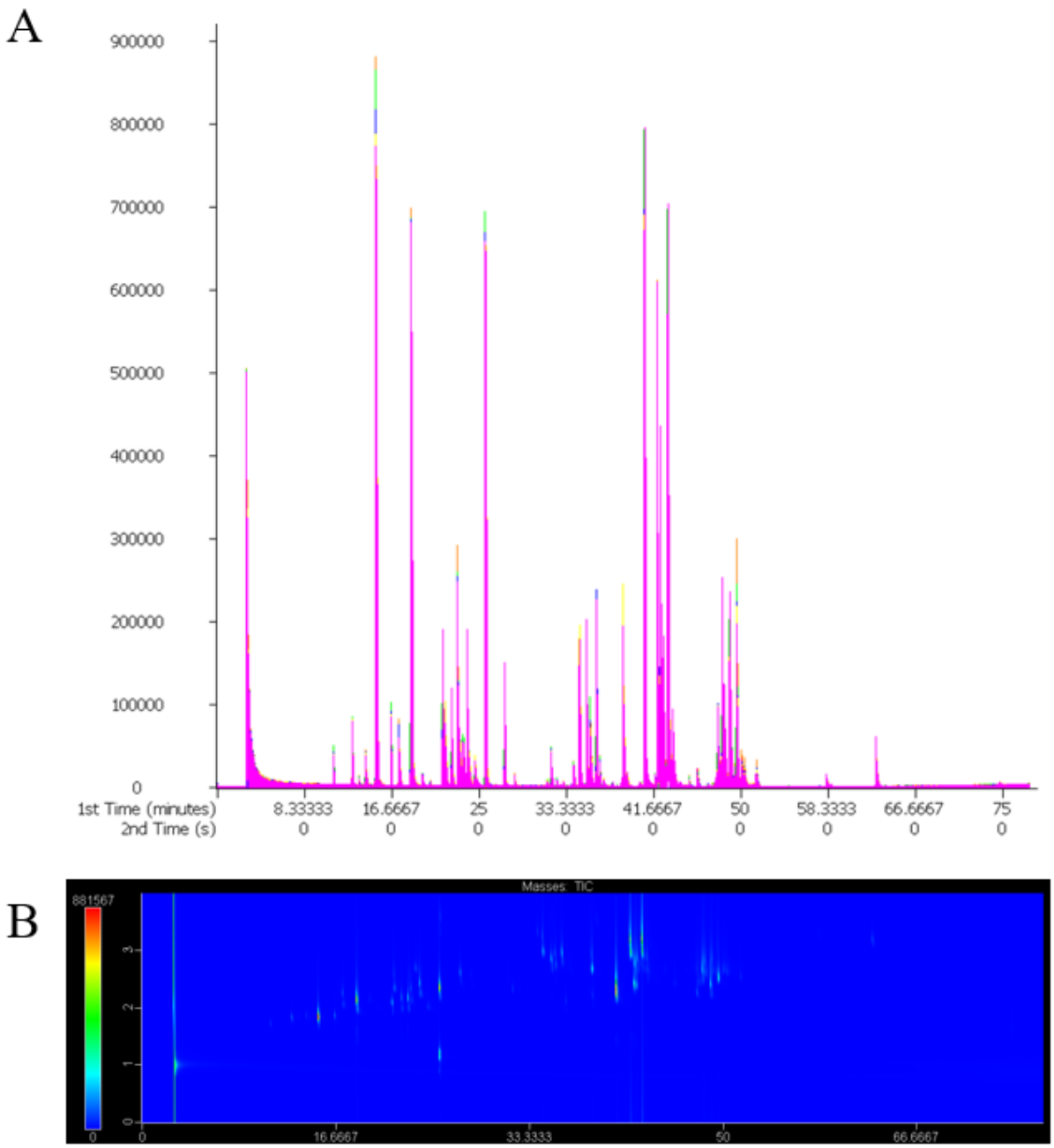

Figure 4.14 Five overlaid replicate injections of the perfume sample shown in 1D view (A) with the corresponding GC×GC contour plot shown below (B).

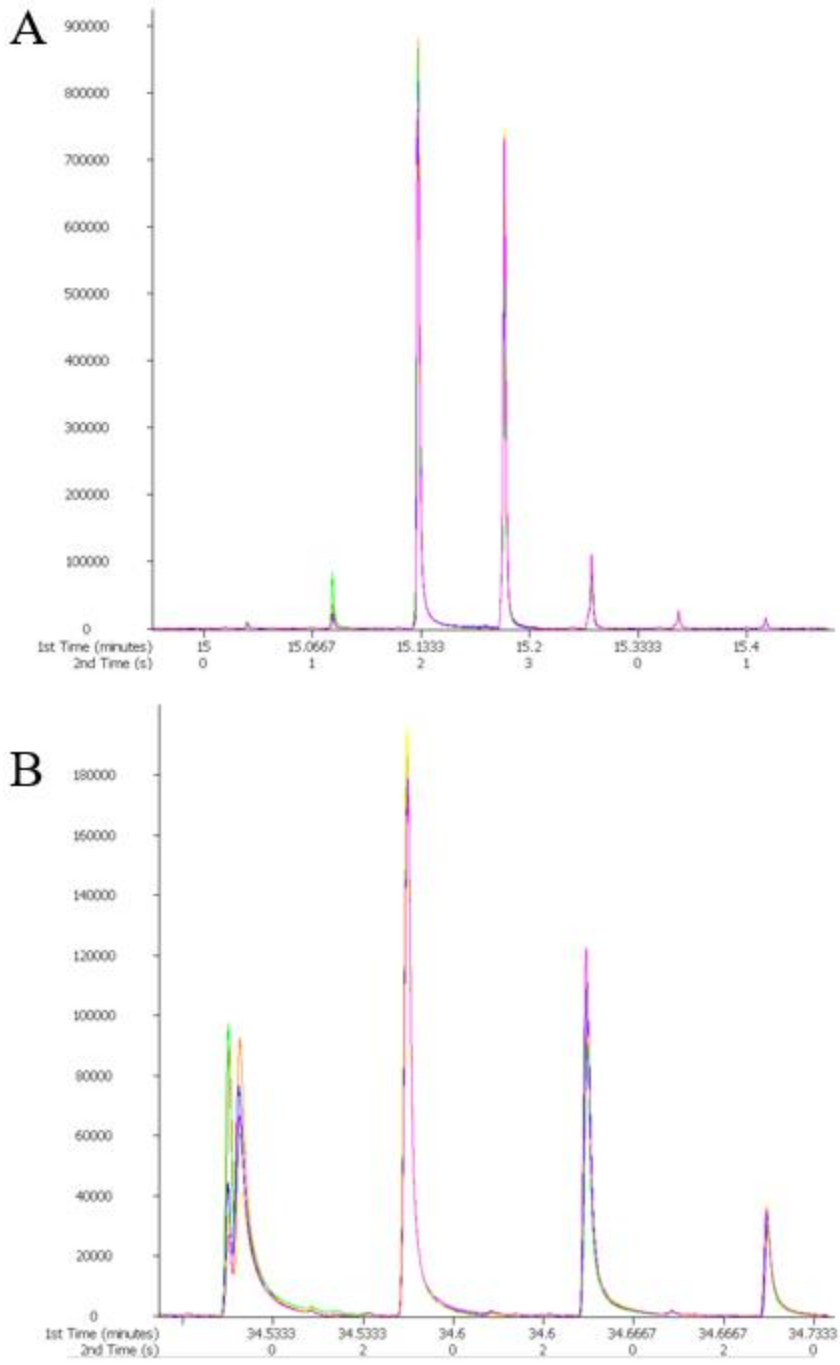

Figure 4.15 Zoomed-in fragments of five overlaid replicate injections of the perfume sample with sub peaks from limonene (A) and ethyl vanillin (B) shown in the 1D view.

Intraday peak area repeatability ranged from as low as 1.3 % to 8.7 % RSD across the six compounds (Figure 4.16). On day two the values were similar, with peak area repeatability ranging from 3.2 % to 8.3 %. Day-to-day reproducibility for peak areas ranged from 2.1 % to 13.7 %. Single column GC separations regularly report peak area RSD values in the 5 % range, so the values recorded in this work align well with those results.

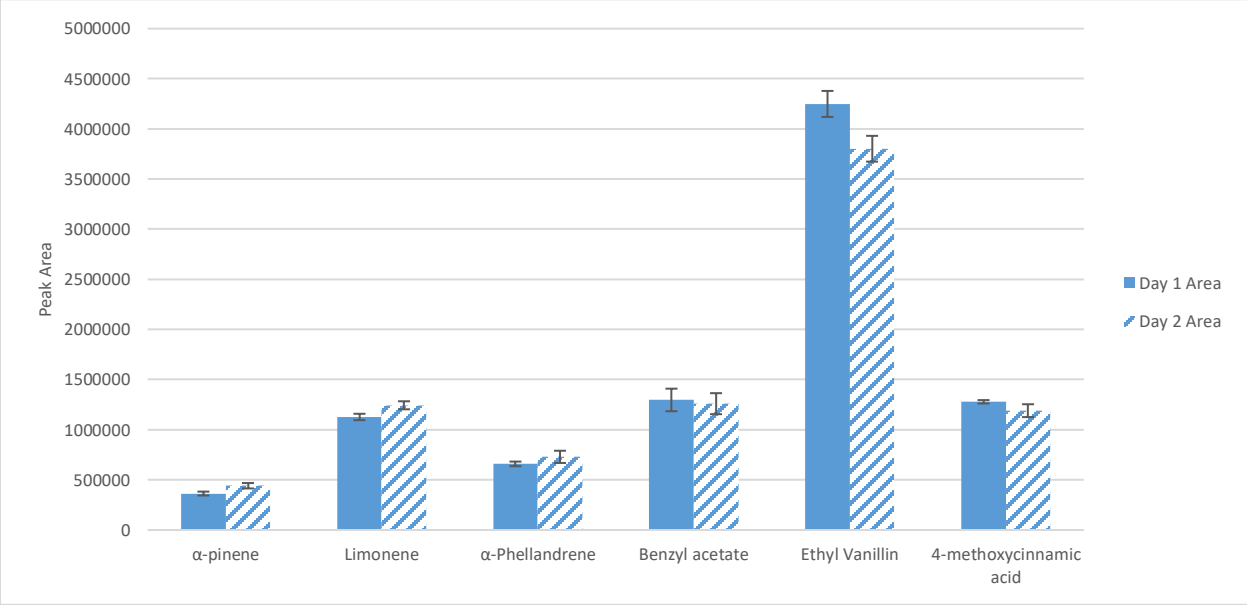

Figure 4.16 Within-day peak area repeatability (N=5) for six fragrance compounds over two days of evaluation. Error bars represent standard deviation.

Compound retention time repeatability was calculated next (Figure 4.17). For the ^{1}D values, the greatest variation in retention time recorded was 3.24 seconds across five replicates. During day one, three compounds were recorded to have no variation in ^{1}D retention time at all. Day to day reproducibility of ^{1}D retention times varied at most by 3 seconds. The remaining compounds varied in ^{1}D retention time by 0.5 seconds or less day to day.

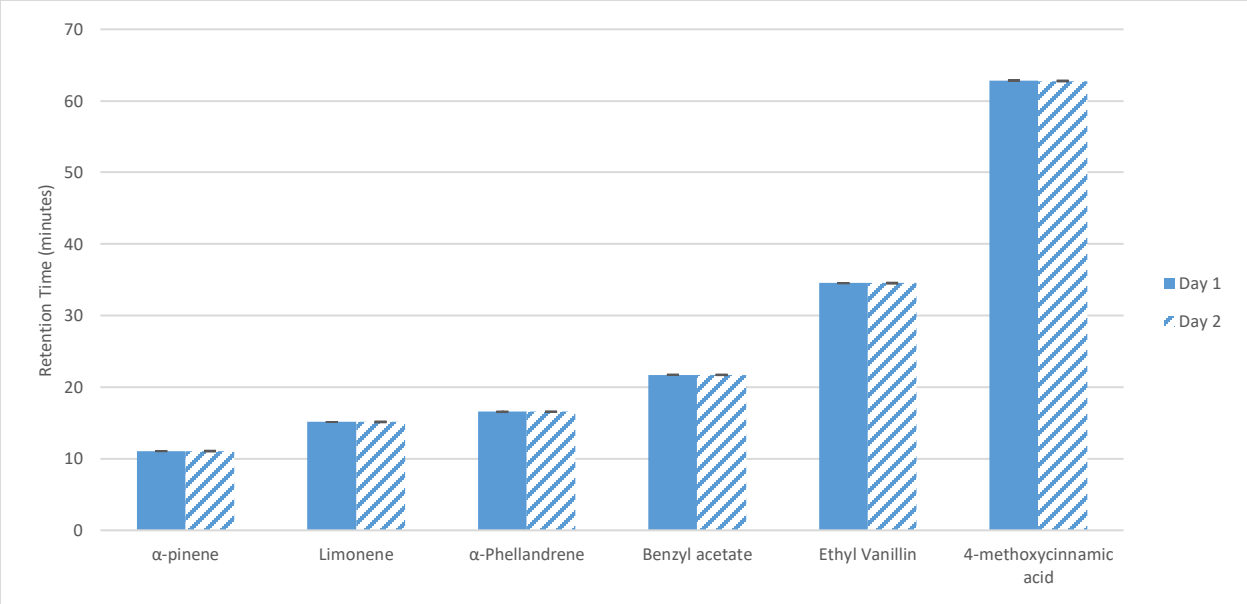

Figure 4.17 Within day ^{1}D retention time repeatability (N=5) for six fragrance compounds over two days of evaluation. Error bars represent standard deviation.

Compound retention time repeatability for the ^{2}D separation was calculated next (Figure 4.18). The greatest variation in retention time recorded was 5.5 ms across five replicates. Day to day reproducibility of ^{2}D retention times varied at most by 14.5 ms for a single compound. Two compounds had no recordable variation in ^{2}D retention time day-to-day.

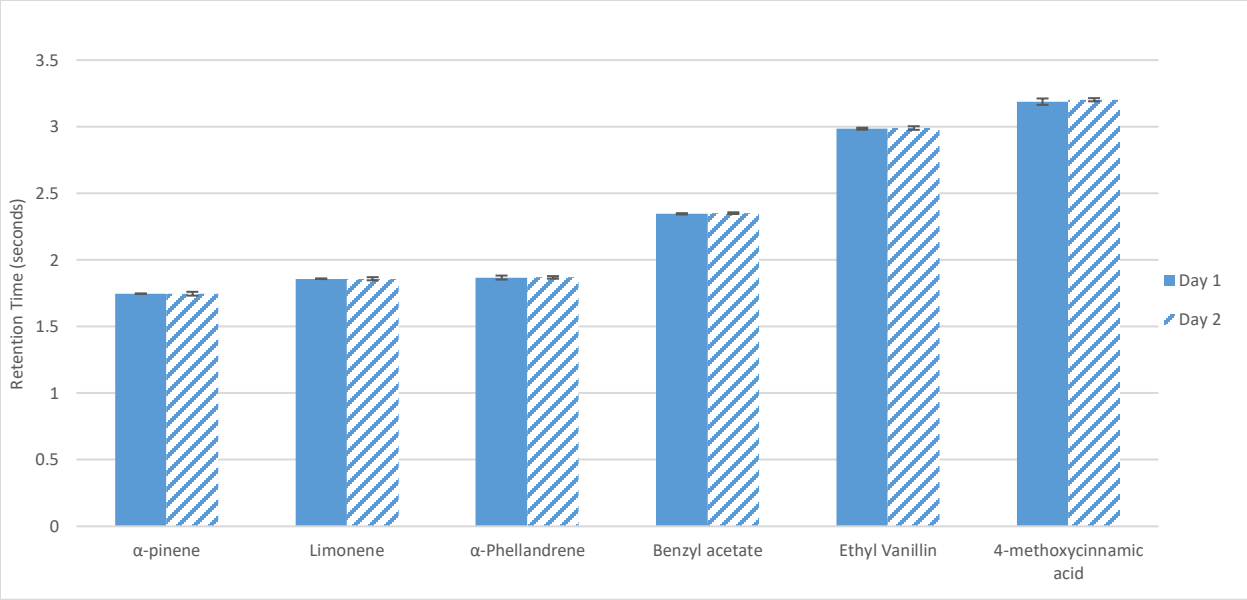

Figure 4.18 Within day ^{2}D retention time repeatability (N=5) for six fragrance compounds over two days of evaluation. Error bars represent standard deviation.

4.4.4 Conclusions

The perfume sample was an interesting mix of fragrance compounds and provided a suitably complex sample for GC×GC analysis. Repeatability and reproducibility of peak areas was observed to be close to acceptable levels for quantitation. Values closer to 5 % RSD for all compounds would have been preferable, but the RSD values under 3 % obtained for some analytes were encouraging. Retention time stability in both dimensions was excellent. It has been demonstrated that retention time stability of this magnitude would allow for the statistical analysis of GC×GC-MS results without the need for chromatographic alignment [312]. In terms of the Mk IV modulator being suitable for the analysis of fragrance allergens, a more in-depth study would be required that would investigate sensitivity and linear dynamic range capabilities alongside TOF MS detection. This modest study demonstrated that the modulator performed basic requirements for quantitation very well and would likely be a suitable device for the application at hand.

Chapter 5. Development of an inlet backflushing device for the improvement of comprehensive two-dimensional gas chromatographic separations[5]

5.1 Introduction

GC×GC is considered an established separation technique and for the last decade focus has shifted away from the development of modulation technology to applying the technique to an ever increasing number of analytical challenges. Fields in which GC×GC applications are popular include petroleum and petrochemicals [313-323]; food, flavours and fragrances [166, 324-336]; metabolomics [337-348] and environmental analysis [349-355]. Although the use of GC×GC has never been more widespread, there are some applications that remain challenging for a chromatographer to perfect. A review of the literature focused on the quality of the chromatographic separations produced revealed frequent sub-optimal results, with long tailing chromatographic bands in applications including e.g. pesticide residue analysis [356], metabolomics [349] and food or fragrance analysis [357]. The aforementioned samples are often investigated for trace levels of target analytes, and thus large volumes of the samples or smaller volumes of highly concentrated sample extracts are typically injected into the column. In these cases, it is very likely that some analytes or interferences might be present in high concentrations. The tailing bands produced by these compounds are problematic, as they can conceal analytes of interest and/or make quantitation difficult. In this study, we investigated both

[5] This section is based on the following publication:

M. Edwards, T. Górecki, "Inlet backflushing device for the improvement of comprehensive two-dimensional gas chromatographic separations," *Journal of Chromatography A*, vol. 1402, pp. 110-123, 2015.

Author contributions include design and manufacture of the Mk IV modulator, original concept, technical, operational and chromatographic analysis, primary manuscript contributor, review and editing.

the source(s) of these tailing chromatographic bands, as well as methods to reduce or even prevent their creation.

The GC inlet has been recognized for some time as producing non-ideal injection bands, especially when highly concentrated samples or those with complicated matrices are evaluated [358-360]. It is possible that polar and/or non-volatile analytes linger within the inlet volatilizing slowly and entering the column over extended time in the form of elongated bands. These bands are then modulated multiple times, producing tailing peaks. There are several possible causes for the extended residency of these analytes within the inlet. Analytes may sorb to active sites within the inlet or onto septum fragments or non-volatile residue from previous injections often found inside the liner. Column connecting ferrules, especially those made of graphite, might also sorb the solvent and the sample components during injection, then gradually release them over the course of the separation. We also investigated the possibility that some compounds trapped within the modulator might undergo only partial desorption during each modulation event, again leading to tailing bands. To determine if the inlet, modulator, or both were responsible for these phenomena, a simple backflushing device was designed consisting of a three way switching valve, a transfer line and a zero dead volume tee. The device was used to study the sources of the tailing bands, as well as to improve separations that are vulnerable to this phenomenon. Several experiments were performed including a GC×GC separation of organochlorine pesticides (OC) and organophosphorous pesticides (OP) in split, splitless and purged splitless modes, as well as analysis of pesticide residues in lemons using the QuEChERS sample preparation method. Analysis of Scotch whisky headspace using solid phase micro extraction (SPME) was also performed.

5.2 Experimental

5.2.1 Chemicals and materials

Standard pesticide mixtures EPA 8270 and EPA 8081(94 % purity or higher) and hexane (99 % purity) were purchased from Sigma-Aldrich Canada Co. (Oakville, ON, Canada). Blended Scotch Whisky (40 % alcohol, v/v) was acquired from the Liquor Control Board of Ontario store in Waterloo, ON, Canada. Acetonitrile (HPLC quality) was purchased from Fisher Scientific (Toronto, ON, Canada). All stock and working solutions were stored at -20 °C. SPME headspace analysis was completed using 85 µm polyacrylate fibers purchased from Supelco (Bellefonte, PA, USA).

QuEChERS supplies including 50 ml centrifuge tubes and extraction salt pouches containing 4 g magnesium sulfate (anhydrous), 1 g sodium chloride, 1 g trisodium citrate dihydrate and 0.5 g disodium hydrogen citrate sesquihydrate were purchased from Restek (Bellefonte, PA, USA).

5.2.2 Sample treatment

Pesticide standard EPA 8270 (2000 µg/ml) was diluted in hexane to 200 µg/ml. A 1 ml aliquot of the dilution was combined with 1 ml of pesticide standard EPA 8081(200 µg/ml) to create a final combined pesticide standard with a concentration of 100 µg/ml. Lemons and limes were obtained from a local grocery chain in Waterloo, Ontario. A 200 g portion of sample was weighed, chopped, and homogenized for 2 minutes at 4500 rpm using an immersion blender from Kitchen Aid (Mississauga, ON, CANADA). A 10 g portion of the sample was weighed in a clean 50 ml tube and 10 ml of in MeCN was added. The tube was then vortexed for 1 minute using a Vortex-Genie mixer from Fisher Scientific (Toronto, ON, CANADA). After mixing, the extraction salt was added. The tube was then vortexed again for 1 minute after which it

underwent centrifugation at 3,000 revolutions per minute (RPM) for five minutes. The resulting supernatant did not undergo any cleanup procedure and was subsequently used for GC×GC analysis.

5.2.3 SPME of Scotch whisky headspace

85 µm polyacrylate fibers were conditioned prior to use within the GC inlet according to the manufacturer's instructions. A 40 ml vial with a PTFE/Silicone septum and a screw top was filled with 20 ml of undiluted whisky. The fiber was exposed to the headspace of the liquid sample stirred at 1200 rpm for a period of 5 minutes. After extraction, the fiber was withdrawn into the needle and immediately inserted into the inlet of the GC kept at 280 °C for a period of 5 minutes.

5.2.4 Instrumentation

GC×GC experiments were performed using an Agilent 6890A gas chromatograph in combination with an FID detector and a split/splitless inlet. The FID data acquisition rate was 100 Hz and the detector temperature was 300 °C. Gas flow rates were as follows: hydrogen, 40 ml/min; air, 450 ml/min and make-up gas (nitrogen) 45 ml/min. Split (2 mm) and splitless (4 mm) deactivated Sky inlet liners were purchased from Restek (Bellefonte, PA, USA). The inlet remained at 280 °C for all analyses. The flow switching device was custom-built to function in both inlet backflush and modulator flush modes. Figures 5.1 and 5.2 show how the device was configured for inlet backflushing and modulator flush, respectively. In inlet backflush mode, the three-way switching valve was activated after a predetermined time following the injection to allow carrier gas to bypass the inlet, and instead enter a tee placed between the inlet and the primary column. This allowed clean carrier gas to flow from the tee into both the primary column and the inlet outlet, which prevented any analytes still present in the inlet from entering

the primary column, effectively isolating the inlet from the [1]D column once the three-way switching valve had been activated. The same principle and device were applied to the modulator. With the three-way switching valve in the same location, the tee was installed between the primary column and the modulator, and the auxiliary gas line was extended from the valve to the tee. Upon activation of the valve, fresh carrier gas travelled to the tee, backflushing the primary column and isolating the modulator from primary column effluent. As modulation was allowed to continue with fresh carrier gas, we were able to observe the modulation events required to remove residual analytes from the modulator.

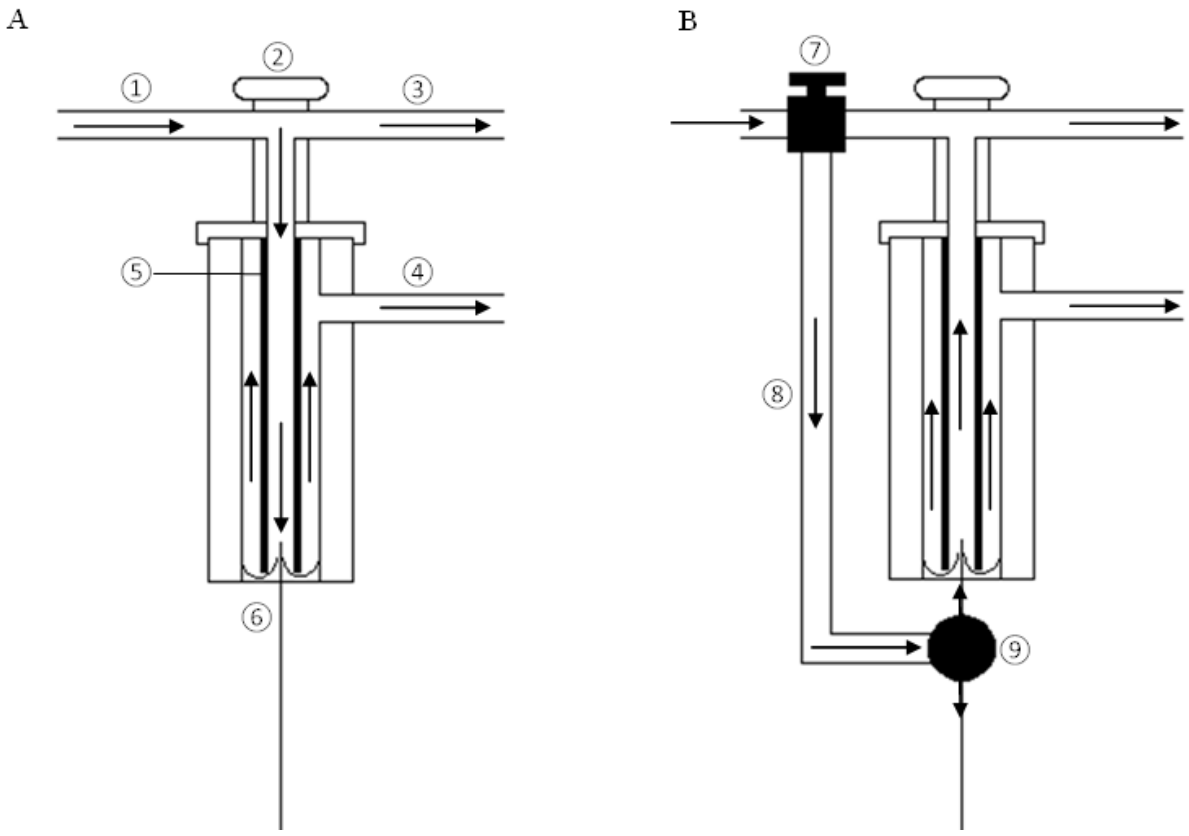

Figure 5.1 (A) A standard split/splitless inlet with a carrier gas inlet line (1), septum nut (2), septum purge line (3), split purge line (4) and glass inlet liner (5) interfaced with a capillary column (6). (B) The inlet backflushing device installed on the same

split/splitless inlet created with a three-way switching valve (7) transfer line (8) and tee (9). Black arrows indicate the direction of carrier gas flow.

Two different low dead volume tees were evaluated for use in the flow switching device. They included a 0.25 mm bore zero dead volume tee from Valco (Brockville, ON, Canada) and an Agilent CFT tee. The 1/8" three-way switching valve used was from Swagelok (Solon, OH, USA). The 3 cm pre-column and transfer lines were created from 0.25 mm Sulfinert deactivated stainless steel capillary tubing from Restek (Bellefonte, PA, USA). The modulator used in this study was the Mk IV modulator previously described in section 2.5. A modulation period of 6 seconds was used for all experiments except the lime pesticide residue experiments which used a modulation period of 4 seconds. No secondary oven or transfer lines were used. A schematic diagram of the modulator was shown in Figure 2.29. All data processing was completed using GC Image software (Version 2.4, GC Image LLC, Lincoln, NE, USA).

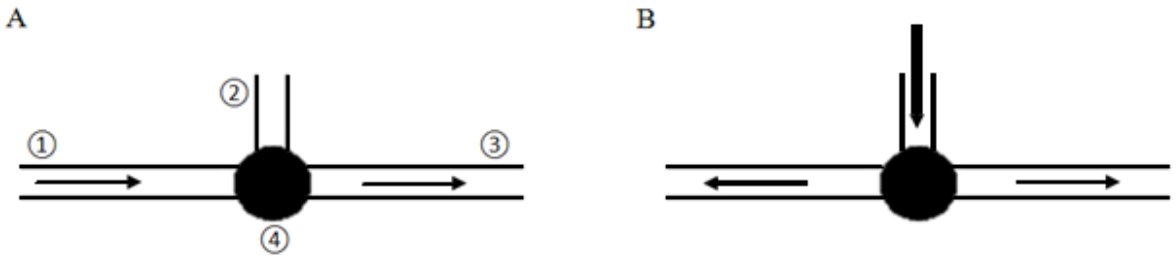

Figure 5.2 (A) The inlet backflush device was modified to direct the transfer line originating at the three way valve (2) to a tee (4) placed between the primary column and modulator entrance (3). (B) Gas flow upon activation of the auxiliary gas. Black arrows indicate the direction of carrier gas flow.

5.2.5 Chromatographic conditions

The column set used consisted of an RTX-5 MS (26 m x 0.25 mm x 0.25 µm; Restek) as the primary column and an Rxi-17 Sil MS (1 m x 0.25 mm x 0.25 µm; Restek) as the secondary column. Hydrogen (99.999 % purity) was used as the carrier gas. All experiments were carried out at a constant carrier gas flow of 1.5 ml/min. Oven temperature programing rates varied with each experiment and were as follows: pesticide standard experiments, 40 °C (hold for 2 min), 8 °C/min to 300 °C, 20 °C/min to 320 °C (hold for 5 min); lemon pesticide residue experiments, 70 °C (hold for 1.1 min), 20 °C/min to 300 (hold for 15 min); lime pesticide residue experiments, 40 °C (hold for 1.0 min), 5 °C/min to 240 °C, 20 °C/min to 300 °C (hold for 5 min); Scotch whisky experiments, 40 °C (hold for 2 minutes), 5 °C/min to 240 °C, 20 °C/min to 300 °C (hold for 5 minutes).

5.3 Results and discussion

5.3.1 Inlet flushing device evaluation

Prior to proceeding with experiments, steps were taken to ensure the system was contamination-free. The inlet was cleaned using a series of solvents and a wirebrush as recommended by the Agilent 5890/6890 inlet cleaning guide [361]. In addition, all consumable parts were replaced. This included the septum, Vespel ferrules, inlet liner, gold seal and Viton o-ring. The column was also subjected to an extended bake-off period at 300 °C for three hours. The backflush device was then installed on the inlet as shown in Figure 5.1 using the Valco zero-dead volume tee. The pesticide standard mixture was used to evaluate three different injection modes: split, splitless and purged splitless. Analysis of the standard mixture was first evaluated in regular GC×GC mode without the use of the backflush device. The same analysis was then completed with the three way switching valve manually activated 6 seconds after the injection had taken

place. The valve remained in the inlet backflush mode throughout the whole analysis and was reset to normal mode when the run was over. To ensure flows and pressure were well balanced, an alkane ladder was run in triplicate with and without inlet backflushing. Deviations of one-dimensional and two-dimensional retention times, as well as peak areas were well within accepted experimental error. The first experiments compared splitless injections to the backflush device. A 100 ng/µL injection of the pesticide standard was used to simulate a worst case scenario whereby the column would be overloaded with analytes and induce tailing bands. In coordination with the backflush device being activated, the split vent flow was turned on, allowing analytes being directed back into the inlet to escape through the purge line at the same flow rate that was applied to the column. In regular GC×GC mode (Figure 5.3 A), the OP analytes along with the sample solvent showed the greatest tendency to produce elongated chromatographic bands. The less polar OC compounds produced narrower peaks with less tailing relative to the OP compounds. A replicate analysis was then completed with the backflush device being activated at 6 seconds (Figure 5.3 B). This short time was clearly insufficient to transfer all the analytes from the inlet to the column, as the analyte transfer is in fact an exponential dilution process requiring 3 inlet volume purges to transfer ~90 % of the analyte to the column. Nevertheless, it represented an interesting extreme case when studying the contribution of the inlet to the generation of tailing bands. As seen in Figure 5.3 B, there was a substantial reduction in peak tailing of both the solvent and the OP compounds. The OC peaks were greatly reduced in width and showed improved resolution. Some late eluting analytes that appear to be missing from the chromatogram were indeed present but were not visible at this particular zoom level. This was due to insufficient transfer time in the inlet prior to the backflush device being activated (as explained above), therefore preventing these compounds from entering

the column in the amounts seen in the previous experiment. Some analyte tailing was to be expected at this concentration as a 1 µL splitless injection containing 100 ng of analyte represented the maximum capacity of a 0.25 mm x 0.25 µm column. Improvement in the overall quality of the separation in this splitless injection experiment was likely due to a combination of two effects: (1) reduction of the amount of analyte directed to the column due to the backflush being activated prior to complete transfer of the analytes inducing a mass discrimination effect and (2) elimination of analyte tails originating in the inlet from entering the column.

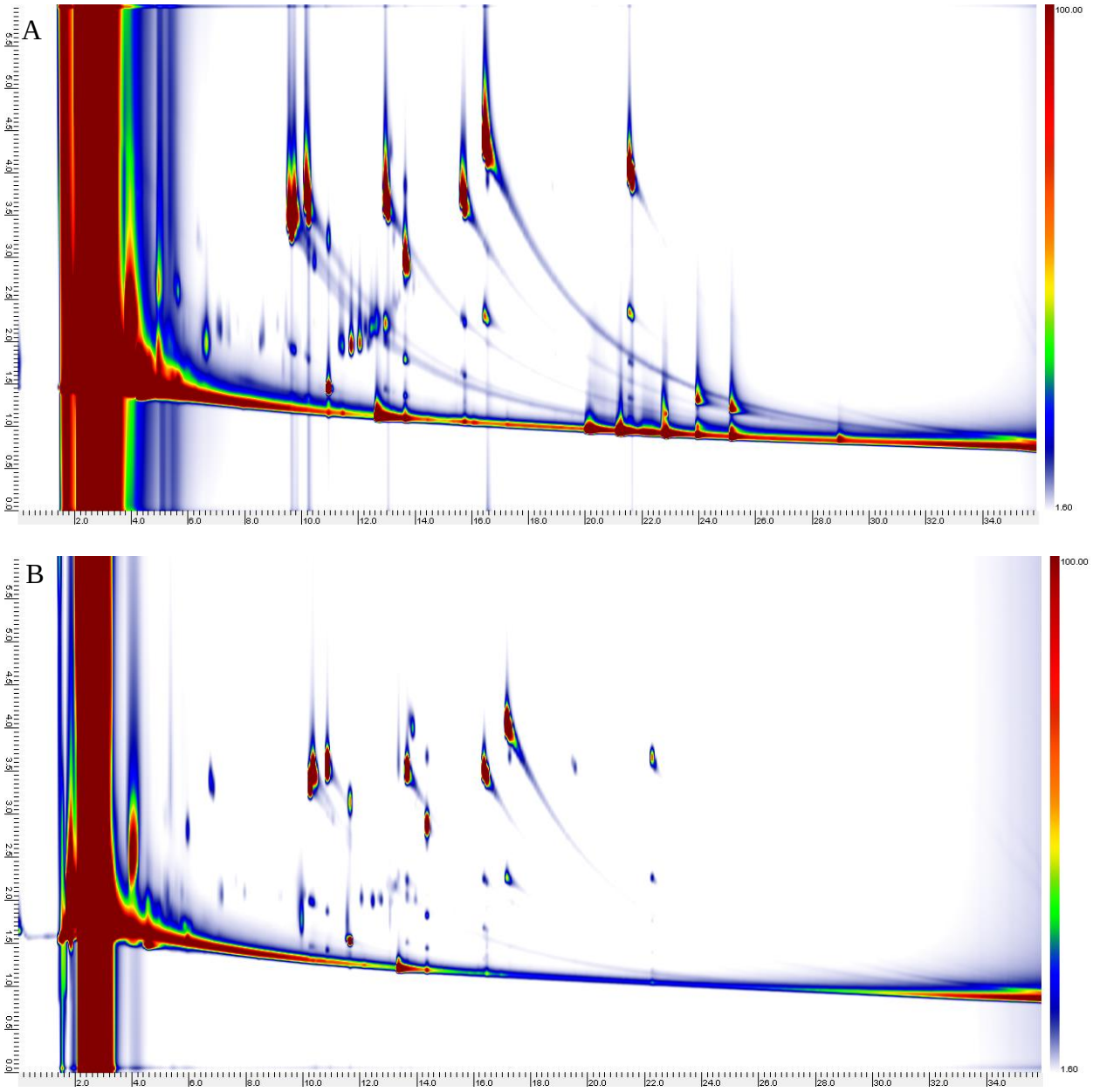

Figure 5.3 GC×GC analysis of OP and CH pesticides. (A) Normal mode with splitless injection. (B) Inlet backflush mode after 6 seconds with splitless injection. Scales are identical in both chromatograms.

d splitless injections are often performed with the goal of reducing the injection band tailing. This is done by opening the split vent and increasing the flow through the inlet at some specified time after injection to quickly remove remnants of the sample from the inlet and deliver clean

carrier gas to the column. To compare the inlet backflush device with purged splitless injection, the 100 ng/µL pesticide mixture was used once again. An injection of 1 µL was completed and after 6 seconds the purge valve was opened and 20 ml/min of the carrier gas was permitted to flow through the inlet. Although the split line was being flushed with high carrier gas flow, both solvent and analyte tailing were still pervasive (Figure 5.4 A). It should be noted that solvent tailing, which occurs at the beginning of the run, should not be confused with the subsequent modulator bleed and column bleed that gives the illusion of solvent tail continuity at the baseline. Whereas solvent bleed can be improved with inlet backflushing, modulator and column bleed cannot. Compared to the splitless injection experiment (Figure 5.3 A), there were improvements in both OC and OP compound peak widths and an overall minor reduction in chromatographic tailing. However, these improvements appeared negligible when compared to the results achieved using inlet backflushing (Figure 5.4 B). This is most apparent when observing the OP compounds and the solvent band, which was clearly still entering the column after the purge valve was opened. Thus, isolating the inlet from the column after an injection provides improved separation relative to purged splitless injection. In addition, inlet backflushing does not require increased gas flows through the inlet to improve splitless injection, resulting in reduced carried gas usage.

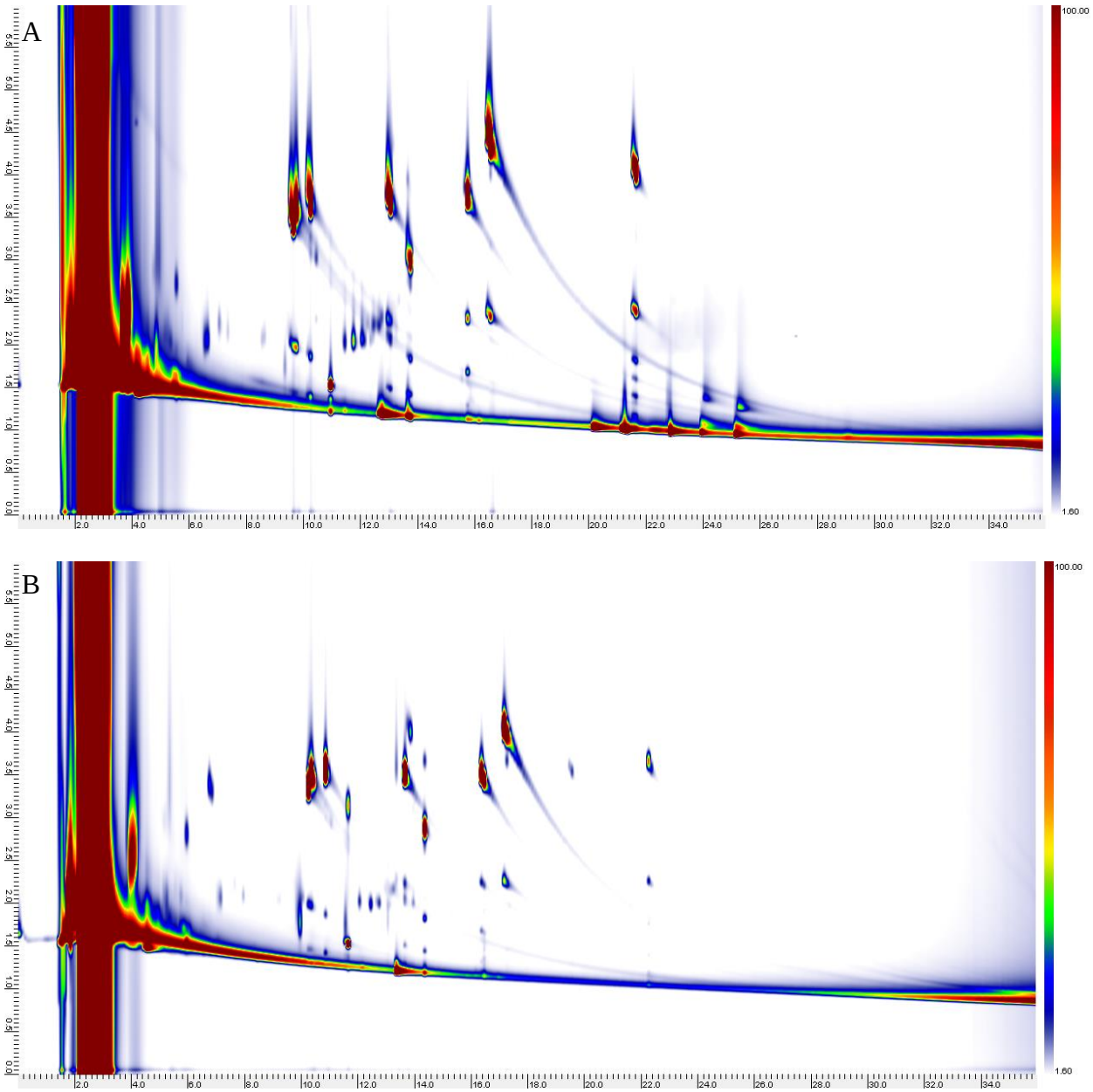

Figure 5.4 GC×GC analysis of OP and CH pesticides. (A) Normal mode with purged splitless injection. (B) Inlet backflush mode after 6 seconds with purged splitless injection. Scales are identical in both chromatograms.

Split injections were evaluated next with the sample and conditions remaining the same with the exception that the 100 ng/µL pesticide sample was split 10:1, resulting in a more reasonable sample quantity of 10 ng entering the column. The results of this experiment revealed the OP compounds still had a tendency to produce tailing even at a concentration an order of magnitude lower than in the splitless experiments (Figure 5.5 A). The OC compounds produced more symmetrical peaks and less tailing than the OP compounds. A replicate analysis was then performed whilst activating the inlet flush device after 6 seconds (Figure 5.5 B). Improvements in OP compound peak characteristics were observed as well as a large reduction in the relative size of the solvent tail.

This series of experiments was carried out to evaluate the inlet backflush device and provide a proof of concept. The experiments brought to light some issues with using this device and areas that needed improvement. The timing of device activation must be given careful consideration prior to use, especially when semi-volatile analytes are present in the sample analysed. Mass discrimination effects were clearly observed in all the experiments with unrepresentative sampling of high molecular weight compounds. This was especially the case in the split injection experiments where the least amount of sample was present (Figure 5.5 B). A period of 6 seconds may be adequate for quickly volatilized, low molecular weight analytes but is not suitable for semi-volatile compounds. The Valco zero dead volume tee was also deemed unsuitable for the inlet flush device. The Valco tee is machined out of a relatively heavy, non-deactivated piece of stainless steel that offers poor thermal response to oven temperature programming due to its mass. Because of this feature, its temperature lagged behind that of the GC oven during temperature ramps, potentially contributing to the tailing effect.

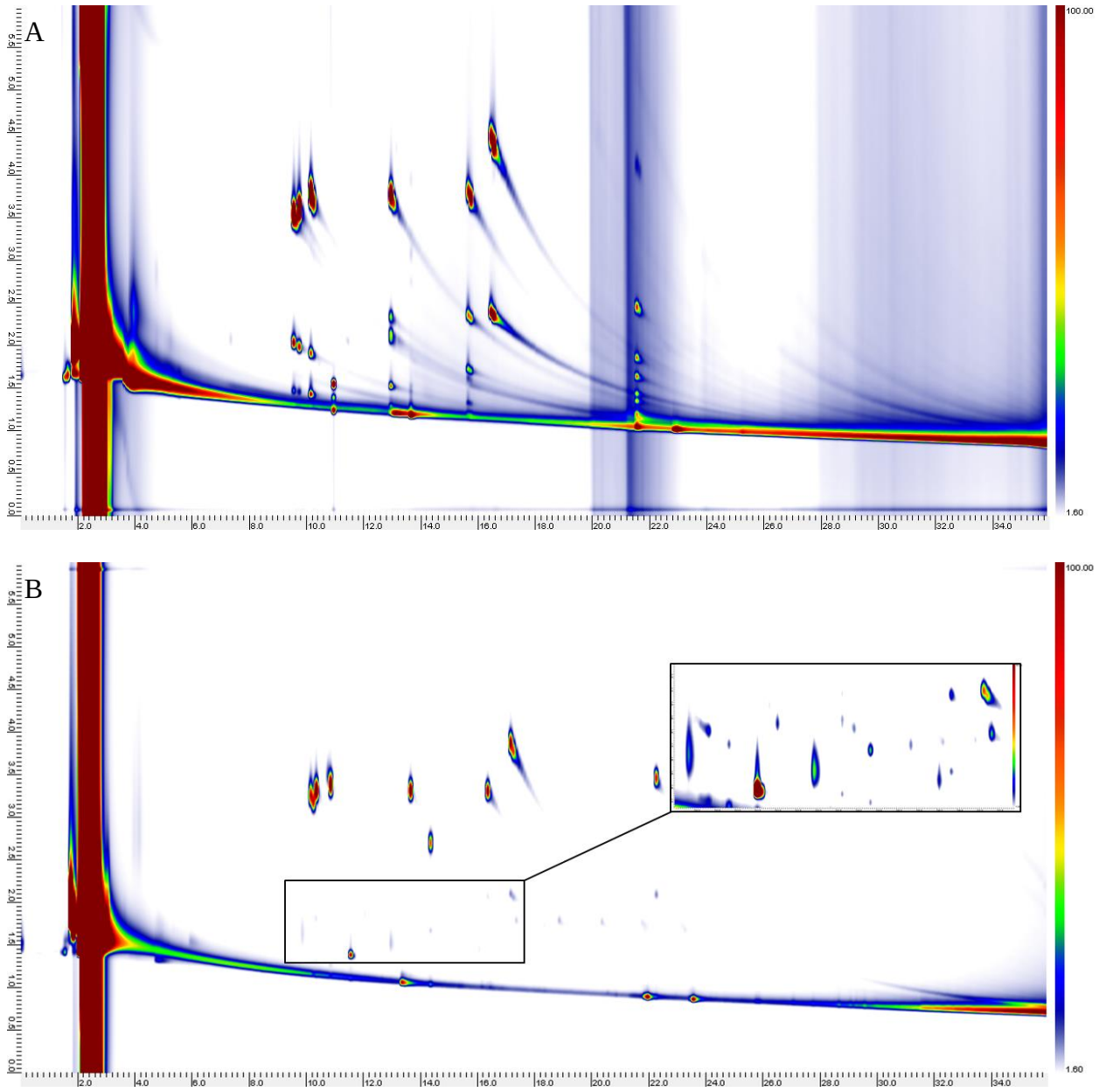

Figure 5.5 GC×GC analysis of OP and CH pesticides. (A) Normal mode with 10:1 split injection. (B) Inlet backflush mode after 6 seconds with 10:1 split injection. Scales are identical in both chromatograms with the exception of the inset image that utilizes greater zoom to reveal the CH pesticides.

The tee also took considerable time to return back to the initial oven temperature after a run had been completed adding unwanted waiting periods between experiments. The non-deactivated nature of the tee may have provided internal active surfaces onto which analytes could adsorb, contributing to the tailing problem we were trying to eliminate. Nuts and ferrules used with this tee were problematic and often resulted in leaks and broken capillaries. Moving forward, the inlet backflush device was improved by replacing the Valco zero dead volume tee with an Agilent CFT tee, which is specifically engineered for GC capillary columns with proper ferrules and nuts for the column set used. It is also made of lightweight, deactivated, thermally conductive materials. No issues with thermal lag or column connectivity were experienced after switching to the Agilent CFT tee.

5.3.2 Application of inlet backflushing to improve chromatography in pesticide residue analysis

To evaluate the inlet backflush device as a tool for improving the separation of samples with complicated matrices, pesticide residue analysis of lemons using the established QuEChERS sample preparation method was performed. Chromatographic conditions were replicated from another study to ensure optimal conditions [362]. In previous experiments, splitless, purged splitless and split injections were evaluated. This experiment utilized the pulsed splitless mode which has been previously recognized as reducing matrix effects by minimising analyte interactions with active sites within the inlet [358, 363, 364]. With optimal conditions established, 1 µL of the lemon extract underwent a pulsed splitless injection with a pulse of 50 psi hydrogen carrier gas for 1.1 minutes. The purge valve opened at 1.0 minute with a flow of 5 ml/min. The chromatogram revealed a complex mixture of many analytes, as well as significant peak tailing (Figure 5.6 A). The same experiment was performed with the inlet backflush device

being activated at the same time as the purge valve was opened (1.0 minute). This allowed fresh carrier gas to enter the inlet and prevented any components remaining in the inlet from entering the column following the activation of the device. Comparing the two chromatograms shown in Figure 5.6 it is clear that after the purge valve was opened, compounds continued to enter the column as elongated bands. Isolating the inlet via backflush prevented these analytes from entering the column, thus reducing the overall degree of tailing and improving resolution. Looking more closely at the tail of the analyte peak eluting at 7.5 minutes (^{2}D retention time 4.2 seconds), it was observed that without inlet backflush, the tail consisted of over 30 individual slices. Slices two and three had peak heights reduced by 30 % and 47 %, respectively, compared to the peak apex value. When inlet backflushing was activated, the tail consisted of only three slices whose peak heights were reduced by 80 % relative to the peak apex. To further demonstrate the reduction of peak tailing, one-dimensional GC×GC data corresponding to Figure 5.6 is shown in Figure 5.7. Without inlet backflushing (Figure 5.7 A), slice height reduction is gradual due to the asymmetrical nature of the analyte band entering the modulator. Using inlet backflushing (Figure 5.7 B) the asymmetrical tail of the analyte band is prevented from entering the column, effectively reducing the total number of slices whilst allowing the bulk of the analyte to enter the column. The residual tailing still seen in the run with inlet backflushing was likely related at least to some extent to the length of time before the purge valve was open: apparently the compounds exhibiting tailing were introduced to the column during this period gradually rather than in a form of a sharp band and were not properly refocused in the column. Other potential sources of the tailing observed included active sites in the tee itself, and/or the ferrules used in the tee.

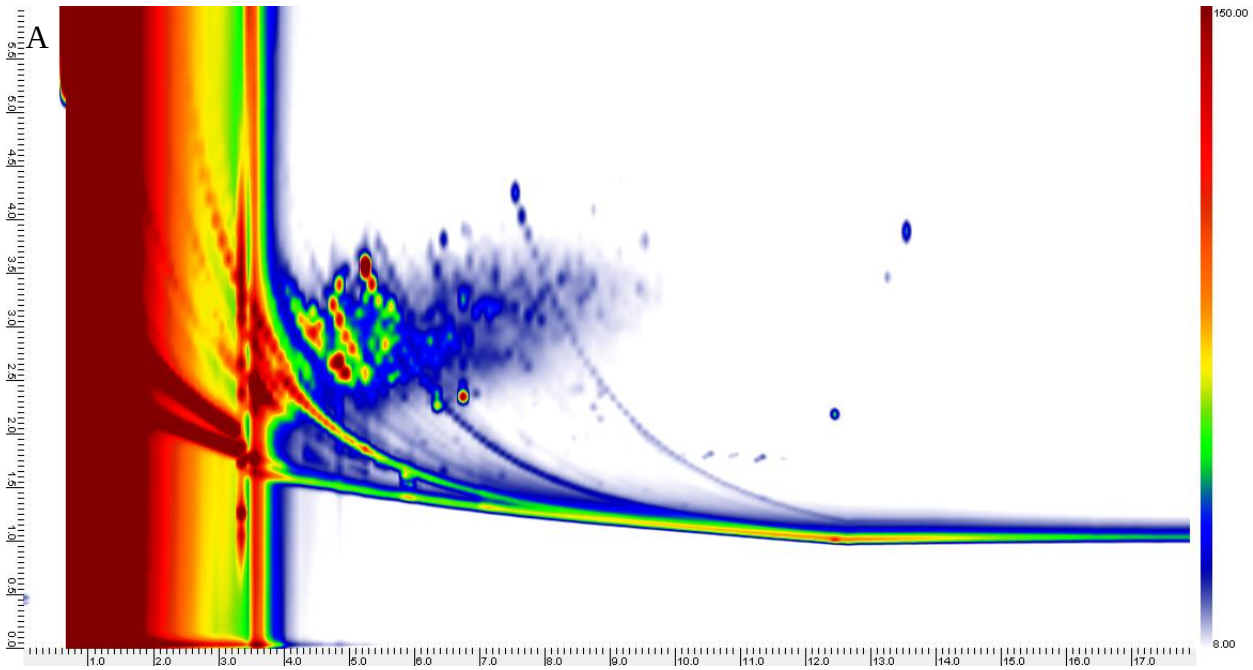
A
150.00
8.00

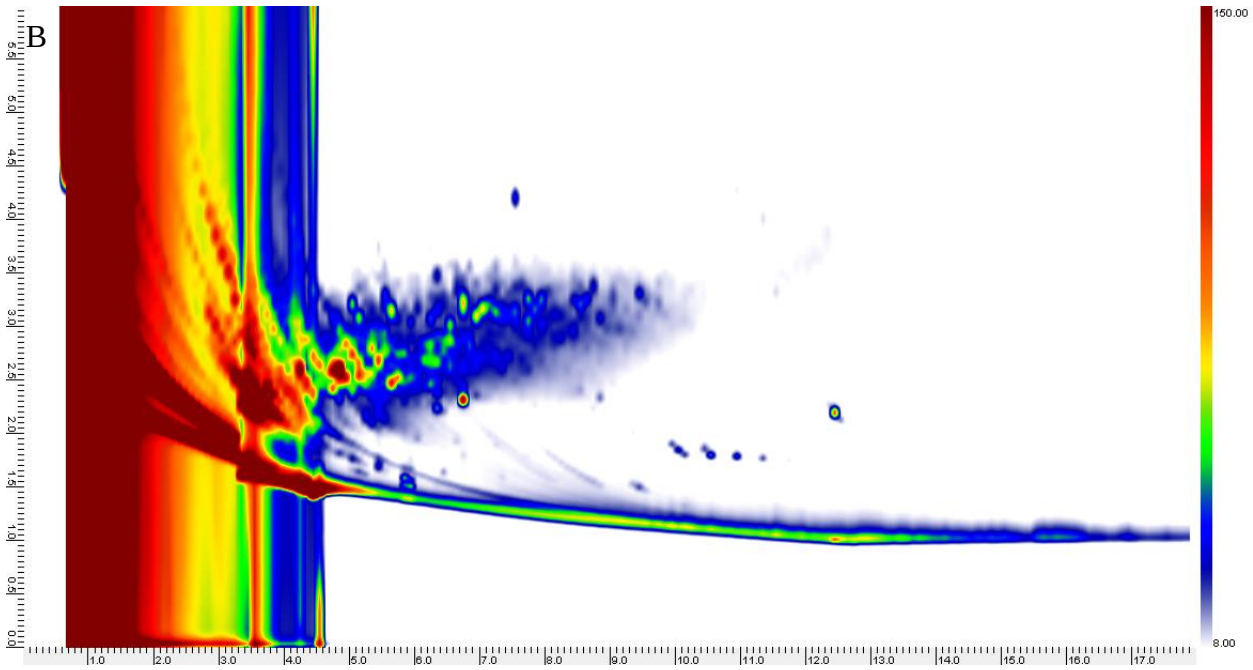
B
150.00
8.00

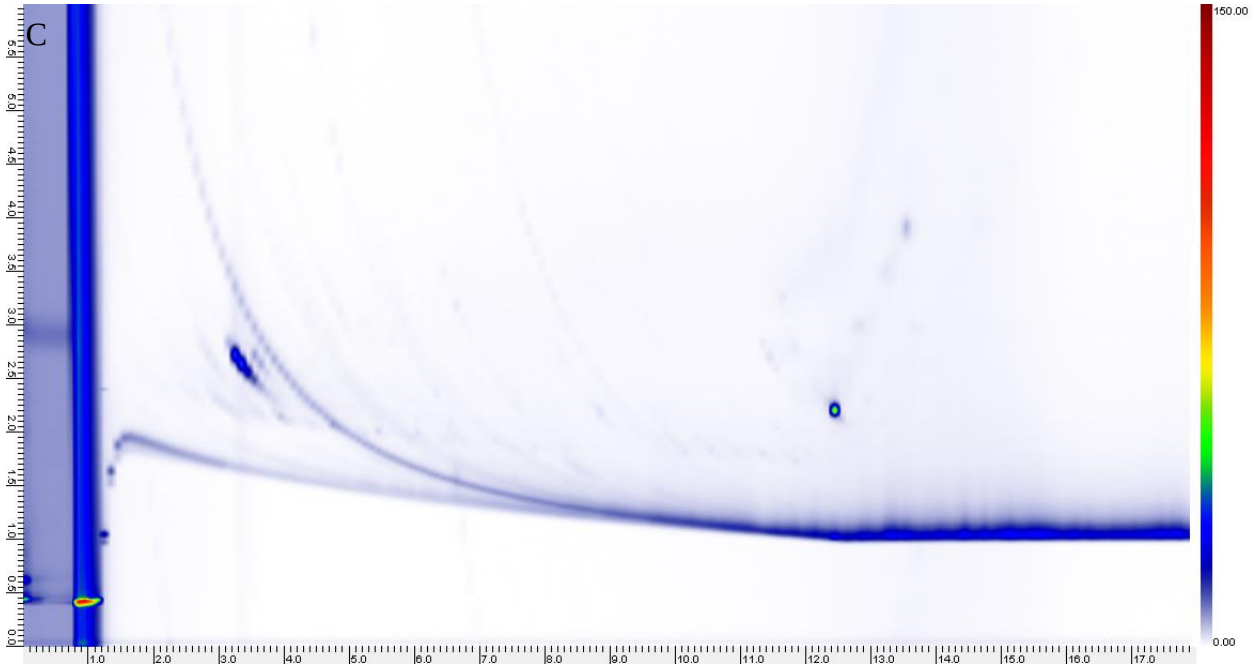
C
150.00
0.00

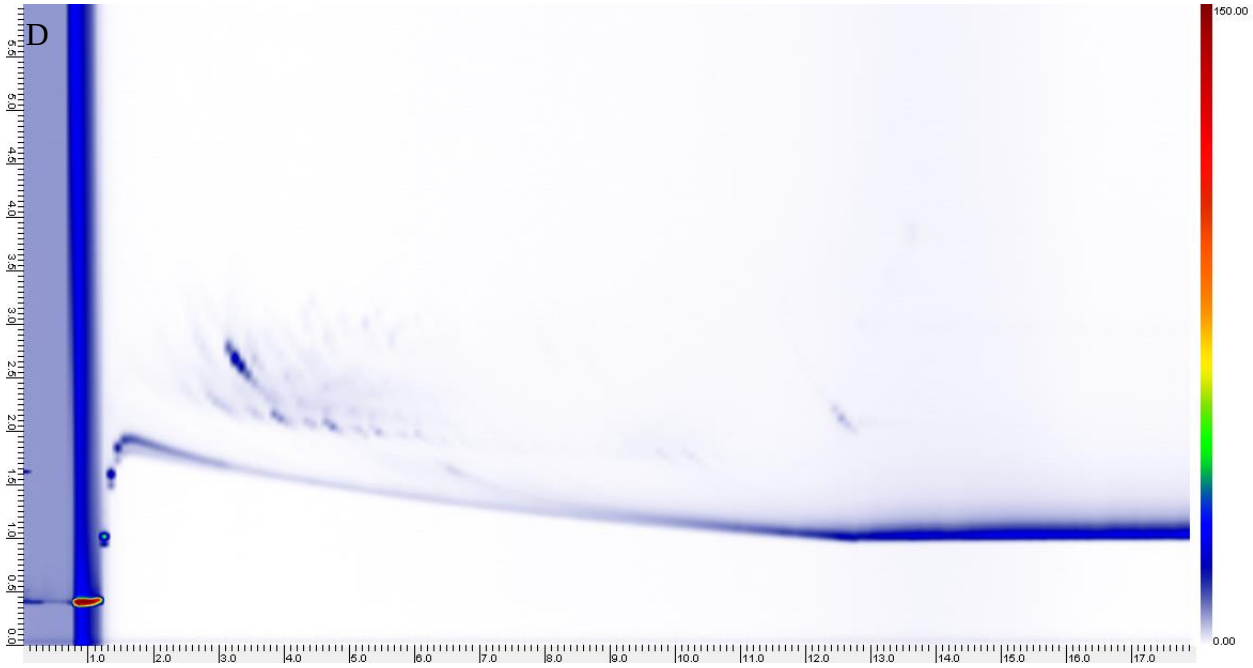
D
150.00
0.00

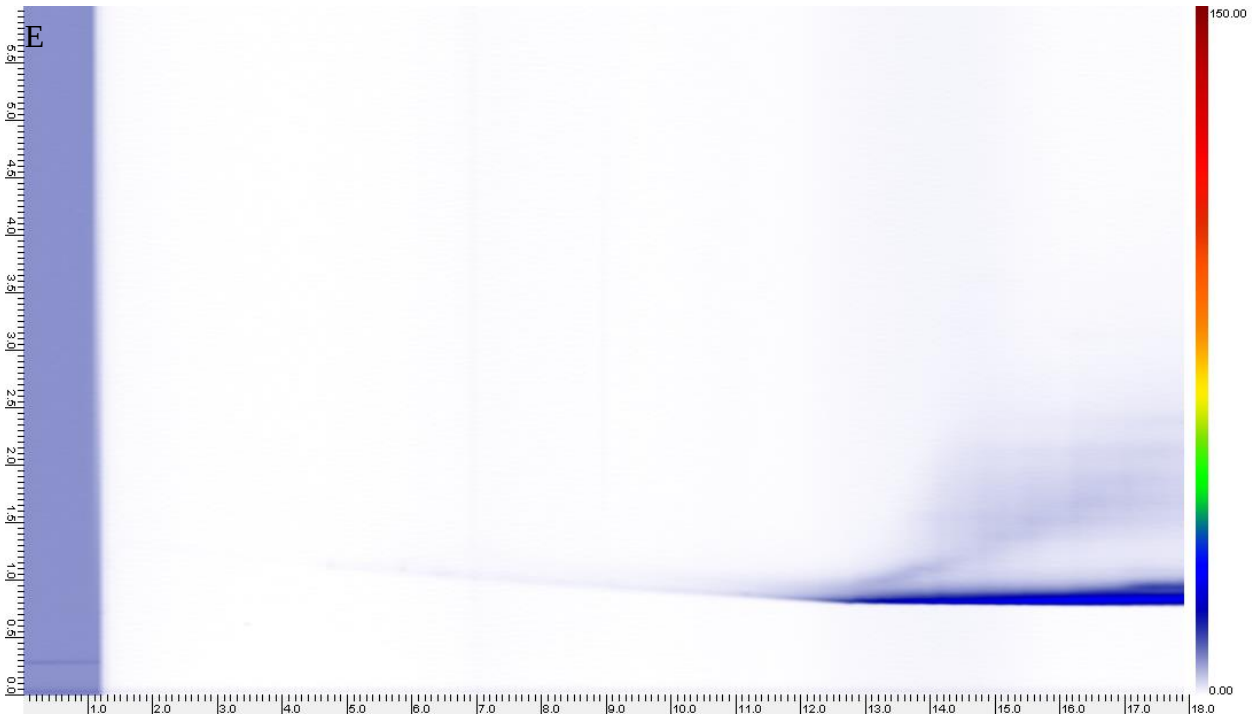

Figure 5.6 GC×GC analysis of lemon extract. (A) Normal pulsed splitless mode (50 psi until 1.1 minutes, 5 ml/min split purge at 1.0 minute). (B) Inlet backflush pulsed splitless mode (50 psi until 1.1 minutes, 5 ml/min split purge at 1.0 minute, backflush device activated at 1.0 minute). (C) Blank performed after normal pulsed splitless mode. (D) Blank performed after backflush pulsed splitless mode. (E) Blank performed with the backflush being activated during the entire analysis. All regular separations have the same scale and all blanks have the same scale. Blank chromatograms have the minimums lowered to reveal carryover. Scales are identical in all chromatograms. (Note: the backflush was not activated during blank runs C and D).

Comparisons of blank analyses were performed after each experiment. Inlet backflushing was not activated during the blank runs to allow any compounds remaining in the inlet to elute into the column for subsequent FID detection. The blank analyses revealed that analyte residues were still present in the inlet (or other parts of the column train) after the run has been completed (Figure 5.6 C and D). The extent of the carryover was only slightly reduced when injection backflush was activated one minute after the beginning of the blank run, with more improvement

observed for later eluting compounds (Figure 5.6 D). To verify that this carryover was not derived from the backflush system itself, an additional blank run was completed with the backflush activated at the beginning of the analysis and remaining on throughout the entire run (Figure 5.6 E). No carryover was observed in this experiment. As the inlet was completely isolated from the column during this run, analytes still remaining within it were prevented from entering the column and exited through the split line as fresh carrier gas entered from below (Figure 5.1). In the next experiment the purge flow was increased to induce greater removal of residual inlet contaminants during the run and achieve improved separation. Once again 1 µL of lemon extract was injected using pulsed splitless injection with a pulse of 50 psi hydrogen carrier gas for 1.1 minutes. The purge valve was opened at 1.0 minute with an increased flow of 25 ml/min. The same experiment was performed with the inlet backflush device being activated at 1.0 minute. A comparison of the chromatograms can be seen in Figure 5.8. Once again tailing was greatly reduced when the inlet was isolated from the column after injection. Improvements in separation in these experiments were not due to mass discrimination effects, as enough time was permitted for analytes within the sample to adequately volatilize and enter the column prior to the backflush device being activated. Comparing the blank runs performed after each experiment (Figures 5.8 C and D), it is clear that increased carrier gas flow through the split line alone was inferior to inlet backflushing during runs for the removal of low volatility, late eluting compounds.

A

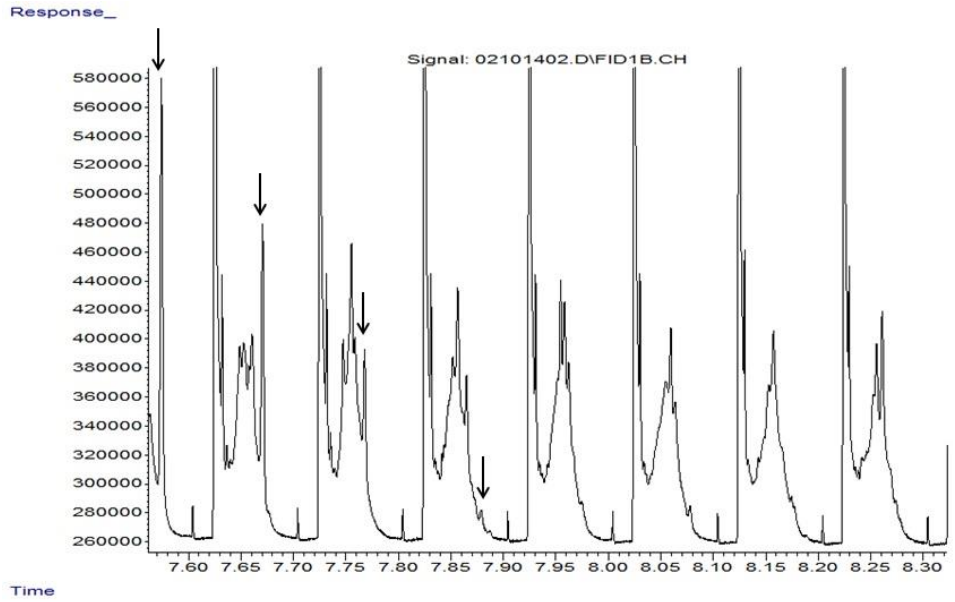

B

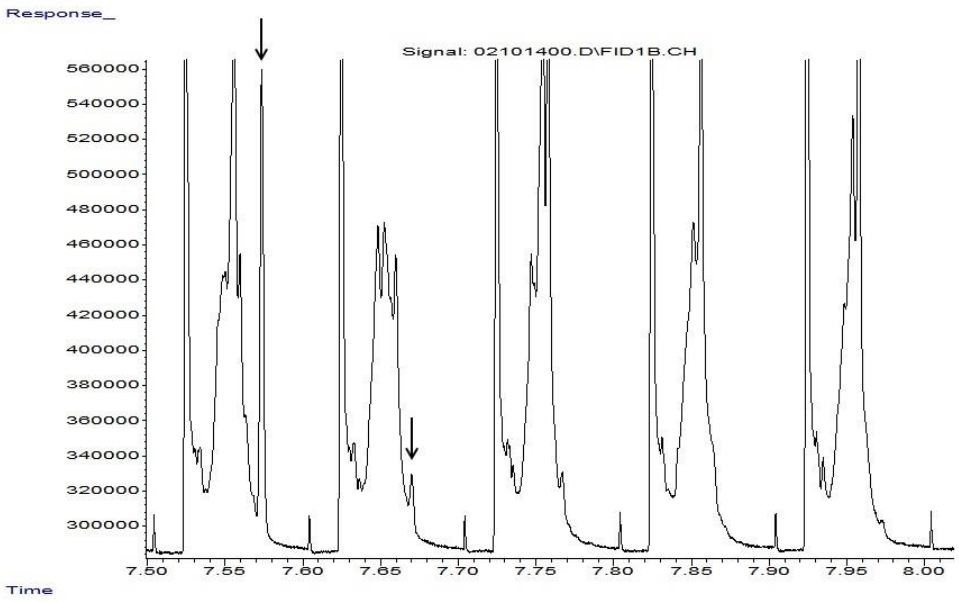

Figure 5.7 One-dimensional representation of GC×GC data of lemon extract. (A) Normal pulsed splitless mode (50 psi until 1.1 minutes, 5 ml/min split purge at 1.0 minute). Arrows indicate the individual slices that represent the tailing band seen in Figure 5.6 A. (B) Inlet backflush pulsed splitless mode (50 psi until 1.1 minutes, 5 ml/min split purge at 1.0 minute, backflush device activated at 1.0 minute). Arrows indicate the individual slices that represent the tailing band seen in Figure 5.6 B.

The most likely reason for that is that in standard operation mode, the bottom part of the inlet including the ferrule sealing the column is exposed to the column flow of the carrier gas only, whereas in the inlet backflush mode this part of the inlet is exposed to the total carrier gas flow, which significantly improves residual analyte removal from this part of the column train.

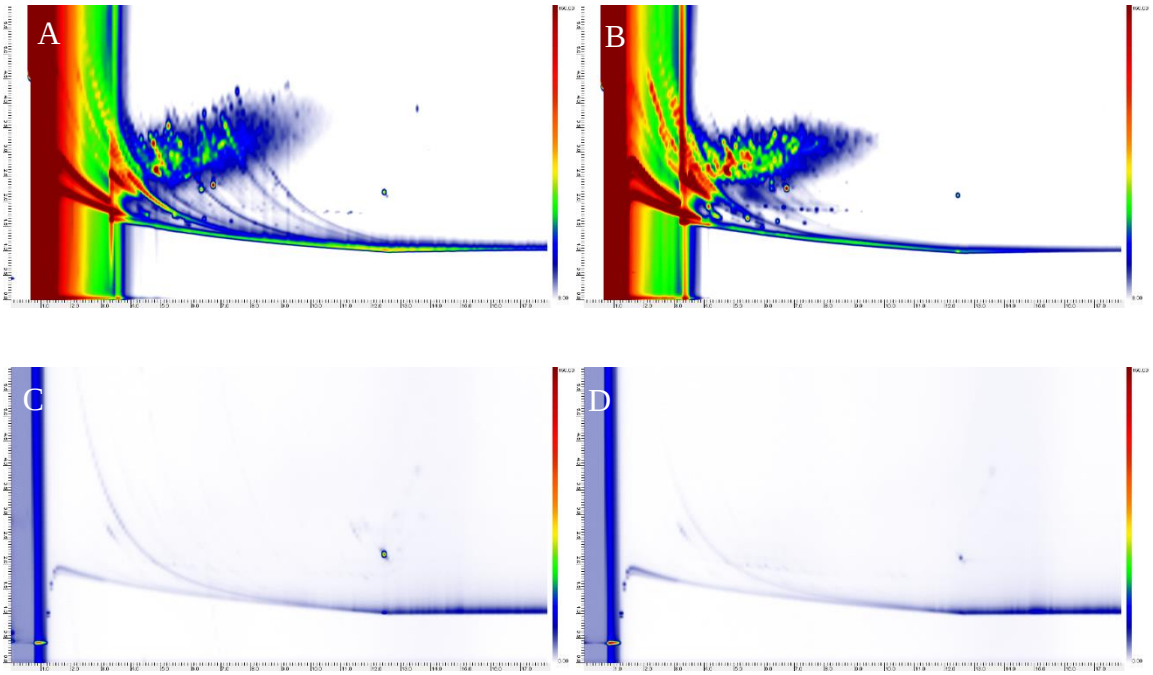

Figure 5.8 GC×GC analysis of lemon extract. (A) Normal pulsed splitless mode (50 psi until 1.1 minutes, 25 ml/min split purge at 1.0 minute). (B) Inlet backflush pulsed splitless mode (50 psi until 1.1 minutes, 25 ml/min split purge at 1.0 minute, backflush device activated at 1.0 minute). (C) Blank performed after normal pulsed splitless injection. (D) Blank performed after inlet backflush pulsed splitless injection. All regular separations have the same scale and all blanks have the same scale. Blank chromatograms have the minimums lowered to reveal carryover. (Note: the backflush was not activated in the blank runs).

5.3.3 Evaluation of the modulator as the source of chromatographic tailing

The modulator used in this study focuses analytes in a specially designed stainless steel capillary trap and injects them into the secondary column via rapid resistive heating. A custom built capacitive discharge power supply delivers electrical current to the steel trap that allows heating

from trapping to desorption temperatures in less than 100 ms. Typical temperature increases are in the range of 300 to 350 °C. It was hypothesized that if analytes were not desorbed quantitatively from this trap in a single modulation event, they could also contribute to chromatographic band tailing. To test this hypothesis, the inlet backflush device was relocated to isolate the primary column from the modulator at the moment the three way switching valve was activated. Schematic diagram showing the setup can be seen in Figure 5.2. After an analyte band had entered the modulator, the valve was switched and clean carrier gas purged the modulator. If tailing was originating from the modulator, the chromatographic bands should continue to elute from it after the primary column was isolated from the system.

An analysis of Scotch whisky headspace using SPME was performed, as this sample contains a wide variety of constituents of varying volatilities and polarities that are likely to produce unwanted tailing. The chromatogram obtained is shown in Figure 5.9 A. As expected, chromatographic tailing was evident throughout the chromatogram. One particular elongated band stood out, as it originated halfway through the run and continued until the experiment had finished. This band was chosen as an ideal candidate, as it did not appear to be originating from the major fibre desorption band at the beginning of the run, but appeared at the middle of the run and suggested an analyte was residing in the system undergoing multiple modulation events. The same analysis was completed with the switching valve being activated at 36.0 minutes.

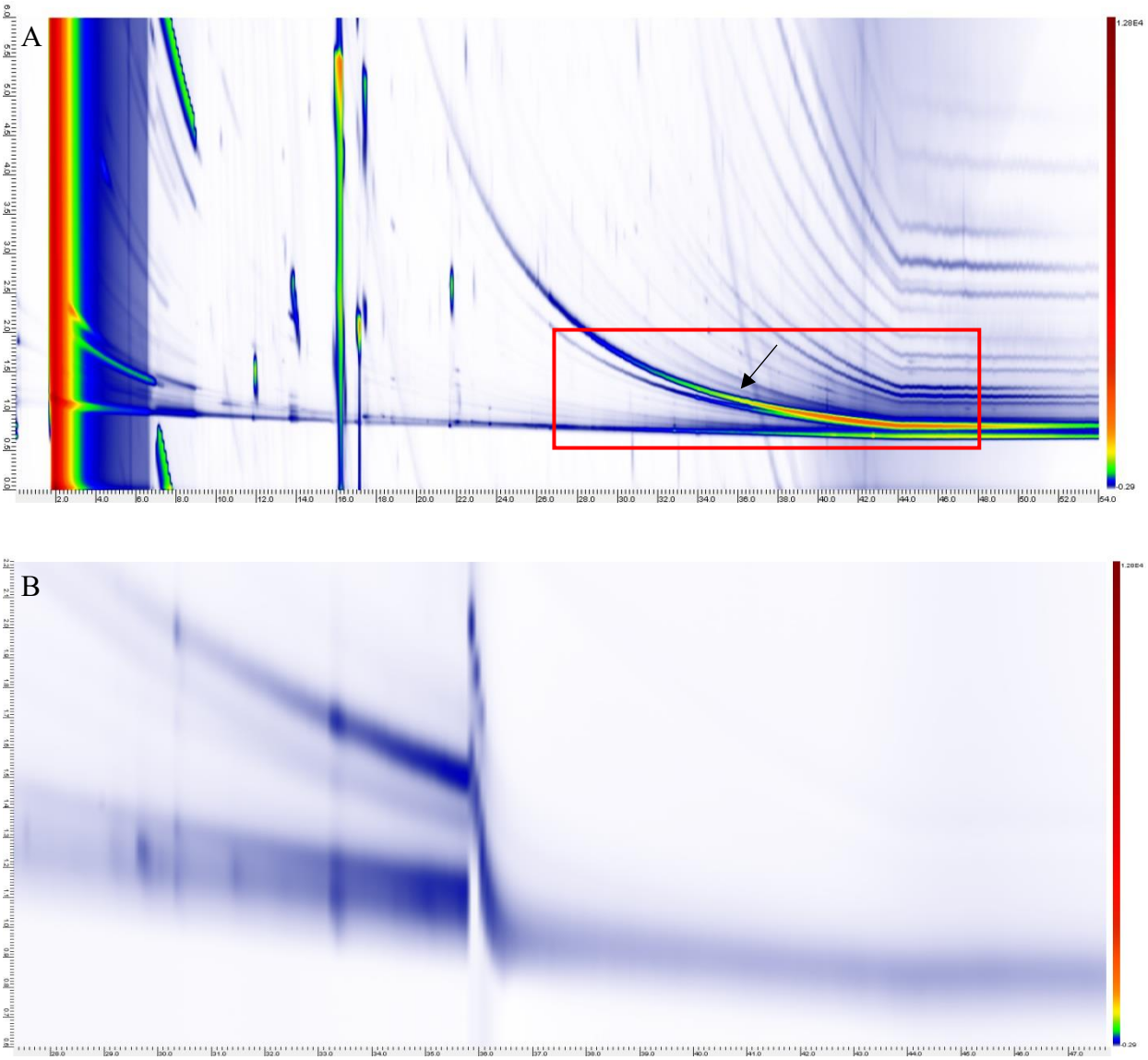

Figure 5.9 GC×GC analysis of Scotch Whisky. (A) Normal splitless mode with an arrow pointing to the targeted band. (B) Targeted band after modulator flush device was activated at 36 minutes. Chromatogram B has an increased zoom level of the selected area shown in (A).

This time was selected because the chromatographic band was at this point past its maximum and nearly halfway through its total width. Once the valve was switched, there was a temporary pressure disturbance after which flow was restored to its normal level. As seen in Figure 5.9 B,

the tailing previously seen was no longer present in the area of its projected trajectory. Thus, the elongated band had most likely been originating from the inlet, eluting over a long period into the column and arriving at the modulator as a heavily tailing analyte. The band at the bottom of the chromatogram was still present after the valve was switched as it corresponded to bleed originating from the proprietary coating of the trap.

A subsequent experiment was performed to further investigate the role of the modulator in the generation of tailing peaks. Continuing with the theme of pesticide residue extractions from fruit, a second QuEChERS extraction was completed, this time using limes. Using a splitless injection, the extract was evaluated and similar to the lemon extract, the sample provided a complex mixture of analytes with several obvious instances of tailing (Figure 5.10 A). A prominent peak eluting at the 10 minute mark was an ideal candidate as a tail extending over 5 minutes could be clearly seen in the chromatogram (Figure 5.10 B). The first two slices of the peak were allowed to elute to ensure the bulk of the analyte had entered the modulator. At this point the modulator was purged with fresh carrier gas using the backflush system (Figure 5.10 C). After several seconds flow from the primary column had been reversed and the tail which had extended in length on the order of several minutes in the previous experiment was now eliminated. This experiment further proved that the modulator was not a contributor to the problem of chromatographic tailing in GC×GC. See Appendix C for further information relating to these results.

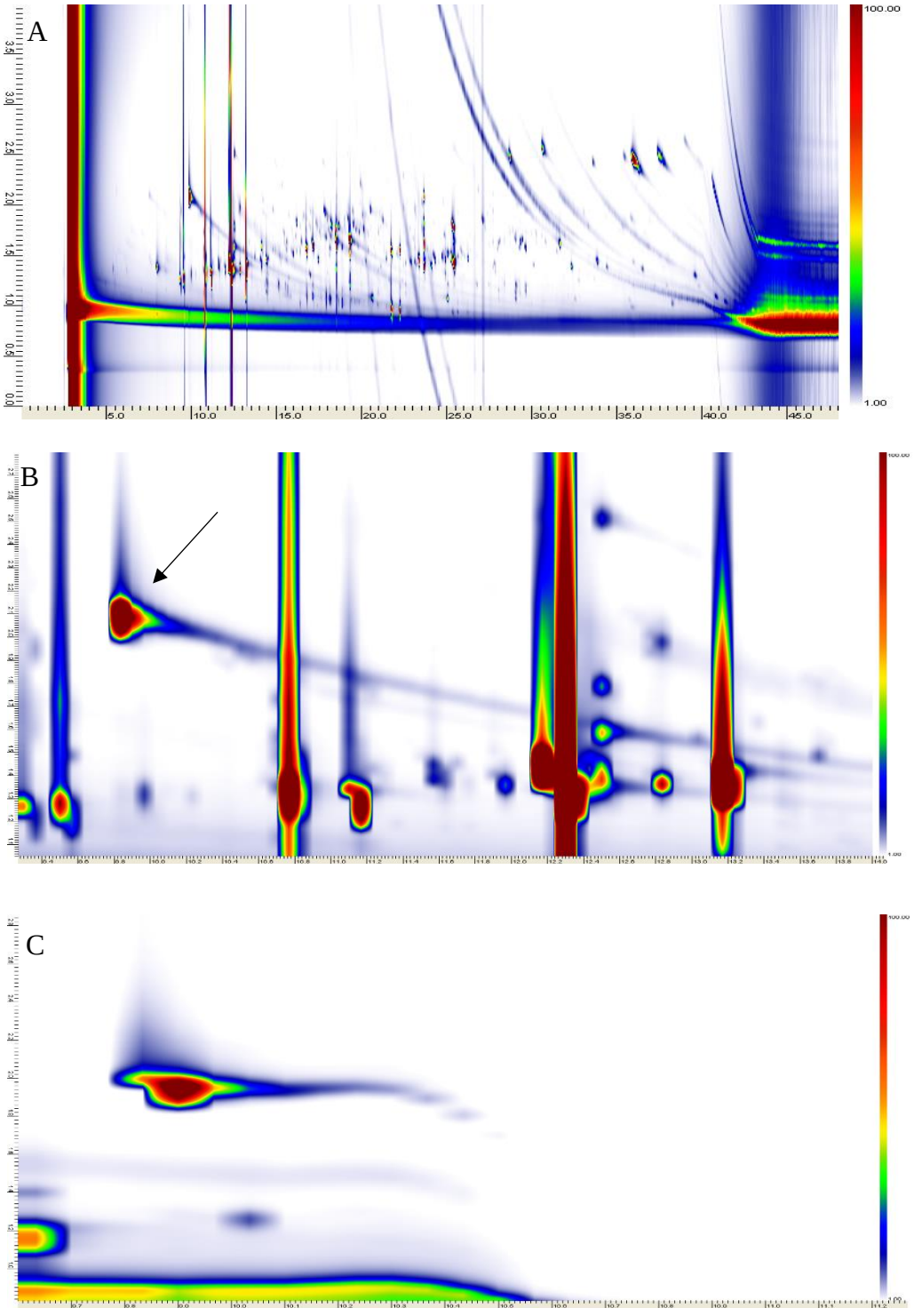

Figure 5.10 GC×GC analysis of lime extract. (A) Full chromatogram showing splitless injection of lime extract. (B) Arrow indicates the tailing peak that was targeted. (C) Modulator purge activated after the bulk of the analyte band has entered the modulator. Figure 5.10 A and Figure 5.10 B are shown with the same scaling.

5.4 Conclusions

In this study, a simple inlet backflushing device was used to investigate the sources of heavily tailing chromatographic bands frequently observed in GC×GC analyses of samples with concentrated and active analytes, those derived from natural products and those with complicated matrices. The device was effective in demonstrating that the inlet plays a significant role in producing chromatographic peaks with bandwidths on the order of minutes. Concentrated, low volatility and polar compounds are likely sorbing to active sites and/or non-volatile residue within the inlet and eluting slowly into the column throughout the analysis. Inlet backflushing is a cheap, simple and effective tool that can be used to isolate the inlet from the chromatographic system, preventing tailing bands from entering the primary column during the analysis. In addition to reducing peak tailing in the first dimension, the backflushing system is also more effective in removing residual analytes from the inlet during the run, reducing run-to-run carryover. When using this device, consideration must be given to when the backflush function is activated to prevent mass discrimination and ensure adequate sample volatilisation and transfer to the analytical column. The design of the device can be further optimized by adding a small trickle flow to remove any components that could enter the side arm via diffusion (thus preventing potential contamination), but at a cost of greater complexity.

Chapter 6. Summary and future work

6.1 Summary

Since its introduction over 30 years ago, GC×GC has emerged as the premier analytical technique for the separation of complex mixtures containing volatile and semi-volatile compounds. Significant development in modulation technology has occurred in that time and is still ongoing today. The work presented in this thesis represents a small contribution to that great story of technological innovation. The work of Panič and McNeish to develop a modulation system using a flattened, lopped trapping capillary with air cooling laid the groundwork for this contribution. Four iterations of single-stage, consumable-free modulators were introduced. The Mk I modulator used the looped 15 cm trapping capillary cooled for the first time by Peltier cooling. Reasonable separations of gasoline components were achieved and analytes as volatile as hexane could be effectively modulated. A counterintuitive result presented itself whereby less stationary phase coating within the trapping capillary resulted in better trapping performance of early eluting species. Thermoelectric cooling proved to be too effective as analytes with boiling points higher than that of *n*-C_{13} required many modulation events to be fully desorbed from the trapping capillary. In addition, the heat sink assemblies used to remove heat from the Peltier coolers failed, rendering the Mk I inoperable. With these results in hand the Mk II modulator was conceived.

A new design allowing better insulation of the heatsinks from hot GC oven air was manufactured. The trapping capillary was shortened to 7 cm total length, 5 cm flattened at its centre and all stationary phase contained within removed with thermal treatment. This process of phase removal would later be understood to be a transformation process as opposed to one of elimination. The trapping capillary placement was modified to be oriented horizontally instead of

in a looped configuration allowing less current to be required to achieve desired temperatures during rapid resistive heating. This modification also allowed better compression of the trap between the TEC coolers, allowing more thorough cooling. Linear alkane standards and diesel fuel samples were analyzed with good results. Early eluting analytes were trapped effectively even with a significant reduction in trapping capillary length. A sequence of diesel fuel replicates demonstrated excellent repeatability of retention times in both the ^{1}D and ^{2}D columns. Although there were some promising results, the system was again found to be ineffective at modulating semi-volatile analytes as the trapping capillary remained too cold during middle to latter segments of analyses. A second failure of the TEC heatsink assemblies also led to the MK II modulator becoming inoperable. With more results and knowledge in hand, a third iteration, the Mk III modulator, was designed and built.

The Mk III modulator was designed with the goal of integrating temperature programming abilities alongside a more robust construction for long term use. CPU heatsinks previously used to remove heat from the TEC devices were replaced with simple extruded aluminum. A new bracket was designed that allowed exposure of these heatsinks to both the GC oven and laboratory air. TEC devised were still in use to cool the trapping capillary, but for the first time the modulator was tested both with and without active cooling. It was found that replacing active heat removal from the TEC devices via computer CPU heat sinks with a passive heatsink design, the heatsink temperature would increase as the GC oven temperature increased during the analytical run. For an actively cooled system this meant that temperatures at both the hot and cold sides of the TEC were elevated relative to temperatures previously seen with the CPU cooler in use. However, these elevated temperatures were not a hinderance on performance and the cooling system could be passively temperature programmed by allowing the GC oven to

regulate heatsink temperature. Further testing established benchmarks for trapping capillary temperatures under a variety of passive and active cooling scenarios. Temperature programming of the system was now possible. A greater variety of samples were tested during this evaluation round including linear alkane standards ranging from *n*-C_6 to *n*-C_{40} and the headspace of whisky, coffee and cigar tobacco preconcentrated on SPME fibers. Chromatographic results were excellent for both volatile and semi-volatile analytes in the test samples. Passive temperature programming allowed the trapping capillary to remain at a higher temperature later in the run compared to the Mk I and Mk II prototypes. This meant the same number of modulation events was needed to fully remove analytes from the trap across the entire run time. Although chromatographic performance was very good, operationally there were issues with the modulator design that made it difficult to use and potentially dangerous for a new user. The next iteration focused on implementing changes to produce a new, user friendly, commercially viable design.

The Mk IV prototype was the last in this series of modulator developments. A new trap compression system inspired by a clothes pin was manufactured to provide even compression of the trapping capillary along its length. This had previously been done using threaded rods and nuts to compress two parts of a bracket system. New compression blocks made with a machinable ceramic material called Macor were built to cool the trap and replace the TEC devices. The TEC unit moved to the top of a new heatsink assembly machined entirely out of copper. A new capacitive discharge delivery system was built that allowed easy installation of the trap between the ceramic blocks whilst providing secure electrical contacts. All electrical leads were insulated and isolated from the user for additional safety. All parts were secured with precision threaded fittings. The device would later be called the “Waterloo Modulator”. The Waterloo modulator was the implementation of all the performance improvements discovered to

that point. Attention was turned next to understanding the unique characteristics of the trapping capillary.

Thermal treatment of the trapping capillary prior to installation in the GC×GC system proved to be an important performance enhancing feature. The nature of how the stationary phase was being transformed was put under investigation. Advanced imaging and material characterization techniques were applied with the assistance of WATLab to reveal changes in the stationary phase coating of the trap. These experiments revealed the PDMS was being converted to carbon doped, oxygen rich silica nanoparticles. These spherical particles coated the internal surface of the capillary evenly and provided an effective and highly sorptive phase for use in GC×GC modulation. Further experiments demonstrated that the use of MXT-1 columns as a starting material provided the most effective trapping capillary.

Validation of the Waterloo modulator's applicability to real world analytical challenges was undertaken. The composition of honeybush tea volatiles was studied in collaboration with scientists from the Stellenbosch University, South Africa. The modulator allowed identification of 84 individual compounds across three species of honeybush tea. Good separations of the complex tea aroma components was achieved with excellent retention time reproducibility, though breakthrough of compounds present at high levels was observed. Overall, the modulator was fit for purpose and provided a consumable-free alternative to other commercially available technologies.

The analysis of polychlorinated biphenyls, organochlorine pesticides and chlorobenzenes was undertaken at the Ministry of the Environment and Climate Change in Etobicoke, Ontario, Canada. This was a head-to-head comparison against a commercially available thermal modulation system using an accredited method. The same target compounds were analyzed with

both systems and the performance of the Waterloo modulator proved to be on par with the commercially available instruments. Experimental data obtained was both accurate and precise when looking at reference standards and certified reference materials. The modulator offered a simple, cost effective and consumable-free alternative to the commercial device without the need to significantly alter the accredited method and without the use of a secondary oven.

A miniaturized, portable version of the Waterloo modulator was designed and manufactured for a collaborative project with the Australian Centre for Research on Separation Science (ACROSS). The study focused on the determination of petroleum content in contaminated soils and the modulator's suitability for analysis with a portable GC. The modulator produced excellent chromatography with peaks averaging less than 100 ms wide and a wide range of analyte concentrations found to be modulated effectively. With good performance achieved and only access to electrical power required for operation, the modulator was deemed suitable for installation into a portable GC for field analysis.

Finally, a perfume sample was delivered to the University of Waterloo from a commercial fragrance manufacturer to evaluate how the modulator would manage this complex mixture. The chromatography produced of high quality with over 500 individual peaks detected. Peak area repeatability was calculated to be close to 10 % RSD with negligible variation in ^{1}D and ^{2}D retention times being observed. Overall, the modulator preformed well and the fragrance manufacturer was pleased with the results.

The final component of this thesis studied the contribution of the inlet to poor chromatography seen on occasion in GC×GC separations. Long tailing bands streaking across the chromatogram can often be seen in application papers in fields such as environmental analysis, petroleum characterization, metabolomics and flavours/fragrances. These tailing bands

are problematic as they conceal analytes of interest and make quantitation more difficult. A simple backflushing device was created to isolate the ^{1}D column from the inlet shortly after an injection had been made. The device was tested by injecting difficult samples of pesticides extracted from limes and whisky headspace preconcentrated with SPME. The hypothesis that the inlet was contributing to the deleterious chromatographic tailing was confirmed as activating backflushing post-injection improved chromatography. The theory that the modulator was responsible for these tailing effects was tested by isolating the primary column from the modulator as a tailing band was observed to be eluting through the modulator. Upon isolation, the tailing band was no longer present in the chromatogram proving that its source was prior to the trapping capillary. The device proved a useful tool to improve chromatography, but more importantly emphasized the importance of inlet maintenance and optimizing injection parameters.

In conclusion, this thesis demonstrates the single-stage, consumable-free GC×GC modulation system described herein is an excellent instrumental option for analysts across a wide breadth of application areas in the world of complex volatile and semi-volatile analysis.

6.2 Future work

Since this work was concluded in 2015, Haleigh Boswell undertook the task of progressing the development of the modulator with a special focus on optimization of the trapping capillary and materials therein [365]. Outside of exploring more sorptive trapping materials, additional efforts to optimize capillary design and capacitive discharge with a focus on reducing metal fatigue would be useful to extend trap lifetime. One of the downsides of the Waterloo modulator was the finite lifetime of the trapping capillary. A commercial vendor may consider this a valuable consumable revenue stream, but practically speaking when connected to

a mass spectrometer under vacuum a broken trapping capillary is a potentially hazardous leak which could damage the ion source and detector. From an application perspective, the modulator would be well suited to use within a routine method such as total petroleum hydrocarbons (TPS) analysis or the recent D8396 method introduced by ASTM. The volatility range or both methods is well suited for the modulator and its excellent repeatability of retention times would allow it to preform well. The use of FID detection in the methods prevents any potential leak issues with broken traps. Further exploration to the modulators use in field portable GC×GC would also have merit.

References

[1] M. Tswett, "Adsorptionsanalyse und chromatographische Methode. Anwendung auf die Chemie des Chlorophylls," *Berichte Der Deutschen Botanischen Gesellschaft,* vol. 24, pp. 384, 1906.

[2] M. Tswett, "Physikalisch-chemische Studien über das chlorophyll. Die Adsorptionen," *Berichte Der Deutschen Botanischen Gesellschaft,* vol. 24, pp. 20, 1906.

[3] L.S. Ettre, "The centenary of "Chromatography"," *LC GC,* vol. 24, pp. 680-692, 2006.

[4] K.K. Unger, E. Machtejevas, " Mehr als nur eine Säule - die Möglichkeiten mehrdimsionaler LC (More than just a column - possibilities of multidimensional LC**)**," *Nachrichten aus der Chemie**,*** vol. 55, pp. 661-664, 2007.

[5] L. Mondello, A.C. Lewis, K.D. Bartle, "Multidimensional chromatography," Hoboken, NJ, USA: John Wiley & Sons, Ltd, 2002.

[6] J.M. Davis, J.C. Giddings, "Statistical-Theory of Component Overlap in Multicomponent Chromatograms," *Analytical Chemistry,* vol. 55, pp. 418-424, 1983.

[7] J.M. Davis, J.C. Giddings, "Statistical-Method for Estimation of Number of Components from Single Complex Chromatograms - Theory, Computer-Based Testing, and Analysis of Errors," *Analytical Chemistry*, vol. 57, pp. 2168-2177, 1985.

[8] P. Rouchon, M. Schonauer, P. Valentin, G. Guiochon, "Numerical simulation of band propagation in nonlinear chromatography," *Separation Science and Technology*, vol. 22, pp. 1793-1833, 1987.

[9] J.C. Giddings, "Sample dimensionality: a predictor of order-disorder in component peak distribution in multidimensional separation," *Journal of Chromatography A*, vol. 703, pp. 3-15, 1995.

[10] T.A. Berger, "Separation of a gasoline on an open tubular column with 1.3 million effective plates," *Chromatographia,* vol. 42, pp. 63-71, 1996.

[11] K.D. Bartle, "Multidimensional chromatography. Chapter 1: introduction," Hoboken, NJ, USA: John Wiley & Sons, 2002,

[12] J.C. Giddings, "Two dimensional Separations: Concept and Promise," *Analytical Chemistry,* vol. 56, pp. 1256, 1984.

[13] J.C. Giddings, "Concepts and Comparisons in Multidimensional Separation," *Journal of High Resolution Chromatography & Chromatography Communications,* vol. 10, pp. 319-323, 1987.

[14] D.W. Armstrong, S.L. Massey Simonich, "Multidimensional Separations," *Analytical Chemistry,* vol. 86, pp. 11473, 2014.

[15] L.M. Blumberg, 'Temperature-programmed gas chromatography," Weinheim, Germany: Wiley-VCH, 2010.

[16] G. Caminiti, "Recent developments in multidimensional GC techniques," *Lab,* vol. 22, pp. 52-57, 2008.

[17] P.W. Carr, J.M. Davis, S.C. Rutan, D.R. Stoll, "Principles of online comprehensive multidimensional liquid chromatography," *Advances in Chromatography,* vol. 50, pp. 139-235, 2012.

[18] H.J. Cortes, "Multidimensional chromatography – techniques and applications," New York, NY, USA: Marcel Dekker, Inc, 1990.

[19] S.A. Cohen, M.R. Schure, Multidimensional liquid chromatography: theory and applications in industrial chemistry and the life sciences," Hoboken, NJ, USA: John Wiley & Sons Inc, 2008.

[20] A.P. de la Mata, J.J. Harynuk, "Limits of detection and quantification in comprehensive multidimensional separations. 1. A theoretical look," *Analytical Chemistry,* vol. 84, pp. 6646-53, 2012.

[21] K. Ding, D. Wu, Y. Guan, "Interface of two-dimensional liquid chromatography," Chinese Journal of Chromatography, vol. 28, pp. 1117-1122, 2010.

[22] P. Dugo, F. Cacciola, T. Kumm, G. Dugo, L. Mondello, "Comprehensive multidimensional liquid chromatography: Theory and applications," *Journal of Chromatography A; 50 Years Journal of Chromatography,* vol. 1184, pp. 353-368, 2008.

[23] J. Cazes, "Encyclopedia of chromatography: 3rd edition," Boca Raton, FL, USA: CRC Press, Taylor and Francis Group, 2010.

[24] T. Gorecki, "Comprehensive multidimensional separations: an introduction," *Pacifichem, Honolulu, HI, USA,* ANYL-140, December 15-20 2010.

[25] W. Grochocki, M.J. Markuszewski, J.P. Quirino, "Multidimensional capillary electrophoresis," *Electrophoresis,* vol. 36, pp. 135-143, 2014.

[26] G. Guiochon, N. Marchetti, K. Mriziq, R.A. Shalliker, "Implementations of two-dimensional liquid chromatography," *Journal of Chromatography A,* vol. 1189, pp. 109-168, 2008.

[27] N. Sharma, R. Sharma, K. Gandhi, N. Sharma, R. Sharma, Y.S. Rajput, B. Mann, R. Singh, K. Gandhi, "Separation methods for milk proteins on polyacrylamide gel electrophoresis:

Critical analysis and options for better resolution," *International Dairy Journal,* vol. 211, pp. 1-11, 2021.

[28] R. Westermeier, "2D gel-based Proteomics: there's life in the old dog yet," *Archives of Physiology and Biochemistry,* vol. 122, pp. 236-237, 2016.

[29] R. Westermeier, Looking at proteins from two dimensions: a review on five decades of 2D electrophoresis," *Archives of Physiology and Biochemistry,* vol. 120, pp. 168-172, 2014.

[30] C.F. Poole, "Thin-layer chromatography: challenges and opportunities," *Journal of Chromatography A,* vol. 1000, pp. 963-984, 2003.

[31] F. Rabel, J. Sherma, "A review of advances in two-dimensional thin-layer chromatography," *Journal of Liquid Chromatography and Related Technology,* vol. 39, pp. 627-639, 2016.

[32] J. Phillips, Z. Liu, "Comprehensive Two-Dimensional Gas Chromatography using an On-Column Thermal Modulator Interface," *Journal of Chromatographic Science,* vol. 29, pp. 227-231, 1991.

[33] R.E. Murphy, M.R. Schure, J.P. Foley, "Effect of sampling rate on resolution in comprehensive two-dimensional liquid chromatography," *Analytical Chemistry,* vol. 70, pp. 1585-1594, 1998.

[34] A. Mostafa, M. Edwards, T. Górecki, "Optimization aspects of comprehensive two-dimensional gas chromatography," *Journal of Chromatography A,* vol. 1255, pp. 38-55, 2012.

[35] Z. Liu, J.B. Phillips, "High-speed gas chromatography using an on-column thermal desorption modulator," *Journal of Microcolumn Separations,* vol. 1, pp. 249-256, 1989.

[36] J.B. Phillips, D.S. Luu, J.B. Pawliszyn, G.C. Carle, "Multiplex gas-ghromatography by thermal modulation of a fused-silica capillary column," *Analytical Chemistry,* vol. 57, pp. 2779-2787, 1985.

[37] C.J. Venkatramani, J.B. Phillips, "Comprehensive two-dimensional gas chromatography applied to the analysis of complex mixtures," *Journal of Microcolumn Separations,* vol. 5, pp. 511-516, 1993.

[38] Z.Y. Liu, S.R. Sirimanne, D.G. Patterson, L.L. Needham, J.B. Phillips, "Comprehensive 2-dimensional gas-chromatography for the fast separation and determination of pesticides extracted from human serum," *Analytical Chemistry,* vol. 66, pp. 3086-3092, 1994.

[39] J.B. Phillips, J.Z. Xu, "Comprehensive multidimensional gas-chromatography," *Journal of Chromatography A,* vol. 703, pp. 327-334, 1995.

[40] J.B. Phillips, J. Beens, "Comprehensive two-dimensional gas chromatography: a hyphenated method with strong coupling between the two dimensions," *Journal of Chromatography A,* vol. 856, pp. 331-347, 1999.

[41] H.J. deGeus, J. deBoer, U.A.T. Brinkman, "Development of a thermal desorption modulator for gas chromatography," *Journal of Chromatography A,* vol. 767, pp. 137-151, 1997.

[42] A.L. Lee, A.C. Lewis, K.D. Bartle, J.B. McQuaid, P.J. Marriott, "A comparison of modulating interface technologies in comprehensive two-dimensional gas chromatography (GC x GC)," *Journal of Microcolumn Separations,* vol. 12, pp. 187-193, 2000.

[43] B.V. Burger, T. Snyman, W.J.G. Burger, W.F. van Rooyen, "Thermal modulator array for analyte modulation and comprehensive two-dimensional gas chromatography," *Journal of Separation Science,* vol. 26, pp. 123-128, 2003.

[44] J.B. Phillips, E.B. Ledford, "Thermal modulation: A chemical instrumentation component of potential value in improving portability," *Field Analytical Chemistry and Technology,* vol. 1, pp. 23-29, 1996.

[45] J.B. Phillips, R.B. Gaines, J. Blomberg, F.W.M. van der Wielen, J.M. Dimandja, V. Green, J. Granger, D. Patterson, L. Racovalis, H.J. de Geus, J. de Boer, P. Haglund, J. Lipsky, V. Sinha, E.B. Ledford, "A robust thermal modulator for comprehensive two-dimensional gas chromatography," *Journal of High Resolution Chromatography,* vol. 22, pp. 3-10, 1999.

[46] H.J. de Geus, A. Schelvis, J. de Boer, U.A.T. Brinkman, "Comprehensive two-dimensional gas chromatography with a rotating thermal desorption modulator and independently temperature-programmable columns," *Journal of High Resolution Chromatography,* vol. 23, pp. 189-196, 2000.

[47] P.J. Marriott, R.M. Kinghorn, R. Ong, P. Morrison, P. Haglund, M. Harju, "Comparison of thermal sweeper and cryogenic modulator technology for comprehensive gas chromatography," *Journal of High Resolution Chromatography,* vol. 23, pp. 253-258, 2000.

[48] J. Beens, R. Tijssen, J. Blomberg, "Prediction of comprehensive two-dimensional gas chromatographic separations - A theoretical and practical exercise," *Journal of Chromatography A,* vol. 822, pp. 233-251, 1998.

[49] J. Beens, H. Boelens, R. Tijssen, J. Blomberg, "Quantitative aspects of comprehensive two-dimensional gas chromatography (GC x GC)," *Journal of High Resolution Chromatography,* vol. 21, pp. 47-54, 1998.

[50] J. Blomberg, P.J. Schoenmakers, J. Beens, R. Tijssen, "Comprehensive two-dimensional gas chromatography (GCxGC) and its applicability to the characterization of complex (petrochemical) mixtures," *Journal of High Resolution Chromatography,* vol. 20, pp. 539-544, 1997.

[51] J. Beens, R. Tijssen, J. Blomberg, "Comprehensive two-dimensional gas chromatography (GC x GC) as a diagnostic tool," *Journal of High Resolution Chromatography,* vol. 21, pp. 63-64, 1998.

[52] R.B. Gaines, E.B. Ledford, J.D. Stuart, "Analysis of water samples for trace levels of oxygenate and aromatic compounds using headspace solid-phase microextraction and comprehensive two-dimensional gas chromatography," *Journal of Microcolumn Separations,* vol. 10, pp. 597-604, 1998.

[53] G.S. Frysinger, R.B. Gaines, E.B. Ledford, "Quantitative determination of BTEX and total aromatic compounds in gasoline by comprehensive two-dimensional gas chromatography (GC x GC)," *Journal of High Resolution Chromatography,* vol. 22, pp. 195-200, 1999.

[54] J. Dalluge, J. Beens, U.A.T. Brinkman, "Comprehensive two-dimensional gas chromatography: a powerful and versatile analytical tool," *Journal of Chromatography A,* vol. 1000, pp. 69-108, 2003.

[55] M. Pursch, K. Sun, B. Winniford, H. Cortes, A. Weber, T. McCabe, J. Luong, "Modulation techniques and applications in comprehensive two-dimensional gas chromatography (GCxGC)," *Analytical and Bioanalytical Chemistry,* vol. 373, pp. 356-367, 2002.

[56] J. Blomberg, P.J. Schoenmakers, U.A.T. Brinkman, "Gas chromatographic methods for oil analysis," *Journal of Chromatography A,* vol. 972, pp. 137-173, 2002.

[57] R.C.Y. Ong, P.J. Marriott, "A review of basic concepts in comprehensive two-dimensional gas chromatography," *Journal of Chromatographic Science,* vol. 40, pp. 276-291, 2002.

[58] T. Hyotylainen, M. Kallio, K. Hartonen, M. Jussila, S. Palonen, M.L. Riekkola, "Modulator design for two-dimensional for comprehensive gas chromatography: quantitative analysis of polyaromatic hydrocarbons and polychlorinated biphenyls," *Analytical Chemistry,* vol. 74, pp. 4441-4446, 2002.

[59] G.S. Frysinger, R.B. Gaines, E.B. Ledford, "Quantitative determination of BTEX and total aromatic compounds in gasoline by comprehensive two-dimensional gas chromatography (GC x GC)," *Journal of High Resolution Chromatography,* vol. 22, pp. 195-200, 1999.

[60] G.S. Frysinger, R.B. Gaines, "Determination of oxygenates in gasoline by GC x GC," *Journal of High Resolution Chromatography,* vol. 23, pp. 197-201, 2000.

[61] G.S. Frysinger, R.B. Gaines, "Separation and identification of petroleum biomarkers by comprehensive two-dimensional gas chromatography," *Journal of Separation Science,* vol. 24, pp. 87-96, 2001.

[62] G.S. Frysinger, R.B. Gaines, C.M. Reddy, "GC x GC - A new analytical tool for environmental forensics," *Environmental Forensics,* vol. 3, pp. 27-34, 2002.

[63] L. Xu, C.M. Reddy, J.W. Farrington, G.S. Frysinger, R.B. Gaines, C.G. Johnson, R.K. Nelson, T.I. Eglinton, "Identification of a novel alkenone in Black Sea sediments," *Organic Geochemistry,* vol. 32, pp. 633-645, 2001.

[64] P.J. Marriott, R.M. Kinghorn, "Longitudinally modulated cryogenic system. A generally applicable approach to solute trapping and mobilization in gas chromatography," *Analytical Chemistry,* vol. 69, pp. 2582-2588, 1997.

[65] P.J. Marriott, R.M. Kinghorn, "Studies on cryogenic trapping of solutes during chromatographic elution in capillary gas chromatography," *Journal of High Resolution Chromatography,* vol. 19, pp. 403-408, 1996.

[66] R.M. Kinghorn, P.J. Marriott, "Comprehensive two-dimensional gas chromatography using a modulating cryogenic trap," *Journal of High Resolution Chromatography,* vol. 21, pp. 620-622, 1998.

[67] P.J. Marriott, R.M. Kinghorn, "Modulation and manipulation of gas chromatographic bands by using novel thermal means," *Analytical Sciences,* vol. 14, pp. 651-659, 1998.

[68] P.J. Marriott, R.M. Kinghorn, "New operational modes for multidimensional and comprehensive gas chromatography by using cryogenic modulation," *Journal of Chromatography A,* vol. 866, pp. 203-212, 2000.

[69] R.M. Kinghorn, P.J. Marriott, P.A. Dawes, "Design and implementation of comprehensive gas chromatography with cryogenic modulation," *Journal of High Resolution Chromatography,* vol. 23, pp. 245-252, 2000.

[70] R. Ong, R. Shellie, P. Marriott, "Observation of non-linear chromatographic peaks in comprehensive two-dimensional gas chromatography," *Journal of Separation Science,* vol. 24, pp. 367-377, 2001.

[71] R. Ong, P. Marriott, P. Morrison, P. Haglund, "Influence of chromatographic conditions on separation in comprehensive gas chromatography," *Journal of Chromatography A,* vol. 962, pp. 135-152, 2002.

[72] P. Marriott, M. Dunn, R. Shellie, P. Morrison, "Targeted Multidimensional Gas Chromatography Using Microswitching and Cryogenic Modulation," *Analytical Chemistry,* vol. 75, pp. 5532-5538, 2003.

[73] T. Gorecki, J. Harynuk, O. Panic, "The evolution of comprehensive two-dimensional gas chromatography (GC x GC)," *Journal of Separation Science,* vol. 27, pp. 359-379, 2004.

[74] E.B. Ledford, *23rd Symposium on Capillary Gas Chromatography,* Riva del Garda, Italy. June 2000.

[75] J. Ledford Edward B, C. Billesbach, "Jet-Cooled Thermal Modulator for Comprehensive Multidimensional Gas Chromatography," *Journal of High Resolution Chromatography,* vol. 23, pp. 202-204, 2000.

[76] J. Beens, M. Adahchour, R.J.J. Vreuls, K. van Altena, U.A. Th. Brinkman, "Simple, non-moving modulation interface for comprehensive two-dimensional gas chromatography," *Journal of Chromatography A,* vol. 919, pp. 127-132, 2001.

[77] M. Adahchour, J. Beens, U.A.T. Brinkman, "Single-jet, single-stage cryogenic modulator for comprehensive two-dimensional gas chromatography (GC × GC)," *Analyst,* vol. 128, pp. 213-216, 2003.

[78] J. Harynuk, T. Gorecki, "Design considerations for a GC x GC system," *Journal of Separation Science,* vol. 25, pp. 304-310, 2002.

[79] E.B. Ledford, C. Billesbach, J. Termaat, "Contribution #2262P," *Pittcon,* New Orleans, LA, USA. March 2002.

[80] R.B. Gaines, G.S. Frysinger, "Temperature requirements for thermal modulation in comprehensive two-dimensional gas chromatography," *Journal of Separation Science,* vol. 27, pp. 380-388, 2004.

[81] E.B. Ledford, "Method and apparatus for measuring velocity of chromatographic pulse," European Patent number EP 1494774A1, 2002.

[82] M. Kallio, T. Hyotylainen, M. Jussila, K. Hartonen, S. Palonen, M. Shimmo, M.L. Riekkola, "Semi-rotating cryogenic modulator for comprehensive two-dimensional gas chromatography," *Analytical and Bioanalytical Chemistry,* vol. 375, pp. 725-731, 2003.

[83] M. Kallio, M. Jussila, P. Raimi, T. Hyotylainen, "Modified semi-rotating cryogenic modulator for comprehensive two-dimensional gas chromatography," *Analytical and Bioanalytical Chemistry,* vol. 391, pp. 2357-2363, 2008.

[84] J. Harynuk, T. Gorecki, "New liquid nitrogen cryogenic modulator for comprehensive two-dimensional gas chromatography," *Journal of Chromatography A,* vol. 1019, pp. 53-63, 2003.

[85] M. Moeder, C. Martin, D. Schlosser, J. Harynuk, T. Gorecki, "Separation of technical 4-nonylphenols and their biodegradation products by comprehensive two-dimensional gas chromatography coupled to time-of-flight mass spectrometry," *Journal of Chromatography A,* vol. 1107, pp. 233-239, 2006.

[86] M. Pursch, P. Eckerle, J. Biel, R. Streck, H. Cortes, K. Sun, B. Winniford, "Comprehensive two-dimensional gas chromatography using liquid nitrogen modulation: set-up and applications," *Journal of Chromatography A,* vol. 1019, pp. 43-51, 2003.

[87] P. Eckerle, M. Pursch, H.J. Cortes, K. Sun, B. Winniford, J. Luong, "Determination of short-chain branching content in polyethylene by pyrolysis comprehensive multidimensional gas chromatography using low thermal mass column technology," *Journal of Separation Science,* vol. 31, pp. 3416-3422, 2008.

[88] A. Mostafa, T. Górecki, "Development and Design of a Single-Stage Cryogenic Modulator for Comprehensive Two-Dimensional Gas Chromatography," *Analytical Chemistry,* vol. 88, pp. 5414-5423, 2016.

[89] M. Libardoni, J.H. Waite, R. Sacks, "Electrically heated, air-cooled thermal modulator and at-column heating for comprehensive two-dimensional gas chromatography," *Analytical Chemistry,* vol. 77, pp. 2786-2794, 2005.

[90] M. Libardoni, E. Hasselbrink, J.H. Waite, R. Sacks, "At-column heating and a resistively heated, liquid-cooled thermal modulator for a low-resource bench-top GC x GC," *Journal of Separation Science,* vol. 29, pp. 1001-1008, 2006.

[91] M. Libardoni, C. Fix, J.H. Waite, R. Sacks, "Design and performance evaluation of a two-stage resistively-heated thermal modulator for GC x GC," *Analytical Methods,* vol. 2, pp. 936-943, 2010.

[92] E. Jover, M. Adahchour, J.M. Bayona, R.J.J. Vreuls, U.A.T. Brinkman, "Characterization of lipids in complex samples using comprehensive two-dimensional gas chromatography with time-of-flight mass spectrometry," *Journal of Chromatography A,* vol. 1086, pp. 2-11, 2005.

[93] I.R. Pizzutti, R.J.J. Vreuls, A. de Kok, R. Roehrs, S. Martel, C.A. Friggi, R. Zanella, "Design of a compressed air modulator to be used in comprehensive multidimensional gas chromatography and its application in the determination of pesticide residues in grapes," *Journal of Chromatography A,* vol. 1216, pp. 3305-3311, 2009.

[94] O. Panić, T. Gorecki, C. McNeish, A.H. Goldstein, B.J. Williams, D.R. Worton, S.V. Hering, N.M. Kreisberg, "Development of a new consumable-free thermal modulator for comprehensive two-dimensional gas chromatography," *Journal of Chromatography A,* vol. 1218, pp. 3070-3079, 2011.

[95] A.H. Goldstein, D.R. Worton, B.J. Williams, S.V. Hering, N.M. Kreisberg, O. Panic, T. Gorecki, "Thermal desorption comprehensive two-dimensional gas chromatography for in-situ measurements of organic aerosols," *Journal of Chromatography A,* vol. 1186, pp. 340-347, 2008.

[96] S. Kim, S.M. Reidy, B.P. Block, K.D. Wise, E.T. Zellers, K. Kurabayashi, "Microfabricated thermal modulator for comprehensive two-dimensional micro gas chromatography: design, thermal modeling, and preliminary testing." *Lab on a Chip,* vol. 10, pp. 1647-1654, 2010.

[97] G. Serrano, D. Paul, S. Kim, K. Kurabayashi, E.T. Zellers, "Comprehensive Two-Dimensional Gas Chromatographic Separations with a Microfabricated Thermal Modulator," *Analytical Chemistry,* vol. 84, pp. 6973-6980, 2012.

[98] S. Kim, S.M. Reidy, B.P. Block, K.D. Wise, E.T. Zellers, K. Kurabayashi, "A low power, high-speed miniaturized thermal modulator for comprehensive 2D gas chromatography," *Mems 2010: 23rd Ieee International Conference on Micro Electro Mechanical Systems, Technical Digest*, pp. 124-127, 2010.

[99] W.R. Collin, A. Bondy, D. Paul, K. Kurabayashi, E.T. Zellers, "µGC × µGC: Comprehensive two-dimensional gas chromatographic separations with microfabricated components," *Analytical Chemistry*, vol. 87, pp. 1630-1637, 2015.

[100] W.R. Collin, N. Nuñovero, D. Paul, K. Kurabayashi, E.T. Zellers, "Comprehensive two-dimensional gas chromatographic separations with a temperature programmed microfabricated thermal modulator," *Journal of Chromatography A*, vol. 1444, pp. 114-122, 2016.

[101] S. Kim, G. Serrano, K.D. Wise, K. Kurabayashi, E.T. Zellers, "Evaluation of a Microfabricated Thermal Modulator for Comprehensive Two-Dimensional Microscale Gas Chromatography," *Analytical Chemistry*, vol. 83, pp. 5556-5562, 2011.

[102] J. Luong, X. Guan, S. Xu, R. Gras, R.A. Shellie, "Thermal Independent Modulator for Comprehensive Two-Dimensional Gas Chromatography," *Analytical Chemistry*, vol. 88, pp. 8428-8432, 2016.

[103] B. Giocastro, M. Zoccali, P.Q. Tranchida, L. Mondello, "Evaluation of different internal diameter coated modulation columns within the context of solid-state modulation," *Journal of Separation Science*, vol. 44, pp. 1923-1930, 2021.

[104] H. Boswell, K. Tarazona Carrillo, T. Górecki, "Evaluation of the performance of cryogen-free thermal modulation-based comprehensive two-dimensional gas chromatography-time-of-flight mass spectrometry (GC×GC-TOFMS) for the qualitative analysis of a complex bitumen sample," *Separations*, vol. 7, pp. 1-12, 2020.

[105] Z.J. An, H.X. Ren, J.K. Jiang, Z. An, H. Ren, M. Xue, X. Guan, J. Jiang, Comprehensive two-dimensional gas chromatography mass spectrometry with a solid-state thermal modulator for in-situ speciated measurement of organic aerosols," *Journal of Chromatography A*, vol. 1625, pp. 461336, 2020.

[106] X. Guan, Z. Zhao, S. Cai, S. Wang, H. Lu, Analysis of volatile organic compounds using cryogen-free thermal modulation based comprehensive two-dimensional gas chromatography coupled with quadrupole mass spectrometry," *Journal of Chromatography A*, vol. 1587, pp. 227-238, 2019.

[107] H.I. Othman, A. Zaid, F. Cacciola, Z. Zhao, X. Guan, J.T. Althakafy, Y.F. Wong, "Evaluation of Cryogen-Free Thermal Modulation-Based Enantioselective Comprehensive Two-Dimensional Gas Chromatography for Stereo-Differentiation of Monoterpenes in Citrus spp. Leaf Oils," *Molecules*, vol. 28, pp. 1381, 2023.

[108] V. Mucedola, L. Vieira, L.W. Hantao, V. Mucédola, L.C.S. Vieira, D. Pierone, A.L. Gobbi, R.J. Poppi, L.W. Hantao, Thermal desorption modulation for comprehensive two-dimensional gas chromatography using a simple and inexpensive segmented-loop fluidic interface," *Talanta***,** vol. 164, pp. 470-476, 2017.

[109] F. Stilo, E. Gabetti, C. Bicchi, A. Carretta, D. Peroni, S.E. Reichenbach, C. Cordero, J. McCurry, "A step forward in the equivalence between thermal and differential-flow modulated comprehensive two-dimensional gas chromatography methods," *Journal of Chromatography A*, vol. 1627, pp. 461396, 2020.

[110] C.A. Bruckner, B.J. Prazen, R.E. Synovec, "Comprehensive two dimensional high-speed gas chromatography with chemometric analysis," *Analytical Chemistry*, vol. 70, pp. 2796-2804, 1998.

[111] C.G. Fraga, B.J. Prazen, R.E. Synovec, "Comprehensive two-dimensional gas chromatography and chemometrics for the high-speed quantitative analysis of aromatic isomers in a jet fuel using the standard addition method and an objective retention time alignment algorithm," *Analytical Chemistry*, vol. 72, pp. 4154-4162, 2000.

[112] B.J. Prazen, K.J. Johnson, A. Weber, R.E. Synovec, "Two-dimensional gas chromatography and trilinear partial least squares for the quantitative analysis of aromatic and naphthene content in naphtha," *Analytical Chemistry*, vol. 73, pp. 5677-5682, 2001.

[113] J.V. Seeley, F. Kramp, C.J. Hicks, "Comprehensive two-dimensional gas chromatography via differential flow modulation," *Analytical Chemistry*, vol. 72, pp. 4346-4352, 2000.

[114] K.J. Johnson, B.J. Prazen, R.K. Olund, R.E. Synovec, "GC x GC temperature programming requirements to produce bilinear data for chemometric analysis," *Journal of Separation Science*, vol. 25, pp. 297-303, 2002.

[115] P.A. Bueno, J.V. Seeley, "Flow-switching device for comprehensive two-dimensional gas chromatography," *Journal of Chromatography A*, vol. 1027, pp. 3-10, 2004.

[116] A.E. Sinha, K.J. Johnson, B.J. Prazen, S.V. Lucas, C.G. Fraga, R.E. Synovec, "Comprehensive two-dimensional gas chromatography of volatile and semi-volatile components using a diaphragm valve-based instrument," *Journal of Chromatography A.* , vol. 983, pp. 195-204, 2003.

[117] A.E. Sinha, B.J. Prazen, C.G. Fraga, R.E. Synovec, "Valve-based comprehensive two-dimensional gas chromatography with time-of-flight mass spectrometric detection: instrumentation and figures-of-merit," *Journal of Chromatography A*, vol. 1019, pp. 79-87, 2003.

[118] P.A. Bueno, J.V. Seeley, "Flow-switching device for comprehensive two-dimensional gas chromatography," *Journal of Chromatography A*, vol. 1027, pp. 3-10, 2004.

[119] N.J. Micyus, J.D. McCurry, J.V. Seeley, "Analysis of aromatic compounds in gasoline with flow-switching comprehensive two-dimensional gas chromatography," *Journal of Chromatography A,* vol. 1086, pp. 115-121, 2005.

[120] J.V. Seeley, E.M. Libby, S.K. Seeley, J.D. McCurry, "Comprehensive two-dimensional gas chromatography analysis of high-ethanol containing motor fuels," *Journal of Separation Science,* vol. 31, pp. 3337-3346, 2008.

[121] R.W. LaClair, P.A. Bueno, J.V. Seeley, "A systematic analysis of a flow-switching modulator for comprehensive two-dimensional gas chromatography," *Journal of Separation Science,* vol. 27, pp. 389-396, 2004.

[122] J. Harynuk, T. Gorecki, "Comprehensive two-dimensional gas chromatography in stop-flow mode," *Journal of Separation Science,* vol. 27, pp. 431-441, 2004.

[123] J. Harynuk, T. Gorecki, "New liquid nitrogen cryogenic modulator for comprehensive two-dimensional gas chromatography," *Journal of Chromatography A,* vol. 1019, pp. 53-63, 2003.

[124] J. Harynuk, T. Gorecki, "Comparison of comprehensive two-dimensional gas chromatography in conventional and stop-flow modes," *Journal of Chromatography A,* vol. 1105, pp. 159-167, 2006.

[125] N. Oldridge, O. Panic, T. Gorecki, "Stop-flow comprehensive two-dimensional gas chromatography with pneumatic switching," *Journal of Separation Science,* vol. 31, pp. 3375-3384, 2008.

[126] J.V. Seeley, N.J. Micyus, J.D. McCurry, S.K. Seeley, "Comprehensive two-dimensional gas chromatography with a simple fluidic modulator," *American Laboratory,* vol. 38, pp. 24-26, 2006.

[127] Agilent Technologies, Comprehensive flow modulated two-dimensional gas chromatography system (Santa Clara, CA, USA), 2007. [Online]. Available: https://www.agilent.com/cs/library/applications/5989-6078EN.pdf. [Accessed May 2023].

[128] M. Poliak, M. Kochman, A. Amirav, "Pulsed flow modulation comprehensive two-dimensional gas chromatography," *Journal of Chromatography A,* vol. 1186, pp. 189-195, 2008.

[129] M. Poliak, A.B. Fialkov, A. Amirav, "Pulsed flow modulation two-dimensional comprehensive gas chromatography-tandem mass spectrometry with supersonic molecular beams," *Journal of Chromatography A,* vol. 1210, pp. 108-114, 2008.

[130] J.V. Seeley, N.J. Micyus, S.V. Bandurski, S.K. Seeley, J.D. McCurry, "Microfluidic Deans switch for comprehensive two-dimensional gas chromatography," *Analytical Chemistry,* vol. 79, pp. 1840-1847, 2007.

[131] F.C. Wang, "New valve switching modulator for comprehensive two-dimensional gas chromatography," *Journal of Chromatography A,* vol. 1188, pp. 274-280, 2008.

[132] H.J. Cortes, B. Winniford, J. Luong, M. Pursch, "Comprehensive two dimensional gas chromatography review," *Journal of Separation Science,* vol. 32, pp. 883-904, 2009.

[133] P.Q. Tranchida, F.A. Franchina, P. Dugo, L. Mondello, "Flow-modulation low-pressure comprehensive two-dimensional gas chromatography," *Journal of Chromatography A,* vol. 1372, pp. 236-244, 2014.

[134] P.Q. Tranchida, F.A. Franchina, P. Dugo, L. Mondello, "A flow-modulated comprehensive gas chromatography–mass spectrometry method for the analysis of fatty acid profiles in marine and biological samples," *Journal of Chromatography A,* vol. 1255, pp. 171-176, 2012.

[135] P.Q. Tranchida, F.A. Franchina, P. Dugo, L. Mondello, "Use of greatly-reduced gas flows in flow-modulated comprehensive two-dimensional gas chromatography-mass spectrometry," *Journal of Chromatography A,* vol. 1359, pp. 271-276, 2014.

[136] F.A. Franchina, M. Maimone, P.Q. Tranchida, L. Mondello, "Flow modulation comprehensive two-dimensional gas chromatography–mass spectrometry using ~4 mL/min gas flows," *Journal of Chromatography A,* vol. 1441, pp. 134-139, 2016.

[137] R.T. Lidster, J.F. Hamilton, A.C. Lewis, "The application of two total transfer valve modulators for comprehensive two-dimensional gas chromatography of volatile organic compounds," *Journal of Separation Science,* vol. 34, pp. 812-821, 2011.

[138] S.J. Edwards, A.C. Lewis, S.J. Andrews, R.T. Lidster, J.F. Hamilton, C.N. Rhodes, "A compact comprehensive two-dimensional gas chromatography (GC× GC) approach for the analysis of biogenic VOCs," *Analytical Methods,* vol. 5, pp. 141-150, 2013.

[139] R.E. Mohler, B.J. Prazen, R.E. Synovec, "Total-transfer, valve-based comprehensive two-dimensional gas chromatography," *Analytica Chimica Acta,* vol. 555, pp. 68-74, 2006.

[140] J.F. Griffith, W.L. Winniford, K. Sun, R. Edam, J.C. Luong, "A reversed-flow differential flow modulator for comprehensive two-dimensional gas chromatography," *Journal of Chromatography A,* vol. 1226, pp. 116-123, 2012.

[141] J. Krupčík, R. Gorovenko, I. Špánik, P. Sandra, M. Giardina, "Comparison of the performance of forward fill/flush and reverse fill/flush flow modulation in comprehensive two-dimensional gas chromatography," *Journal of Chromatography A,* vol. 1466, pp. 113-128, 2016.

[142] M. Giardina, J.D. McCurry, P. Cardinael, G. Semard-Jousset, C. Cordero, C. Bicchi, "Development and validation of a pneumatic model for the reversed-flow differential flow modulator for comprehensive two-dimensional gas chromatography," *Journal of Chromatography A,* vol. 1577, pp. 72-81, 2018.

[143] O. Vyviurska, N. Koljančić, A.A. Gomes, I. Špánik, "Optimization of enantiomer separation in flow-modulated comprehensive two-dimensional gas chromatography by response surface methodology coupled to artificial neural networks: Wine analysis case study," *Journal of Chromatography A,* vol. 1675, pp. 463189, 2022.

[144] J. Ayala-Cabrera, L. Montero, T. Sahlabji, O.J. Schmitz, "Comprehensive two-dimensional gas chromatography with flow modulator coupled via tube plasma ionization to an atmospheric pressure high-resolution mass spectrometer for the analysis of vermouth volatile profile," *Analytical and Bioanalytical Chemistry,* vol. 415, pp. 2561-2573, 2023.

[145] J. Kindell, C. Bridge, "Error rate and similarity determination of latent fingerprint chemistry via 1D GC and GC × GC–MS," *Forensic Chemistry,* vol. 35, pp. 100521, 2023.

[146] SepSolve Analytical, INSIGHT flow modulator (Peterborough, UK), 2022. [Online]. Available: https://www.sepsolve.com/gas-chromatography/insight-flow-modulator-for-gcxgc.aspx. [Accessed May 2023].

[147] H.R. Yamanaka, C. Cheung, J.S. Mendoza, D.J. Oliva, K. Elzey-Aberilla, K.A. Perrault, Pilot Study on Exhaled Breath Analysis for a Healthy Adult Population in Hawaii*Molecules* **26** (2021) 3726

[148] E. Daulton, A.N. Wicaksono, A. Tiele, H.M. Kocher, S. Debernardi, T. Crnogorac-Jurcevic, J.A. Covington, "Volatile organic compounds (VOCs) for the non-invasive detection of pancreatic cancer from urine," *Talanta,* vol. 221, pp. 121604, 2021.

[149] A.C. Paiva, D. Simões Oliveira, L.W. Hantao, "A Bottom-Up Approach for Data Mining in Bioaromatization of Beers Using Flow-Modulated Comprehensive Two-Dimensional Gas Chromatography/Mass Spectrometry," *Separations,* vol. 6, 2019.

[150] LECO Corporation, FLUX GCxGC The operation, use, and concepts behind a diverting flow technique (St. Joseph, MI, USA), 2022. [Online}. Available: https://eu.leco.com/images/SepSci-Application-Library/FLUX_MODULATOR_WHITE_PAPER.pdf. [Accessed May 2023]

[151] A. Ghosh, C.T. Bates, S.K. Seeley, J.V. Seeley, "High speed Deans switch for low duty cycle comprehensive two-dimensional gas chromatography," *Journal of Chromatography A,* vol. 1291, pp. 146-154, 2013.

[152] F. Stilo, E. Gabetti, C. Bicchi, A. Carretta, D. Peroni, S.E. Reichenbach, C. Cordero, J. McCurry, "A step forward in the equivalence between thermal and differential-flow modulated comprehensive two-dimensional gas chromatography methods," *Journal of Chromatography A,* vol. 1627, pp. 461396, 2020.

[153] L.M. Blumberg, "Comprehensive two-dimensional gas chromatography: metrics, potentials, limits," *Journal of Chromatography A,* vol. 985, pp. 29-38, 2003.

[154] J. Harynuk, T. Gorecki, "Experimental variables in GCxGC: A complex interplay," *American Laboratory,* vol. 39, pp. 36-39, 2007.

[155] M. Edwards, H. Boswell, T. Gorecki, "Comprehensive Multidimensional Chromatography," *Current Chromatography,* vol. 2, pp. 80-109, 2015.

[156] P. Marriott, R. Shellie, "Principles and applications of comprehensive two-dimensional gas chromatography," *Trends in Analytical Chemistry,* vol. 21, pp. 573-583, 2002.

[157] E.B. Ledford, J.B. Phillips, J.Z. Xu, R.B. Gaines, J. Blomberg, "Ordered chromatograms: A powerful methodology in gas chromatography," *American Laboratory,* vol. 28, pp. 22, 1996.

[158] M. Jennerwein, M. Eschner, T. Wilharm, T. Gröger, R. Zimmermann, "Evaluation of reversed phase versus normal phase column combination for the quantitative analysis of common commercial available middle distillates using GC × GC-TOFMS and Visual Basic Script," *Fuel,* vol. 235, pp. 336-338, 2019.

[159] F. Adam, F. Bertoncini, V. Coupard, N. Charon, D. Thiébaut, D. Espinat, M. Hennion, "Using comprehensive two-dimensional gas chromatography for the analysis of oxygenates in middle distillates: I. Determination of the nature of biodiesels blend in diesel fuel," *Journal of Chromatography A,* vol. 1186, pp. 236-244, 2008.

[160] A. Kohl, J. Cochran, D.M. Cropek, "Characterization of military fog oil by comprehensive two-dimensional gas chromatography," *Journal of Chromatography A,* vol. 1217, pp. 550-557, 2010.

[161] D. Ryan, P. Morrison, P. Marriott, "Orthogonality considerations in comprehensive two-dimensional gas chromatography," *Journal of Chromatography A,* vol. 1071, pp. 47-53, 2005.

[162] D. Ryan, R. Shellie, P. Tranchida, A. Casilli, L. Mondello, P. Marriott, "Analysis of roasted coffee bean volatiles by using comprehensive two-dimensional gas chromatography–time-of-flight mass spectrometry," *Journal of Chromatography A,* vol. 1054, pp. 57-65, 2004.

[163] L. Mondello, A. Casilli, P.Q. Tranchida, P. Dugo, R. Costa, S. Festa, G. Dugo, "Comprehensive multidimensional GC for the characterization of roasted coffee beans," *Journal of Separation Science,* vol. 27, pp. 442-450, 2004.

[164] L. Mondello, A. Casilli, P.Q. Tranchida, R. Costa, B. Chiofalo, P. Dugo, G. Dugo, "Evaluation of fast gas chromatography and gas chromatography–mass spectrometry in the analysis of lipids," *Journal of Chromatography A,* vol. 1035, pp. 237-247, 2004.

[165] M. Adahchour, J. Beens, R.J.J. Vreuls, A.M. Batenburg, U.A.T. Brinkman, "Comprehensive two-dimensional gas chromatography of complex samples by using a 'reversed-type' column combination: application to food analysis," *Journal of Chromatography A,* vol. 1054, pp. 47-55, 2004.

[166] B.T. Weldegergis, A. de Villiers, C. McNeish, S. Seethapathy, A. Mostafa, T. Gorecki, A.M. Crouch, "Characterisation of volatile components of Pinotage wines using comprehensive two-dimensional gas chromatography coupled to time-of-flight mass spectrometry (GC×GC-TOFMS)," *Food Chemistry,* vol. 129, pp. 188-199, 2011.

[167] A.C. Lewis, N. Carslaw, P.J. Marriott, R.M. Kinghorn, P. Morrison, A.L. Lee, K.D. Bartle, M.J. Pilling, "A larger pool of ozone-forming carbon compounds in urban atmospheres," *Nature,* vol. 405, pp. 778-781, 2000.

[168] M. Harju, P. Haglund, "Comprehensive two-dimensional gas chromatography (GC×GC) of atropisomeric PCBs, combining a narrow bore β-cyclodextrin column and a liquid crystal column," *Journal of Microcolumns Separations,* vol. 13, pp. 300-305, 2001.

[169] J.D. Dimandja, S.B. Stanfill, J. Grainger, D.G. Patterson Jr, "Application of Comprehensive Two-Dimensional Gas Chromatography (GC×GC) to the Qualitative Analysis of Essential Oils," *Journal of High Resolution Chromatography,* vol. 23, pp. 208-214, 2000.

[170] X. Lu, J. Cai, H. Kong, M. Wu, R. Hua, M. Zhao, J. Liu, G. Xu, "Analysis of Cigarette Smoke Condensates by Comprehensive Two-Dimensional Gas Chromatography/Time-of-Flight Mass Spectrometry I Acidic Fraction," *Analytical Chemistry,* vol. 75, pp. 4441-4451, 2003.

[171] M. Zapadlo, J. Krupčík, P. Májek, D.W. Armstrong, P. Sandra, "Use of a polar ionic liquid as second column for the comprehensive two-dimensional GC separation of PCBs," *Journal of Chromatography A,* vol. 1217, pp. 5859-5867, 2010.

[172] J.V. Seeley, C.T. Bates, J.D. McCurry, S.K. Seeley, "Stationary phase selection and comprehensive two-dimensional gas chromatographic analysis of trace biodiesel in petroleum-based fuel," *Journal of Chromatography A,* vol. 1226, pp. 103-109, 2012.

[173] C. Cordero, P. Rubiolo, B. Sgorbini, M. Galli, C. Bicchi, "Comprehensive two-dimensional gas chromatography in the analysis of volatile samples of natural origin: a multidisciplinary approach to evaluate the influence of second dimension column coated with mixed stationary phases on system orthogonality," *Journal of Chromatography A,* vol. 1132, pp. 268-279, 2006.

[174] J.L. Anderson, J. Ding, T. Welton, D.W. Armstrong, "Characterizing ionic Liquids on the basis of multiple solvation interactions," *Journal of the American Chemical Society,* vol. 124, pp. 14247-14254, 2002.

[175] J.L. Anderson, D.W. Armstrong, "High-stability ionic liquids. A new class of stationary phases for gas chromatography," *Analytical Chemistry,* vol. 75, pp. 4851-4858, 2003.

[176] J.L. Anderson, D.W. Armstrong, "Immobilized ionic liquids as high-selectivity/high-temperature/high-stability gas chromatography stationary phases," *Analytical Chemistry,* vol. 77, pp. 6453-6462, 2005.

[177] Z.S. Breitbach, D.W. Armstrong, "Characterization of phosphonium ionic liquids through a linear solvation energy relationship and their use as GLC stationary phases," *Analytical and Bioanalytical Chemistry,* vol. 390, pp. 1605-1617, 2008.

[178] V.R. Reid, J.A. Crank, D.W. Armstrong, R.E. Synovec, "Characterization and utilization of a novel triflate ionic liquid stationary phase for use in comprehensive two-dimensional gas chromatography," *Journal of Separation Science,* vol. 31, pp. 3429-3436, 2008.

[179] J. Dallüge, M. van Rijn, J. Beens, R.J.J. Vreuls, U.A.T. Brinkman, "Comprehensive two-dimensional gas chromatography with time-of-flight mass spectrometric detection applied to the determination of pesticides in food extracts," *Journal of Chromatography A,* vol. 965, pp. 207-217, 2002.

[180] D. Van Marieke, J. Beens, J. Reijenga, P. Lipman, C. Cramers, J. Blomberg, "Group-type identification of oil samples using comprehensive two-dimensional gas chromatography coupled to a time-of-flight mass spectrometer (GC×GC-TOF)," *Journal of High Resolution Chromatography,* vol. 23, pp. 507-510, 2000.

[181] R. Shellie, P. Marriott, P. Morrison, "Concepts and preliminary observations on the triple-dimensional analysis of complex volatile samples by using GCxGC-TOFMS," *Analytical Chemistry,* vol. 73, pp. 1336-1344, 2001.

[182] P. Hess, J. de Boer, W.P. Cofino, P.E.G. Leonards, D.E. Wells, "Critical review of the analysis of non- and mono-ortho-chlorobiphenyls," *Journal of Chromatography A,* vol. 703, pp. 417-465, 1995.

[183] M. Adahchour, J. Beens, R.J.J. Vreuls, A.M. Batenburg, U.A.T. Brinkman, "Comprehensive two-dimensional gas chromatography of complex samples by using a 'reversed-type' column combination: application to food analysis," *Journal of Chromatography A,* vol. 1054, pp. 47-55, 2004.

[184] J. Harynuk, T. Gorecki, J. de Zeeuw, "Overloading of the second-dimension column in comprehensive two-dimensional gas chromatography," *Journal of Chromatography A,* vol. 1071, pp. 21-27, 2005.

[185] Z. Zhu, J. Harynuk, T. Gorecki, "Effect of first-dimension column film thickness on comprehensive two-dimensional gas chromatographic separation," *Journal of Chromatography A,* vol. 1105, pp. 17-24, 2006.

[186] R. Ong, R. Shellie, P. Marriott, "Observation of non-linear chromatographic peaks in comprehensive two-dimensional gas chromatography," *Journal of Separation Science,* vol. 24, pp. 367-377, 2001.

[187] M. Adahchour, E. Jover, J. Beens, R.J.J. Vreuls, U.A.T. Brinkman, "Twin comprehensive two-dimensional gas chromatographic system: concept and applications," *Journal of Chromatography A,* vol. 1086, pp. 128-134, 2005.

[188] J. Harynuk, T. Gorecki, J. de Zeeuw, "Overloading of the second-dimension column in comprehensive two-dimensional gas chromatography," *Journal of Chromatography A,* vol. 1071, pp. 21-27, 2005.

[189] J. Dallüge, R.J.J. Vreuls, J. Beens, U.A.T. Brinkman, "Optimization and characterization of comprehensive two-dimensional gas chromatography with time-of-flight mass spectrometric detection (GC×GC–TOF MS)," *Journal of Separation Science,* vol. 25, pp. 201-214, 2002.

[190] R. Shellie, P. Marriott, P. Morrison, L. Mondello, "Effects of pressure drop on absolute retention matching in comprehensive two-dimensional gas chromatography," *Journal of Separation Science,* vol. 27, pp. 503-512, 2004.

[191] P.Q. Tranchida, A. Casilli, P. Dugo, G. Dugo, L. Mondello, "Generation of improved gas linear velocities in a comprehensive two-dimensional gas chromatography system," *Analytical Chemistry,* vol. 79, pp. 2266-2275, 2007.

[192] P.Q. Tranchida, G. Purcaro, L. Conte, P. Dugo, G. Dugo, L. Mondello, "Optimized use of a 50 μm internal diameter secondary column in a comprehensive two-dimensional gas chromatography system," *Analytical Chemistry,* vol. 81, pp. 8529-8537, 2009.

[193] P.Q. Tranchida, G. Purcaro, L. Conte, P. Dugo, G. Dugo, L. Mondello, "Enhanced resolution comprehensive two-dimensional gas chromatography applied to the analysis of roasted coffee volatiles," *Journal of Chromatography A,* vol. 1216, pp. 7301-7306, 2009.

[194] C.J. Venkatramani, J.Z. Xu, J.B. Phillips, "Separation orthogonality in temperature-programmed comprehensive two-dimensional gas chromatography," *Analytical Chemistry,* vol. 68, pp. 1486-1492, 1996.

[195] A. Mostafa, T. Gorecki, P.Q. Tranchida, L. Mondello, “Comprehensive chromatography in combination with mass spectrometry,” Hoboken, NJ, USA: John Wiley & Sons, Inc, 2011.

[196] H.J. Chow, T. Górecki, "Temperature Programming of the Second Dimension in Comprehensive Two-Dimensional Gas Chromatography," *Analytical Chemistry,* vol. 89, pp. 8207-8211, 2017.

[197] H.Y.J. Chow, T. Górecki, "Second dimension temperature programming system for comprehensive two-dimensional gas chromatography with true temperature control," *Journal of Chromatography Open,* vol. 2, pp. 100062, 2022.

[198] H.Y.J. Chow, T. Górecki, "Second-Dimension Temperature Programming System for Comprehensive Two-Dimensional Gas Chromatography. Part 1: Precise Temperature Control Based on Column Electrical Resistance," *Analytical Chemistry,* vol. 95, pp. 8156-8163, 2023.

[199] H.Y.J. Chow, T. Górecki, "Second-Dimension Temperature Programming System for Comprehensive Two-Dimensional Gas Chromatography. Part 2: Technical Improvements and Compatibility with Flow Modulation and Time-of-Flight Mass Spectrometry," *Analytical Chemistry,* vol. 95, pp. 8164-8171, 2023.

[200] M. Adahchour, J. Beens, U.A.T. Brinkman, "Recent developments in the application of comprehensive two-dimensional gas chromatography," *Journal of Chromatography A,* vol. 1186, pp. 67-108, 2008.

[201] J. Beens, A.T. Udo, "Comprehensive two-dimensional gas chromatography—a powerful and versatile technique," *Analyst,* vol. 130, pp. 123-127, 2005.

[202] A.M. Muscalu, E.J. Reiner, S.N. Liss, T. Chen, G. Ladwig, D. Morse, "A routine accredited method for the analysis of polychlorinated biphenyls, organochlorine pesticides, chlorobenzenes and screening of other halogenated organics in soil, sediment and sludge by GCxGC-Î¼ECD," *Analytical and Bioanalytical Chemistry,* vol. 401, pp. 2403-2413, 2011.

[203] A.M. Muscalu, M. Edwards, T. Gorecki, E.J. Reiner, "Evaluation of a single-stage consumable-free modulator for comprehensive two-dimensional gas chromatography: Analysis of polychlorinated biphenyls, organochlorine pesticides and chlorobenzenes," *Journal of Chromatography A,* vol. 1391, pp. 93-101, 2015.

[204] E.P. Mateus, M.D.R. Gomes da Silva, A.B. Ribeiro, P.J. Marriott, "Qualitative mass spectrometric analysis of the volatile fraction of creosote-treated railway wood sleepers by using comprehensive two-dimensional gas chromatography," *Journal of Chromatography A,* vol. 1178, pp. 215-222, 2008.

[205] D. Ryan, P. Marriott, "Studies on thermionic ionisation detection in comprehensive two-dimensional gas chromatography," *Journal of Separation Science,* vol. 29, pp. 2375-2382, 2006.

[206] W. Khummueng, C. Trenerry, G. Rose, P.J. Marriott, "Application of comprehensive two-dimensional gas chromatography with nitrogen-selective detection for the analysis of fungicide residues in vegetable samples," *Journal of Chromatography A,* vol. 1131, pp. 203-214, 2006.

[207] T.C. Tran, G.A. Logan, E. Grosjean, J. Harynuk, D. Ryan, P. Marriott, "Comparison of column phase configurations for comprehensive two dimensional gas chromatographic analysis of crude oil and bitumen," *Organic Geochemistry,* vol. 37, pp. 1190-1194, 2006.

[208] L. Mahe, T. Dutriez, M. Courtiade, D. Thiebaut, H. Dulot, F. Bertoncini, "Global approach for the selection of high temperature comprehensive two-dimensional gas chromatography experimental conditions and quantitative analysis in regards to sulfur-containing compounds in heavy petroleum cuts," *Journal of Chromatography A,* vol. 1218, pp. 534-44, 2011.

[209] R. Hua, J. Wang, H. Kong, J. Liu, X. Lu, G. Xu, "Analysis of sulfur-containing compounds in crude oils by comprehensive two-dimensional gas chromatography with sulfur chemiluminescence detection," *Journal of Separation Science,* vol. 27, pp. 691-8, 2004.

[210] R. Hua, Y. Li, W. Liu, J. Zheng, H. Wei, J. Wang, X. Lu, H. Kong, G. Xu, "Determination of sulfur-containing compounds in diesel oils by comprehensive two-dimensional gas chromatography with a sulfur chemiluminescence detector," *Journal of Chromatography A,* vol. 1019, pp. 101-109, 2003.

[211] F.C. Wang, W.K. Robbins, F.P. Di Sanzo, F.C. McElroy, "Speciation of sulfur-containing compounds in diesel by comprehensive two-dimensional gas chromatography," *J. Chromatographic Science,* vol. 41, pp. 519-523, 2003.

[212] E.M. Kristenson, P. Korytár, C. Danielsson, M. Kallio, M. Brandt, J. Mäkelä, R.J.J. Vreuls, J. Beens, U.A.T. Brinkman, "Evaluation of modulators and electron-capture detectors for comprehensive two-dimensional GC of halogenated organic compounds," *Journal of Chromatography A,* vol. 1019, pp. 65-77, 2003.

[213] B.L. Winniford, K. Sun, J.F. Griffith, J.C. Luong, "Universal and discriminative detection using a miniaturized pulsed discharge detector in comprehensive two-dimensional GC," *Journal of Separation Science,* vol. 29, pp. 2664-2670, 2006.

[214] K.A. Schug, I. Sawicki, D.D.J. Carlton, H. Fan, H.M. McNair, J.P. Nimmo, P. Kroll, J. Smuts, P. Walsh, D. Harrison, "Vacuum ultraviolet detector for gas chromatography," *Analytical Chemistry,* vol. 86, pp. 8329-8335, 2014.

[215] B. Gruber, T. Groeger, D. Harrison, R. Zimmermann, "Vacuum ultraviolet absorption spectroscopy in combination with comprehensive two-dimensional gas chromatography for the monitoring of volatile organic compounds in breath gas: A feasibility study," *Journal of Chromatography A,* vol. 1464, pp. 141-146, 2016.

[216] J. Heyne, D. Bell, J. Feldhausen, Z. Yang, R. Boehm, "Towards fuel composition and properties from Two-dimensional gas chromatography with flame ionization and vacuum ultraviolet spectroscopy," *Fuel,* vol. 312, pp. 122709, 2022.

[217] P.J. Marriott, S. Chin, B. Maikhunthod, H. Schmarr, S. Bieri, "Multidimensional gas chromatography," *Trends in Analytical Chemistry,* vol. 34, pp. 1-21, 2012.

[218] E. Reiner, A. Ladak, L. Mullin, J.V. Seeley, K.J. Jobst, "Enhancing the sensitivity of atmospheric pressure ionization mass spectrometry using flow modulated gas chromatography," *LC GC,* vol. 14. Pp. 22-28, 2018.

[219] P.Q. Tranchida, S. Salivo, F.A. Franchina, L. Mondello, "Flow-modulated comprehensive two-dimensional gas chromatography combined with a high-resolution time-of-flight mass spectrometer: a proof-of-principle study," *Analytical Chemistry,* vol. 87, pp. 2925-2930, 2015.

[220] N. Ochiai, T. Ieda, K. Sasamoto, Y. Takazawa, S. Hashimoto, A. Fushimi, K. Tanabe, "Stir bar sorptive extraction and comprehensive two-dimensional gas chromatography coupled to high-resolution time-of-flight mass spectrometry for ultra-trace analysis of organochlorine pesticides in river water," *Journal of Chrmoatography A,* vol. 1218, pp. 6851-6860, 2011.

[221] O. Vyviurska, I. Špánik, "Assessment of Tokaj varietal wines with comprehensive two-dimensional gas chromatography coupled to high resolution mass spectrometry," *Microchemical Journal*, vol. 152, pp. 104385, 2020.

[222] L.M. Dubois, P. Stefanuto, L. Heudt, J. Focant, K.A. Perrault, "Characterizing decomposition odor from soil and adipocere samples at a death scene using HS-SPME-GC×GC-HRTOFMS," *Forensic Chemistry*, vol. 8, pp. 11-20, 2018.

[223] E.M.M. Wanda, B.B. Mamba, T.A.M. Msagati, "Comparative analysis of performance of fabricated nitrogen-doped carbon-nanotubes, silicon/germanium dioxide embedded polyethersulfone membranes for removal of emerging micropollutants from water," *Physics and Chemistry of the Earth*, vol. 127, pp. 103164, 2022.

[224] L. McGregor, N. Bukowski, D. Barden, "A New Outlook on Soft Ionization for GC-MS." *Current Trends in Mass Spectrometry*, vol. 12, 2014

[225] B. Mitrevski, P.J. Marriott, "Evaluation of quadrupole-time-of-flight mass spectrometry in comprehensive two-dimensional gas chromatography," *Journal of Chromatography A*, vol. 1362, pp. 262-269, 2014.

[226] F.A. Franchina, M.E. Machado, P.Q. Tranchida, C.A. Zini, E.B. Caramao, L. Mondello, "Determination of aromatic sulphur compounds in heavy gas oil by using (low-)flow modulated comprehensive two-dimensional gas chromatography-triple quadrupole mass spectrometry," *Journal of Chromatography A*, vol. 1387, pp. 86-94, 2015.

[227] P. Donato, F. Cacciola, P.Q. Tranchida, P. Dugo, L. Mondello, "Mass spectrometry detection in comprehensive liquid chromatography: Basic concepts, instrumental aspects, applications and trends," *Mass Spectrometry Reviews*, vol. 31, pp. 523-559, 2012.

[228] P.Q. Tranchida, G. Purcaro, D. Sciarrone, P. Dugo, G. Dugo, L. Mondello, "Accurate quadrupole MS peak reconstruction in optimized gas-flow comprehensive two-dimensional gas chromatography," *Journal of Separation Science*, vol. 33, pp. 2791-2795, 2010.

[229] P.Q. Tranchida, G. Purcaro, C. Fanali, P. Dugo, G. Dugo, L. Mondello, "Optimized use of a 50 μm ID secondary column in comprehensive two-dimensional gas chromatography–mass spectrometry," *Journal of Chromatography A*, vol. 1217, pp. 4160-4166, 2010.

[230] R. Costa, C. Fanali, G. Pennazza, L. Tedone, L. Dugo, M. Santonico, D. Sciarrone, F. Cacciola, L. Cucchiarini, M. Dachà, "Screening of volatile compounds composition of white truffle during storage by GCxGC-(FID/MS) and gas sensor array analyses," *LWT-Food Science and Technology*, vol. 60, pp. 905-913, 2015.

[231] T.H. Nievierowski, F.F. Veras, R.D. Silveira, B. Giocastro, I. Aloisi, P.Q. Tranchida, P. Dugo, A. Brandelli, C.A. Zini, J.E. Welke, "A Bacillus-based biofungicide agent prevents ochratoxins occurrence in grapes and impacts the volatile profile throughout the Chardonnay winemaking stages," *International Journal of Food Microbiology*, vol. 389, pp. 110107, 2023.

[232] K. Song, Y. Gong, S. Guo, D. Lv, H. Wang, Z. Wan, Y. Yu, R. Tang, T. Li, R. Tan, W. Zhu, R. Shen, S. Lu, "Investigation of partition coefficients and fingerprints of atmospheric gas- and particle-phase intermediate volatility and semi-volatile organic compounds using pixel-based approaches," *Journal of Chromatography A*, vol. 1665, pp. 462808, 2022.

[233] C. Cheung, J.D. Baker, J.M. Byrne, K.A. Perrault, "Investigating volatiles as the secondary metabolome of Piper methysticum from root powder and water extracts using comprehensive two-dimensional gas chromatography," *Journal of Ethnopharmacology*, vol. 294, pp. 115346, 2022.

[234] J. Harynuk, T. Gorecki, "Experimental variables in GCxGC: A complex interplay," *Americal Laboratory*, vol. 39, pp. 36-39, 2007.

[235] N.H. Snow, "GCxGC: From research to routine," *LC GC North America*, vol. 37, 2019.

[236] K. Magrini, J. Olstad, B. Peterson, R. Jackson, Y. Parent, C. Mukarakate, K. Iisa, E. Christensen, R. Seiser, "Feedstock and catalyst impact on bio-oil production and FCC Co-processing to fuels," *Biomass and Bioenergy*, vol. 163, pp. 106502, 2022.

[237] F. Liu, J. Wu, M. Jin, D.L. Hardman, D. Cannon, “From reservoir characterization to reservoir monitoring: an integrated workflow to optimize field development using geochemical fingerprinting technology,” *SPE/AAPG/SEG Unconventional Resources Technology Conference*, D013S016R003, 2022

[238] M. Jin, S. Esmaili, A. Harris, M. Pavlovic, A. Serna, T. Lv, J. Wu, F. Liu, “Reservoir characterization and monitoring using geochemical fingerprinting technology with case studies in the delaware basin,” *SPE/AAPG/SEG Unconventional Resources Technology Conference*, D021S033R004, 2022.

[239] M. Jafarian, P. Haseli, S. Saxena, B. Dally, Emerging technologies for catalytic gasification of petroleum residue derived fuels for sustainable and cleaner fuel production - an overview,” *Energy Reports*, vol. 9, pp. 3248-3272. 2023.

[240] E. Colleoni, V.G. Samaras, P. Guida, A. Frassoldati, T. Faravelli, W.L. Roberts, Unraveling the complexity of pyrolysates from residual fuels by Py-GCxGC-FID/SCD/TOF-MS with an innovative data processing method.” *Journal of Analytical and Applied Pyrolysis*, vol. 175, pp. 106204, 2023.

[241] ASTM, "Method D8396,” 2023.

[242] N. Koljancic, O. Vyviurska, I. Spánik, N. Koljančić, O. Vyviurska, I. Špánik, “Aroma compounds in essential oils: analyzing chemical composition using two-dimensional gas chromatography high resolution time-of-flight mass spectrometry combined with chemometrics,” *Plants*, vol. 12, pp. 2362, 2023.

[243] J.E. Welke, K.P. Nicolli, C.A. Zini, J.E. Welke, K.P. Nicolli, K.C. Hernandes, A.C.T. Biasoto, C.A. Zini, “Adaptation of an olfactometric system in a GC-FID in combination with GCxGC/MS to evaluate odor-active compounds of wine,” *Food Chemistry,* vol. 310, pp. 131004, 2022.

[244] C. Cordero, P. Rubiolo, C. Bicchi, C. Cordero, P. Rubiolo, S.E. Reichenbach, A. Carretta, L. Cobelli, M. Giardina, C. Bicchi, “Method translation and full metadata transfer from thermal to differential flow modulated comprehensive two dimensional gas chromatography: Profiling of suspected fragrance allergens,” *Journal of Chromatography A,* vol. 1480, pp. 70-82, 2017.

[245] L. Gimenes, J. Silva, M. Marques, L. Gimenes, J.C.R.L. Silva, R. Facanali, L.W. Hantao, W.J. Siqueira, M.O.M. Marques, “Essential oils of new lippia alba genotypes analyzed by flow-modulated comprehensive two-dimensional gas chromatography (gc×gc) and chemometric analysis,” *Molecules,* vol. 26, pp. 2332, 2021.

[246] A.M. Muscalu, D. Morse, T. Górecki, A.M. Muscalu, D. Morse, E.J. Reiner, T. Górecki, “The quantification of short-chain chlorinated paraffins in sediment samples using comprehensive two-dimensional gas chromatography with μECD detection,” *Analytical and Bioanalytical Chemistry,* vol. 409, pp. 2065-2074, 2017.

[247] D. Huang, L.R. Gao, S. Wang, D. Huang, L. Gao, M. Zheng, L. Qiao, C. Xu, K. Wang, S. Wang, Screening organic contaminants in soil by two-dimensional gas chromatography high-resolution time-of-flight mass spectrometry: A non-target analysis strategy and contaminated area case study,” *Environmental Research,* vol. 205, pp. 112420, 2022.

[248] K. Murtada, D. Bowman, M. Edwards, J. Pawliszyn, "Thin-film microextraction combined with comprehensive two-dimensional gas chromatography time-of-flight mass spectrometry screening for presence of multiclass organic pollutants in drinking water samples," *Talanta,* vol. 242, pp. 123301, 2022.

[249] C.E. Freye, P.R. Bowden, M.T. Greenfield, B.C. Tappan, "Non-targeted discovery-based analysis for gas chromatography with mass spectrometry: A comparison of peak table, tile, and pixel-based Fisher ratio analysis," *Talanta,* vol. 211, pp. 120668, 2020.

[250] J.E. Welke, K.C. Hernandes, K.P. Nicolli, J.A. Barbará, A.C.T. Biasoto, C.A. Zini, “Role of gas chromatography and olfactometry to understand the wine aroma: achievements denoted by multidimensional analysis,” *Journal of Separation Science,* vol. 44, pp. 135-168, 2021.

[251] T. Ieda, S. Hashimoto, “GC × GC and computational strategies for detecting and analyzing environmental contaminants,” *Trends in Analytical Chemistry,* vol. 165, pp. 117117, 2023.

[252] A. Zaid, M.S. Khan, D. Yan, P.J. Marriott, Y.F. Wong, “Comprehensive two-dimensional gas chromatography with mass spectrometry: an advanced bioanalytical technique for clinical metabolomics studies,” *The Analyst,* vol. 147, pp. 3974-3995, 2022.

[253] M.F.S. Mota, H.D. Waktola, Y. Nolvachai, P.J. Marriott, “Gas chromatography – mass spectrometry for characterisation, assessment of quality and authentication of seed and vegetable oils,” *Trends in Analytical Chemistry*, vol. 138, pp. 116238, 2021.

[254] D. Zanella, M. Romagnoli, S. Malcangi, M. Beccaria, T. Chenet, C. De Luca, F. Testoni, L. Pasti, U. Visentini, G. Morini, A. Cavazzini, F.A. Franchina, “The contribution of high-resolution GC separations in plastic recycling research,” *Analytical and Bioanalytical Chemistry*, vol. 415, pp. 2343-2355, 2023.

[255] F. Stilo, C. Bicchi, A. Robbat, S.E. Reichenbach, C. Cordero, “Untargeted approaches in food-omics: The potential of comprehensive two-dimensional gas chromatography/mass spectrometry,” *Trends in Analytical Chemistry*, vol. 135, pp. 116162, 2021.

[256] R.A. Hand, T. Bassindale, N. Turner, G. Morgan, "Application of comprehensive 2D chromatography in the anti-doping field: Sample identification and quantification," *Journal of Chromatography B*, vol. 1178, pp. 122584, 2021.

[257] Y. Pico, A.H. Alfarhan, D. Barcelo, "How recent innovations in gas chromatography-mass spectrometry have improved pesticide residue determination: An alternative technique to be in your radar," *Trends in Analytical Chemistry*, vol. 122, pp. 115720, 2020.

[258] M. Biedermann, K. Grob, "Advantages of comprehensive two-dimensional gas chromatography for comprehensive analysis of potential migrants from food contact materials," *Analitica Chimica Acta*, vol. 1057, pp. 11-17, 2019.

[259] E. Tammekivi, C. Geantet, C. Lorentz, K. Faure, "Two-dimensional chromatography for the analysis of valorisable biowaste: A review," *Analitica Chimica Acta*, vol. 1283, pp. 341855, 2023.

[260] O. Panić, *Development of a Cost-Effective and Consumable-Free Interface for Comprehensive Two-Dimensional Gas Chromatography* (Unpublished MSc Thesis). University of Waterloo, Waterloo, Ontario, Canada, (2007)

[261] O. Panić, T. Górecki, C. McNeish, A.H. Goldstein, B.J. Williams, D.R. Worton, S.V. Hering, N.M. Kreisberg, "Development of a new consumable-free thermal modulator for comprehensive two-dimensional gas chromatography," *Journal of Chromatography A*, vol. 1218, pp. 3070-3079, 2011.

[262] NIST, Type K Thermocouples -- thermoelectric voltage as a function of temperature (°C); reference junctions at 0 °C (NIST, Gaithersburg, MD, USA), 1995. [Online]. Available: https://srdata.nist.gov/its90/type_k/1200to1372.html. [Accessed May 2023]

[263] M.P. Pedroso, L.A.F. de Godoy, E.C. Ferreira, R.J. Poppi, F. Augusto, "Identification of gasoline adulteration using comprehensive two-dimensional gas chromatography combined to multivariate data processing," *Journal of Chromatography A*, vol. 1201, pp. 176-182, 2008.

[264] P.L. Ashmore, A. DuBois, E. Tomasino, J.F. Harbertson, T.S. Collins, "Impact of Dilution on Whisky Aroma: A Sensory and Volatile Composition Analysis," *Foods*, vol. 12, 2023.

[265] X. Fang, Y. Chen, J. Gao, Z. Run, H. Chen, R. Shi, Y. Li, H. Zhang, Y. Liu, "Application of GC-GC-TOF/MS and GC×GC-TOF/MS to Discriminate Coffee Products in Three States (Bean, Powder, and Brew)," *Foods*, vol. 12, pp. 3123, 2023.

[266] J. Fan, G. Kong, H. Yao, Y. Wu, G. Zhao, F. Li, G. Zhang, "Widely targeted metabolomic analysis reveals that volatile metabolites in cigar tobacco leaves dynamically change during fermentation," *Biochemistry and Biophysics Reports*, vol. 35, pp. 101532, 2021.

[267] Corning, MACOR Machinable Glass Ceramic For Industrial Applications (Corning, Avon Cedex, France), 2012. [Online]. Available: https://www.corning.com/media/worldwide/csm/documents/71759a443535431395eb34ebead091cb.pdf. [Accessed July 2023]

[268] V.G. Antunes, C.A. Figueroa, F. Alvarez, "A comprehensive study of the TiN/Si interface by X-ray photoelectron spectroscopy," *Applied Surface Science*, vol. 448, pp. 502-509, 2018.

[269] P. Louette, F. Bodino, J. Pireaux, "Poly(dimethyl siloxane) (PDMS) XPS Reference Core Level and Energy Loss Spectra," *Surface Science Spectra*, vol. 12, pp. 38-43, 2006.

[270] M. Adahchour, S. van Leo L, J. Beens, R.J.J. Vreuls, M.A. Batenburg, U.A.T. Brinkman, "Comprehensive two-dimensional gas chromatography with time-of-flight mass spectrometric detection for the trace analysis of flavour compounds in food," *Journal of Chromatography A*, vol. 1019, pp. 157-72, 2003.

[271] E. Joubert, M.E. Joubert, C. Bester, D. de Beer, J.H. De Lange, "Honeybush (Cyclopia spp.): From local cottage industry to global markets — The catalytic and supporting role of research," *South African Journal of Botany*, vol. 77, pp. 887-907, 2011.

[272] K.A. Theron, M. Muller, M. van der Rijst, J.C. Cronje, M. le Roux, E. Joubert, "Sensory profiling of honeybush tea (Cyclopia species) and the development of a honeybush sensory wheel," *Food Research International*, vol. 66, pp. 12-22, 2014.

[273] E. Joubert, W.C.A. Gelderblom, A. Louw, D. de Beer, "South African herbal teas: Aspalathus linearis, Cyclopia spp. and Athrixia phylicoides—A review," *Journal of Ethnopharmacology*, vol. 119, pp. 376-412, 2008.

[274] J. Lin, Y. Dai, Y. Guo, H. Xu, X. Wang, "Volatile profile analysis and quality prediction of Longjing tea (Camellia sinensis) by HS-SPME/GC-MS," *Journal of Zhejiang University SCIENCE B*, vol. 13, pp. 972-980, 2012.

[275] M.A. Drake, G.V. Civille, "Flavor Lexicons," *Comprehensive Reviews in Food Science and Food Safety*, vol. 2, pp. 33-40, 2003.

[276] M. Le Roux, J.C. Cronje, E. Joubert, B.V. Burger, "Chemical characterization of the constituents of the aroma of honeybush, Cyclopia genistoides," *South African Journal of Botany*, vol. 74, pp. 139-143, 2008.

[277] M.L. Roux, J.C. Cronje, B.V. Burger, E. Joubert, "Characterization of volatiles and aroma-active compounds in honeybush (cyclopia subternata) by GC-MS and GC-O analysis," *Journal of Agriculture and Food Chemistry*, vol. 60, pp. 2657-2664, 2012.

[278] J.C. Cronje, *Chemical characterisation of the aroma of honeybush (Cyclopia) species* (Unpublished PhD Thesis). Stellenbosch University, Stellenbosch, South Africa, (2019) Canada, (2010)

[279] L.M. Erasmus, K.A. Theron, M. Muller, M. Van der Rijst, E. Joubert, "Optimising high-temperature oxidation of Cyclopia species for maximum development of characteristic aroma notes of honeybush herbal tea infusions," *South African Journal of Botany*, vol. 110, pp. 144-151, 2017.

[280] R. van der Westhuizen, M. Ajam, P. De Coning, J. Beens, A. de Villiers, P. Sandra, "Comprehensive two-dimensional gas chromatography for the analysis of synthetic and crude-derived jet fuels," *Journal of Chromatography A*, vol. 1218, pp. 4478-4486, 2011.

[281] J. Dallüge, R.J.J. Vreuls, J. Beens, U.A.T. Brinkman, "Optimization and characterization of comprehensive two-dimensional gas chromatography with time-of-flight mass spectrometric detection (GC×GC–TOF MS)," *Journal of Separation Science*, vol. 25, pp. 201-214, 2002.

[282] A. Mostafa, M. Edwards, T. Górecki, "Optimization aspects of comprehensive two-dimensional gas chromatography," *Journal of Chromatography A*, vol. 1255, pp. 38-55, 2012.

[283] R. Weber, A. Watson, F. Oliaei, R. Weber, A. Watson, M. Forter, F. Oliaei, "Review Article: Persistent organic pollutants and landfills - a review of past experiences and future challenges," *Waste Management & Research*, vol. 29, pp. 107-121, 2011.

[284] A.M. Muscalu, E.J. Reiner, S.N. Liss, T. Chen, G. Ladwig, D. Morse, "A routine accredited method for the analysis of polychlorinated biphenyls, organochlorine pesticides, chlorobenzenes and screening of other halogenated organics in soil, sediment and sludge by GCxGC-μECD," *Analytical and Bioanalytical Chemistry*, vol. 401, pp. 2403-2413, 2011.

[285] P. Dimitriou-Christidis, A. Bonvin, S. Samanipour, J. Hollender, R. Rutler, J. Westphale, J. Gros, J.S. Arey, "GC×GC Quantification of priority and emerging nonpolar halogenated micropollutants in all types of wastewater matrices: analysis methodology, chemical occurrence, and partitioning," *Environmental Science and Technology*, vol. 49, pp. 7914-7925, 2015.

[286] Ontario Ministry of the Environment and Climate Change, "Method E3487," 2010.

[287] J.V. Seeley, S.K. Seeley, "Multidimensional Gas Chromatography: Fundamental Advances and New Applications," *Analytical Chemistry*, vol. 85, pp. 557-578, 2013.

[288] M.R. Jacobs, E.F. Hilder, R.A. Shellie, “Applications of resistive heating in gas chromatography: A review,” *Analytica Chimica Acta,* vol. 803, pp. 2-14, 2013.

[289] J. Harynuk, T. Gorecki, "Design considerations for a GC×GC system," *Journal of Separation Science,* vol. 25, pp. 304-310, 2002.

[290] M. Libardoni, “Analysis of human breath samples with a multi-bed sorption trap and comprehensive two-dimensional gas chromatography (GC×GC),” *Journal of Chromatography A,* vol. 842, pp. 13-21, 2006.

[291] R.C. Blase, K. Llera, A. Luspay-Kuti, M. Libardoni, "The Importance of Detector Acquisition Rate in Comprehensive Two-Dimensional Gas Chromatography (GC×GC)," *Separation Science and Technology,* vol. 49, pp. 847-853, 2014.

[292] J.L. Rayner, I. Snape, J.L. Walworth, P.M. Harvey, S.H. Ferguson, "Petroleum–hydrocarbon contamination and remediation by microbioventing at sub-Antarctic Macquarie Island," *Cold Regions Science and Technology,* vol. 48, pp. 139-153, 2007.

[293] S.M. Powell, J.P. Bowman, S.H. Ferguson, I. Snape, "The importance of soil characteristics to the structure of alkane-degrading bacterial communities on sub-Antarctic Macquarie Island," *Soil Biology and Biochemistry,* vol. 42, pp. 2012-2021, 2010.

[294] S. Furbo, A.B. Hansen, T. Skov, J.H. Christensen, "Pixel-based analysis of comprehensive two-dimensional gas chromatograms (color plots) of petroleum: A tutorial," *Analytical Chemistry,* vol. 86, pp. 7160-7170, 2014.

[295] T. Tin, Z.L. Fleming, K.A. Hughes, D.G. Ainley, P. Convey, C.A. Moreno, S. Pfeiffer, J. Scott, I. Snape, "Impacts of local human activities on the Antarctic environment," *Antarctic Science,* vol. 21, pp. 3-33, 2009.

[296] J.M. Aislabie, M.R. Balks, J.M. Foght, E.J. Waterhouse, "Hydrocarbon Spills on Antarctic Soils: Effects and Management," *Environmental Science and Technology,* vol. 38, pp. 1265-1274, 2004.

[297] J. Gros, C.M. Reddy, C. Aeppli, R.K. Nelson, C.A. Carmichael, J.S. Arey, "Resolving biodegradation patterns of persistent saturated hydrocarbons in weathered oil samples from the deepwater horizon disaster," *Environmental Science and Technology*, vol. 48, pp. 1628-1637, 2014.

[298] C. Aeppli, R.K. Nelson, J.R. Radović, C.A. Carmichael, D.L. Valentine, C.M. Reddy, "Recalcitrance and Degradation of Petroleum Biomarkers upon Abiotic and Biotic Natural Weathering of Deepwater Horizon Oil," *Environmental Science and Technology,* vol. 48, pp. 6726-6734, 2014.

[299] P.M. Harvey, R.A. Shellie, "Data Reduction in Comprehensive Two-Dimensional Gas Chromatography for Rapid and Repeatable Automated Data Analysis," *Analytical Chemistry,* vol. 84, pp. 6501-6507, 2012.

[300] G.S. Frysinger, R.B. Gaines, "Forensic Analysis of Ignitable Liquids in Fire Debris by Comprehensive Two-Dimensional Gas Chromatography," *Journal of Forensic Science,* vol. 47, pp. 471-482, 2002.

[301] G.S. Frysinger, R.B. Gaines, L. Xu, C.M. Reddy, "Resolving the Unresolved Complex Mixture in Petroleum-Contaminated Sediments," *Environmental Science and Technology,* vol. 37, pp. 1653-1662, 2003.

[302] R.K. Nelson, B.M. Kile, D.L. Plata, S.P. Sylva, L. Xu, C.M. Reddy, R.B. Gaines, G.S. Frysinger, S.E. Reichenbach, "Tracking the weathering of an oil spill with comprehensive two-dimensional gas chromatography," *Environmental Forensics,* vol. 7, pp. 33-44, 2006.

[303] S.K. Seeley, S.V. Bandurski, R.G. Brown, J.D. McCurry, J.V. Seeley, "A Comprehensive two-dimensional gas chromatography method for analyzing extractable petroleum hydrocarbons in water and soil," *Journal of Chromatographic Science,* vol. 45, pp. 657-663, 2007.

[304] W. Zhang, S. Zhu, S. He, Y. Wang, "Screening of oil sources by using comprehensive two-dimensional gas chromatography/time-of-flight mass spectrometry and multivariate statistical analysis," *Journal of Chromatography A,* vol. 1380, pp. 162-170, 2015.

[305] T.J. Mooney, C.K. King, J. Wasley, N.R. Andrew, "Toxicity of diesel contaminated soils to the subantarctic earthworm Microscolex macquariensis," *Environmental Toxicology and Chemistry,* vol. 32, pp. 370-377, 2013.

[306] A.C. Olivieri, "Practical guidelines for reporting results in single- and multi-component analytical calibration: A tutorial," *Analytica Chimica Acta,* vol. 868, pp. 10-22, 2015.

[307] I. Snape, P.M. Harvey, S.H. Ferguson, J.L. Rayner, A.T. Revill, "Investigation of evaporation and biodegradation of fuel spills in Antarctica I. A chemical approach using GC–FID," *Chemosphere,* vol. 61, pp. 1485-1494, 2005.

[308] European Union “DIRECTIVE 2003/15/EC of the European Parliament and of the Council of 27 february 2003 amending Council Directive 76/768/EEC on the approximation of the laws of the Member States relating to cosmetic products,” *Official Journal of the European Union,* vol. 66, pp. 26-34, 2003.

[309] European Union “Regulation of (EC) No 1223/2009 of the European Parliament and of the Council of 30 November 2009 on cosmetic products,” *Official Journal of the European Union,* vol. 342, pp. 59-209, 2009.

[310] The International Fragrance Association, “Analytical method to quantify 57 suspected allergens (and isomers) in ready to inject fragrance materials by gas chromatography and mass

spectrometry," IFRA (Brussels, Belgium), 2016. [Online]. Available: https://ifrafragrance.org/docs/default-source/guidelines/23754_gd_2017_04_11_ifra_analytical_method_to_quantify_57_suspected_allergens_(and_isomers)_in_ready_to_inject_fragrance_materials_by_gc-ms-(3).pdf?sfvrsn=ad55ac1_6. [Accessed July 2023]

[311] G. Ntlhokwe, A.G.J. Tredoux, T. Górecki, M. Edwards, J. Vestner, M. Muller, L. Erasmus, E. Joubert, J. Christel Cronje, A. de Villiers, "Analysis of honeybush tea (Cyclopia spp.) volatiles by comprehensive two-dimensional gas chromatography using a single-stage thermal modulator," *Analytical and Bioanalytical Chemistry,* vol. 409, pp. 4127-4138, 2017.

[312] K.D. Nizio, J.J. Harynuk, "Analysis of alkyl phosphates in petroleum samples by comprehensive two-dimensional gas chromatography with nitrogen phosphorus detection and post-column Deans switching," *Journal of Chromatography A,* vol. 1252, pp. 171-176, 2012.

[313] G. Wang, S. Shi, P. Wang, T.-. Wang, "Analysis of diamondoids in crude oils using comprehensive two-dimensional gas chromatography/time-of-flight mass spectrometry," *Fuel,* vol. 107, pp. 706-714, 2013.

[314] S. Li, J. Cao, S. Hu, D. Zhang, R. Fan, "Analysis of terpanes in biodegraded oils from China using comprehensive two-dimensional gas chromatography with time-of-flight mass spectrometry," *Fuel,* vol. 133, pp. 153-162, 2014.

[315] C.R. Oliveira, A.A. Ferreira, C.J.F. Oliveira, D.A. Azevedo, E.V. Santos Neto, F.R. Aquino Neto, "Biomarkers in crude oil revealed by comprehensive two-dimensional gas chromatography time-of-flight mass spectrometry: Depositional paleoenvironment proxies," *Organic Geochemistry,* vol. 46, pp. 154-164, 2012.

[316] C.R. Oliveira, C.J.F. Oliveira, A.A. Ferreira, D.A. Azevedo, F.R. Aquino Neto, "Characterization of aromatic steroids and hopanoids in marine and lacustrine crude oils using comprehensive two dimensional gas chromatography coupled to time-of-flight mass spectrometry (GCxGC-TOFMS)," *Organic Geochemistry,* vol. 53, pp. 131-136, 2012.

[317] R.C. Silva, R.S.F. Silva, E.V.R. de Castro, K.E. Peters, D.A. Azevedo, "Extended diamondoid assessment in crude oil using comprehensive two-dimensional gas chromatography coupled to time-of-flight mass spectrometry," *Fuel,* vol. 112, pp. 125-133, 2013.

[318] W. Hexana, P. Coning, S. Jali, R. Westhuizen, B. Brack, A. Houwelingen, R. Nel, "Comprehensive two-dimensional GC for the analysis of low-molecular-weight oxygenates in three different matrices from a petrochemical pilot plant using a single calibration," *Journal of Separation Science,* vol. 37, pp. 566-572, 2014.

[319] K. Lissitsyna, S. Huertas, L.C. Quintero, L.M. Polo, "Novel simple method for quantitation of nitrogen compounds in middle distillates using solid phase extraction and comprehensive two-dimensional gas chromatography," *Fuel,* vol. 104, pp. 752-757, 2013.

[320] H. Lu, Q. Shi, J. Lu, G. Sheng, P. Peng, C.S. Hsu, "Petroleum sulfur biomarkers analyzed by comprehensive two-dimensional gas chromatography sulfur-specific detection and mass spectrometry," *Energy and Fuels,* vol. 27, pp. 7245-7251, 2013.

[321] K. Lissitsyna, S. Huertas, L.C. Quintero, L.M. Polo, "Quantitation method of N,N'-disalicylidene-1,2-propanediamine by comprehensive two-dimensional gas chromatography coupled to a nitrogen chemiluminescence detector," *Journal of Separation Science,* vol. 36, pp. 1768-1773, 2013.

[322] G.T. Ventura, B.R.T. Simoneit, R.K. Nelson, C.M. Reddy, "The composition, origin and fate of complex mixtures in the maltene fractions of hydrothermal petroleum assessed by comprehensive two-dimensional gas chromatography," *Organic Geochemistry,* vol. 45, pp. 48-65, 2012.

[323] L. Zhang, Z. Zeng, C. Zhao, H. Kong, X. Lu, G. Xu, "A comparative study of volatile components in green, oolong and black teas by using comprehensive two-dimensional gas chromatography-time-of-flight mass spectrometry and multivariate data analysis," *Journal of Chromatography A,* vol. 1313, pp. 245-52, 2013.

[324] Y. Ding, L. Zhu, S. Liu, H. Yu, Y. Dai, "Analytical method of free and conjugated neutral aroma components in tobacco by solvent extraction coupled with comprehensive two-dimensional gas chromatography-time-of-flight mass spectrometry," *Journal of Chromatography A,* vol. 1280, pp. 122-7, 2013.

[325] K. Samykanno, E. Pang, P.J. Marriott, "Chemical characterisation of two Australian-grown strawberry varieties by using comprehensive two-dimensional gas chromatography-mass spectrometry," *Food Chemistry,* vol. 141, pp. 1997-2005, 2013.

[326] G. Purcaro, P. Morrison, S. Moret, L.S. Conte, P.J. Marriott, "Determination of polycyclic aromatic hydrocarbons in vegetable oils using solid-phase microextraction-comprehensive two-dimensional gas chromatography coupled with time-of-flight mass spectrometry," *Journal of Chromatography A,* vol. 1161, pp. 284-91, 2007.

[327] Y. Qiu, X. Lu, T. Pang, C. Ma, X. Li, G. Xu, "Determination of radix ginseng volatile oils at different ages by comprehensive two-dimensional gas chromatography/time-of-flight mass spectrometry," *Journal of Separation Science,* vol. 31, pp. 3451-7, 2008.

[328] J. Kiefl, P. Schieberle, "Evaluation of process parameters governing the aroma generation in three hazelnut cultivars (Corylus avellana L.) by correlating quantitative key odorant profiling with sensory evaluation," *Journal of Agriculture and Food Chemistry,* vol. 61, pp. 5236-5244, 2013.

[329] A. Nosheen, B. Mitrevski, A. Bano, P.J. Marriott, "Fast comprehensive two-dimensional gas chromatography method for fatty acid methyl ester separation and quantification using dual ionic liquid columns," *Journal of Chromatography A,* vol. 1312, pp. 118-23, 2013.

[330] S. Chin, G.T. Eyres, P.J. Marriott, "Identification of potent odourants in wine and brewed coffee using gas chromatography-olfactometry and comprehensive two-dimensional gas chromatography," *Journal of Chromatography A,* vol. 1218, pp. 7487-98, 2011.

[331] J. Filippi, E. Belhassen, N. Baldovini, H. Brevard, U.J. Meierhenrich, "Qualitative and quantitative analysis of vetiver essential oils by comprehensive two-dimensional gas chromatography and comprehensive two-dimensional gas chromatography/mass spectrometry," *Journal of Chromatography A,* vol. 1288, pp. 127-48, 2013.

[332] S.P. Pyl, C.M. Schietekat, K.M. Van Geem, M. Reyniers, J. Vercammen, J. Beens, G.B. Marin, "Rapeseed oil methyl ester pyrolysis: On-line product analysis using comprehensive two-dimensional gas chromatography," *Journal of Chromatography A,* vol. 1218, pp. 3217-3223, 2011.

[333] G. Du, Y. Xiao, H. Yang, L. Wang, Y. Song, Y. Wang, "Rapid determination of pesticide residues in herbs using selective pressurized liquid extraction and fast gas chromatography coupled with mass spectrometry," *Journal of Separation Science,* vol. 35, pp. 1922-1932, 2012.

[334] M.S. Klee, L.J. Gajdos, B.D. Quimby, "System for integrated backflush in a gas chromatograph," U.S. Patent number 8,210,026, 2012.

[335] C. Ma, H. Wang, X. Lu, H. Li, B. Liu, G. Xu, "Analysis of Artemisia annua L. volatile oil by comprehensive two-dimensional gas chromatography time-of-flight mass spectrometry," *Journal of Chromatography A,* vol. 1150, pp. 50-53, 2007.

[336] M. Caldeira, R. Perestrelo, A.S. Barros, M.J. Bilelo, A. Morete, J.S. Camara, S.M. Rocha, "Allergic asthma exhaled breath metabolome: A challenge for comprehensive two-dimensional gas chromatography," *Journal of Chromatography A,* vol. 1254, pp. 87-97, 2012.

[337] Z. Yun, H. Gao, P. Liu, S. Liu, T. Luo, S. Jin, Q. Xu, J. Xu, Y. Cheng, X. Deng, "Comparative proteomic and metabolomic profiling of citrus fruit with enhancement of disease resistance by postharvest heat treatment," *BMC Plant Biology,* vol. 13, pp. 44, 2013.

[338] P. Wojtowicz, J. Zrostlikova, V. St'astna, E. Dostalova, L. Zidkova, P. Bruheim, T. Adam, "Comprehensive two-dimensional gas chromatography coupled tp time-of-flight mass spectrometry in human metabolomics," Rijeka, Croatia: InTech, 2012

[339] A. Knorr, A. Monge, M. Stueber, A. Stratmann, D. Arndt, E. Martin, P. Pospisil, "Computer-Assisted Structure Identification (CASI)-An Automated Platform for High-Throughput Identification of Small Molecules by Two-Dimensional Gas Chromatography Coupled to Mass Spectrometry," *Analytical Chemistry,* vol. 85, pp. 11216-11224, 2013.

[340] S.M. Rocha, M. Caldeira, J. Carrola, M. Santos, N. Cruz, I.F. Duarte, "Exploring the human urine metabolomic potentialities by comprehensive two-dimensional gas chromatography coupled to time of flight mass spectrometry," *Journal of Chromatography A,* vol. 1252, pp. 155-163, 2012.

[341] S.M. Rocha, R. Freitas, P. Cardoso, M. Santos, R. Martins, E. Figueira, "Exploring the potentialities of comprehensive two-dimensional gas chromatography coupled to time of flight mass spectrometry to distinguish bivalve species: Comparison of two clam species (Venerupis decussata and Venerupis philippinarum)," *Journal of Chromatography A,* vol. 1315, pp. 152-161, 2013.

[342] A.W. Culbertson, W.B. Williams, A.G. Mckee, X. Zhang, K.L. Marchs, S. Naylor, S.J. Valentine, "Inside the personalized medicine toolbox: GC X GC-mass spectrometry for high-throughput profiling of the human plasma metabolome," *LCGC North America,* vol. 26, pp. 74-81, 2008.

[343] J. Jeong, X. Shi, X. Zhang, S. Kim, C. Shen, "Model-based peak alignment of metabolomic profiling from comprehensive two-dimensional gas chromatography mass spectrometry," *BMC Bioinformatics,* vol. 13, pp. 27, 2012.

[344] K.A. Kouremenos, J.J. Harynuk, W.L. Winniford, P.D. Morrison, P.J. Marriott, "One-pot microwave derivatization of target compounds relevant to metabolomics with comprehensive two-dimensional gas chromatography," *Journal of Chromatography B,* vol. 878, pp. 1761-1770, 2010.

[345] S. Ly-Verdu, A. Schaefer, M. Kahle, T. Groeger, S. Neschen, J. Arteaga-Salas, M. Ueffing, M.H. Angelis, R. Zimmermann, "The impact of blood on liver metabolite profiling - a combined metabolomic and proteomic approach," *Biomedical Chromatography,* vol. 28, pp. 231-240, 2014.

[346] K.K. Pasikanti, K. Esuvaranathan, Y. Hong, P.C. Ho, R. Mahendran, N.M. Raman, E. Chiong, E.C.Y. Chan, "Urinary metabotyping of bladder cancer using two-dimensional gas chromatography time-of-flight mass spectrometry," *Journal of Proteome Research,* vol. 12, pp. 3865-3873, 2013.

[347] M.M. Koek, B. Muilwijk, L.L.P. van Stee, T. Hankemeier, "Higher mass loadability in comprehensive two-dimensional gas chromatography-mass spectrometry for improved analytical performance in metabolomics analysis," *Journal of Chromatography A,* vol. 1186, pp. 420-429, 2008.

[348] C.E. West, A.G. Scarlett, J. Pureveen, E.W. Tegelaar, S.J. Rowland, "Abundant naphthenic acids in oil sands process-affected water: studies by synthesis, derivatization and two-dimensional gas chromatography/high-resolution mass spectrometry," *Rapid Communications in Mass Spectrometry,* vol. 27, pp. 357-365, 2013.

[349] S. Zhu, L. Gao, M. Zheng, H. Liu, B. Zhang, L. Liu, Y. Wang, "Determining indicator toxaphene congeners in soil using comprehensive two-dimensional gas chromatography-tandem mass spectrometry," *Talanta,* vol. 118, pp. 210-216, 2014.

[350] M. Beldean-Galea, J. Vial, D. Thiebaut, "Development of a screening method for the determination of xenobiotic organic pollutants in municipal landfill leachate using solvent

extraction and comprehensive GCxGC-qMS analysis," *Central European Journal of Chemistry*, vol. 11, pp. 1563-1574, 2013.

[351] M. Pena-Abaurrea, F. Ye, J. Blasco, L. Ramos, "Evaluation of comprehensive two-dimensional gas chromatography-time-of-flight-mass spectrometry for the analysis of polycyclic aromatic hydrocarbons in sediments," *Journal of Chromatography A*, vol. 1256, pp. 222-231, 2012.

[352] D. Megson, R. Kalin, P.J. Worsfold, C. Gauchotte-Lindsay, D.G. Patterson, M.C. Lohan, S. Comber, T.A. Brown, G. O'Sullivan, "Fingerprinting polychlorinated biphenyls in environmental samples using comprehensive two-dimensional gas chromatography with time-of-flight mass spectrometry," *Journal of Chromatography A*, vol. 1318, pp. 276-283, 2013.

[353] D. Nabi, J. Gros, P. Dimitriou-Christidis, J.S. Arey, "Mapping Environmental Partitioning Properties of Nonpolar Complex Mixtures by Use of GC×GC," *Environmental Science and Technology*, vol. 48, pp. 6814-6826, 2014.

[354] C.M. Rochman, C. Manzano, B.T. Hentschel, S.L.M. Simonich, E. Hoh, "Polystyrene Plastic: A Source and Sink for Polycyclic Aromatic Hydrocarbons in the Marine Environment," *Environmental Science and Technology*, vol. 47, pp. 13976-13984, 2013.

[355] F.L. Dorman, P.D. Schettler, L.A. Vogt, J.W. Cochran, "Using computer modeling to predict and optimize separations for comprehensive two-dimensional gas chromatography," *Journal of Chromatography A*, vol. 1186, pp. 196-201, 2008.

[356] B.T. Weldegergis, A.M. Crouch, T. Gorecki, V.A. de, "Solid phase extraction in combination with comprehensive two-dimensional gas chromatography coupled to time-of-flight mass spectrometry for the detailed investigation of volatiles in South African red wines," *Analytica Chimica Acta*, vol. 701, pp. 98-111, 2011.

[357] K. Mastovska, P.L. Wylie, "Evaluation of a new column backflushing set-up in the gas chromatographic-tandem mass spectrometric analysis of pesticide residues in dietary supplements," *Journal of Chromatography A*, vol. 1265, pp. 155-164, 2012.

[358] J.S. Nadeau, R.B. Wilson, B.D. Fitz, J.T. Reed, R.E. Synovec, "Utilizing a constant peak width transform for isothermal gas chromatography," *Journal of Chromatography A*, vol. 1218, pp. 3718-3724, 2011.

[359] K. Mastovska, J. Hajslova, S.J. Lehotay, "Ruggedness and other performance characteristics of low-pressure gas chromatography-mass spectrometry for the fast analysis of multiple pesticide residues in food crops," *Journal of Chromatography A*, vol. 1054, pp. 335-349, 2004.

[360] Agilent Technologies, Split/Splitless Inlet Cleaning Procedure 5890 and 6890 Split/Splitless Inlets (Santa Clara, CA, USA), 2015. [Online]. Available: https://www.agilent.com/cs/library/support/documents/a16022.pdf. [Accessed June 2023]

[361] J. Zrostlikova, J. Hajslova, T. Cajka, "Evaluation of two-dimensional gas chromatography-time-of-flight mass spectrometry for the determination of multiple pesticide residues in fruit," *Journal of Chromatography A*, vol. 1019, pp. 173-186, 2003.

[362] P.L. Wylie, "Improved gas chromatographic analysis of organophosphorus pesticides with pulsed splitless injection," *Journal of AOAC International*, vol. 79, pp. 571-577, 1996.

[363] M. Godula, J. Hajslova, K. Alterova, "Pulsed splitless injection and the extent of matrix effects in the analysis of pesticides," *Journal of High Resolution Chromatography*, vol. 22, pp. 395-402, 1999.

[364] H. Boswell, *In Search of an Ideal Modulator for Comprehensive Two-Dimensional Gas Chromatography* (Unpublished PhD Thesis). University of Waterloo, Waterloo, Ontario, Canada, (2019)

Appendix A

Supplementary materials from section 4.1

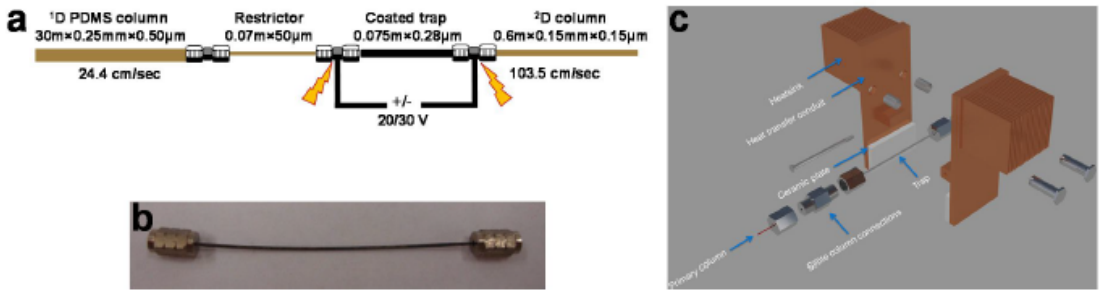

Fig. S1 Overview of the single-stage thermal modulator used in this study. (a) Schematic illustration of the columns, restrictor and trap used, (b) photograph of the trap, and (c) placement of the trap between two ceramic plates which are passively cooled by the heatsinks placed outside the GC oven (adapted from [10])

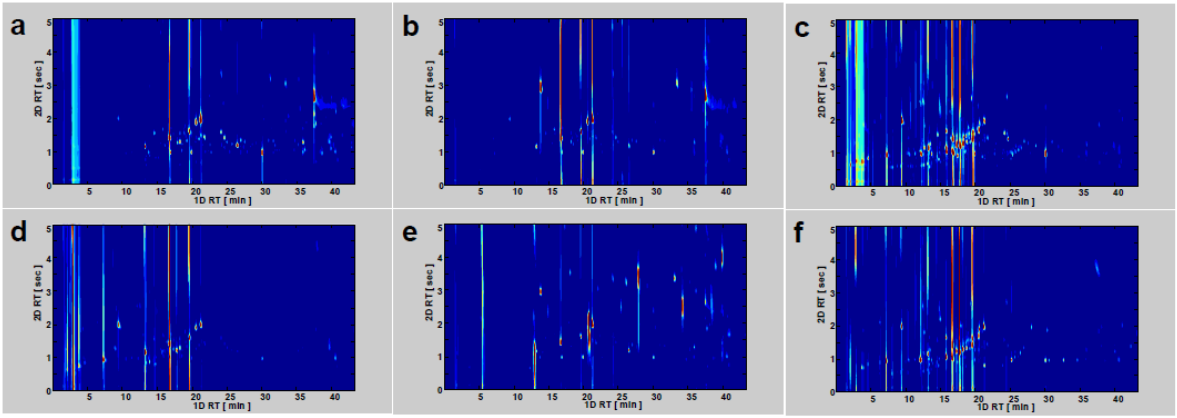

Fig. S2 GC×GC-FID contour plots of honeybush tea volatiles obtained for different SPME fibres (a) PDMS, (b) PA, (c) DVB/CAR/PDMS, (d) CAR/PDMS, (e) PEG and (f) PDMS/DVB. The analyses were performed on a HP-5MS × Stabilwax column combination at an inlet head-pressure of 151.7 kPa; initial flow = 2.06 mL/min; oven temperature ramping rate = 5.5 °C/min (refer to section 2.5.1 for further experimental details)

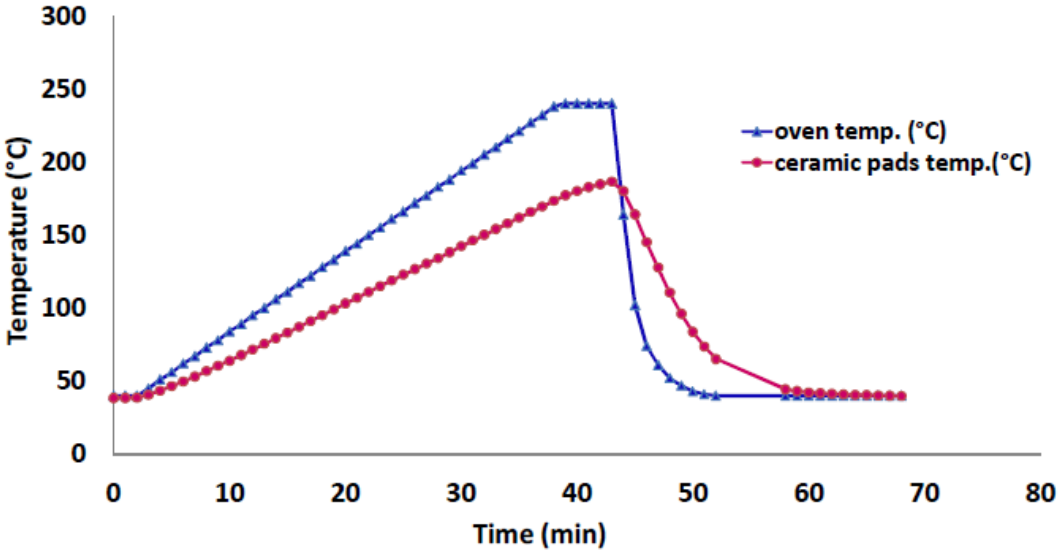

Fig. S3 Temperature difference between the modulator's ceramic plates (as measured using a thermocouple placed between them) and the oven temperature (according to the GC), determined at an oven temperature ramping rate of 5.5°C/min from 40°C to 240°C

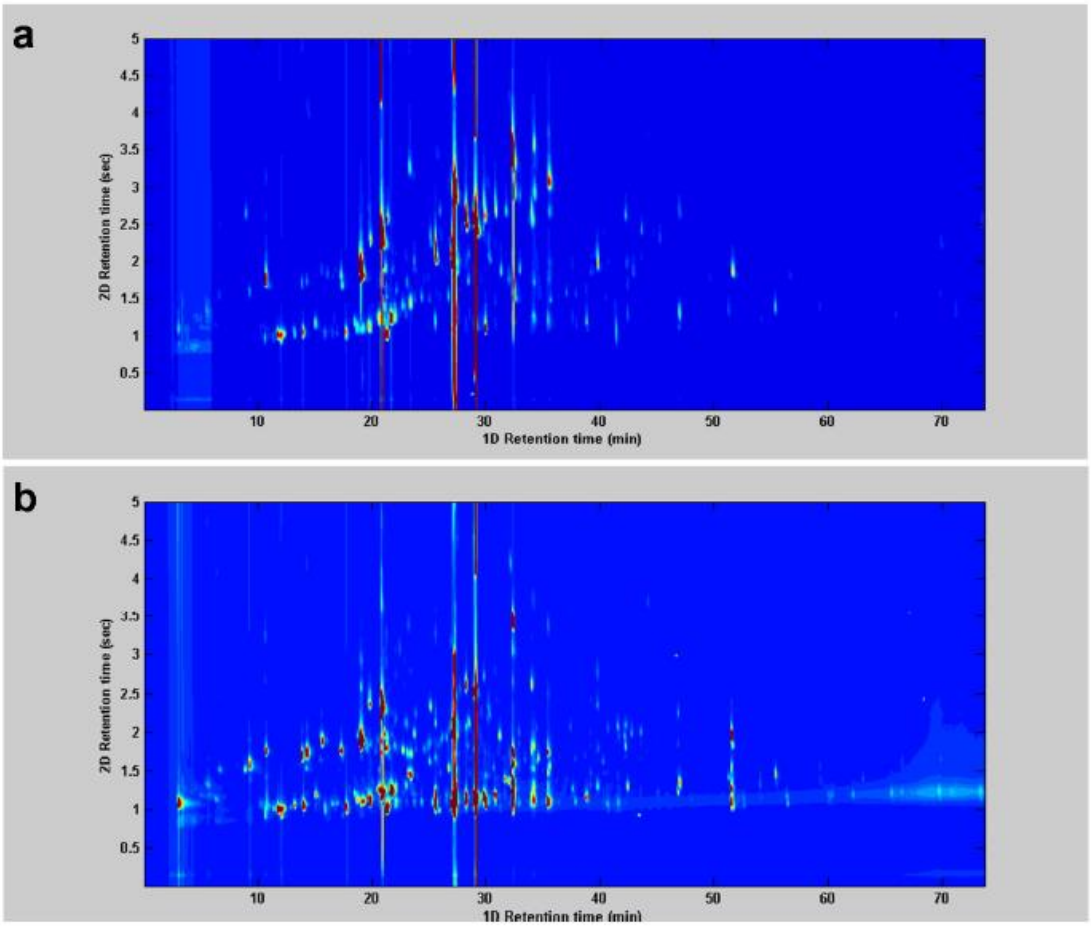

Fig. S4 Illustration of the effect of the modulator discharge voltage on the GC×GC separation of honeybush tea volatile compounds: (a) 20 V and (b) 30 V discharge voltages. Analyses were performed using the optimised conditions (Section 2.5.2)

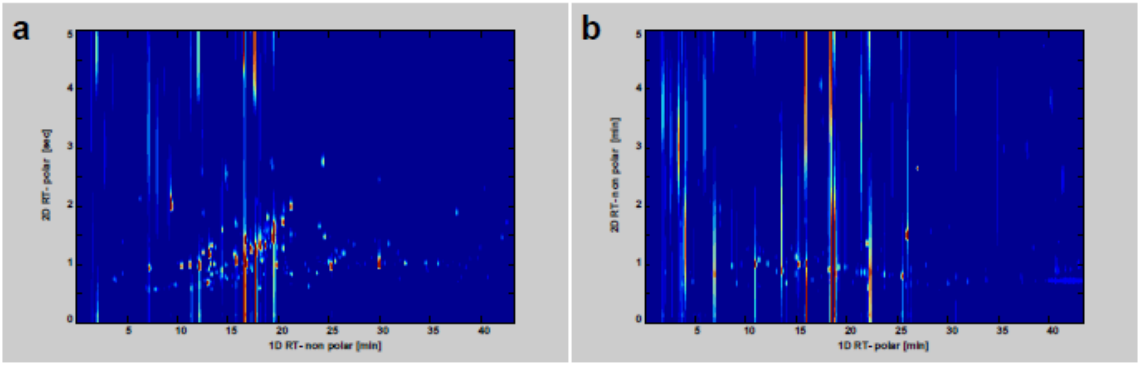

Fig. S5 GC×GC-FID contour plots obtained for the analysis of honeybush tea volatile components on different column sets: (a) non-polar × polar (HP-5MS × Stabilwax) and (b) polar × non-polar (DB-WAXETR× Rxi-5Sil MS). Analytes were extracted by HS-SPME using a PDMS/DVB SPME fibre and chromatographic conditions are as specified in Fig. S2

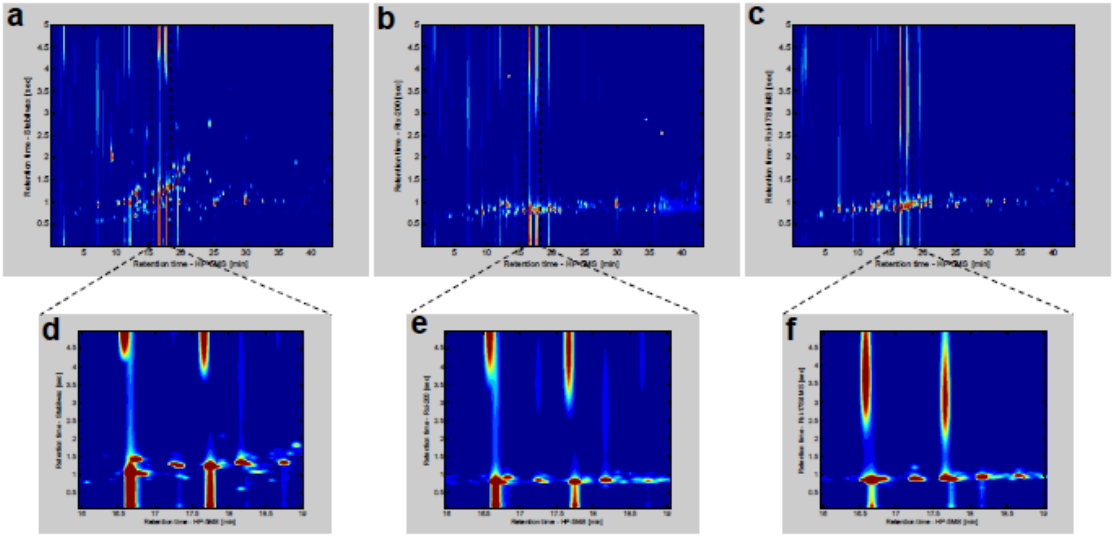

Fig. S6 Influence of polarity of the second dimension column on wraparound in the GC×GC separation of honeybush tea volatile components. A HP-5 MS column was used in ^{1}D, together with (a) Stabilwax, (b) Rtx-200 and (**c**) Rxi-17Sil MS columns in ^{2}D. Zoomed contour plots show the degree of wraparound for two major compounds on the (d) Stabilwax, (e) Rtx-200 and (f) Rxi-17Sil MS ^{2}D columns. A PDMS/DVB SPME fibre was used for extraction of analytes and chromatographic conditions are the same as in Fig. S2

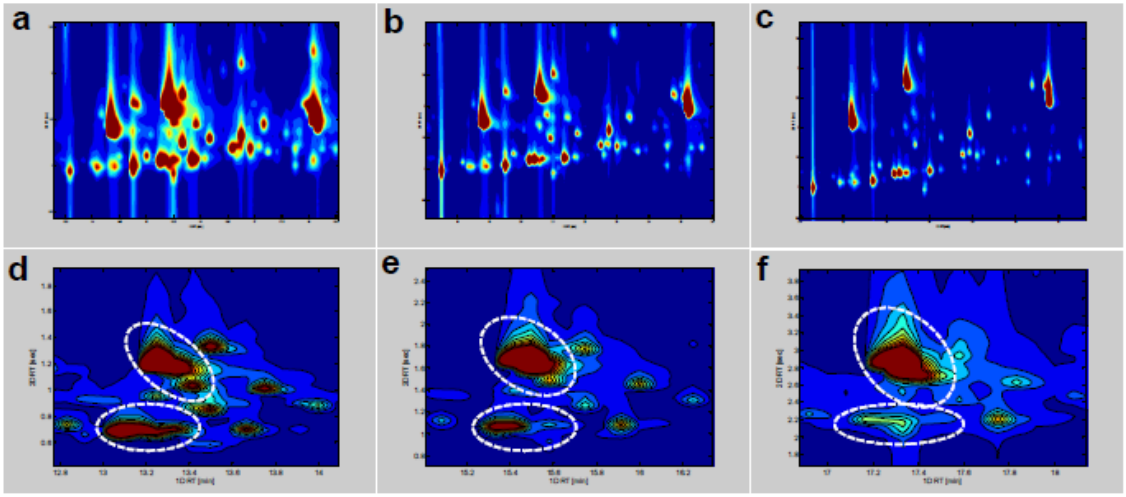

Fig. S7 Illustration of the effect of oven ramping rate and carrier gas flow rate on the GC×GC separation of honeybush tea volatiles. The effect of the oven ramping rate is illustrated for selected parts of the GC×GC-FID contour plots at a flow rate of 2.06 mL/min in (a) 5.5°C/min, (b) 3°C/min and (c) 2°C/min. The effect of flow rate is shown at 5.5°C/min (d) 151.7 kPa (u_{1D} = 39.4 cm/sec, u_{2D} = 191 cm/sec), (e) 100 kPa (u_{1D} = 24.4 cm/sec, u_{2D} = 103 cm/sec), and (f) 75 kPa (u_{1D}= 20.4 cm/sec, u_{2D}=79.6 cm/sec). Analyses were performed on PDMS × Stabilwax column set; SPME fibre = PDMS/DVB. Other chromatographic conditions are as specified in Section 2.5.1

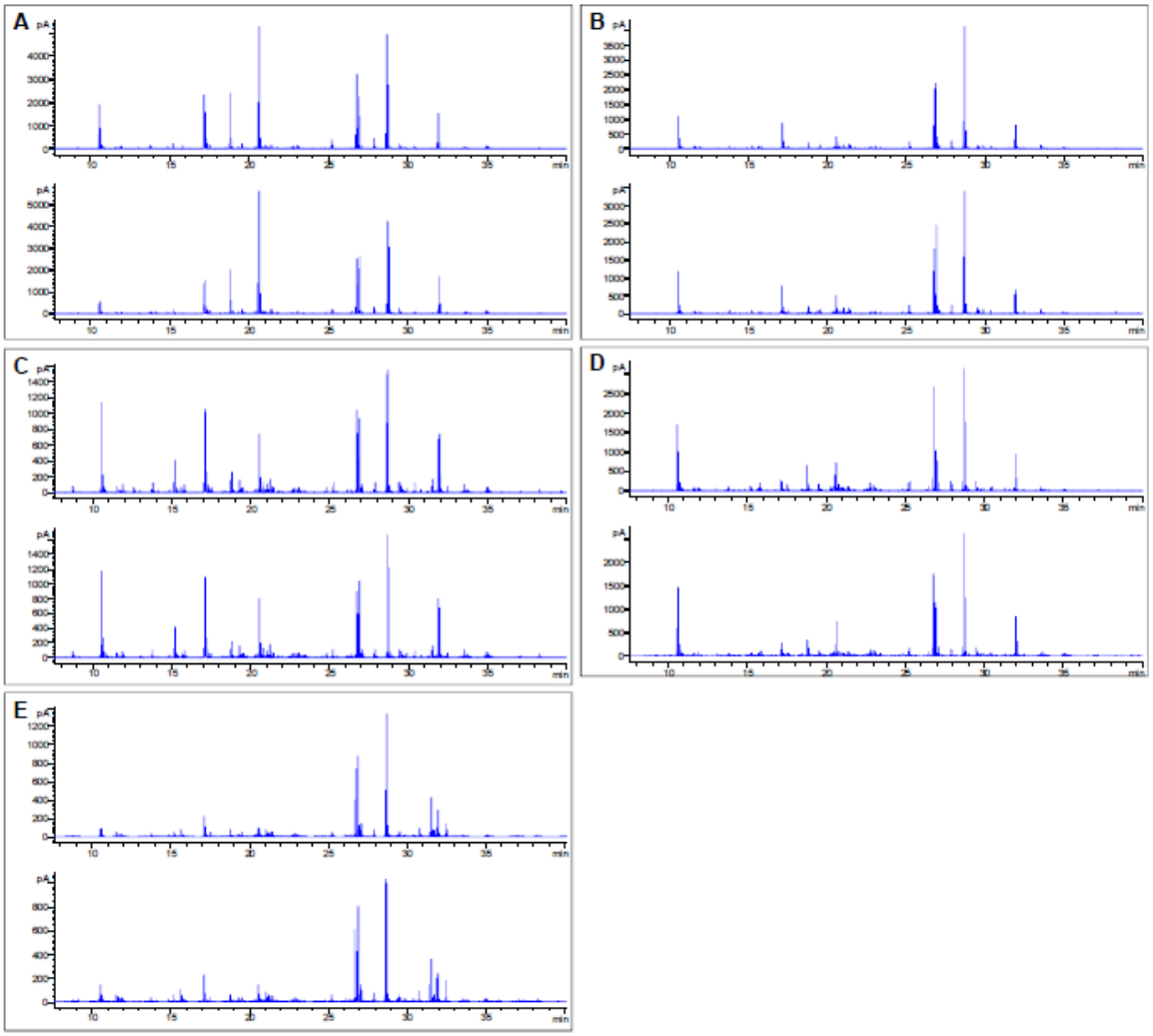

Fig. S8 Raw chromatograms obtained for the duplicate analyses of *C. subternata* samples (A) SUB-B8, (B) SUB-B4, (C) SUB-B6, (D) SUB-B3 and (E) SUB-B5 illustrate the differences between the samples of the same species and the reproducibility of duplicate analyses of the same sample

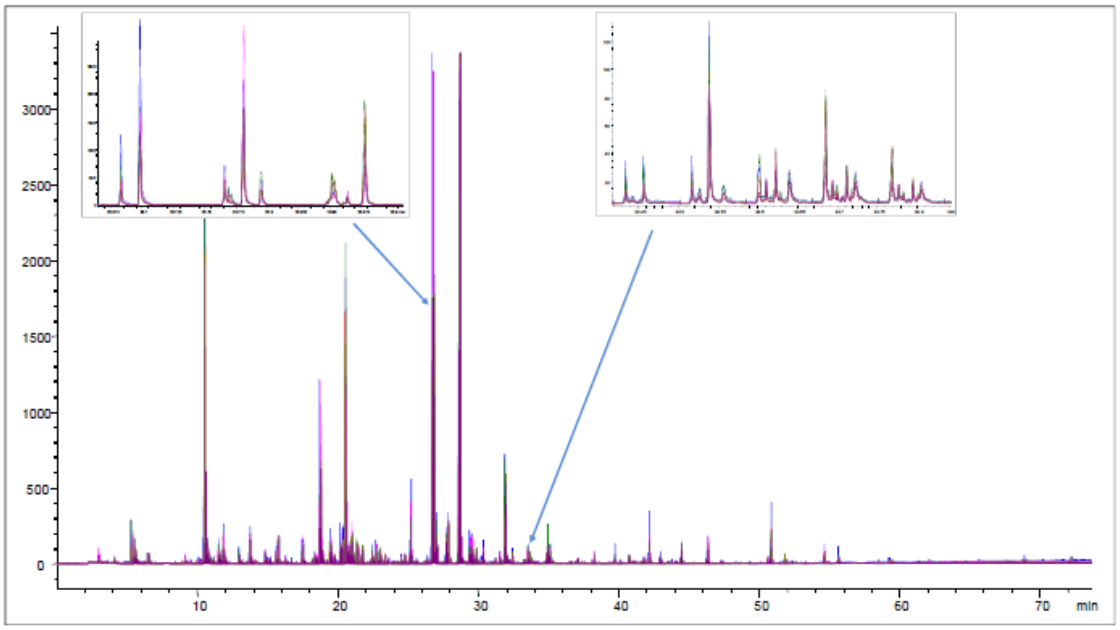

Fig. S9 Representative chromatograms of *C. genistoides* obtained for the inter-day repeatability study (n = 6)

Appendix B

Supplementary materials from section 4.2

Within-run - Full Width at Half Height (FWHH)

N=10 Replicates	LN_2 Modulator				Uof Waterloo Modulator			
Name	**^{1}D Retention Time (s)**	**^{2}D Retention Time (s)**	**FWHH Avg. (s)**	**FWHH Std. Deviation (s)**	**^{1}D Retention Time (s)**	**^{2}D Retention Time (s)**	**FWHH Avg. (s)**	**FWHH Std. Deviation (s)**
PCB4/PCB10	884	0.240	0.151	0.001	879	0.124	0.192	0.004
PCB6	960	0.524	0.164	0.001	952	0.568	0.207	0.003
PCB8	972	0.660	0.169	0.001	964	0.776	0.215	0.004
PCB15	1072	1.346	0.189	0.001	1061	1.854	0.245	0.003
PCB16	1108	1.014	0.174	0.001	1171	1.450	0.233	0.020
PCB18	1064	0.844	0.172	0.001	1058	1.028	0.223	0.005
PCB19	1012	0.718	0.168	0.001	1205	1.308	0.236	0.031
PCB22	1212	1.506	0.183	0.001	1202	2.004	0.240	0.003
PCB28/PCB31	1176	1.384	0.189	0.001	1164	1.870	0.268	0.013
PCB33	1196	1.310	0.182	0.002	1188	1.682	0.237	0.003
PCB37	1312	2.046	0.211	0.000	1342	2.156	0.250	0.004
PCB40	1352	1.678	0.188	0.001	1342	2.156	0.250	0.004
PCB41	1336	1.602	0.185	0.001	1326	2.048	0.245	0.003
PCB44	1304	1.522	0.187	0.001	1297	1.952	0.258	0.012
PCB49	1272	1.384	0.186	0.001	1261	1.850	0.245	0.004
PCB52	1260	1.344	0.182	0.001	1250	1.816	0.246	0.005
PCB54	1136	1.108	0.178	0.001	1129	1.324	0.235	0.006
PCB66	1412	1.926	0.209	0.002	1402	2.604	0.273	0.011

PCB70	1407	1.857	0.182	0.005	1394	2.538	0.279	0.007
PCB74*	n/a	n/a	n/a	n/a	1383	2.572	0.249	0.022
PCB77	1560	2.536	0.219	0.001	1548	3.460	0.300	0.004
PCB81	1536	2.434	0.214	0.016	1526	3.288	0.295	0.004
PCB84	1464	1.872	0.198	0.006	1455	2.398	0.266	0.004
PCB85	1548	2.086	0.218	0.009	1538	2.770	0.284	0.017
PCB87	1536	2.028	0.199	0.006	1528	2.638	0.265	0.005
PCB90/PCB101	1479	1.712	0.191	0.003	1467	2.306	0.254	0.004
PCB95	1416	1.664	0.234	0.018	1406	2.186	0.267	0.022
PCB97	1528	1.844	0.200	0.015	1518	2.394	0.260	0.004
PCB99**	1488	1.790	0.205	0.004	1485	2.354	0.258	0.010
PCB104	1300	1.310	0.182	0.001	1291	1.638	0.246	0.004
PCB105	1688	2.578	0.210	0.000	1678	3.360	0.281	0.003
PCB110	1564	2.044	0.198	0.000	1553	2.676	0.266	0.006
PCB114	n/a	n/a	n/a	n/a	1646	3.124	0.322	0.028
PCB118	1632	2.276	0.206	0.001	1620	3.066	0.288	0.009
PCB119	1508	1.822	0.192	0.001	1498	2.392	0.258	0.004
PCB123	1624	2.204	0.202	0.001	1614	2.904	0.275	0.005
PCB126	1776	2.828	0.222	0.001	1764	3.782	0.308	0.005
PCB128	1816	2.620	0.211	0.000	1806	3.324	0.285	0.004
PCB129	1776	2.252	0.201	0.001	1765	2.812	0.270	0.005
PCB135	1612	1.842	0.196	0.000	1601	2.344	0.265	0.009
PCB137	1739	2.184	0.219	0.017	1727	2.796	0.273	0.004
PCB138	1756	2.306	0.203	0.001	1746	2.936	0.276	0.004
PCB141	1724	2.128	0.197	0.001	1714	2.710	0.266	0.003
PCB149	1628	1.906	0.212	0.003	1619	2.440	0.267	0.003
PCB151	1603	1.848	0.196	0.001	1593	2.372	0.326	0.072
PCB153	1696	2.012	0.199	0.001	1661	2.546	0.269	0.009
PCB155	1460	1.452	0.184	0.001	1493	2.002	0.256	0.017
PCB156	1884	2.728	0.224	0.001	1872	3.560	0.307	0.008

PCB157	1892	2.774	0.216	0.001	1869	3.496	0.291	0.006
PCB158	1764	2.342	0.204	0.000	1689	2.832	0.270	0.014
PCB167* **	1832	2.500	0.210	0.001	n/a	n/a	n/a	n/a
PCB168	1704	1.932	0.195	0.001	1693	2.484	0.265	0.005
PCB169	1980	3.054	0.225	0.001	1993	3.718	0.302	0.005
PCB170	1996	2.676	0.213	0.001	1985	3.322	0.289	0.004
PCB174	1860	2.206	0.200	0.000	1850	2.708	0.270	0.004
PCB177	1872	2.382	0.207	0.001	1862	2.966	0.278	0.004
PCB178	1788	1.990	0.197	0.001	1778	2.478	0.267	0.004
PCB180	1932	2.390	0.205	0.001	1911	2.978	0.276	0.005
PCB183	1820	2.088	0.198	0.001	1821	2.622	0.268	0.003
PCB187	1808	2.038	0.198	0.001	1786	2.518	0.270	0.005
PCB188	1680	1.784	0.201	0.001	1722	2.386	0.268	0.015
PCB189	2072	2.918	0.217	0.001	1916	3.292	0.281	0.034
PCB191	1952	2.386	0.206	0.001	1845	2.798	0.270	0.020
PCB193	1940	2.360	0.204	0.000	1931	2.956	0.277	0.004
PCB194	2160	2.718	0.213	0.001	2149	3.360	0.293	0.005
PCB199	2028	2.314	0.204	0.001	2020	2.782	0.275	0.002
PCB200	1960	2.336	0.203	0.001	1952	2.750	0.273	0.006
PCB201	1908	2.110	0.200	0.000	1900	2.512	0.269	0.005
PCB202	1888	2.064	0.202	0.001	1881	2.450	0.272	0.009
PCB203	2044	2.378	0.203	0.001	2032	2.898	0.278	0.005
PCB205	2176	2.758	0.213	0.001	2166	3.398	0.292	0.002
PCB206	2254	2.624	0.218	0.007	2245	3.152	0.288	0.005
PCB207	2132	2.394	0.204	0.001	2124	2.778	0.274	0.003
PCB208	2116	2.300	0.202	0.001	2106	2.676	0.273	0.006
PCB209	2328	2.596	0.210	0.000	2322	2.942	0.288	0.006
HCB	996	0.854	0.163	0.001	989	0.938	0.204	0.005
HCBD	536	2.744	0.117	0.001	n/a	n/a	n/a	n/a
HCE	417	2.768	0.118	0.002	n/a	n/a	n/a	n/a

1,2,3,4-TCB	656	3.426	0.131	0.000	654	2.920	0.155	0.005
1,2,3,5-/1,2,4,5-TCB	620	3.206	0.129	0.001	616	2.606	0.158	0.004
1,2,3-TCB	522	3.038	0.127	0.001	520	2.452	0.153	0.017
1,2,4-TCB	495	3.000	0.130	0.002	492	2.428	0.163	0.031
1,3,5-TBB	696	3.650	0.136	0.002	692	3.214	0.159	0.004
1,3,5-TCB	461	2.910	0.125	0.002	458	2.330	0.161	0.009
2,3,6-TCT	600	3.114	0.128	0.001	599	2.528	0.154	0.008
2,4,5-TCT	592	3.092	0.127	0.001	590	2.516	0.157	0.006
P5CB	793	0.020	0.145	0.002	784	3.770	0.174	0.004
A2,6-TCT	628	3.286	0.129	0.002	625	2.738	0.151	0.007
A-BHC	957	0.950	0.163	0.001	950	1.166	0.210	0.005
G-BHC	1024	1.300	0.174	0.001	1016	1.704	0.223	0.005
A-CHLA**	1496	1.940	0.193	0.001	1485	2.354	0.258	0.010
Oxy-CHLA	1408	1.624	0.213	0.012	1397	1.920	0.241	0.007
Aldrin	1312	1.354	0.177	0.001	1302	1.480	0.224	0.003
Endrin	1596	2.638	0.208	0.001	1586	3.142	0.270	0.002
Dieldrin	1548	2.364	0.238	0.012	1541	2.820	0.295	0.040
Endos 1	1488	2.184	0.198	0.001	1477	2.630	0.286	0.025
Endos 2	1604	3.482	0.234	0.001	1699	0.856	0.334	0.003
Endos S	1705	3.680	0.240	0.001	1699	0.856	0.334	0.003
Heptachlor	1224	1.206	0.172	0.001	1214	1.370	0.224	0.004
OCSTYR	1402	1.186	0.172	0.001	1393	1.372	0.220	0.004
Trans-Nonachlor	1516	1.826	0.195	0.011	1506	2.226	0.255	0.003
o,p'-DDT	1660	1.960	0.196	0.003	1651	2.452	0.289	0.007
p,p'-DDD	1640	2.522	0.206	0.004	1628	3.520	0.290	0.007
p,p'-DDE	1548	1.840	0.233	0.010	1537	2.510	0.284	0.018
p,p'-DDT	1744	2.380	0.208	0.011	1733	3.128	0.285	0.013
Mirex	2000	3.436	0.239	0.001	1971	0.046	0.317	0.004
p-Mirex***	1832	2.990	0.223	0.007	n/a	n/a	n/a	n/a

G-CHLA/PCB60*	1452	2.182	0.204	0.001	1442	2.838	0.276	0.005
DMDT/PCB171	1880	2.416	0.270	0.003	1872	3.020	0.303	0.009
Cis-Nonachlor/PCB114	1660	2.356	0.205	0.001	n/a	n/a	n/a	n/a
H-Epoxide/PCB74	1396	1.840	0.195	0.001	n/a	n/a	n/a	n/a
H-Epoxide	n/a	n/a	n/a	n/a	1386	2.244	0.295	0.018
Cis-Nonachlor	n/a	n/a	n/a	n/a	1650	2.894	0.295	0.026
PCB99/Alpha-Chlordane	n/a	n/a	n/a	n/a	1485	2.354	0.258	0.010
PCB167/Photo-Mirex	n/a	n/a	n/a	n/a	1810	3.242	0.293	0.011

*PCB74/H-epoxide coelutopn - LN2 modulator

**PCB99/alpha-chlordane coelution - new modulator

***PCB167/photo-Mirex coelution - new modulator

Within-run - Peak Heights

N=10 Replicates	**LN_2 Modulator**		**Uof Waterloo Modulator**	
Name	**Avg.**	**Std. Deviation**	**Avg.**	**Std. Deviation**
PCB4/PCB10	7.28E+04	1.87E+03	8.29E+04	5.17E+03
PCB6	4.71E+04	1.41E+03	5.68E+04	3.17E+03
PCB8	5.43E+04	1.60E+03	6.42E+04	3.51E+03

PCB15	1.63E+04	5.90E+02	2.00E+04	7.63E+02
PCB16	8.21E+04	1.55E+03	1.37E+05	1.38E+05
PCB18	5.89E+04	1.19E+03	6.64E+04	4.31E+03
PCB19	4.92E+04	3.81E+03	1.08E+05	1.04E+05
PCB22	1.45E+05	4.01E+03	1.68E+05	8.23E+03
PCB28/PCB31	2.16E+05	6.33E+03	2.28E+05	1.45E+04
PCB33	9.96E+04	2.54E+03	1.13E+05	5.03E+03
PCB37	4.06E+04	1.63E+03	1.57E+05	9.01E+03
PCB40	1.35E+05	2.75E+03	1.57E+05	9.01E+03
PCB41	1.33E+05	3.15E+03	1.49E+05	7.99E+03
PCB44	7.51E+04	4.59E+03	1.43E+05	9.15E+03
PCB49	9.37E+04	9.71E+02	1.10E+05	6.90E+03
PCB52	8.05E+04	1.76E+03	9.12E+04	4.48E+03
PCB54	4.80E+04	3.14E+03	5.69E+04	3.93E+03
PCB66	9.50E+04	1.43E+04	1.51E+05	8.50E+03
PCB70	1.12E+05	2.88E+04	1.37E+05	9.22E+03
PCB74*	n/a	n/a	1.63E+05	1.54E+04
PCB77	6.82E+04	2.75E+03	7.89E+04	2.37E+03
PCB81	8.46E+04	1.06E+04	1.09E+05	4.12E+03
PCB84	1.20E+05	1.33E+04	1.41E+05	8.27E+03
PCB85	1.87E+05	2.86E+04	2.31E+05	7.81E+04
PCB87	1.82E+05	6.88E+03	2.21E+05	1.41E+04
PCB90/PCB101	2.53E+05	2.82E+04	3.14E+05	1.66E+04
PCB95	1.19E+05	4.91E+04	1.16E+05	9.93E+03
PCB97	1.28E+05	1.40E+04	1.54E+05	7.83E+03
PCB99**	5.41E+04	4.03E+04	5.28E+05	5.78E+04
PCB104	7.36E+04	1.93E+03	8.90E+04	4.71E+03
PCB105	2.14E+05	7.30E+03	2.44E+05	1.13E+04
PCB110	1.75E+05	3.51E+03	2.48E+05	1.17E+04
PCB114	n/a	n/a	2.88E+05	4.62E+04

PCB118	1.37E+05	4.23E+03	1.66E+05	7.21E+03
PCB119	1.78E+05	7.05E+03	2.02E+05	1.33E+04
PCB123	1.64E+05	5.50E+03	1.79E+05	1.37E+04
PCB126	1.10E+05	5.24E+03	1.30E+05	3.75E+03
PCB128	2.25E+05	6.90E+03	2.73E+05	1.22E+04
PCB129	2.05E+05	5.48E+03	2.41E+05	1.11E+04
PCB135	1.27E+05	2.70E+03	1.53E+05	7.27E+03
PCB137	2.25E+05	6.50E+03	2.63E+05	1.40E+04
PCB138	1.90E+05	6.29E+03	2.19E+05	1.12E+04
PCB141	2.54E+05	7.29E+03	2.94E+05	1.47E+04
PCB149	1.12E+05	2.56E+03	1.53E+05	9.52E+03
PCB151	1.29E+05	3.24E+03	1.75E+05	1.69E+04
PCB153	1.61E+05	1.57E+04	1.80E+05	2.86E+04
PCB155	1.09E+05	2.40E+03	1.48E+05	5.64E+04
PCB156	2.49E+05	1.40E+04	2.94E+05	1.40E+04
PCB157	2.17E+05	8.44E+03	2.76E+05	1.39E+04
PCB158	2.43E+05	7.62E+03	2.77E+05	6.54E+04
PCB167* **	1.89E+05	6.67E+03	n/a	n/a
PCB168	1.70E+05	1.52E+04	2.11E+05	2.99E+04
PCB169	1.63E+05	9.44E+03	2.24E+05	1.29E+04
PCB170	2.53E+05	9.88E+03	2.95E+05	1.20E+04
PCB174	1.93E+05	5.71E+03	2.26E+05	1.08E+04
PCB177	1.83E+05	5.95E+03	2.20E+05	1.11E+04
PCB178	1.69E+05	4.05E+03	1.96E+05	1.05E+04
PCB180	2.61E+05	9.99E+03	2.60E+05	1.94E+04
PCB183	2.04E+05	6.06E+03	2.29E+05	1.74E+04
PCB187	1.75E+05	5.66E+03	1.87E+05	2.09E+04
PCB188	1.33E+05	3.17E+03	1.73E+05	4.02E+04
PCB189	3.00E+05	1.49E+04	2.40E+05	7.28E+04
PCB191	2.87E+05	1.12E+04	2.85E+05	7.85E+04

PCB193	2.49E+05	9.29E+03	2.56E+05	2.83E+04
PCB194	3.22E+05	1.45E+04	3.07E+05	1.29E+04
PCB199	2.35E+05	8.92E+03	2.38E+05	1.02E+04
PCB200	2.42E+05	7.05E+03	2.78E+05	1.46E+04
PCB201	1.71E+05	4.65E+03	1.90E+05	1.09E+04
PCB202	1.49E+05	4.19E+03	1.65E+05	8.87E+03
PCB203	3.42E+05	1.16E+04	3.07E+05	1.34E+04
PCB205	3.26E+05	1.58E+04	2.84E+05	1.19E+04
PCB206	3.25E+05	1.60E+04	3.11E+05	1.51E+04
PCB207	3.05E+05	9.38E+03	2.76E+05	1.21E+04
PCB208	2.75E+05	9.37E+03	2.46E+05	1.06E+04
PCB209	2.70E+05	1.21E+04	2.32E+05	1.18E+04
HCB	3.98E+05	8.26E+03	3.79E+05	2.38E+04
HCBD	7.69E+05	1.10E+04	n/a	n/a
HCE	8.43E+05	2.44E+04	n/a	n/a
1,2,3,4-TCB	2.27E+05	5.55E+03	2.40E+05	1.59E+04
1,2,3,5-/1,2,4,5-TCB	2.70E+05	1.69E+04	2.84E+05	3.50E+04
1,2,3-TCB	1.28E+05	3.91E+03	1.25E+05	1.81E+04
1,2,4-TCB	7.12E+04	1.42E+03	7.02E+04	9.12E+03
1,3,5-TBB	5.23E+05	1.44E+04	5.23E+05	5.04E+04
1,3,5-TCB	8.62E+04	1.98E+03	7.01E+04	1.73E+04
2,3,6-TCT	1.15E+05	2.58E+03	1.13E+05	1.17E+04
2,4,5-TCT	6.62E+04	3.38E+03	6.94E+04	5.96E+03
P5CB	3.16E+05	4.78E+04	3.73E+05	2.76E+04
A2,6-TCT	3.68E+05	1.23E+04	3.98E+05	4.25E+04
A-BHC	5.06E+05	9.33E+03	5.71E+05	3.91E+04
G-BHC	4.08E+05	9.80E+03	4.69E+05	3.23E+04
A-CHLA**	3.44E+05	4.47E+03	5.28E+05	5.78E+04
Oxy-CHLA	2.79E+05	7.93E+03	3.59E+05	2.40E+04
Aldrin	4.47E+05	6.65E+03	5.18E+05	3.49E+04

Endrin	1.47E+05	1.68E+04	1.46E+05	3.85E+04
Dieldrin	3.08E+05	7.69E+03	3.50E+05	5.34E+04
Endos 1	2.65E+05	1.29E+04	3.84E+05	3.50E+04
Endos 2	2.10E+05	9.62E+03	2.38E+05	1.20E+04
Endos S	2.14E+05	4.39E+03	2.38E+05	1.20E+04
Heptachlor	2.96E+05	1.07E+04	2.75E+05	2.38E+04
OCSTYR	4.32E+05	8.84E+03	5.09E+05	3.10E+04
Trans-Nonachlor	2.98E+05	4.71E+04	3.99E+05	2.59E+04
o,p'-DDT	1.53E+05	5.75E+03	1.60E+05	7.66E+03
p,p'-DDD	2.45E+05	4.82E+03	2.75E+05	1.14E+04
p,p'-DDE	3.43E+05	7.07E+03	4.00E+05	2.79E+04
p,p'-DDT	1.90E+05	3.32E+04	1.46E+05	1.29E+04
Mirex	1.68E+05	3.27E+03	1.55E+05	2.82E+03
p-Mirex* **	1.78E+05	3.72E+03	n/a	n/a
G-CHLA/PCB60*	5.38E+05	9.20E+03	6.35E+05	3.38E+04
DMDT/PCB171	2.32E+05	7.62E+03	2.88E+05	8.64E+03
Cis-Nonachlor/PCB114	6.04E+05	1.32E+04	n/a	n/a
H-Epoxide/PCB74	4.51E+05	7.61E+03	n/a	n/a
H-Epoxide	n/a	n/a	4.38E+05	2.55E+04
Cis-Nonachlor	n/a	n/a	3.72E+05	4.87E+04
PCB99/Alpha-Chlordane	n/a	n/a	5.28E+05	5.78E+04
PCB167/Photo-Mirex	n/a	n/a	4.80E+05	9.08E+04

*PCB74/H-epoxide coelutopn - LN_2 modulator

**PCB99/alpha-chlordane coelution - new modulator

***PCB167/photo-Mirex coelution - new modulator

Name	LN_2 Modulator (N=9)				Univ. of Waterloo Modulator (N=5)			
	Avg. (ng/mL)	Std. Deviation	%RSD	IDL (ng/mL)	Avg. (ng/mL)	Std. Deviation	%RSD	IDL (ng/mL)
PCB4/PCB10	1.99	0.10	4.85	0.29	1.90	0.06	3.14	0.18
PCB6	0.97	0.10	10.17	0.30	0.99	0.18	18.32	0.55
PCB8	0.95	0.05	5.77	0.16	0.81	0.09	11.33	0.28
PCB15	1.07	0.08	7.79	0.25	0.78	0.11	14.45	0.34
PCB16	1.06	0.03	3.13	0.10	1.02	0.04	3.62	0.11
PCB18	1.05	0.02	1.99	0.06	0.89	0.05	5.15	0.14
PCB19	1.06	0.02	1.89	0.06	0.86	0.12	14.24	0.37
PCB22	0.90	0.03	3.14	0.08	1.07	0.04	3.74	0.12
PCB28/PCB31	1.78	0.03	1.08	0.08	2.07	0.07	3.26	0.20
PCB33	0.89	0.05	5.42	0.14	1.03	0.07	6.43	0.20
PCB37	1.01	0.11	11.14	0.34	1.04	0.06	6.12	0.19
PCB40	1.01	0.04	3.95	0.12	1.04	0.06	6.12	0.19
PCB41	1.08	0.03	3.23	0.10	1.03	0.03	2.87	0.09
PCB44	0.94	0.06	6.02	0.17	1.10	0.06	5.89	0.19
PCB49	0.88	0.05	5.27	0.14	0.96	0.07	7.27	0.21
PCB52	0.94	0.12	12.50	0.35	1.04	0.07	6.56	0.20
PCB54	1.06	0.09	8.34	0.26	0.90	0.04	3.95	0.11
PCB66	0.98	0.04	3.82	0.11	1.01	0.04	4.39	0.13
PCB70	0.98	0.07	7.17	0.21	0.96	0.05	5.37	0.16
PCB74*	n/a	n/a	n/a	n/a	1.17	0.01	1.15	0.04
PCB77	1.01	0.04	3.91	0.12	1.01	0.11	11.03	0.34
PCB81	1.14	0.05	4.09	0.14	1.05	0.09	8.69	0.27
PCB84	0.97	0.04	3.63	0.11	1.01	0.04	4.05	0.12
PCB85	1.04	0.02	1.52	0.05	0.97	0.07	6.87	0.20
PCB87	1.07	0.07	6.13	0.20	1.25	0.03	2.36	0.09
PCB90/PCB101	2.04	0.11	5.40	0.33	2.12	0.03	1.31	0.08
PCB95	1.09	0.05	4.81	0.16	1.05	0.04	3.95	0.12
PCB97	1.07	0.07	6.13	0.20	1.03	0.08	7.39	0.23
PCB99**	n/a	n/a	n/a	n/a	2.18	0.07	3.40	0.22
PCB104	0.94	0.06	5.95	0.17	0.86	0.06	7.03	0.18
PCB105	0.98	0.03	3.47	0.10	1.10	0.04	3.39	0.11

PCB110	0.97	0.03	3.03	0.09	0.99	0.04	3.57	0.11
PCB114	n/a	n/a	n/a	n/a	0.92	0.12	12.78	0.35
PCB118	1.07	0.03	3.02	0.10	1.12	0.23	20.10	0.68
PCB119	1.06	0.03	2.75	0.09	1.10	0.10	8.72	0.29
PCB123	1.00	0.04	3.99	0.12	1.09	0.29	26.26	0.86
PCB126	1.11	0.02	2.25	0.07	0.96	0.04	3.81	0.11
PCB128	0.91	0.05	5.63	0.15	1.05	0.02	2.23	0.07
PCB129	1.15	0.03	2.30	0.08	1.05	0.02	2.07	0.07
PCB135	1.11	0.05	4.20	0.14	0.95	0.14	14.30	0.41
PCB137	1.13	0.04	3.79	0.13	1.10	0.01	1.11	0.04
PCB138	1.12	0.03	2.36	0.08	0.93	0.04	4.30	0.12
PCB141	1.06	0.03	3.26	0.10	1.03	0.01	1.10	0.03
PCB149	0.98	0.03	3.28	0.10	1.05	0.03	3.11	0.10
PCB151	0.92	0.03	3.38	0.09	1.03	0.10	9.95	0.31
PCB153	1.00	0.04	4.08	0.12	0.89	0.04	4.63	0.12
PCB155	1.01	0.03	3.43	0.10	1.02	0.07	6.39	0.20
PCB156	1.05	0.05	4.47	0.14	1.10	0.01	1.11	0.04
PCB157	1.03	0.05	4.81	0.15	1.19	0.02	1.75	0.06
PCB158	1.09	0.03	2.54	0.08	1.09	0.03	2.93	0.10
PCB167* **	1.00	0.03	2.54	0.08	n/a	n/a	n/a	n/a
PCB168	0.98	0.05	4.60	0.14	1.17	0.04	3.28	0.12
PCB169	1.08	0.04	3.89	0.13	1.06	0.03	3.22	0.10
PCB170	1.13	0.03	3.05	0.10	1.06	0.02	1.63	0.05
PCB174	1.10	0.03	2.44	0.08	1.05	0.05	4.76	0.15
PCB177	1.20	0.05	4.44	0.16	0.98	0.03	2.83	0.08
PCB178	1.07	0.11	10.40	0.33	0.93	0.06	6.18	0.17
PCB180	1.07	0.04	3.67	0.12	0.94	0.03	2.76	0.08
PCB183	0.96	0.03	3.06	0.09	1.01	0.02	2.38	0.07
PCB187	1.15	0.02	2.06	0.07	0.97	0.06	6.44	0.19
PCB188	0.98	0.06	5.78	0.17	0.95	0.07	7.73	0.22
PCB189	1.08	0.03	2.38	0.08	1.12	0.03	2.66	0.09
PCB191	1.07	0.06	5.37	0.17	1.08	0.02	1.73	0.06
PCB193	no data	no data	no data	no data	1.11	0.04	3.28	0.11
PCB194	1.08	0.03	3.02	0.10	1.05	0.03	2.56	0.08
PCB199	1.01	0.03	3.15	0.10	1.04	0.05	4.57	0.14
PCB200	1.07	0.03	2.82	0.09	1.06	0.06	5.94	0.19
PCB201	0.99	0.02	2.52	0.07	1.00	0.03	2.87	0.09
PCB202	1.04	0.04	3.38	0.11	0.91	0.05	5.10	0.14
PCB203	0.99	0.03	3.10	0.09	1.08	0.01	1.25	0.04
PCB205	1.12	0.03	2.56	0.09	1.10	0.09	8.05	0.26
PCB206	1.02	0.11	11.02	0.34	1.00	0.03	3.32	0.10

PCB207	1.05	0.03	2.95	0.09	1.06	0.03	2.50	0.08
PCB208	1.14	0.03	2.58	0.09	1.04	0.03	2.88	0.09
PCB209	1.05	0.02	2.06	0.07	1.13	0.02	1.45	0.05
HCB	0.83	0.03	3.24	0.08	1.11	0.02	1.76	0.06
HCBD	1.10	0.04	4.04	0.13	n/a	n/a	n/a	n/a
HCE	1.21	0.14	11.33	0.41	n/a	n/a	n/a	n/a
1,2,3,4-TCB	1.09	0.09	8.31	0.27	1.07	0.09	8.00	0.26
1,2,3,5-/1,2,4,5-TCB	1.86	0.09	4.97	0.28	2.09	0.06	3.11	0.19
1,2,3-TCB	1.05	0.15	14.06	0.44	0.89	0.04	5.06	0.13
1,2,4-TCB	0.92	0.10	11.28	0.31	0.68	0.15	21.78	0.45
1,3,5-TBB	1.00	0.02	1.96	0.06	1.08	0.03	3.14	0.10
1,3,5-TCB	1.05	0.12	10.99	0.35	1.31	0.19	14.62	0.57
2,3,6-TCT	1.19	0.09	7.66	0.27	0.81	0.06	7.78	0.19
2,4,5-TCT	0.90	0.04	4.84	0.13	0.98	0.14	14.71	0.43
P5CB	0.87	0.06	6.38	0.17	1.14	0.02	1.92	0.07
A2,6-TCT	0.85	0.03	3.05	0.08	1.09	0.09	8.53	0.28
A-BHC	0.89	0.04	4.11	0.11	1.30	0.02	1.54	0.06
G-BHC	0.77	0.01	1.52	0.04	1.20	0.06	5.33	0.19
A-CHLA**	1.00	0.03	3.14	0.09	2.18	0.07	3.40	0.22
Oxy-CHLA	1.03	0.02	2.05	0.07	1.05	0.08	7.65	0.24
Aldrin	1.05	0.03	3.14	0.10	1.21	0.04	3.22	0.12
Endrin	1.10	0.02	1.42	0.05	1.30	0.05	3.67	0.14
Dieldrin	0.97	0.03	2.80	0.09	1.05	0.08	7.70	0.24
Endos 1	0.94	0.02	2.22	0.06	1.19	0.02	2.09	0.07
Endos 2	0.99	0.03	2.71	0.08	1.16	0.11	9.65	0.34
Endos S	0.74	0.03	3.17	0.09	1.16	0.11	9.65	0.34
Heptachlor	0.85	0.02	2.71	0.06	1.08	0.34	31.55	1.02
OCSTYR	0.86	0.02	2.03	0.05	1.15	0.04	3.10	0.11
Trans-Nonachlor	0.98	0.02	1.88	0.05	1.11	0.06	4.98	0.17
o,p'-DDT	1.31	0.04	4.02	0.12	0.99	0.17	17.05	0.51
p,p'-DDD	0.87	0.14	10.76	0.42	1.17	0.02	2.04	0.07
p,p'-DDE	1.02	0.04	4.17	0.11	1.23	0.03	2.42	0.09
p,p'-DDT	1.40	0.02	2.43	0.07	1.17	0.10	8.74	0.31
Mirex	0.82	0.05	3.50	0.15	1.08	0.09	8.39	0.27
p-Mirex***	0.97	0.02	1.97	0.05	n/a	n/a	n/a	n/a
G-CHLA/PCB60*	2.21	0.05	2.40	0.16	2.12	0.02	0.71	0.05
DMDT/PCB171	2.01	0.03	1.73	0.10	2.35	0.12	5.08	0.36

Cis-Nonachlor/PCB114	1.89	0.06	3.26	0.17	n/a	n/a	n/a	n/a
H-Epoxide/PCB74	1.96	0.04	1.81	0.10	n/a	n/a	n/a	n/a
H-Epoxide	n/a	n/a	n/a	n/a	1.19	0.03	2.40	0.09
Cis-Nonachlor	n/a	n/a	n/a	n/a	1.02	0.12	12.09	0.37
PCB99/Alpha-Chlordane	n/a	n/a	n/a	n/a	2.18	0.07	3.40	0.22
PCB167/Photo-Mirex	n/a	n/a	n/a	n/a	2.13	0.05	2.44	0.16

*PCB74/H-epoxide coelutopn - LN_2modulator

**PCB99/alpha-chlordane coelution - new modulator

***PCB167/photo-Mirex coelution - new modulator

Within-run - Calculated concentration

N=10 Replicates	**Design (ng/mL)**	**LN_2 Modulator**			**Uof Waterloo Modulator**		
Name		**Avg. (ng/mL)**	**%RSD**	**Std. Deviation**	**Avg. (ng/mL)**	**%RSD**	**Std. Deviation**
PCB4/PCB10	40	47.6	7.0	3.4	41.0	2.7	1.1
PCB6	20	23.0	3.9	0.9	20.2	4.0	0.8
PCB8	20	21.2	2.7	0.6	20.3	3.1	0.6
PCB15	20	21.7	7.7	1.7	21.1	5.2	1.1
PCB16	20	21.3	2.2	0.5	21.8	24.6	5.4
PCB18	20	20.4	2.9	0.6	21.1	2.3	0.5
PCB19	20	20.5	8.2	1.7	20.3	6.8	1.4
PCB22	20	19.8	1.2	0.2	19.1	2.7	0.5
PCB28/PCB31	40	41.8	3.8	1.6	38.8	2.6	1.0
PCB33	20	20.1	1.2	0.2	19.7	3.3	0.6
PCB37	20	22.2	5.2	1.1	19.4	2.5	0.5
PCB40	20	22.6	3.2	0.7	19.4	2.5	0.5
PCB41	20	20.9	2.0	0.4	19.3	3.1	0.6
PCB44	20	15.4	11.3	1.7	20.0	7.0	1.4
PCB49	20	20.3	3.0	0.6	19.2	3.9	0.7
PCB52	20	20.5	0.7	0.1	20.1	3.4	0.7
PCB54	20	21.2	7.4	1.6	20.4	4.1	0.8
PCB66	20	19.9	6.6	1.3	19.0	6.6	1.3
PCB70	20	22.0	10.7	2.4	19.8	7.5	1.5
PCB74*	20	n/a	n/a	n/a	20.1	9.2	1.9
PCB77	20	20.6	3.3	0.7	19.1	6.0	1.1

PCB81	20	17.9	2.2	0.4	18.9	4.2	0.8
PCB84	20	23.0	3.0	0.7	19.8	3.0	0.6
PCB85	20	23.2	3.8	0.9	19.6	21.8	4.3
PCB87	20	19.2	4.1	0.8	19.0	4.4	0.8
PCB90/PCB101	40	43.2	1.2	0.5	38.2	2.6	1.0
PCB95	20	18.8	8.7	1.6	19.8	4.4	0.9
PCB97	20	20.0	1.2	0.2	18.9	3.2	0.6
PCB99**	20	17.8	3.7	0.7	n/a	n/a	n/a
PCB104	20	19.1	2.5	0.5	20.0	3.4	0.7
PCB105	20	19.2	1.9	0.4	18.8	3.6	0.7
PCB110	20	19.1	2.5	0.5	20.2	4.3	0.9
PCB114	20	n/a	n/a	n/a	21.3	13.2	2.8
PCB118	20	18.0	5.8	1.0	21.1	5.3	1.1
PCB119	20	20.7	3.3	0.7	21.4	5.7	1.2
PCB123	20	21.4	3.8	0.8	21.4	6.2	1.3
PCB126	20	20.2	4.2	0.8	19.5	5.1	1.0
PCB128	20	19.7	2.0	0.4	18.8	3.7	0.7
PCB129	20	23.1	2.9	0.7	18.4	3.7	0.7
PCB135	20	19.5	15.3	3.0	20.6	6.1	1.3
PCB137	20	22.5	6.3	1.4	19.0	4.7	0.9
PCB138	20	20.2	2.9	0.6	18.8	4.8	0.9
PCB141	20	20.7	3.6	0.7	19.1	3.2	0.6
PCB149	20	19.0	2.4	0.5	18.4	3.2	0.6
PCB151	20	20.3	13.8	2.8	21.2	6.6	1.4
PCB153	20	22.8	7.8	1.8	18.8	12.9	2.4
PCB155	20	20.3	0.6	0.1	19.7	4.1	0.8
PCB156	20	18.9	4.0	0.8	18.4	4.1	0.7
PCB157	20	18.9	2.4	0.5	19.5	4.7	0.9
PCB158	20	20.0	4.0	0.8	19.5	3.9	0.8
PCB167***	20	21.2	3.8	0.8	n/a	n/a	n/a
PCB168	20	17.4	8.0	1.4	20.7	14.1	2.9
PCB169	20	20.6	7.7	1.6	18.3	3.6	0.7
PCB170	20	19.3	2.8	0.5	18.8	3.9	0.7
PCB174	20	20.5	1.7	0.4	19.1	3.0	0.6
PCB177	20	21.2	2.1	0.5	19.3	3.1	0.6
PCB178	20	21.8	2.6	0.6	20.6	2.6	0.5
PCB180	20	21.7	4.6	1.0	19.0	6.9	1.3
PCB183	20	20.6	2.0	0.4	19.5	6.6	1.3
PCB187	20	21.9	2.3	0.5	19.3	3.2	0.6
PCB188	20	20.5	2.5	0.5	19.2	4.0	0.8
PCB189	20	20.9	6.6	1.4	18.5	4.0	0.8
PCB191	20	21.5	3.6	0.8	19.0	8.5	1.6
PCB193	20	21.2	2.7	0.6	18.9	3.9	0.7
PCB194	20	21.7	6.5	1.4	18.7	3.7	0.7
PCB199	20	21.4	4.3	0.9	18.8	2.8	0.5
PCB200	20	20.8	2.1	0.4	20.1	2.3	0.5
PCB201	20	21.8	2.5	0.5	20.1	2.8	0.6

PCB202	20	21.5	1.9	0.4	19.6	3.3	0.7
PCB203	20	23.7	4.8	1.1	19.0	3.3	0.6
PCB205	20	20.3	6.2	1.2	18.9	3.2	0.6
PCB206	20	21.8	7.9	1.7	19.4	3.6	0.7
PCB207	20	23.4	5.3	1.2	18.8	3.1	0.6
PCB208	20	22.1	5.1	1.1	18.8	3.1	0.6
PCB209	20	20.7	6.9	1.4	18.7	4.2	0.8
HCB	20	22.3	3.4	0.8	19.8	5.8	1.1
HCBD	20	23.2	3.2	0.7	n/a	n/a	n/a
HCE	20	22.2	4.3	1.0	n/a	n/a	n/a
1,2,3,4-TCB	20	21.3	3.7	0.8	21.0	4.7	1.0
1,2,3,5-/1,2,4,5-TCB	40	39.9	6.3	2.5	40.5	6.4	2.6
1,2,3-TCB	20	21.8	3.3	0.7	20.6	4.4	0.9
1,2,4-TCB	20	22.6	2.0	0.4	19.7	6.7	1.3
1,3,5-TBB	20	21.9	4.4	1.0	20.7	5.0	1.0
1,3,5-TCB	20	22.3	2.5	0.5	18.7	23.2	4.3
2,3,6-TCT	20	20.9	3.4	0.7	20.3	5.8	1.2
2,4,5-TCT	20	20.1	7.2	1.5	22.8	7.9	1.8
P5CB	20	22.4	5.7	1.3	20.3	6.2	1.3
A2,6-TCT	20	19.5	4.5	0.9	19.7	6.0	1.2
A-BHC	20	20.2	6.9	1.4	18.0	5.8	1.0
G-BHC	20	17.9	9.2	1.6	19.4	6.5	1.3
A-CHLA**	20	20.3	2.5	0.5	36.4	11.8	4.3
Oxy-CHLA	20	19.1	7.9	1.5	19.7	6.5	1.3
Aldrin	20	21.4	2.1	0.5	19.5	6.5	1.3
Endrin	20	17.8	13.7	2.5	12.0	24.6	2.9
Dieldrin	20	18.1	9.8	1.8	20.0	12.9	2.6
Endos 1	20	17.2	11.0	1.9	19.3	10.8	2.1
Endos 2	20	15.9	11.1	1.8	18.5	4.7	0.9
Endos S	20	16.6	8.7	1.4	18.5	4.7	0.9
Heptachlor	20	15.8	8.2	1.3	22.1	6.8	1.5
OCSTYR	20	20.0	7.9	1.6	19.5	6.2	1.2
Trans-Nonachlor	20	18.7	7.5	1.4	18.4	6.5	1.2
o,p'-DDT	20	16.9	3.2	0.5	22.2	5.1	1.1
p,p'-DDD	20	15.9	8.4	1.3	18.5	3.8	0.7
p,p'-DDE	20	18.8	3.3	0.6	18.2	4.7	0.9
p,p'-DDT	20	18.6	8.8	1.6	19.6	5.4	1.1
Mirex	20	18.1	7.7	1.4	18.5	2.3	0.4
p-Mirex***	40	18.4	8.6	1.6	n/a	n/a	n/a
G-CHLA/PCB60*	40	38.5	2.3	0.9	39.0	2.0	0.8
DMDT/PCB171	40	41.4	8.1	3.4	34.2	2.7	0.9
Cis-Nonachlor/PCB114	40	39.1	6.5	2.5	n/a	n/a	n/a

H-Epoxide/PCB74	**40**	36.8	5.2	1.9	n/a	n/a	n/a
H-Epoxide	**20**	n/a	n/a	n/a	20.8	11.5	2.4
Cis-Nonachlor	**20**	n/a	n/a	n/a	22.8	16.8	3.8
PCB99/Alpha-Chlordane	**40**	n/a	n/a	n/a	36.4	11.8	4.3
PCB167/Photo-Mirex	**40**	n/a	n/a	n/a	36.0	13.9	5.0

***PCB74/H-epoxide coelutopn - LN_2 modulator**
****PCB99/alpha-chlordane coelution - new modulator**
*****PCB167/photo-Mirex coelution - new modulator**

Name	**Design (ng/mL)**	**LN_2 Commercial Modulator**			**Uof Waterloo Modulator (N=5)**		
		Avg.	%RSD	Std. Deviation	**Avg. (ng/mL)**	**%RSD**	**Std. Deviation**
PCB4/PCB10	40	47.60	7.04	3.35	40.6	3.9	1.57
PCB6	20	22.97	3.91	0.90	20.2	6.1	1.23
PCB8	20	21.21	2.70	0.57	20.1	5.1	1.02
PCB15	20	21.71	7.75	1.68	21	7.1	1.5
PCB16	20	21.28	2.16	0.46	19.9	4.3	0.85
PCB18	20	20.43	2.95	0.60	21	4.7	1
PCB19	20	20.50	8.19	1.68	20.1	8.6	1.72
PCB22	20	19.76	1.19	0.24	19	4.8	0.91
PCB28/PCB31	40	41.83	3.81	1.59	38.6	1.6	0.63
PCB33	20	20.07	1.24	0.25	19.8	3.9	0.77
PCB37	20	22.22	5.15	1.15	19.1	3.6	0.69
PCB40	20	22.56	3.24	0.73	19.1	3.6	0.69
PCB41	20	20.93	1.98	0.41	19.2	5	0.97
PCB44	20	15.36	11.30	1.74	20.1	5.7	1.14
PCB49	20	20.35	2.99	0.61	18.9	3.5	0.65
PCB52	20	20.51	0.71	0.15	19.6	5	0.97
PCB54	20	21.15	7.36	1.56	20.2	5.2	1.05
PCB66	20	19.90	6.63	1.32	19.3	5.8	1.12
PCB70	20	22.00	10.75	2.36	18.8	10.8	2.04
PCB74*	20	n/a	n/a	n/a	20	14.3	2.87

PCB77	20	20.60	3.30	0.68	19.2	7.3	1.4
PCB81	20	17.92	2.16	0.39	18.4	5.5	1.01
PCB84	20	23.02	2.97	0.68	19.3	4.9	0.94
PCB85	20	23.18	3.82	0.89	15.9	28.2	4.49
PCB87	20	19.20	4.13	0.79	18.5	4.8	0.89
PCB90/PCB101	40	43.18	1.20	0.52	37.4	3.2	1.19
PCB95	20	18.81	8.68	1.63	19.1	3.9	0.75
PCB97	20	20.00	1.17	0.23	18.6	4.2	0.79
PCB99**	20	17.78	3.75	0.67	37.4	11.9	4.45
PCB104	20	19.13	2.54	0.49	18.7	15	2.8
PCB105	20	19.20	1.94	0.37	18.5	4.3	0.8
PCB110	20	19.11	2.49	0.48	19.4	5.1	1
PCB114	20	n/a	n/a	n/a	17.5	11.9	2.09
PCB118	20	17.96	5.80	1.04	19.8	5	1
PCB119	20	20.70	3.30	0.68	21.2	3.3	0.71
PCB123	20	21.40	3.82	0.82	20.5	13.1	2.68
PCB126	20	20.17	4.19	0.85	19.1	6.5	1.24
PCB128	20	19.71	2.01	0.40	18.2	4.9	0.89
PCB129	20	23.06	2.93	0.68	18.1	4.4	0.79
PCB135	20	19.54	15.31	2.99	19.5	6.2	1.21
PCB137	20	22.49	6.28	1.41	18.5	4.9	0.9
PCB138	20	20.15	2.89	0.58	18.6	5.6	1.04
PCB141	20	20.67	3.56	0.73	18.7	3.9	0.73
PCB149	20	19.05	2.40	0.46	17.9	3.8	0.67
PCB151	20	20.28	13.85	2.81	20.8	7.9	1.64
PCB153	20	22.81	7.81	1.78	14.3	57.1	8.19
PCB155	20	20.27	0.63	0.13	19.4	3.9	0.76
PCB156	20	18.87	3.99	0.75	17.9	6.5	1.17
PCB157	20	18.94	2.44	0.46	18.8	6.4	1.2
PCB158	20	20.03	4.01	0.80	18.6	6.1	1.15
PCB167***	20	21.15	3.82	0.81	n/a	n/a	n/a
PCB168	20	17.43	8.04	1.40	21.1	7.8	1.64
PCB169	20	20.63	7.70	1.59	17.5	6.9	1.21
PCB170	20	19.31	2.78	0.54	18.1	7	1.28
PCB174	20	20.54	1.71	0.35	18.5	5	0.93
PCB177	20	21.19	2.14	0.45	18.5	4.7	0.86
PCB178	20	21.77	2.63	0.57	19.7	4.9	0.97

PCB180	20	21.68	4.64	1.00	18	7.1	1.28
PCB183	20	20.57	2.01	0.41	18.8	6.8	1.28
PCB187	20	21.87	2.29	0.50	18.7	5.2	0.98
PCB188	20	20.52	2.51	0.52	18.9	4	0.75
PCB189	20	20.88	6.59	1.37	17.9	6.3	1.13
PCB191	20	21.54	3.57	0.77	18.7	11.6	2.16
PCB193	20	21.18	2.70	0.57	18.2	7.7	1.39
PCB194	20	21.75	6.48	1.41	18.2	5.3	0.96
PCB199	20	21.41	4.33	0.93	18.1	6.1	1.1
PCB200	20	20.80	2.12	0.44	19.3	6.4	1.24
PCB201	20	21.79	2.47	0.54	19.5	4.8	0.93
PCB202	20	21.48	1.95	0.42	18.3	7.2	1.32
PCB203	20	23.69	4.84	1.15	18.4	5.4	0.99
PCB205	20	20.27	6.16	1.25	18.5	5	0.92
PCB206	20	21.83	7.88	1.72	18.9	4.8	0.9
PCB207	20	23.44	5.29	1.24	18.3	4.4	0.81
PCB208	20	22.14	5.13	1.14	18.2	6.2	1.12
PCB209	20	20.72	6.90	1.43	17.8	5	0.89
HCB	20	22.30	3.45	0.77	19.8	7.6	1.51
HCBD	20	23.24	3.17	0.74	n/a	n/a	n/a
HCE	20	22.25	4.29	0.95	n/a	n/a	n/a
1,2,3,4-TCB	20	21.29	3.67	0.78	21.1	7.2	1.51
1,2,3,5-/1,2,4,5-TCB	40	39.93	6.25	2.50	39.6	8.3	3.28
1,2,3-TCB	20	21.82	3.30	0.72	20.4	8.2	1.67
1,2,4-TCB	20	22.57	1.96	0.44	19	5	0.94
1,3,5-TBB	20	21.95	4.36	0.96	20.7	6.9	1.43
1,3,5-TCB	20	22.32	2.45	0.55	19.3	28.3	5.48
2,3,6-TCT	20	20.89	3.37	0.70	20.3	7.2	1.45
2,4,5-TCT	20	20.10	7.22	1.45	21.9	12.1	2.65
P5CB	20	22.44	5.72	1.28	20.2	6.9	1.38
A2,6-TCT	20	19.51	4.49	0.88	19.8	9.8	1.94
A-BHC	20	20.24	6.88	1.39	18.1	8.8	1.59
G-BHC	20	17.89	9.16	1.64	19.3	13.3	2.57
A-CHLA**	20	20.28	2.52	0.51	37.4	11.9	4.45
Oxy-CHLA	20	19.08	7.90	1.51	19.6	8.4	1.64

Aldrin	20	21.37	2.14	0.46	19.3	10	1.94
Endrin	20	17.85	13.74	2.45	14.3	33.4	4.79
Dieldrin	20	18.14	9.83	1.78	22.6	9.1	2.05
Endos 1	20	17.20	11.02	1.90	16.5	18.9	3.12
Endos 2	20	15.95	11.10	1.77	18.4	11.4	2.09
Endos S	20	16.63	8.71	1.45	18.4	11.4	2.09
Heptachlor	20	15.80	8.20	1.29	20.8	51.7	10.73
OCSTYR	20	20.04	7.88	1.58	19.3	9	1.73
Trans-Nonachlor	20	18.65	7.51	1.40	18.3	10.8	1.99
o,p'-DDT	20	16.93	3.22	0.55	23.8	34.9	8.31
p,p'-DDD	20	15.91	8.45	1.34	18.6	11.6	2.16
p,p'-DDE	20	18.76	3.34	0.63	18.5	5.5	1.01
p,p'-DDT	20	18.61	8.76	1.63	20.4	44.8	9.15
Mirex	20	18.13	7.75	1.40	18	6.1	1.1
p-Mirex***	40	18.36	8.62	1.58	n/a	n/a	n/a
G-CHLA/PCB60*	40	38.53	2.27	0.88	38.4	2.2	0.83
DMDT/PCB171	40	41.42	8.11	3.36	34.6	13.4	4.62
Cis-Nonachlor/PCB114	40	39.12	6.51	2.55	n/a	n/a	n/a
H-Epoxide/PCB74	40	36.81	5.16	1.90	n/a	n/a	n/a
H-Epoxide	20	n/a	n/a	n/a	20.1	9.3	1.87
Cis-Nonachlor	20	n/a	n/a	n/a	23.3	27	6.28
PCB99/Alpha-Chlordane	40	n/a	n/a	n/a	37.4	11.9	4.45
PCB167/Photo-Mirex	40	n/a	n/a	n/a	36.5	3.5	1.28

Appendix C

Supplementary materials from Chapter 5

Without Backflush

Run 1

Analyte	^1t_R (min)	^2t_R (s)	Area
C11	7.50	3.46	1094
C12	9.20	3.54	1440
C13	10.80	3.63	1841
C14	12.40	3.63	1817

Areas

Analyte Areas	Std Dev	Average	RSD (%)
C11	65.00	1131.00	**5.74**
C12	130.00	1328.00	**9.76**
C13	202.00	1994.00	**10.14**
C14	92.00	1877.00	**4.92**

Run 2

Analyte	^1t_R (min)	^2t_R (s)	Area
C11	7.50	3.44	1206
C12	9.20	3.53	1186
C13	10.80	3.63	2223
C14	12.40	3.62	1983

^1t_R

^1t_R	Std Dev	Average	RSD (%)
C11	0.00010	7.50	**0.00**
C12	0.00010	9.20	**0.00**
C13	0.00010	10.80	**0.00**
C14	0.00010	12.40	**0.00**

Run 3

Analyte	^1t_R (min)	^2t_R (s)	Area
C11	7.50	3.45	1093
C12	9.20	3.54	1358
C13	10.80	3.64	1917
C14	12.40	3.65	1830

^2t_R

2D tR	Std Dev	Average	RSD (%)
C11	0.0100	3.45	**0.29**
C12	0.0058	3.54	**0.16**
C13	0.0058	3.63	**0.16**
C14	0.0153	3.63	**0.42**

With Backflush after one minute

Run 1

Analyte	^1t_R (min)	^2t_R (s)	Area
C11	7.40	3.45	1203
C12	9.10	3.53	1105
C13	10.80	3.50	1361
C14	12.40	3.48	1000

Areas

Analyte Areas	Std Dev	Average	RSD (%)
C11	36.00	1180.00	**3.09**
C12	298.00	1449.00	**20.59**
C13	307.00	1662.00	**18.48**
C14	48.00	1037.00	**4.66**

Run 2

Analyte	^1t_R (min)	^2t_R (s)	Area
C11	7.40	3.46	1138
C12	9.10	3.54	1640
C13	10.80	3.51	1975
C14	12.40	3.49	1092

Run 3

Analyte	^1t_R (min)	^2t_R (s)	Area
C11	7.40	3.47	1199
C12	9.10	3.55	1601
C13	10.80	3.51	1650
C14	12.40	3.49	1020

^1t_R

^1t_R	Std Dev	Average	RSD (%)
C11	0.00010	7.40	**0.00**
C12	0.00010	9.10	**0.00**
C13	0.00010	10.80	**0.00**
C14	0.00010	12.40	**0.00**

^2t_R

^2t_R	Std Dev	Average	RSD (%)
C11	0.0100	3.46	**0.29**
C12	0.0100	3.54	**0.28**
C13	0.0058	3.51	**0.16**
C14	0.0058	3.49	**0.17**